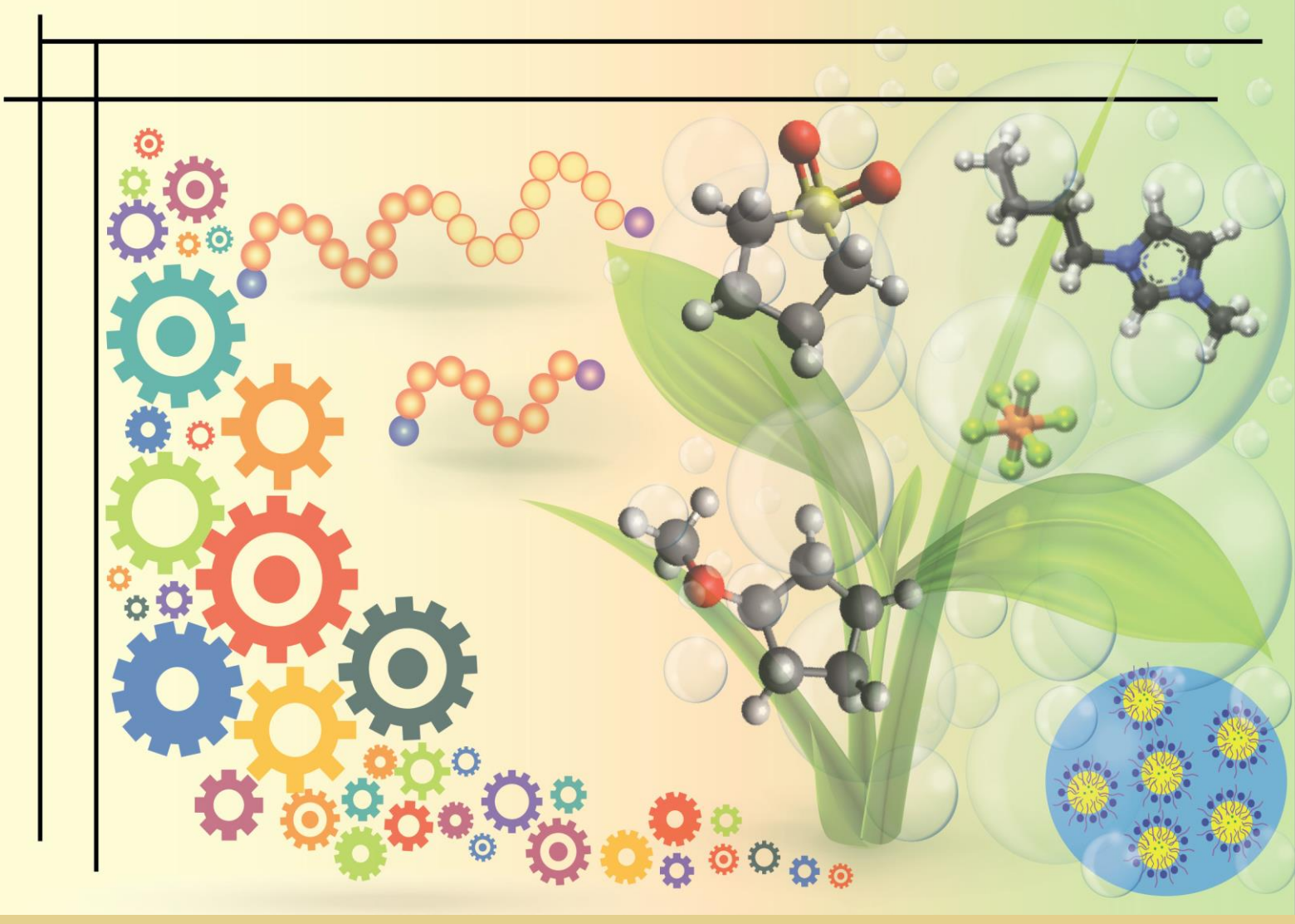

Joana Serra e Moura Pacheco Mendes

Supplemental Activator and Reducing Agent Atom Transfer Radical Polymerization: exploring new solvent systems and development of tailor-made block copolymers

Doctoral Thesis in Chemical Engineering, supervised by Professor Doctor Arménio Serra, Doctor Ana Fonseca and Professor Doctor Jorge Coelho, submitted to the Department of Chemical Engineering, Faculty of Science and Technology, University of Coimbra

Agosto, 2017

· U C ·

UNIVERSIDADE DE COIMBRA

Joana Serra e Moura Pacheco Mendes

Supplemental Activator and Reducing Agent Atom Transfer Radical Polymerization: exploring new solvent systems and development of tailor-made block copolymers

Thesis submitted to Faculty of Sciences and Technology, University of Coimbra to obtain the Degree of Doctor in Chemical Engineering.

Agosto
2017

UNIVERSIDADE DE COIMBRA

Joana Serra e Moura Pacheco Mendes

Supplemental Activator and Reducing Agent Atom Transfer Radical Polymerization: exploring new solvent systems and development of tailor-made block copolymers

Thesis submitted to Faculty of Sciences and Technology, University of Coimbra to obtain the Degree of Doctor in Chemical Engineering.

Supervisors:

Prof. Dr. Arménio Coimbra Serra

Dr. Ana Clotilde Amaral Loureiro da Fonseca

Prof. Dr. Jorge Fernando Jordão Coelho

Host institutions:

CEMMPRE - Centre for Mechanical Engineering, Materials and Processes, Department of Chemical Engineering, Faculty of Sciences and Technology of the University of Coimbra

Agosto

2017

UNIVERSIDADE DE COIMBRA

"O único homem que está isento de erros é aquele que não arrisca acertar"

Albert Einstein

Acknowledgments

Ao Jorge Coelho que me lançou nesta aventura da investigação e ao longo destes anos sempre me apoiou, motivou e acreditou em mim. Agradeço o desafio científico que me deste, agradeço todo o conhecimento que me transmitiste e agradeço toda a ajuda.

Ao Professor Arménio Serra, que sempre me orientou. Agradeço toda a disponibilidade, todo o conhecimento e sugestões que me deu durante este trabalho.

Aos meus colegas que contribuíram direta ou indiretamente para este trabalho. Obrigada pelo conhecimento que partilharam, pela simpatia e boa disposição, e claro, por aturarem as minhas frustrações laboratoriais.

Ao Departamento de Engenharia Química e a todos os seus funcionários, agradeço todas as condições proporcionadas.

Não poderia deixar de agradecer à minha família por todo o apoio que sempre me deram e pelo carinho que sempre me prestam. Obrigada pais, avós e gémeos por me apoiarem incondicionalmente, obrigada pelos vossos beijos e abraços em todos os momentos da minha vida. Obrigada minha Tininha, tens uma paciência de santa e nunca me dizes que não.

Por último, mas não menos importantes, os meus amigos. Muito Obrigada! Não vos inúmero porque vocês sabem quem são e o que são para mim. Obrigada pela paciência que demonstraram nestes últimos meses, obrigada por me permitirem descontrair e divertir, obrigada por me desafiarem e por me fazerem crescer, obrigada por me darem o melhor de vocês. Obrigada, obrigada, obrigada.

Abstract

This project was envisaged to develop new reaction systems for Atom Transfer Radical Polymerization (ATRP). The focus of the work was centred on the use of different solvents, namely "greener" alternatives to the use of toxic solvents.

The first study involved the polymerization of methyl acrylate (MA) by Supplemental Activation and Reducing Agent (SARA) ATRP in sulfolane. This system required only very low amounts of soluble copper (catalytic system) to afford the control over the polymerization of MA, methyl methacrylate (MMA) and vinyl chloride (VC). Under the same reaction conditions, similar kinetic data have been obtained with sulfolane and dimethyl sulfoxide (DMSO). However, contrary to DMSO, a commonly used solvent in ATRP, sulfolane also allowed to afford the controlled polymerization of styrene (St). This feature is particularly relevant to access a portfolio of block copolymers using the afore mentioned monomers in a single solvent (Chapter 2).

In order to increase the rate of the polymerization, small amounts of water were added to the reaction mixture. In addition, the presence of water allowed to use $Na_2S_2O_4$ as SARA agent as alternative to copper wire, turning the system "greener" (Chapter 3).

Following published reports showing an acceleration effect induced by using ionic liquids in radical-based polymerization, the solvent system DMSO/1-Butyl-3-methylimidazolium hexafluorophosphate ([BMIM]-[PF_6]) was studied for polymerization of MA catalyzed by $Na_2S_2O_4$/ $CuBr_2$ / Me_6TREN (Me_6TREN: Tris [2-(dimethylamino) ethyl] amine. An unexpected synergistic effect between these two solvents was observed. The results revealed an enormous acceleration of the reaction and also an optimum mixture ratio of DMSO/[BMIM]-[PF_6]= 50/50 (v/v) (Chapter 4).

A study of SARA ATRP of several monomers using different sulfolane based mixtures ([BMIM]-[PF_6], triethylene glycol and water) was carried out at room temperature (Chapter 5).

Aiming to replace tetrahydrofuran (THF), it was proposed the use of cyclopentyl methyl ether (CPME)/ethanol/water mixtures as a "greener" solvent mixture for SARA ATRP of MA, glycidyl methacrylate, St and VC (Chapter 6).

The work continued with the study of the SARA ATRP using a miniemulsion system. For the first time, butyl acrylate (BA) and St were polymerized in the presence $CuBr_2$/EHA_6TREN or BPMODA* complexes mediated by $Na_2S_2O_4$ as the SARA agent. The obtained polymers had a controlled structure and narrow molecular weight

distribution ($Đ \leq 1.2$). However, the conversion obtained was always low (~20 %). Different strategies were studied to improve the monomer conversion with no success (Chapter 7).

Finally, copolymers prepared by ATRP were applied in the stabilization of superparamagnetic iron oxide nanoparticles (hydrophilic and hydrophobic). Different amphiphilic copolymers of poly(ethylene glycol)-block-poly(vinylpyridine) with different compositions and molecular weights were synthesized and used to prepare hybrid nanoaggregates via "self-assembly" in aqueous medium. Theses structures were achieved via tritation or solvent exchange method (tritation method: 24.7 to 613 nm; solvent exchange method: 17.6 to 35.7 nm) (Chapter 8).

Resumo

Este projeto foi elaborado para desenvolver novos sistemas de reação para polimerização radicalar por transferência de átomo (ATRP: "*Atom Transfer Radical Polymerization"*). O foco do trabalho foi centrado no uso de diferentes solventes, nomeadamente alternativas "mais verdes" ao uso de solventes tóxicos.

O primeiro estudo envolveu a polimerização de acrilato de metilo (MA) por ATRP na presença de um agente de redução e ativação suplementar (SARA) em sulfolano. Este sistema exigiu apenas quantidades muito baixas de cobre solúvel (sistema catalítico) para permitir o controlo sobre a polimerização de MA, metacrilato de metilo (MMA) e cloreto de vinilo (VC). Sob as mesmas condições de reação, dados cinéticos similares foram obtidos com sulfolano e dimetil sulfóxido (DMSO). No entanto, contrariamente ao DMSO, um solvente vulgarmente utilizado em ATRP, o sulfolano permitiu também a polimerização controlada do estireno (St). Esta característica é particularmente relevante para sintetizar um portfólio de copolímeros de bloco usando os monómeros acima mencionados num único solvente (Capítulo 2).

Com o objetivo de aumentar a velocidade da reação de polimerização, foram adicionadas à mistura reacional pequenas quantidades de água. Além disso, a presença de água permitiu usar $Na_2S_2O_4$ como agente SARA, em alternativa ao fio de cobre e tornar o sistema "mais verde" (Capítulo 3).

Na sequência de artigos científicos publicados que mostram um efeito de aceleração induzido pela utilização de líquidos iónicos na polimerização radicalar, o sistema solvente DMSO / hexafluorofosfato de 1-butil-3-metilimidazólio ([BMIM]-[PF_6]) foi estudado para polimerização do MA catalisado por $Na_2S_2O_4$, $CuBr_2$ / Me_6TREN (Me_6TREN: Tris [2- (dimetilamino) etil] amina. Com este trabalho, observou-se um efeito sinergístico inesperado entre estes dois solventes. Os resultados revelaram uma enorme aceleração da reação e também uma proporção óptima de mistura de DMSO / [BMIM]-[PF_6] = 50/50 (v / v) (Capítulo 4). O estudo de SARA ATRP de vários monómeros com diferentes misturas à base de sulfolano ([BMIM]-[PF_6], trietileno glicol e água) foi realizado a temperatura ambiente (Capítulo 5).

Com o objetivo de substituir o tetrahidrofurano (THF), propôs-se o uso de misturas de éter ciclopentilmetil (CPME) / etanol / água como uma mistura solvente "mais verde" para SARA ATRP do MA, metacrilato de glicidilo (GMA), St e VC (Capítulo 6).

O trabalho continuou com o estudo do SARA ATRP usando um sistema de miniemulsão. Pela primeira vez foram polimerizados acrilato de butilo (BA) e St na presença de complexos de $CuBr_2$ / EHA_6TREN ou BPMODA* mediados por $Na_2S_2O_4$ como agente de SARA. Os polímeros obtidos tinham uma estrutura controlada e uma polidispersividade baixa ($Đ \leq 1,2$). No entanto, a conversão obtida foi sempre baixa (~ 20%). Foram ainda estudadas diferentes estratégias para melhorar a conversão da polimerização mas sem sucesso (Capítulo 7).

Finalmente, copolímeros preparados por ATRP foram aplicados na estabilização de nanopartículas superparamagnéticas de óxido de ferro (hidrofílicas e hidrofóbicas). Foram sintetizados diferentes copolímeros anfifílicos de poli(etileno glicol)-bloco-poli(vinilpiridina) com diferentes composições e pesos moleculares e utilizados para preparar nanoagregados híbridos por "*self-assembly*" em meio aquoso. Essas estruturas foram obtidas por métodos de titulação ou método de troca de solvente (método de titulação: 24,7 a 613 nm, método de troca de solvente: 17,6 a 35,7 nm) (Capítulo 8).

List of publications

Papers published from the research work presented in this thesis:

Rocha, N.; Mendonça, P. V.; Mendes, J. P.; Simões, P. N.; Popov, A. V.; Guliashvili, T.; Serra, A. C.; Coelho, J. F. J., *Facile Synthesis of Well-Defined Telechelic Alkyne-Terminated Polystyrene in Polar Media Using ATRP With Mixed Fe/Cu Transition Metal Catalyst*. **Macromolecular Chemistry and Physics** 2013, 214 (1), 76-84. (Chapter 2, Part II)

Rocha, N.; Mendes, J.; Duraes, L.; Maleki, H.; Portugal, A.; Geraldes, C. F. G. C.; Serra, A.; Coelho, J., *Poly(ethylene glycol)-block-poly(4-vinyl pyridine) as a versatile block copolymer to prepare nanoaggregates of superparamagnetic iron oxide nanoparticles*. **Journal of Materials Chemistry B** 2014, 2 (11), 1565-1575. (Chapter 8, Part III)

Mendes, J. P.; Branco, F.; Abreu, C. M. R.; Mendonça, P. V.; Popov, A. V.; Guliashvili, T.; Serra, A. C.; Coelho, J. F. J., *Synergistic Effect of 1-Butyl-3-methylimidazolium Hexafluorophosphate and DMSO in the SARA ATRP at Room Temperature Affording Very Fast Reactions and Polymers with Very Low Dispersity*. **ACS Macro Letters** 2014, 3 (6), 544-547. (Chapter 4, Part II)

Mendes, J. P.; Branco, F.; Abreu, C. M. R.; Mendonça, P. V.; Serra, A. C.; Popov, A. V.; Guliashvili, T.; Coelho, J. F. J., *Sulfolane: an Efficient and Universal Solvent for Copper-Mediated Atom Transfer Radical (co)Polymerization of Acrylates, Methacrylates, Styrene, and Vinyl Chloride*. **ACS Macro Letters** 2014, 3 (9), 858-861. (Chapter 2, Part II)

Maximiano, P., Mendes, J. P., Mendonça, P. V., Abreu, C. M. R., Guliashvili, T., Serra, A. C. and Coelho, J. F. J. , *Cyclopentyl methyl ether: A new green co-solvent for supplemental activator and reducing agent atom transfer radical polymerization.* **Journal of Polymer Science Part A: Polymer Chemistry**, 2015, 53, 2722–2729. (Chapter 6, Part II)

Mendes, J. P.; Mendonca, P. V.; Maximiano, P.; Abreu, C. M. R.; Guliashvili, T.; Serra, A. C.; Coelho, J. F. J., *Getting faster: low temperature copper-mediated SARA ATRP of methacrylates, acrylates, styrene and vinyl chloride in polar media using sulfolane/water mixtures*, **RSC Advances**, 2016, 6 (12), 9598-9603. (Chapter 3, Part II)

Mendes, J. P.; Góis, J. R.; Costa, J. R. C.; Maximiano, P.; Serra, A. C.; Guliashvili, T.; Coelho, J. F. J., *Ambient temperature SARAATRP for meth(acrylates), styrene, and vinyl chloride using sulfolane/1-butyl-3-methylimidazolium hexafluorophosphate-based mixtures*, **Journal of Polymer Science Part A: Polymer Chemistry**, n/a-n/a, 2017. (Chapter 5, Part II)

Papers published from the collaboration in other projects during the PhD program:

Cordeiro, R. A.; Rocha, N.; Mendes, J. P.; Matyjaszewski, K.; Guliashvili, T.; Serra, A. C.; Coelho, J. F. J., Synthesis of well-defined poly(2-(dimethylamino)ethyl methacrylate) under mild conditions and its co-polymers with cholesterol and PEG using Fe(0)/Cu(II) based SARA ATRP. **Polymer Chemistry** 2013, 4 (10), 3088-3097.

Cordeiro, R., G.L. Santos, H. Faneca, J.P. Mendes, A.C. Serra, and J.F.J. Coelho, Evaluation of the biocompatibility of cholesterol-poly[2-(dimethylamino)ethyl methacrylate] synthesized by atom transfer radical polymerization. **European Cells and Materials**, 2013. 26(SUPPL.6): p. 58

Monteiro, S.; Dias, A.; Mendes, A. M.; Mendes, J. P.; Serra, A. C.; Rocha, N.; Coelho, J. F. J.; Magalhães, F. D., Stabilization of nano-TiO2 aqueous dispersions with poly(ethylene glycol)-b-poly(4-vinyl pyridine) block copolymer and their incorporation in photocatalytic acrylic varnishes. **Progress in Organic Coatings** 2014, 77 (11), 1741-1749.

Submitted papers, waiting for decision

Mendes, J. P.; Góis, J. R.; Costa, Trino, A.; Catalão, F. P.; Serra, A. C.; Coelho, J. F. J., *Miniemulsion SARA-ATRP of butyl acrylate and styrene mediated by sodium dithionite* (Chapter 7, Part II).

Thesis outline

This document is organized in four parts subdivided into different chapters.

The first part, corresponding to Chapter 1, is a literature review covering the main relevant aspects concerning the reversible deactivation radical polymerization (RDRP) methods with a particular focus on Atom Transfer Radical Polymerization (ATRP) techniques in homogeneous and heterogeneous media.

The second part concerns the experimental work carried out in Supplemental Activation and Reducing Agent (SARA) ATRP using different solvent systems: Sulfolane (Chapter 2), sulfolane/water mixtures (Chapter 3), ionic liquid (Chapter 4), sulfolane/3-Butyl-3-methylimidazolium mixtures ([BMIM]-[PF_6]) (Chapter 5) and cyclopentyl methyl ether (CPME) (Chapter 6). The results of the SARA ATRP heterogeneous polymerization using miniemulsion approach are also described (Chapter 7).

In Chapter 2, sulfolane was used for the first time on the RDRP area, as a "universal" solvent for acrylates, methacrylates, styrene and vinyl chloride. Block copolymers of these monomers were prepared by SARA ATRP employing tiny amounts of soluble copper. The robustness of the system was demonstrated through the synthesis of block copolymers that had never been reported (*e.g.,* poly(methyl acrylate)-*b*-poly(vinyl chloride)-*b*-poly(methyl acrylate)). Although the kinetic results presented between dimethyl sulfoxide (DMSO) and sulfolane are similar, unlike DMSO, sulfolane also allows the polymerization of styrene. The use of this polar aprotic solvent allowed us to overcome one of the most limiting aspects of the preparation of block copolymers, namely the differences in the solubility of the different polymeric segments in the same solvent.

In Chapter 3, based on the previous data, the rate of polymerization of the different monomers was increased significantly by using a small amount of water as a co-solvent, while maintaining the controlled features of the polymerization. The addition of water also allowed the use of FDA-approved sulfites as SARA agents which could not be used in pure sulfolane due to insolubility of the catalytic system.

In Chapter 4, it was observed a synergistic effect of [BMIM]-[PF_6] /DMSO for SARA ATRP of methyl acrylate using $Na_2S_2O_4$/$CuBr_2$/Me_6TREN as the catalytic system. Following this research line, a study of SARA ATRP of several monomers using different sulfolane based mixtures was carried out at room temperature (Chapter 5).

CPME presented an opportunity to introduce a "green" solvent approach to a proved and robust system, such as SARA ATRP. In Chapter 6 it is reported for the first time the use of this solvent as a suitable substitute for the commonly used toxic tetrahydrofuran (THF).

In Chapter 7, the SARA ATRP method was carried out in miniemulsion to evaluate the potential of this controlled polymerization strategy to be used in heterogeneous media.

The third part of this thesis refers to the application of different block copolymers prepared by SARA ATRP for the stabilization of superparamagnetic iron oxide nanoparticles (SPIONs). Amphiphilic block copolymers based on poly(ethylene glycol)-block-poly(4-vinyl pyridine) (mPEG-*b*-P4VP) with different compositions and molecular weights were used to afford stable SPIONs.

Finally, the fourth part of this thesis presents the main conclusions from this work, and some suggestions for future work.

List of acronyms

AA	Ascorbic acid
ABA	Triblock copolymer
AGET	Activators generated by electron transfer
AIBN	Azobisisobutyronitrile
ARGET	Activators regenerated by electron transfer
ATRA	Atom transfer radical addition
ATRP	Atom transfer radical polymerization
Azido-BiB	2-Azidoethyl 2-bromoisobutyrate
[BMIM]-[PF_6]	1-Butyl-3-methylimidazolium hexafluorophosphate
bpy	2,2'-Bipyridine
BPMODA	Bis(2-pyridylmethyl)octadecylamine
BPMODA*	bis[2-(4-methoxy-3,5-dimethyl)pyridylmethyl]octadecylamine
BPN	2-bromopropionitrile
4f-BiB	Pentaerythritol tetrakis(2-bromoisobutyrate)
CPME	Cyclopentyl methyl ether
CPA	Chloropropionamide
CPC	2-chloropropionyl chloride
CTAB	Cetyltrimethylammonium bromide
DCM	Dichloromethane
dn/dc	Refractive Index Increment
DMAP	4-Dimetilaminopiridina
dNbpy	4,4′-Dinonyl-2,2′-dipyridyl (),
DHB	2,5-Dihydroxybenzoic acid
DMF	Dimethylformamide
DMSO	Dimethyl sulfoxide
DP	Degree of polymerization
DT	Degenerative transfer
DV	Differential viscometer
*e*ATRP	Electrochemically mediated atom transfer radical polymerization
EBiB	Ethyl α-bromoisobutyrate
EBPA	α-bromophenylacetate
ECP	Ethyl 2-chloropropionate

EHA_6TREN	Tris(2-bis(3-(2-ethylhexoxy)-3-oxopropyl)aminoethyl)amine
EtOH	Ethanol
FDA	Food and Drug Administration
FRP	Free radical polymerization
FTIR-ATR	Fourier transform infrared attenuated total reflection
GBP	Glycidol 2-bromopropionate
HABA	2-(4-Hydroxyphenylazo)benzoic acid
HBiB	2-hydroxyethyl α-bromoisobutyrate
HBP	2-hydroxyethyl 2-bromopropanoate
HEA	2-hydroxyethyl acrylate
HLB	Hydrophilic-lipophilic balance
HMTETA	1,1,4,7,10,10-Hexamethyltriethylenetetramine
HPLC	High performance liquid chromatography
ICAR	Initiators for continuous activator regeneration
IL	Ionic liquid
IUPAC	International Union of Pure and Applied Chemistry
LALLS	Low-angle laser-light scattering
MADIX	Macromolecular design via the interchange of xanthates
MALDI-TOF	Matrix assisted laser desorption/ionization time-of-flight mass
MA	Methyl acrylate
MBP	Methylbromopropionate
MePEOMA	2-Phenoxyethyl methacrylate
MMA	Methyl methacrylate
Me_6TREN	Tris[2-(dimethylamino)ethyl]amine)
*n*BA	butyl acrylate
*n*BMA	butyl methacrylate
NMP	Nitroxide mediated polymerization
NMR	Nuclear magnetic resonance
OMRP	Organometallic mediated radical polymerization
PBiB	Propargyl 2-bromoisobutyrate
PEG	Poly(ethylene glycol)
PEBr	1-phenyl ethylbromide
PeBr4	2,2-dibromomethyl-1,3-dibromopropane
PMA	Poly(methyl acrylate)

PMDETA	*N*,*N*,*N*′,*N*″,*N*‴-Pentamethyldiethylenetriamine
P*n*BA	Poly(butyl acrylate)
P*n*MBA	Poly(butyl methacrylate)
ppm	Parts per million
PRE	Persistent radical effect
PSt	Polystyrene
PTFE	Polytetrafluoroethylene
PVA	Poly(vinyl alcohol)
PVC	Poly(vinyl chloride)
RALLS	Right-angle laser-light scattering
RAFT	Reversible addition-fragmentation chain transfer
RDC	Reversible deactivation by coupling or reversible termination
RDAT	Reversible deactivation by atom transfer
RDRP	Reversible deactivation radical polymerization
RI	Refractive index
SARA	Supplemental activator and reducing agent
SET	Single-electron transfer
SEC	Size exclusion chromatography
SDS	Sodium dodecyl sulfate
SR&NI	Simultaneous reverse and normal initiation
St	Styrene
TEA	Triethylamine
TEMPO	2,2,6,6-Tetramethylpiperidinyl-1-oxy
THF	Tetrahydrofuran
TMS	Tetramethylsilane
tNtpy	4,4',4''-tris(5-nonyl)-2,2':6',2''-terpyridine
TPMA	Tris(pyridin-2-ylmethyl)amine
TREN	Tris(2-aminoethyl)amine
TsCl	Tosyl chloride
UV-Vis	Ultraviolet-visible
VClAc	Vinyl cloro acetate

Nomenclature

$Đ$	Dispersity
D_h	Hydrodynamic diameter
M_n^{NMR}	Number-average molecular mass determined by NMR spectroscopy
M_n^{SEC}	Number-average molecular mass determined by SEC
M_n^{Th}	Theoretical number-average molecular mass
M_w	Theoretical mass-average molecular mass
k_p^{app}	Apparent rate constant of propagation
k_a	Activation rate constant
k_d	Deactivation rate constant
k_t	Activation/deactivation rate constant
k_{disp}	Disproportionation rate constant
k_{comp}	Comproportionation rate constant
K^{ATRP}	ATRP equilibrium constant
T	Temperature

Contents

ACKNOWLEDGMENTS ..... **VII**

ABSTRACT ..... **IX**

RESUMO ..... **XI**

LIST OF PUBLICATIONS ..... **XIII**

Papers published from the research work presented in this thesis: XIII

Papers published from the collaboration in other projects during the PhD program: XIV

SUBMITTED PAPERS, WAITING FOR DECISION ..... **XIV**

THESIS OUTLINE ..... **XV**

LIST OF ACRONYMS ..... **XVII**

NOMENCLATURE ..... **XXI**

LIST OF FIGURES ..... **XXXI**

LIST OF SCHEMES ..... **XLIII**

LIST OF TABLES ..... **XLV**

MOTIVATION, TARGETS AND RESEARCH SIGNIFICANCE ..... **XLVII**

Part I **1**

Literature review 1

Chapter 1 3

1.1 Radical Polymerization: from “free” to “controlled” polymers 3

1.2 Reversible deactivation radical polymerization – most used methods 4

1.3 Fundamentals of atom transfer radical polymerization 7

1.4 Components of the ATRP System 9

1.4.1 Monomers 9

1.4.2 Initiators 9
1.4.3 Catalysts and Ligands 11
1.4.4 Solvents 12
1.5 ATRP: limitations, variations and "*greener*" strategies 13
1.5.1 Single Electron Transfer Living Radical Polymerization (SET–LRP) 15
1.6 Green solvents 17
1.6.1 Ionic liquids 17
1.6.2 Water-based systems 19
1.7 Heterogeneous Polymerization: suspension, emulsion and miniemulsion 20
1.7.1 ATRP in aqueous dispersed media – focus on miniemulsion 25
1.8 References 29

Part II 35
Synthesis Method 35
Chapter 2 37
Sulfolane – an Efficient and Universal Solvent for Copper-Mediated Atom Transfer Radical (co)Polymerization of Acrylates, Methacrylates, Styrene and Vinyl Chloride 37
2.1 Abstract 39
2.2 Introduction 39
2.3 Experimental Section 41
2.3.1 Materials 41
2.3.2 Techniques 42
2.3.3 Procedures 43
2.3.3.1 Typical procedure for the $[Cu(0)]_0/[CuBr_2]_0/[Me_6TREN]_0$ = Cu(0) wire/0.1/1.1 catalyzed SARA ATRP of MA (DP = 222) 43
2.3.3.2 Typical procedure for the $[Cu(0)]_0/[CuBr_2]_0/[bpy]_0$ = Cu(0) wire/0.1/2.2 catalyzed SARA ATRP of MMA (DP = 222) 44
2.3.3.3 Typical procedure for the $[Cu(0)]_0/[CuBr_2]_0/[PMDETA]_0$ = Cu(0) wire/0/1.1 catalyzed ATRP of St (DP = 222) 44
2.3.3.4 Typical procedure for the $[Fe(0)]_0/[CuBr_2]_0/[Me_6TREN]_0$ = 1/0.1/1.1 catalyzed ATRP of Sty (DP = 125) in DMF. 45
2.3.3.5 Typical procedure for the $[Cu(0)]_0/[CuCl_2]_0/[PMDETA]_0$ = Cu(0) wire/0.1/1.1 catalyzed ATRP of St (DP = 222) 45
2.3.3.6 Typical procedure for the $[Cu(0)]_0/[TREN]_0$ = Cu(0) wire/1 catalyzed SARA ATRP of VC (DP = 222) 46
2.3.3.7 Typical procedure for chain extension of –Br terminated PMA 46
2.3.3.8 Typical procedure for chain extension of –Br terminated PMMA 47
2.3.3.9 Typical procedure for chain extension of –Br terminated PS 47
2.3.3.10 Typical procedure for the synthesis of PMA-*b*-PVC-*b*-PMA block copolymers by $[Cu(0)]_0/[Me_6TREN]_0$=Cu(0) wire/1.1 catalyzed SARA ATRP . 48

2.3.3.11 Typical procedure for the synthesis of PS-*b*-PVC-*b*-PS block copolymers by $[Cu(0)]_0/[PMDETA]_0$ = Cu(0) wire/1.1 catalyzed SARA ATRP 48
2.3.3.12 Typical procedure for the synthesis of PMA-*b*-PVC-*b*-PMA block copolymers by "one-pot" $[Cu(0)]_0/[TREN]_0$ = Cu(0) wire/1 catalyzed SARA ATRP 49
2.3.3.13 UV-vis spectroscopic study of the catalytic systems 49
2.4 Results and discussion 50
2.5 Conclusions 64
2.6 References 65

Chapter 3 69
Getting faster: low temperature copper-mediated ATRP of methacrylates, acrylates, styrene and vinyl chloride in polar media using sulfolane/water mixtures 69
3.1 Abstract 71
3.2 Introduction 71
3.3 Experimental Section 73
3.3.1 Materials 73
3.3.2 Techniques 74
3.3.3 Procedures 74
3.3.3.1 Typical procedure for the $[Cu(0)]_0/[CuBr_2]_0/[Me_6TREN]_0$ = Cu(0) wire/0.1/1.1 catalyzed SARA ATRP of MA in sulfolane/water = 90/10 (v/v) 74
3.3.3.2 Typical procedure for the $[Cu(0)]_0/[TREN]_0$ = Cu(0) wire/1 catalyzed SARA ATRP of VC 75
3.3.3.3 Typical procedure for the synthesis of PMA-*b*-PVC-*b*-PMA block copolymers by "one-pot" $[Cu(0)]_0/[TREN]_0$ = Cu(0) wire/1 catalyzed SARA ATRP 75
3.4 Results and discussion 76
3.4.1 SARA ATRP of (meth)acrylates, styrene and vinyl chloride in sulfolane /water = 90/10 (v/v) 78
3.4.2 Influence of the catalytic system 80
3.4.3 Synthesis of a PMA-*b*-PVC-*b*-PMA triblock copolymer by "one-pot" SARA ATRP 81
3.5 Conclusions 83
3.6 References 83

Chapter 4 85
Synergistic effect of 1-butyl-3-methylimidazolium hexafluorophosphate and DMSO in the SARA ATRP at room temperature affording very fast reactions and polymers with very low dispersity 85
4.1 Abstract 87
4.2 Introduction 87

4.3 Experimental Section 88
4.3.1 Materials 88
4.3.2 Techniques 89
4.4 Procedures 90
4.4.1.1 Typical Procedure for the $[Na_2S_2O_4]/[CuBr_2]/[Me_6TREN]$ = 1/0.1/0.1 catalyzed SARA ATRP of MA (DP=222) in [BMIM]-$[PF_6]$/DMSO = 50/50 (v/v) 90
4.4.1.2 Chain extension experiment of –Br terminated PMA 91
4.4.1.3 UV/Vis spectroscopy of $Na_2S_2O_4/CuBr_2/Me_6TREN$ in [BMIM]-$[PF_6]$/DMSO = 50/50 (v/v) 91
4.4.1.4 Determination of $E_T(30)$ in [BMIM]-$[PF_6]$/DMSO mixtures 91
4.5 Results and discussion 92
4.6 Conclusion 102
4.7 References 102

Chapter 5 105
Ambient Temperature SARA ATRP for meth(acrylates), styrene and vinyl chloride using sulfolane/1-butyl-3-methylimidazolium hexafluorophosphate based mixtures 105
5.1 Abstract 107
5.2 Introduction 107
5.3 Experimental Section 108
5.3.1 Materials 108
5.3.2 Techniques 109
5.3.3 Procedures 110
5.3.3.1 Typical procedure for the $[Cu(0)]_0/[CuBr_2]_0/[Me_6TREN]_0$ = Cu(0) wire/0.1/1.1 catalyzed SARA ATRP of MA (DP = 222) 110
5.3.3.2 Typical procedure for the $[Cu(0)]_0/[CuBr_2]_0/[bpy]_0$ = Cu(0) wire/0.1/2.2 catalyzed SARA ATRP of MMA (DP = 222) 110
5.3.3.3 Typical procedure for the $[Cu(0)]_0/[CuBr_2]_0/[PMDETA]_0$ = Cu(0) wire/0/1.1 catalyzed ATRP of St (DP = 222) 111
5.3.3.4 Typical procedure for chain extension of PMA-Br 111
5.3.3.5 UV/Vis spectroscopy of Cu(0) wire/$CuBr_2/Me_6TREN$ in mixtures of DMSO/BMIM-PF_6 and Sulfolane/[BMIM]-$[PF_6]$ = 100/0, 75/25, 50/50 and 25/75 (v/v) 112
5.4 Results and discussion 112
5.4.1 Absorption spectra of Reichardt's dye (30) 115
5.4.2 Comproportionation studies in the solvent mixtures 116
5.4.3 Effect of TEG and water in the sulfolane mixtures 117
5.4.4 SARA ATRP of MMA, St and VC in a mixture of sulfolane/[BMIM]-$[PF_6]$ 118
5.4.5 ^{1}H NMR analysis 119
5.4.6 Reinitiation experiment 122

5.5 Conclusions 122
5.6 References 123

Chapter 6 127
Cyclopentyl Methyl Ether: a New Green Co-Solvent for Supplemental Activator and Reducing Agent Atom Transfer Radical Polymerization 127
6.1 Abstract 129
6.2 Introduction 129
6.3 Experimental Section 131
6.3.1 Materials 131
6.3.2 Techniques 132
6.3.3 Procedures 133
6.3.3.1 Typical procedure for the $[Cu(0)]_0/[CuBr_2]_0/[Me_6TREN]_0$ = Cu(0) wire/0.1/1.1 catalyzed SARA ATRP of MA 133
6.3.3.2 Typical procedure for the $[Fe(0)]_0/[CuBr_2]_0/[Me_6TREN]_0$ = Cu(0) wire/0.1/1.1 catalyzed SARA ATRP of MA 134
6.3.3.3 Typical procedure for the $[Na_2S_2O_4)]_0/[CuBr_2]_0/[Me_6TREN]_0$ = Cu(0) wire/0.1/0.5 catalyzed SARA ATRP of MA 134
6.3.3.4 Typical procedure for the $[Cu(0)]_0/[CuBr_2]_0/[PMDETA]_0$ = Cu(0) wire/0/1.1 catalyzed SARA ATRP of St 135
6.3.3.5 Typical procedure for the $[Fe(0)]_0/[CuBr_2]_0/[TPMA]_0$ = 1/0/1.1 catalyzed SARA ATRP of GMA 135
6.3.3.6 Typical procedure for the $[Cu(0)]_0/[CuBr_2]_0/[TREN]_0$ = Cu(0) wire/0.1/1.1 catalyzed SARA ATRP of VC 136
6.3.3.7 Typical procedure for the synthesis of PMA-*b*-PVC-*b*-PMA block copolymer by "one-pot" $[Cu(0)]_0/[CuBr_2]_0/[TREN]_0$ = Cu(0) wire/0.1/1.1 catalyzed SARA ATRP 136
6.4 Results and discussion 137
6.4.1 Influence of the solvent mixture composition 137
6.4.2 Influence of the catalytic system 140
6.4.3 Influence of the degree of polymerization 141
6.4.4 Polymerization of styrene, vinyl chloride and glycidyl methacrylate 142
6.5 Conclusions 146
6.6 References 147

Chapter 7 151
Miniemulsion SARA ATRP of butyl acrylate and styrene mediated by sodium dithionite
7.1 Abstract 153
7.2 Introduction 153
7.3 Experimental Section 155
7.3.1 Materials 155

7.3.2 Techniques 155
7.3.3 Procedures 156
7.3.3.1 Typical procedure for SARA ATRP of *n*BA in miniemulsion catalyzed by $[Na_2S_2O_4]_0/[CuBr_2]_0/[BPMODA^*]_0$ = 0.2/0.4/0.4 (DP = 200) 156
7.3.3.2 Typical procedure for SARA ATRP of St in miniemulsion catalyzed by $[Na_2S_2O_4]_0/[CuBr_2]_0/[BPMODA^*]_0$ = 0.2/0.4/0.4 (DP = 200) 157
7.3.3.3 Typical procedure for chain extension of P*n*BA- Br 158
7.3.3.4 Typical procedure for chain extension of PS–Br 158
7.4 Results and discussion 159
7.4.1 Influence of ligand structure 159
7.4.2 Effect of the deactivator concentration 161
7.4.3 Effect of $Na_2S_2O_4$ concentration 162
7.4.4 St Polymerization 168
7.4.5 Evaluation of chain-end functionality 169
7.5 Conclusions 172
7.6 References 172

Part III 177
Application 177
Chapter 8 179
8.1 Abstract 181
8.2 Introduction 181
8.3 Experimental Section 184
8.3.1 Materials 184
8.3.2 Techniques 185
8.3.3 Procedures 187
8.3.3.1 Synthesis of poly(ethylene glycol) monomethyl ether chloride ($mPEG_{113}$-Cl) 187
8.3.3.2 Synthesis of $mPEG_{113}$-*b*-$P4VP_{124}$ block copolymer 187
8.3.3.3 Synthesis of hydrophilic Fe_3O_4 SPIONs (hSPIONs) 188
8.3.3.4 Self-assembly of mPEG-*b*-P4VP block copolymers 188
8.3.3.5 Self-assembly of mPEG-*b*-P4VP block copolymers in the presence of SPIONs 189
8.4 Results and discussion 189
8.4.1 Synthesis and characterization of mPEG-*b*-P4VP block copolymers 189
8.4.2 Preparation and characterization of mPEG-*b*-P4VP micellar structures 192
8.1.1 Preparation and characterization of SPIONs aggregates based on mPEG-*b*-P4VP self-assembly 195

8.1.2 Relaxometry of self-assembled mPEG-*b*-P4VP and SPIONs as aqueous dispersions 200
8.5 Conclusions 203
8.6 References 203

Part IV 207
Final Remarks 207
Chapter 9 209
9.1 Conclusions 209
9.2 Future work 211

List of figures

Figure 1.1 Bromine-functional initiators typically used in ATRP: α-bromophenylacetate (EBPA), α-bromoisobutyrate (EBIB), methylbromopropionate (MBP), 1-phenyl ethylbromide (PEBr).....10

Figure 1.2 Initiators typically used in ATRP with different chemical groups: 2-hydroxyethyl 2-bromopropanoate (HBP), vinyl cloro acetate (VClAc), 2-bromopropionitrile(BPN), propargyl 2-bromoisobutyrate (PBiB), 2-azidoethyl 2-bromoisobutyrate (Azido-BiB), glycidol 2-bromopropionate (GBP), chloropropionamide (CPA), 2,2-dibromomethyl-1,3-dibromopropane (PeBr4), *p*-toluene sulfonyl chloride (TsCl).....10

Figure 1.3 Nitrogen-based ligands typically used in ATRP: tris(2-pyridylmethyl)amine (TPMA) , tris[2-(dimethylamino)ethyl]amine (Me_6TREN), 2,2'-bipyridine (Bpy) *N,N,N′ ,N′ ′ ,N′ ′* -pentamethyldiethylenetriamine (PMDETA).....11

Figure 1.4 ATRP variation techniques 15

Figure 1.5 Copper-catalysed SET-LRP and SARA-ATRP mechanism.....16

Figure 1.6 Typical ligands successfully used in ATRP miniemulsion: bis(2-pyridylmethyl)octadecylamine (BPMODA)4,4 ′ -Dinonyl-2,2 ′ -dipyridyl (dNbpy), 4,4',4"-tris(5-nonyl)-2,2':6',2"-terpyridine (tNtpy), tris(2-bis(3-(2-ethylhexoxy)-3-oxopropyl)aminoethyl)amine (EHA_6TREN).....26

Figure 1.7 Typical nonionic surfactants used in ATRP miniemulsion: poly(vinyl alcohol) (PVA), polyoxyethylene (20) oleyl ether (Brij 98), polyethylene glycol sorbitan monooleate (Tween 80) 27

Figure 1.8 Typical ionic surfactants: cetrimonium bromide (CTAB) and sodium dodecyl sulfate (SDS).....28

Figure 2.1 Kinetic plots of conversion and $\ln[M]_0/[M]$ *vs*. time (left) and plot of number-average molecular weights (M_n^{SEC}) and $Đ$ *vs*. conversion (right) for the SARA ATRP of MA catalyzed by Cu(0) wire/$CuBr_2$/Me_6TREN in sulfolane (black circle and blue square symbols) or DMSO (red triangle symbols) at 30 °C. Conditions: $[MA]_0$/[solvent] = 2/1 (v/v); $[MA]_0/[EBiB]_0$/Cu(0) wire/$[CuBr_2]$/$[Me_6TREN]_0$ = 222/1/Cu(0) wire/0 or 0.1/1.1 (molar); Cu (0): d = 1 mm, l = 5 cm. 51

Figure 2.2 - Evolution of UV−vis spectra in comproportionation experiments at 30 ºC: (a) Cu(0) wire: l = 5 cm and d = 1 mm, $[CuBr_2]_0$ = 7.50 mM and $[Me_6TREN]_0$ =

82.5 mM in DMSO (2.5 mL); (b) Cu(0) wire: l = 5 cm and d = 1 mm, $[CuBr_2]_0$ = 7.50 mM and $[Me_6TREN]_0$ = 82.5 mM in sulfolane (2.5 mL); (c) Relative amount of $CuBr_2$ reduced during the comproportionation of Cu(0) and $CuBr_2$ in DMSO or sulfolane at 30 ºC. The values were determined by UV-vis spectroscopy. 52

Figure 2.3 – Kinetic plots of conversion and $\ln[M]_0/[M]$ *vs*. time and plot of number-average molecular weights (M_n^{SEC}) and *Đ vs*. conversion for the SARA ATRP of (a) MMA, (b) St and (c) VC using Cu(0) wire as a supplemental activator and reducing agent in sulfolane. Conditions: (a) $[MMA]_0/[EBPA]_0$/Cu(0) wire/ $[CuBr_2]_0/[bpy]_0$ = 222/1/Cu(0) wire/0 (blue circle) or 0.1 (red triangle)/2.2 (molar), $[MMA]_0$/[Sulfolane] = 1/1 (v/v) and T = 40 ºC; (b) $[St]_0/[EBiB]_0$/Cu(0) wire/$[PMDETA]_0$ = 222/1/Cu(0) wire/1.1 (molar), $[St]_0$/[Sulfolane] = 2/1 (v/v) and T = 60 ºC; (c) $[VC]_0/[CHBr_3]_0/$[Cu(0) wire]$_0$/ $[TREN]_0$ = 222/1/ Cu(0) wire/1.1, $[VC]_0$/[Sulfolane] = 1/1and T = 42 ºC; Cu (0): d = 1 mm, l = 5 cm. 54

Figure 2.4 – (a) Kinetic plots of $\ln[M]_0/[M]$ *vs*. time and plot of number-average molecular weights (M_n^{SEC}) and *Đ vs.* conversion for the SARA ATRP of St using Cu(0) wire as supplemental activator and reducing agent in sulfolane at 30 ºC (blue circle symbols), 60 ºC (black square symbols) and 90 ºC (red triangle symbols) . Conditions: $[St]_0$/[sulfolane] = 2/1 (v/v); $[St]_0/[EBiB]_0$/Cu(0)wire /$[PMDETA]_0$ = 222/1/Cu(0) wire/1.1 (molar); Cu (0): d = 1 mm, l = 5 cm. 55

Figure 2.5 – Kinetic plots of conversion and $\ln[M]_0/[M]$ vs. time and plot of number-average molecular weights (M_n^{SEC}) and Đ vs. conversion for the SARA ATRP of St using Cu(0) wire as a supplemental activator and reducing agent in sulfolane. Conditions: $[St]_0/[EBiB]_0$/Cu(0) wire/$[PMDETA]_0$=222/1/Cu(0) wire/1.1 (molar), $[St]_0$/[Sulfolane] = 1/1 (v/v) and T = 60 ºC; Cu (0): d = 1 mm, l = 5 cm. 55

Figure 2.6 Kinetic plots of conversion and $\ln[M]_0/[M]$ *vs.* time and (b) plot of number average molecular weights (M_n^{SEC}) and *Đ vs.* conversion for ATRP of St catalyzed with mixed catalyst system (Fe(0) and $CuBr_2/Me_6TREN$ at 70 ºC and 90 ºC in DMF. Conditions: $[St]_0/[EBiB]_0/[Fe(0)]_0/[CuBr_2]_0/$[ligand] = 125/1/1/0.1/1.1 (molar); $[St]_0$/[DMF] = 2/1 (v/v) and T = 70 ºC (circle black); $[St]_0$/[DMF] = 2/1 (v/v) and T = 90ºC (triangle red); $[St]_0$/[DMF] = 1/1 (v/v) and T = 70 ºC (square blue).....56

Figure 2.7 - ^{1}H NMR spectrum of PMA-Br (M_n^{SEC} = 15.9 x 10^3; *Đ* =1.08) in $CDCl_3$. 57

Figure 2.8 - ^{1}H NMR spectrum of PMMA-Br (M_n^{SEC} = 52500; *Đ* =1.46) in $CDCl_3$. ...58

Figure 2.9 - ^{1}H NMR spectrum of PS-Br (M_n^{SEC} = 24.7 x 10^3; $Đ$ = 1.24) in $CDCl_3$. ...59
Figure 2.10 - The ^{1}H NMR spectrum of Br-PVC-Br (M_n^{SEC} = 9100; $Đ$ = 1.55) in THF-d_8. ...59
Figure 2.11 - a) MALDI-TOF-MS in the linear mode (using HABA as matrix) of PMA-Br (M_n^{SEC} = 15900, $Đ$ = 1.08); b) Enlargement of the MALDI-TOF-MS from m/z 15250 to 15850 of PMA-Br ...60
Figure 2.12 - a) MALDI-TOF-MS in the linear mode (using HABA as matrix) of Br-PVC-Br (M_n^{SEC} = 9100, $Đ$ = 1.55); b) Enlargement of the MALDI-TOF-MS from m/z 2750 to 3200 of Br-PVC-Br 61
Figure 2.13 - Displacement of the SEC trace (RI signal) of a –Br-terminated (a) PMA (b) PMMA and (c) PS obtained by SARA ATRP (black line), towards high molecular weight values after a chain-extension experiment (blue line). Conditions: $[MA]_0$/[solvent] = 2/1 (v/v); $[MA]_0/[EBiB]_0$/Cu(0) wire /$[Me_6TREN]_0$= 222/1/ Cu(0) wire /1.1 (molar); $[MMA]_0$/[solvent] = 2/1 $[MMA]_0/[EBPA]_0$/Cu(0)wire/$[PMDETA]_0$ = 222/1/Cu(0) wire/1.1 (molar); $[St]_0$/[solvent] = 2/1 (v/v); $[St]_0/[EBiB]_0$/Cu(0) wire/$[PMDETA]_0$ = 222/1/Cu(0) wire/1.1 (molar); Cu (0): d = 1 mm, l = 5 cm. ...62
Figure 2.14 – (a) SEC traces of the Br-PVC-Br (conv.$_{VC}$ = 48.4%, M_n^{th} = 5500, M_n^{SEC} = 9100, $Đ$ = 1.55) macroinitiator (black line), and the PMA-*b*-PVC-*b*-PMA (conv.$_{MA}$ = 86.5%, M_n^{th} = 53800, M_n^{SEC} = 59400, $Đ$ = 1.87) (blue line) and PS-*b*-PVC-*b*-PS (conv.$_{St}$ = 57.5%, M_n^{th} = 45000, M_n^{SEC} = 63300, $Đ$ = 2.34) block copolymers (red line). (b) SEC traces of the Br-PVC-Br (conv.$_{VC}$ = 62.2%, M_n^{th} = 3000, M_n^{SEC} = 3900, $Đ$ = 1.69) macroinitiator (black line), and the PMA-*b*-PVC-*b*-PMA (conv.$_{MA}$ = 85.7%, M_n^{th} = 17800, M_n^{SEC} = 18300, $Đ$ = 1.83) block copolymer (blue line) prepared by “one-pot” SARA ATRP chain extension. ...62
Figure 2.15 - The ^{1}H NMR spectrum of PMA-*b*-PVC-*b*-PMA block copolymer (M_n^{SEC} = 59400; $Đ$ = 1.87) in THF- d_8. ...63
Figure 2.16 - ^{1}H NMR spectrum of PS-*b*-PVC-*b*-PS block copolymer (M_n^{SEC} = 63300; $Đ$ = 2.34) in THF-d_8. ...64
Figure 3.1 - Kinetic plots of (a) $\ln[M]_0/[M]$ *vs*. time and plot of number-average molecular weights (M_n^{SEC}) and $Đ$ *vs.* conversion for the SARA ATRP of MA using Cu(0) wire as supplemental activator and reducing agent in different sulfolane/water mixtures at 30 ºC. Conditions: $[MA]_0$/[solvent] = 2/1 (v/v);

$[MA]_0/[EBiB]_0/Cu(0)wire /[Me_6TREN]_0$ = 222/1/Cu(0) wire/1.1 (molar); Cu (0): d = 1 mm, l = 5 cm. 78

Figure 3.2 Kinetic plots of conversion and $\ln[M]_0/[M]$ *vs*. time and plot of number-average molecular weights (M_n^{SEC}) and $Đ$ (M_w/M_n) *vs*. conversion for the SARA ATRP of (a) MA, (b) MMA, (c) St and (d) VC using Cu(0) wire as the SARA agent in solvent sulfolane/water = 90/10 (v/v). Conditions: (a) $[MA]_0/[EBiB]_0/Cu(0)wire/[Me_6TREN]_0$ = 222/1/Cu(0) wire/1.1 (molar), $[MA]_0/[Solvent]$ = 2/1 (v/v) and T = 30 °C; (b) $[MMA]_0/[EBPA]_0/Cu(0)$ wire/ $[CuBr_2]_0/[bpy]_0$ = 222/1/Cu(0) wire/0.1/2.2 (molar), $[MMA]_0/[Solvent]$ = 1/1 (v/v) and T = 40 °C; (c) $[St]_0/[EBiB]_0/Cu(0)$ wire/$[PMDETA]_0$ = 222/1/Cu(0) wire/1.1 (molar), $[St]_0/[Solvent]$ = 2/1 (v/v) and T = 60 °C; (d) $[VC]_0/[CHBr_3]_0/[Cu(0)\ wire]_0/[TREN]_0$ = 222/1/ Cu(0) wire/1, $[VC]_0/[Solvent]$ = 1/1 and T = 42 °C; Cu (0): d = 1 mm, l = 5 cm.....79

Figure 3.3 – SEC chromatograms of a α,ω-di(bromo)PVC ($conv._{VC}$ = 47.3 %, M_n^{th} = 3.8 x 10^3, M_n^{SEC} = 7.8 x 10^3, $Đ$ = 1.69) macroinitiator (black line) and PMA-b-PVC-b-PMA triblock copolymer ($conv._{MA}$ = 84.3%, M_n^{th} = 56.4 x 10^3, M_n^{SEC} = 36.3 x 10^3, $Đ$ = 1.48) (blue line), after "one-pot" chain extension by SARA ATRP in sulfolane/water = 90/10 (v/v). 81

Figure 3.4 - ^{1}H NMR spectrum (solvent: THF-d_8) of a Br-PVC-Br (M_n^{SEC} = 7.8 x 10^3 ; $Đ$ = 1.69) sample obtained by SARA ATRP.....82

Figure 3.5^{1}H NMR spectrum (solvent: THF-d_8) of a purified PMA-*b*-PVC-*b*-PMA (M_n^{SEC} = 36.3 x 10^3, $Đ$ = 1.48) triblock copolymer obtained by "one-pot" SARA ATRP in sulfolane/water = 90/10 (v/v). 82

Figure 4.1 Kinetic plots of conversion and $\ln[M]_0/[M]$ *vs*. time and plots of number average molecular weights (M_n^{SEC}) and $Đ$ *vs*. conversion for the SARA ATRP of MA catalyzed by $Na_2S_2O_4/CuBr_2//Me_6TREN$ in [BMIM]-[PF_6]/DMSO = 5/95 (circle, black) and [BMIM]-[PF_6]/DMSO = 50/50 (triangle, red). Conditions: $[MA]_0/[solvent]$ = 2/1(v/v); $[MA]_0/[EBiB]_0/[Na_2S_2O_4]_0/[CuBr_2]_0/[Me_6TREN]_0$ = 222/1/1/0.1/0.1 (molar); T = 30 °C.....92

Figure 4.2 Chromatograms of PS standards (red and blue lines) and PMA samples (black lines) collected during the SARA ATRP of MA catalyzed by $Na_2S_2O_4/CuBr_2/Me_6TREN$ in [BMIM]-[PF_6]/DMSO = 50/50. Conditions: $[MA]_0/[solvent]$ = 2/1 (v/v); $[MA]_0/[EBiB]_0/[Na_2S_2O_4]_0/[CuBr_2]_0/[Me_6TREN]_0$ = 222/1/1/0.1/0.1 (molar); T = 30 °C.....93

Figure 4.3 Kinetic plots of conversion and $\ln[M]_0/[M]$ *vs*. time and plots of number average molecular weights M_n^{SEC} and *Đ vs*. conversion for the SARA ATRP of MA catalyzed by $Na_2S_2O_4/CuBr_2/Me_6TREN$ in [BMIM]-[PF_6]/DMSO = 95/5 (circle, black), [BMIM]-[PF_6]/DMSO = 75/25 (triangle, red) and [BMIM]-[PF_6]/DMSO = 25/75 (square, blue). Conditions: $[MA]_0/[solvent]$ = 2/1 (v/v); $[MA]_0/[EBiB]_0/[Na_2S_2O_4]_0/[CuBr_2]_0/[Me_6TREN]_0$ = 222/1/1/0.1/0.1 (molar); T = 30 °C. 93

Figure 4.4 k_p^{app} values of the SARA ATRP of MA catalyzed by $Na_2S_2O_4/CuBr_2/Me_6TREN$ in [BMIM]-[PF_6]/DMSO mixtures, for different contents of [BMIM]-[PF_6] in the reaction mixture. Conditions: $[MA]_0/[solvent]$ = 2/1 (v/v); $[MA]_0/[EBiB]_0/[Na_2S_2O_4]_0/[CuBr_2]_0/[Me_6TREN]_0$ = 222/1/1/0.1/0.1 (molar); T = 30 °C 94

Figure 4.5 (a) UV-Vis spectra in different [BMIM]-[PF_6]/DMSO mixtures with Reichardt's dye 30 (50 μM); (b) Experimental $E_T(30)$ value in different [BMIM]-[PF_6]/DMSO mixtures (the dashed line represents the predicted $E_T(30)$). 95

Figure 4.6 Kinetic plots of conversion and $\ln[M]_0/[M]$ *vs*. time and plots of number average molecular weights (M_n^{SEC}) and *Đ vs*. conversion for the SARA ATRP of MA catalyzed by $Na_2S_2O_4$/TBA-$PF_6/CuBr_2/Me_6TREN$ in DMSO. Conditions: $[MA]_0/[solvent]$ = 2/1 (v/v); $[MA]_0/[EBiB]_0/[Na_2S_2O_4]_0/[TBA\text{-}PF_6]_0/[CuBr_2]_0/[Me_6TREN]_0$ = 222/1/1/3/0.1/0.1 (molar); T = 30 °C. 95

Figure 4.7 Kinetic plots of conversion and $\ln[M]_0/[M]$ *vs*. time and plots of number average molecular weights (M_n^{SEC}) and *Đ vs*. conversion for the SARA ATRP of MA catalyzed by $Na_2S_2O_4/CuBr_2/Me_6TREN$ in [BMIM]-[PF_6]/DMSO = 50/50 (v/v) for different targeted DP values: (a) DP = 100; (b) DP = 222; (c) DP = 1100. Conditions: $[MA]_0/[solvent]$ = 2/1 (v/v); $[MA]_0/[EBiB]_0/[Na_2S_2O_4]_0/[CuBr_2]_0/[Me_6TREN]_0$ = DP/1/1/0.1/0.1 (molar); T = 30 °C. 96

Figure 4.8 Kinetic plots of conversion and $\ln[M]_0/[M]$ *vs*. time and plots of number average molecular weights (M_n^{SEC}) and *Đ vs*. conversion for the SARA ATRP of MA initiated by a four-arm initiator and catalyzed by $Na_2S_2O_4/CuBr_2/Me_6TREN$, in [BMIM-$PF_6$]/DMSO = 50/50 (v/v) for a targeted DP of 400. Conditions: $[MA]_0/[solvent]$ = 2/1 (v/v); $[MA]_0/[4f\text{-}BiB]_0/[Na_2S_2O_4]_0/[CuBr_2]_0/[Me_6TREN]_0$ = 400/1/1/0.4/0.4 (molar); T = 30 °C. 96

Figure 4.9 Chromatograms of PS standards (red and blue lines) and star-shaped PMA samples (black lines) collected during the SARA ATRP of MA catalyzed by

$Na_2S_2O_4$/$CuBr_2$/Me_6TREN in [BMIM]-[FPF_6]/DMSO = 50/50 (v/v). Conditions: $[MA]_0$/[solvent] = 2/1 (v/v); $[MA]_0$/$[4f\text{-}BiB]_0$/$[Na_2S_2O_4]_0$/$[CuBr_2]_0$/$[Me_6TREN]_0$ = 400/1/1/0.4/0.4 (molar); T = 30 °C 97

Figure 4.10 Viscosity as a function of the amount of [BMIM]-[PF_6] in the [BMIM]-[PF_6]/DMSO solvent mixture. 99

Figure 4.11 UV-Vis spectra of reduction of $CuBr_2$/Me_6TREN by $Na_2S_2O_4$ in a) pure DMSO, b) [BMIM]-[PF_6]/DMSO (25/75) and c) [BMIM]-[PF_6]/DMSO (50/50) at 30 °C. 99

Figure 4.12 Chromatograms of the PMA before (black curve) and after the chain extension (blue curve) experiment. 100

Figure 4.13 a) MALDI-TOF-MS in the linear mode (using HABA as matrix) of PMA-Br (M_n^{SEC} = 6.9 x 10^3, $Đ$ = 1.05) obtained by SARA ATRP of MA catalyzed by $Na_2S_2O_4$/$CuBr_2$/Me_6TREN, in [BMIM]-[PF_6]/DMSO = 50/50 (v/v). b) Enlargement of the MALDI-TOF-MS from m/z 6450 to 7050. Conditions: $[MA]_0$/[solvent] = 2/1 (v/v); $[MA]_0$/$[EBiB]_0$/$[Na_2S_2O_4]_0$/$[CuBr_2]_0$/$[Me_6TREN]_0$ = 222/1/1/0.1/0.1 (molar); T = 30 °C. 100

Figure 4.14 ^{1}H NMR spectrum, in $CDCl_3$, of PMA-Br obtained at high conversion ($M_{n,GPC}$ = 6900, Đ = 1.05, $M_{n,NMR}$ = 6600; active chain-end functionality = 92%). The PMA is atactic: [dr] = [dm] = 0.5. 101

Figure 5.1 Kinetic plots of $ln[M]_0/[M]$ *vs*. time and plot of number-average molecular weights (M_n^{SEC}) and $Đ$ (M_w/M_n) *vs.* conversion for the SARA ATRP of MA using Cu(0) wire as supplemental activator and reducing agent in DMSO (blue symbols) or sulfolane (green symbols)/ [BMIM]-[PF_6] mixtures at 30 ºC. Conditions: $[MA]_0$/[solvent mixture] = 2/1 (v/v); $[MA]_0$/$[EBiB]_0$/Cu(0)wire/ $[CuBr_2]$/$[Me_6TREN]_0$ = 222/1/Cu(0) wire/0.1/1.1 (molar); Cu (0): d = 1 mm, l = 5 cm. 114

Figure 5.2 k_p^{app} values for SARA ATRP of MA catalyzed by Cu(0)/$CuBr_2$/Me_6TREN in sulfolane/[BMIM[-[PF_6] (green symbols) and DMSO/[BMIM]-[PF_6] (blue symbols) mixtures.....114

Figure 5.3 Experimental $E_T(30)$ value in different [BMIM]-[PF_6]/sulfolane mixtures (the dashed line represents the predicted $E_T(30)$). 115

Figure 5.4 Percentage of $CuBr_2$ reduced during the comproportionation of Cu(0) and $CuBr_2$ in DMSO/[BMIM]-[PF_6] or sulfolane/[BMIM]-[PF_6] at 30 ºC. The values were determined by UV-vis spectroscopy. 116

Figure 5.5 Kinetic plots of $\ln[M]_0/[M]$ *vs*. time and plot of number-average molecular weights (M_n^{SEC}) and $Đ$ (M_w/M_n) *vs*. conversion for the SARA ATRP of MMA using Cu(0) wire as supplemental activator and reducing agent in sulfolane/[BMIM]-[PF_6]=75/25(v/v) mixture at 40 ºC. Conditions: $[MMA]_0$/[solvent mixture] = 1/1 (v/v); $[MMA]_0/[EBPA]_0$/Cu(0)wire/ $[CuBr_2]/[bpy]_0$ = 222/1/Cu(0) wire/0.1/2.2 (molar); Cu (0): d = 1 mm, l = 5 cm. 119

Figure 5.6 ^{1}H NMR spectrum of purified PMA-Br (M_n^{SEC} = 16.0 x 10^3; $Đ$ =1.06) in $CDCl_3$. Reaction conditions: $[MA]_0/[EBiB]_0/[Cu(0)\ wire]_0/[CuBr_2]_0/[Me_6TREN]_0$ =222/1/Cu(0) wire/0.1/1.1 (molar); $[MA]_0$/[solvent mixture]= 2/1 (v/v), sulfolane/[BMIM]-[PF_6]=75/25 (v/v), T = 30 ºC. 119

Figure 5.7 ^{1}H NMR spectrum of PMMA-Br (M_n^{SEC} = 24.7 x 10^3; $Đ$ =1.02) in $CDCl_3$. 120

Figure 5.8 ^{1}H NMR spectrum of PS-Br (M_n^{SEC} =39.5 x 10^3; $Đ$ =1.33) in $CDCl_3$.....121

Figure 5.9 The ^{1}H NMR spectrum of Br-PVC-Br (M_n^{SEC} = 9100; $Đ$ = 1.55) in THF-d_8. 121

Figure 5.10 Displacement of the SEC trace (RI signal) of a –Br-terminated PMA, obtained by SARA ATRP (black line), towards high molecular weight values after a chain-extension experiment (blue line) using the solvent mixture sulfolane/[BMIM]-[PF_6]= 75/25 (v/v). Conditions: $[MA]_0$/[solvent mixture] = 1/1 (v/v); $[MA]_0/[PMA\text{-}Br]_0$/Cu(0) wire/$[Me_6TREN]_0$= 550/1/ Cu(0) wire/1.1 (molar); Cu (0): d = 1 mm, l = 5 cm. 122

Figure 6.1 Chemical structure of cyclopentyl methyl ether and some of its "green" aspects. 131

Figure 6.2 Kinetic plots of conversion and $\ln[M]_0/[M]$ *vs*. time (triangle) and plot of number-average molecular weights (M_n^{SEC}) and $Đ$ *vs*. monomer conversion (circle) for the SARA ATRP of MA in CPME/DMSO = 70/30 (v/v) at 30 °C. Reaction conditions: $[MA]_0$/[solvent] = 2/1 (v/v); $[MA]_0/[EBiB]_0$/Cu(0)/ $[CuBr_2]_0/[Me_6TREN]_0$= 222/1/Cu(0) wire/0.1/1.1. 138

Figure 6.3 Kinetic plots of conversion and $\ln[M]_0/[M]$ *vs*. time (triangle) and plot of number-average molecular weights (M_n^{SEC}) and $Đ$ *vs*. monomer conversion (circle) for the SARA ATRP of MA in CPME/EtOH/H_2O = 70/28/2 (v/v/v) at 30 °C. Reaction conditions: $[MA]_0$/[solvent] = 2/1 (v/v); $[MA]_0/[EBiB]_0$/Cu(0)/ $[CuBr_2]_0/[Me_6TREN]_0$= 222/1/Cu(0) wire/0.1/1.1. 138

Figure 6.4 ^{1}H NMR spectrum of a PMA sample (M_n^{SEC} = 10 600 ; $Đ$ = 1.28) obtained by SARA ATRP in CPME/EtOH/H_2O = 70/28/2 (v/v/v) at 30 °C. 139

Figure 6.5 Enlargement of the MALDI-TOF-MS from m/z 8800 to 9400 in the linear mode (using HABA as matrix) of PMA-Br (M_n^{SEC} = 10600, $Đ$ =1.28). 139

Figure 6.6 Kinetic plots of conversion and ln$[M]_0$/[M] *vs.* time (triangle) and plot of number-average molecular weights (M_n^{SEC}) and $Đ$ *vs.* monomer conversion (circle) for the SARA ATRP of MA in CPME/EtOH/H_2O = 70/28/2 (v/v/v) at 30 °C, using different SARA agents. Reaction conditions: $[MA]_0$/[solvent] = 2/1 (v/v); $[MA]_0$/$[EBiB]_0$/SARA agent/$[CuBr_2]_0$/$[Me_6TREN]_0$= 222/1/Cu(0) wire (blue) or Fe(0) powder (green)/0.1/1.1. 140

Figure 6.7 Kinetic plots of conversion and ln$[M]_0$/[M] *vs.* time (triangle) and plot of number-average molecular weights (M_n^{SEC}) and $Đ$ *vs.* monomer conversion (cirdcle) for the SARA ATRP of MA in CPME/EtOH/H_2O = 70/28/2 (v/v/v) at 30 °C, for different targeted DP values. Reaction conditions: $[MA]_0$/[solvent] = 2/1 (v/v); $[MA]_0$/$[EBiB]_0$/Cu(0)/$[CuBr_2]_0$/$[Me_6TREN]_0$= DP/Cu(0) wire/0.1/1.1. ...141

Figure 6.8 Kinetic plots of conversion and ln$[M]_0$/[M] *vs.* time (triangle) and plot of number-average molecular weights (M_n^{SEC}) and $Đ$ *vs.* monomer conversion (circle) for the SARA ATRP of St in CPME/DMF = 70/30 (v/v) at 60 °C. Reaction conditions: $[St]_0$/[solvent] = 2/1 (v/v); $[St]_0$/$[EBiB]_0$/Cu(0)/ $[CuBr_2]_0$/$[PMDETA]_0$= 222/1/Cu(0) wire/0.1/1.1 142

Figure 6.9 ^{1}H NMR spectrum of a PS sample ($M_n^{|SEC}$ = 3800 ; $Đ$ =1.14; conversion = 27 %; functionality = 90 %) obtained by SARA ATRP; solvent: $CDCl_3$ 143

Figure 6.10 SEC chromatograms of a PS-Br macroinitiator (black line) and self-extended PS (blue line) by SARA ATRP. 143

Figure 6.11 ^{1}H NMR spectrum of a PGMA sample (M_n^{SEC} = 46600; $Đ$ = 1.39) obtained by SARA ATRP; solvent: $CDCl_3$ 144

Figure 6.12 ^{1}H NMR spectrum of a PVC sample (M_n^{SEC} = 6100; $Đ$ =1.57) obtained by SARA ATRP; solvent: d_8-THF. 145

Figure 6.13 SEC chromatograms of a α,ω-di(bromo)PVC (conv.$_{VC}$ = 61.8%, M_n^{th} = 5000, M_n^{SEC} = 6100, $Đ$ = 1.57) macroinitiator (black line) and PMA-*b*-PVC-*b*-PMA (conv.$_{MA}$ = 77.3%, M_n^{th} = 39400, M_n^{SEC} = 40700, $Đ$ = 1.49) triblock copolymer (blue line), after "one-pot" chain extension by SARA ATRP in CPME/DMSO = 70/30 (v/v).....145

Figure 6.14 ^{1}H NMR of a purified PMA-*b*-PVC-*b*-PMA (M_n^{SEC} = 40700, $Đ$ = 1.49) triblock copolymer obtained by "one-pot" SARA ATRP in CPME/DMSO = 70/30 (v/v); solvent: d_8-THF. 146

Figure 7.1 Structure of bis(2-pyridylmethyl) octadecylamine (BPMODA) and bis[2-(4-methoxy-3,5-dimethyl)pyridylmethyl]octadecylamine (BPMODA*) ligands. 159

Figure 7.2 Kinetic plots of conversion and $\ln[M]_0/[M]$ *vs*. time (left) and plot of number-average molecular weights (M_n^{SEC}) and $Đ$ *vs*. conversion (right) for ATRP of *n*BA in miniemulsion catalyzed by $Na_2S_2O_4$ in the presence of EHA_6TREN (triangle red symbols) or BPMODA* (round blue symbols) at 80 °C. Conditions: $[Brij98]_0/[Hexadecane]_0$ = 2.3/3.6 % *vs* *n*BA; $[n\text{BA}]_0/[EBiB]_0/[CuBr_2]_0/[ligand]/[Na_2S_2O_4]_0$ = 200/1/0.4/0.4/0.2 (mol). 160

Figure 7.3 Kinetic plots of conversion and $\ln[M]_0/[M]$ *vs*. time (left) and plot of number-average molecular weights (M_n^{SEC}) and $Đ$ *vs*. conversion (right) for ATRP of *n*BA in miniemulsion catalyzed by AA in the presence of EHA_6TREN (triangle red symbols) or BPMODA* (round blue symbols) at 80 °C. Conditions: $[Brij98]_0/[Hexadecane]_0$=2.3/3.6 % *vs* *n*BA; $[n\text{BA}]_0/[EBiB]_0/[AA]/[CuBr_2]/[EHA_6TREN]_0$=200/1/0.2/0.4/0.4 (mol) and $[n\text{BA}]_0/[EBiB]_0/[AA]/[CuBr_2]/[BPMODA^*]_0$ = 200/1/0.2/0.4/0.4 (mol). 161

Figure 7.4 Kinetic plots of conversion and $\ln[M]_0/[M]$ *vs*. time (left) and plot of number-average molecular weights (M_n^{SEC}) and $Đ$ *vs*. conversion (right) for ATRP of *n*BA in miniemulsion catalysed by $Na_2S_2O_4/CuBr_2/BPMODA^*$ with $CuBr_2/BPMODA^*$ = 0.4/0.4 (round blue symbols) or 1/1 (triangle red symbols) at 80 °C. Conditions: $[Brij98]_0/[Hexadecane]_0$ = 2.3/3.6 % *vs* *n*BA; $[n\text{BA}]_0/[EBiB]_0/[CuBr_2]/[BPMODA^*]_0/[Na_2S_2O_4]$ = 200/1/1/1/0.127 (mol) or $[n\text{BA}]_0/[EBiB]_0/[CuBr_2]_0/[BPMODA^*]_0/[Na_2S_2O_4]_0$ = 200/1/0.4/0.4/0.127 (mol). 162

Figure 7.6 Kinetic plots of conversion and $\ln[M]_0/[M]$ *vs*. time (left) and plot of number-average molecular weights (M_n^{SEC}) and $Đ$ *vs*. conversion (right) for ATRP of *n*BA in miniemulsion catalysed by $Na_2S_2O_4/CuBr_2/BPMODA^*$ with $[Na_2S_2O_4]$= 0.127 (blue symbols) or $[Na_2S_2O_4]$= 0.244 (red symbols) at 80 °C. Conditions: $[Brij98]_0/[Hexadecane]_0$ = 2.3/3.6 % *vs* *n*BA; $[n\text{BA}]_0/[EBiB]_0/[CuBr_2]_0/[BPMODA^*]_0/[Na_2S_2O_4]_0/$ = 200/1/1/1/(0.127 or 0.244) (mol). 163

Figure 7.7 Kinetic plots of conversion and $\ln[M]_0/[M]$ *vs*. time (left) and plot of number-average molecular weights (M_n^{SEC}) and *Đ* (M_w/M_n) *vs*. conversion (right) for ATRP of *n*BA in miniemulsion catalyzed by $Na_2S_2O_4$/$CuBr_2$/BPMODA* = 0.12/1/1 at 80 °C with successive addition of $Na_2S_2O_4$ (blue symbols). Conditions: [Brij*98*]$_0$/[Hexadecane]$_0$ = 2.3/3.6 % vs *n*BA; [*n*BA]$_0$/[EBiB]$_0$/ [$CuBr_2$]$_0$/[BPMODA*]$_0$/[$Na_2S_2O_4$]$_0$ = 200/1/1/1/ 0.12 (mol). 164

Figure 7.8 Kinetic plots of conversion and $\ln[M]_0/[M]$ *vs*. time (left) and plot of number-average molecular weights (M_n^{SEC}) and *Đ vs*. conversion (right) for ATRP of *n*BA in miniemulsion catalyzed by $Na_2S_2O_4$ at 80 °C. Conditions: [Brij*98*]$_0$/[Hexadecane]$_0$ = 2.3/3.6 % vs *n*BA; [*n*BA]$_0$/[EBiB]$_0$/[$CuBr_2$]$_0$/[BPMODA*]$_0$/[$Na_2S_2O_4$]$_0$ = 200/1/0.4/0.4/0.2(mol). 400 µl of an aqueous solution of $Na_2S_2O_4$ (57 mM) was injected into the reaction medium using a syringe pump at a rate of 1 µL.min^{-1}.....164

Figure 7.9 Kinetic plots of conversion and $\ln[M]_0/[M]$ *vs*. time (left) and plot of number-average molecular weights (M_n^{SEC}) and *Đ vs*. conversion (right) for ATRP of *n*BA in miniemulsion catalyzed by $Na_2S_2O_4$ at 80 °C in the presence of PTC. Conditions: [Brij*98*]$_0$/[Hexadecane]$_0$ = 2.3/3.6 % *vs n*BA; [*n*BA]$_0$/[EBiB]$_0$/ [$CuBr_2$]$_0$/[BPMODA*]$_0$/[$Na_2S_2O_4$]$_0$/[PTC]$_0$ = 200/1/0.4/0.4/0.2 /0.7 (mol).....166

Figure 7.10 Kinetic plots of conversion and $\ln[M]_0/[M]$ *vs*. time (left) and plot of number-average molecular weights (M_n^{SEC}) and *Đ vs*. conversion (right) for ATRP of *n*BA in miniemulsion catalyzed by $Na_2S_2O_4$ at 80 °C. Conditions: [SDS]$_0$/[Hexadecane]$_0$ = 2.3/3.6 % *vs n*BA; [*n*BA]$_0$/[EBiB]$_0$/[$CuBr_2$]$_0$/[BPMODA*]$_0$/[$Na_2S_2O_4$]$_0$ = 200/1/0.4/0.4/0.2(mol).167

Figure 7.11 Kinetic plots of conversion and $\ln[M]_0/[M]$ *vs*. time (left) and plot of number-average molecular weights (M_n^{SEC}) and *Đ vs*. conversion (right) for ATRP of *n*BA in miniemulsion catalyzed by 6-o-palmitoyl-l-ascorbic acid (dissolved in ethanol) at 80 °C. Conditions: [Brij*98*]$_0$/[Hexadecane]$_0$ = 2.3/3.6 % *vs n*BA; [*n*BA]$_0$/[EBiB]$_0$/[$CuBr_2$]$_0$/[BPMODA*]$_0$[AA_{org}]$_0$/ = 200/1/0.4/0.4/0.2 (mol). 167

Figure 7.12 Chromatograms of PS standard (red and blue lines) and PS sample obtained by ATRP of St in miniemulsion (black lines) catalysed by $Na_2S_2O_4$/$CuBr_2$/BPMODA* = 0.2/0.4/0.4. Conditions: [Brij*98*]$_0$/ [Hexadecane]$_0$ = 2.3/3.6 % vs St [St]$_0$/[EBiB]$_0$/[$Na_2S_2O_4$]$_0$/[$CuBr_2$]$_0$/[BPMODA*]$_0$ = 200/1/0.2 /0.4/0.4 (mol); T = 80 °C. 168

Figure 7.13 ^{1}H NMR spectrum of P*n*BA-Br (M_n^{SEC} = 5.0 x 10^3; $Đ$ = 1.2) in $CDCl_3$. 169

Figure 7.14 ^{1}H NMR spectrum of PS-Br (M_n^{SEC} = 4.78 x 10^3; $Đ$ =1.11) in $CDCl_3$. ...169

Figure 7.15 - Movement of the SEC trace (RI signal) of a –Br-terminated P*n*Ba, obtained by ATRP in miniemulsion (left, red line), towards high molecular weight values after a chain-extension experiment (right, blue line). Conditions of miniemulsion experiment: [Brij*98*]$_0$/[Hexadecane]$_0$ = 2.3/3.6 % vs *n*Ba; [*n*Ba]$_0$/[EBiB]$_0$/[$Na_2S_2O_4$]/[Cu(II)Br_2]/[BPMODA*]$_0$ = 200/1/0.2/0.4/0.4 (mol); T=80 ºC. Condition of chain-extension experiment : [*n*BA]$_0$/[EtOH] = 1/1 (v/v); [*n*BA]$_0$/[P*n*BA-Br]$_0$/[Cu(0)]$_0$/[Cu(II)Br_2]$_0$/[Me_6TREN]$_0$=600/1/ Cu(0) wire/0.5/1 (mol); T = 30 ºC.....171

Figure 7.16 Movement of the SEC trace (RI signal) of a –Br-terminated PS, obtained by ATRP in miniemulsion (left, blue line), towards high molecular weight values after a chain-extension experiment (right, red line). Conditions: [Brij*98*]$_0$/[Hexadecane]$_0$ = 2.3/3.6 % vs St; [St]$_0$/[EBiB]$_0$/[$Na_2S_2O_4$]/[$CuBr_2$]/[BPMODA*]$_0$ = 200/1/0.1/1/1 (mol); T=80 ºC. Condition of chain-extension experiment : [St]$_0$/[DMF] = 1/1 (v/v); [St]$_0$/[EBiB]$_0$/[Fe(0)]$_0$/[$CuBr_2$]$_0$/[Me_6TREN]$_0$= 350/1/1/0.1/1.1 (mol); T = 70 ºC.....171

Figure 8.1 SEC traces (RI signal) of a mPEG-*b*-P4VP block copolymers obtained by SARA ATRP with : (a) $mPEG_{45}$-Cl and (b) $mPEG_{113}$-Cl macroinitiators.....190

Figure 8.2 - ^{1}H NMR spectrum of $mPEG_{45}$-*b*-$P4VP_{56}$-Cl block copolymer. Their chemical structure and the proton identification scheme adopted for the NMR spectral assignments are also indicated. 191

Figure 8.3 $mPEG_{113}$-*b*-$P4VP_{40}$ kinetic plots of conversion and ln[M]$_0$/[M] *vs*. time (left) and plot of number-average molecular weights (M_n^{SEC}) and $Đ$ *vs*. conversion (right) for ATRP of 4VP catalyzed by $CuCl_2$/Me_6TREN in isopropanol at 40 °C. Conditions: [4VP]$_0$/ [IPA]= 1/1 (v/v); [4VP]$_0$/[PEG_{113}-Cl]$_0$ /[$CuCl_2$]$_0$/[Me_6TREN] = 100/1/1/1 (molar).....191

Figure 8.4 Representation of mPEG-*b*-P4VP self-assembly in aqueous media via titration and solvent exchange methods.....192

Figure 8.5 Particle size distribution in intensity determined by DLS for $mPEG_{113}$-*b*-$P4VP_{40}$ at different pH conditions. 193

Figure 8.6 Hydrodynamic diameter (D_h) of $mPEG_{113}$-b-$P4VP_{78}$ self-assembled in the presence of Hydrophilic SPIONs (hSPIONs) measured at different pH values using the titration method. 194

Figure 8.7 TEM images of self-assembled block copolymers of (a) $mPEG_{113}$-*b*-$P4VP_{40}$ obtained by titration method and (b) at $mPEG_{45}$-*b*-$P4VP_{96}$ prepared by solvent exchange. 195

Figure 8.8 Schematic representation of the self-assembly of mPEG-*b*-P4VP in the presence of Fe_3O_4-based SPIONs, via titration and via solvent exchange methods. 196

Figure 8.9 TEM micrographs of self-assembled block copolymers with hSPIONs prepared with (a, c) $mPEG_{113}$-*b*-$P4VP_{40}$ by titration and (b, d) $mPEG_{45}$-*b*-$P4VP_{32}$ by solvent exchange. (a) and (b) micrographs were taken at Mag. x60,000 and highlight the presence of the nanoaggregates (black circles), whereas (c) and (d) micrographs were taken at Mag. x200,000.....197

Figure 8.10 Particle size distributions, determined by DLS, for mPEG-*b*-P4VP block copolymers that were self-assembled in the presence of OaSPIONs. The block copolymers were based on (a) $mPEG_{45}$ and (b) $mPEG_{113}$ respectively as the steric stabilizer.....198

Figure 8.11 TEM micrographs of SPIONs aggregates, prepared with oleic acid-coated SPIONs nanoaggregates based on the self-assembly of $mPEG_{45}$-*b*-$P4VP_{32}$: (a) was taken at a Mag. x60,000 and (b) at Mag. x300,000.....199

Figure 8.12 The paramagnetic contribution to the water proton relaxation rates (20 MHz, 25ºC) (a) for T_1 and (b) for T_2 relaxation rates (represented, respectively, as $r_{1,p}$ and $r_{2,p}$ in s^{-1}) as a function of iron concentration (in mM) for hSPION-loaded-$mPEG_{45}$-*b*-$P4VP_{32}$ and $mPEG_{113}$-*b*-$P4VP_{78}$ micelles, prepared, respectively, by the titration (Tit) and solvent exchange (SE) methods. 200

Figure 8.13 Comparison of aqueous dispersions of hSPIONs-loaded $mPEG_{45}$-*b*-$P4VP_{32}$ micelles (a) before, (b) during, and (c) after being subjected to an external magnetic field. 202

List of schemes

Scheme 1.1 General scheme for RDRP mechanism. 5
Scheme 1.2 General ATRP mechanism. 8
Scheme 3.1 General scheme mechanism of the Cu(0)/CuX_2/L-catalyzed SARA ATRP (L: ligand and X: halide). 72
Scheme 4.1 General mechanism of ATRP 87
Scheme 6.1 General mechanism of the Cu(0)/CuX_2/L-catalyzed SARA ATRP (L: ligand and X: halide). 130

List of tables

Table 1.1 SET-LRP and SARA ATRP - differences and similarities[46, 50] 17

Table 1.2 The differences between the heterogeneous polymerization systems[67-68] ...21

Table 2.1 Kinetic data for the SARA ATRP of MA. Conditions: $[MA]_0/[EBiB]_0/[Cu(0)wire]_0/[CuBr_2]_0/[Me_6TREN]_0$=222/1/1/1.1. $[MA]_0$/[Sulfolane]= 2/1 (v/v); 50

Table 2.2 - Kinetic data for the SARA ATRP of MMA, St and VC with $[Monomer]_0$/[Sulfolane]= 2/1 (v/v).....53

Table 3.1 Kinetic data for the Cu(0)-mediated SARA ATRP of MA in sulfolane/water mixtures. Conditions: $[MA]_0$/[solvent] = 2/1 (v/v); $[MA]_0/[EBiB]_0/[Cu(0)\ wire]_0/[CuBr_2]_0/[Me_6TREN]_0$ = 222/1/1/0/1.1; T = 30 °C.....77

Table 3.2 - Molecular weight parameters of the PMA-Br prepared by SARA ATRP in sulfolane and sulfolane/water = 90/10 (v/v) at 30 °C, using different SARA agents. Reaction conditions: $[MA]_0/[EBiB]_0$ = 222; $[MA]_0$/[solvent] = 2/1 (v/v); $[Cu(0)]_0/[CuBr_2]_0/[Me_6TREN]_0$ = Cu(0) wire/0.1/1.1; $[Na_2S2O_4]_0/[CuBr_2]_0/[Me_6TREN]_0$ = 1/0.1/0.2. 80

Table 4.1 Kinetic data for the SARA ATRP of MA in [BMIM]-$[PF_6]$/DMSO mixtures. Conditions: $[MA]_0$/[solvent] = 2/1 (v/v); $[MA]_0/[EBiB]_0/[Na_2S_2O_4]_0/[CuBr_2]_0/[Me_6TREN]_0$ = 222/1/1/0.1/0.1; T = 30 ºC.....98

Table 5.1 Kinetic data for the SARA ATRP of MA using DMSO or sulfolane/[BMIM]-$[PF_6]$ solvent mixture. Conditions: $[MA]_0/[EBiB]_0/[Cu(0)\ wire]_0/[CuBr_2]_0/[Me_6TREN]_0$=222/1/Cu(0) wire/0.1/1.1 (molar); $[MA]_0$/[solvent mixture]$_0$= 2/1 (v/v), Cu (0): d = 1 mm, l = 5 cm, T = 30 ºC.....113

Table 5.2 Kinetic data for the SARA ATRP of MA using sulfolane/[BMIM]-$[PF_6]$ solvent mixture. Conditions: $[MA]_0/[EBiB]_0/[Cu(0)\ wire]_0/[CuBr_2]/[Me_6TREN]_0$ =222/1/Cu(0) wire/0.1/1.1 (molar); $[MA]_0$/[solvent mixture]= 2/1 (v/v), Cu (0): d = 1 mm, l = 5 cm, T = 30 ºC. 117

Table 5.3 Kinetic data for the SARA ATRP of MMA, Sty and VC using sulfolane/ [BMIM]-$[PF_6]$=75/25 (v/v) as solvent mixture at T = 40 ºC (MMA), 60 ºC (Sty) and 42 ºC (VC); Cu (0): d = 1 mm, l = 5 cm. 118

Table 6.1 Molecular weight parameters of the PMA-Br prepared by SARA ATRP in CPME/EtOH/H_2O = 70/28/2 (v/v/v) at 30 °C, using different SARA agents.

Reaction conditions: $[MA]_0/[EBiB]_0$ = 222; $[MA]_0$/[solvent] = 2/1 (v/v); [Fe(0) or Cu(0)]/$[CuBr_2]_0/[Me_6TREN]_0$ = Cu(0) wire or Fe(0) powder/0.1/1.1; $[Na_2S_2O_4]/[CuBr_2]_0/[Me_6TREN]_0$ = 1/0.1/0.5 141

Table 6.2 Molecular weight parameters of the PS-Br, PGMA-Br and Br-PVC-Br prepared by SARA ATRP in CPME-based mixtures. 144

Table 7.1 Kinetic data of miniemulsion polymerization of *n*BA with [*n*BA]/[EBiB] = DP/1, [Brij*98*]$_0$/[Hexadecane]$_0$ = 2.3/3.6 % *vs n*BA at T = 80 ºC. 165

Table 7.2 Kinetic data of the influence of copper(II) 2-ethylhexanoate chloroform and toluene in miniemulsion polymerization of *Ba* with [*n*BA]$_0$/[EBiB]$_0$=200/1; [Brij*98*]$_0$/[Hexadecane]$_0$ = 2.3/3.6 % *vs nBA* at T=80 ºC. 166

Table 7.3 – Kinetic data of miniemulsion polymerization of St with [St]/[EBiB] = 200/1, [Brij*98*]$_0$/[Hexadecane]$_0$ = 2.3/3.6 % *vs* St at T = 80 ºC. 168

Table 7.4 – Kinetic data of chain extension reaction in a homogeneous medium for of the P*n*BA-Br and PS–Br obtained through the miniemulsion method 170

Table 8.1 M_n and $Đ$ values determined by ^{1}H NMR and SEC and residual copper content determined by elemental analysis for the mPEG-*b*-P4VP block copolymer product. 190

Table 8.2 D_h and PDI of aqueous block copolymer dispersions, as determined by DLS, prepared by titration and by solvent exchange methods 193

Table 8.3 - Dh and PDI values for mPEG-*b*-P4VP, self-assembled in the presence of hSPIONs..... 196

Table 8.4 Longitudinal (r_1), transverse (r_2) relaxivities, and relaxivity ratios (r_2/r_1), obtained from relaxometry measurements, for different block copolymers and SPIONs-self-assembled samples, (at 20 MHz, 25ºC, 0.47T) 201

Motivation, targets and research significance

Reversible deactivation radical polymerization (RDRP) processes and mostly ATRP have been the focus of an extraordinary interest by numerous academic researchers and also by industrial laboratories. ATRP allows the synthesis of a wide range of polymer families with well-defined architecture, composition, molecular weight and chain-end functionality. ATRP also has the following important features: it is tolerant to a wide range of monomer functionalities; most of the compounds required are commercially available; involves mild reaction conditions; and facilitates an easy setup.

The application of the classical ATRP method at an industrial scale can be limited by several difficulties: oxygen sensibility; use of toxic solvents; the high amounts of catalytic complexes used in the system; polymer purification; and expensive ligands. Considering environmental issues, different strategies have been proposed trying to mitigate those problems.

In this work, different solvent mixtures have been used aiming a deeper understanding of the SARA ATRP method, and also developing "greener" routes to afford controlled (co)polymers with high chain-end functionality.

As a proof-of-concept, new block copolymers for stabilization of superparamagnetic iron oxide nanoparticles have been synthesized and used to prepare tailor-made nanoaggregates.

Part I

Literature review

Chapter 1

1.1 Radical Polymerization: from "free" to "controlled" polymers

Conventional free-radical polymerization (FRP) accounts for about 50% of the worldwide production of polymers due to its: applicability to a wide range of monomers with carbon-carbon double bond; tolerance to different functionalities; easy implementation at an industrial scale; tolerance to protic solvents (*e.g* water); possibility to be employed in different technologies (*e.g.*, solution, emulsion, suspension or bulk); good reproducibility regarding the final properties of the products. [1-3]

In most cases, FRP proceeds via three basic steps [1]: initiation, propagation, and termination. In the initiation step, a conventional initiator is decomposed by temperature, radiation, and/or chemically to form radical species which will begin a consecutive monomer addition (propagation step). The propagation occurs with a first-order kinetics, in respect to the propagating radicals concentration. Finally, each active radical growing chain terminates either via combination or disproportionation. Therefore, the resulting polymers have dead chain-ends, and there is no control over the structure or molecular weight, in part because the monomer addition is a very fast process (a polymer with very high molecular weight can be produced in 1s [4]). In addition, due to the high reactivity of the radicals some chain transfer reactions between propagating radicals and monomers, polymers, transfer agents or solvent may occur. As such, there are several strong limitations associated to FRP that influence the final properties of the polymers: the lack of control over the molecular weight, polymer dispersity and chain-end functionalities.[2] In order to create new tailor made materials with improved properties, many efforts have been made in radical polymerization to develop processes that can suppress chain termination reactions (and side reactions) and still allowing for propagation reactions to occur. In order to achieve this important goal a dynamic equilibrium between propagating radicals and dormant species can be used to substantially reduce the concentration of active

radicals. In this case, chains cannot terminate and can be intermittently deactivated and reactivated.[5]

For both radical polymerizations (free and controlled), termination reactions occur. However, in FRP all the chains terminate by radical combination or disproportionation. In controlled polymerizations, this fraction of chains is residual (typically between 1 and 10 mol %) because most polymer chains remain in their dormant state (without activity).[6]

For some years, these processes which afford control over the polymerization were described as "living radical", "controlled", "controlled/living", "quasi-living" or "living radical polymerization".[7] Nowadays, the IUPAC recommends the term reversible-deactivation radical polymerization (RDRP).[5]

1.2 Reversible deactivation radical polymerization – most used methods

RDRP methods are based on an equilibrium between active carbon-centred radicals (activation) and dormant species (without activity) to allow the effective reduction of growing radicals. The complete consumption of the initiator at the beginning of the reaction and the equilibrium allow the controlled growth of the polymer chains. Tipically, the RDRP methods are characterized by: a linear evolution of the molecular weight with conversion, an internal first-order kinetics with respect to the monomer conversion; low dispersity of final polymer ($1< Đ <1.5$); the occurrence of negligible chain transfers or termination reactions; and long-lived radical polymer chains. RDRP allows the control over the molecular weight, topology (*e.g* stars, comb-like, brushes, regular networks), composition (*e.g* block, graft, alternating, gradient copolymers), functionalities and tacticity of the polymers.[2, 5, 8]

There are three main RDRP mechanisms that are distinguished by the nature of the deactivation process (Scheme 1.1).[9] These differences are due to the use of different functional controlling groups as well as the activation/deactivation mechanisms, and they render each method unique requirements in terms of required compounds and reaction characteristics.

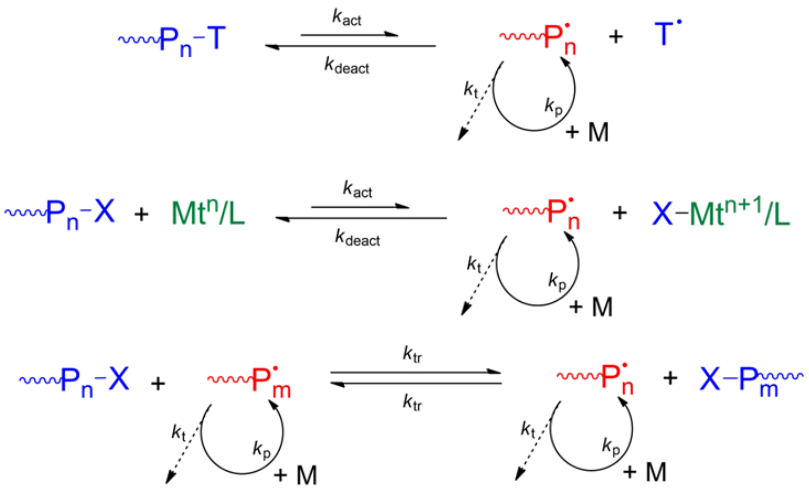

Scheme 1.1 General scheme for RDRP mechanism.

According to Scheme 1.1 these processes are divided in three major categories: (1) reversible deactivation by coupling or reversible termination (RDC), (2) reversible deactivation by atom transfer (RDAT) and (3) degenerative transfer (DT) radical methods.

In order to understand the first two categories it is mandatory to detail the persistent radical effect (PRE) mechanism, since process (1) and (2) (Scheme 1.1) are mediated by this effect with minor differences.

PRE also called *spin trap* provides a self-regulating effect.[5] This effect discovered by Fisher[10] describes the reaction between a transient radical (R_x) and a persistent radical (R_y) that results in the formation of a cross-coupling product (R_x-R_y). At the beginning there is the accumulation of R_y in the system due to self-termination of a very small amount of R_x thus promoting the formation of R_x-R_y.

In RDC (Scheme 1.1 (1)) at an early stage of the polymerization and due to the PRE, the active radicals can propagate (k_p) but also terminate in a low percentage (k_t), resulting in an accumulation of deactivatied species (stable radicals or catalytic complex), which will be persistent during the polymerization (P_n-T).[11] The dormant species (P_n-T) are activated by homolytic cleavage, with temperature, light or with an appropriate catalyst to provide growing radical chain species ($P_n^{\bullet}$) and a persistent free radical ($T^{\bullet}$). This species should not react with itself or the monomer. In the deactivation step, the propagating radical chain ($P_n^{\bullet}$) is trapped by a stable radical such as a nitroxide (nitroxide mediated radical polymerizations (NMP)) or organometallic species such as cobalt (organometallic mediated radical

polymerization (OMRP)). Since the availability of trapping agents has to be proportional to all growing chains, these methods use stoichiometric amounts of mediating species. The polymeritazion rate (k_{deac}/k_{act}) is strongly dependent on the reaction conditions, such as initiator, solvent, monomer, additives and temperature.

In Scheme 1.1 (2) RDAT is also mediated by PRE. However, the dormant species (P_n-X) is activated by the redox-active metalic complex (Mt^n/L) that has an akyl halide which in a lower oxidation-state also catalyses the homolytic cleavage of P_n-X resulting in the formation of active macroradical ($P_n^{\bullet}$). On the other hand, the active radical species are deactivated by a metalic complex in higher oxidation state (Mt^{n+1}/L), yielding dormant species and regenerating the activator (P_n-X + Mt^n/L). Since controlled polymerization can be obtained with lower amounts of metal complex, it can be used in substoichiometric quantities, which will allow to carry out these polymerization with catalytic amounts of copper complexes. The most studied RDAT method is the atom transfer radical polymerization (ATRP) using copper as metal that forms a catalytic complex with nitrogen-based ligands.[11]

Finally, in Scheme 1.1 (3) is shown another system based on degenerative transfer. This system unlike the ones described above does not rely on PRE, because it is based on a thermodynamically neutral biomolecular exchange between growing radicals ($P_m^{\bullet}$) and dormant species (P_n-X). It involves an atom exchange (*e.g* iodine mediated polymerization), a group transfer (*e.g* cobalt)) or addition-fragmentation process (*e.g*. reversible addition–fragmentation chain transfer (RAFT) and macromolecular design via the interchange of xanthates (MADIX)).[12] The equilibrium is regulated by a reversible exchange of an unstable end-group between the two species (active and dormant). This degenerative chain transfer mechanism can be accomplished by direct end-group exchange, or by addition-fragmentation. In these processes, the first radicals are tipically formed by the decomposition of a conventional initiator (like in FRP).

The reaction mechanism evolves according to a steady state of growing radicals, which results from balancing the activation and deactivation rates. This also means that the initiation is slow (low concentration of radicals) and termination is fast (due to the increase of molecular weight of the active/dormant species). In addition, a critical factor for the control over the polymerization process is the concentration of chain transfer agent (CTA), since it mediates the slow initiation and is responsible for

the formation of dormant species.[13-14] Therefore its structure and suitability for the system plays a critical role in the control achieved over the polymerization.

The different RDRP techniques have advantages and limitations, but according to their radical nature, all processes are characterized by specific reactivity ratios, a limited control over taticity and inevitably some radical termination.[11]

In the last 20 years, RDRP processes and mostly ATRP have been the focus of an extraordinary interest by numerous academic researchers and also by industrial laboratories.[5] ATRP has the particularity that can be used for a wide range of monomers, greater availability of initiators, mild reaction conditions, and vast range of techniques for the preparation of polymers, leading to materials with complex topology, composition and functionality.[5]

Therefore, the focus of this section is the ATRP status, future perspectives and applications. The state of the art, the mechanistic aspects and the synthetic procedures are presented in the next topics.

1.3 Fundamentals of atom transfer radical polymerization

In ATRP, the possibility of adjusting the rate of polymerization by the simple change of the structure of the transition metal-catalyst and the possibility of applying this technique to a wide variety of monomers (acrylonitrile, (meth)acrylates, styrenics, and water-soluble monomers) makes it the most popular RDRP technique.

The polymerization initiates via abstraction of the halogen atom (X) by the transition metal/ligand complex in a lower oxidation state (Mt^n/L, activator) to create the growing active radical species ($P_n^{\bullet}$) and a deactivator (transition metal/ligand complex in an higher state (X-Mt^{n+1}/L, deactivator)). The $P_n^{\bullet}$ species can propagate by monomer addition and/or be deactivated by the action of the deactivator. In this case, the reversible activation (k_{act}) and deactivation (k_{deact}) occurs as a dynamic equilibrium mediated by a redox mechanism (Scheme 1.2). The dormant species (P_n-X) are either an alkyl halide (or pseudohalide) initiator or a halogen-terminated macromolecule. Mt^n represents the transition metal in the oxidized state *n* and *L* represents the ligand. The termination reactions are negligible due to the PRE. The most used transition metals for ATRP are copper (Cu), molybdenum (Mo), manganese (Mn), ruthenium (Ru), iron (Fe), cobalt (Co), rhodium (Rh), nickel (Ni) and palladium (Pd).[11] The ligand is required to stabilize the two oxidation states of the

metal catalysts, in order to regulate their activity and to solubilize the metal centre in the reaction mixture.

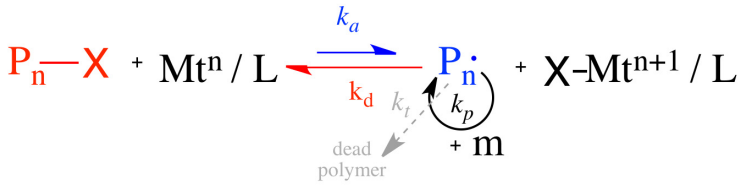

Scheme 1.2 General ATRP mechanism.

In ATRP, the value of the constants of activation (k_a), deactivation (k_d) and K_{ATRP} (K_{ATRP}= k_a/k_d) play a key role in the reaction rate (Equation 1) as well as on the control over the polymerization (dispersity, Equation 2).[5]

$$R_p = k_p[M][P_n^{\cdot}] = k_p K_{ATRP}[P_nX]\frac{[M_t^n X_m/L][M]}{[M_t^{n+1}X_{m+1}/L]} \quad (1)$$

$$Đ = \frac{M_w}{M_n} = 1 + \frac{1}{DP_n}\left(\frac{[P_nX]_0 k_p}{k_d[M_t^{n+1}X_{m+1}/L]}\right)\left(\frac{2}{conv.} - 1\right) \quad (2)$$

The rate of ATRP depends on the rate constant of propagation (k_p), on the concentration of monomer and on the concentration of growing radicals.[5] In order to ensure the control over the polymerization, the k_d should be as high as possible (low K_{ATRP}), but still affording fast polymerization (reasonable k_a) in order to maintain a low concentration of radicals and prevent termination reactions.[15] K_{ATRP} is influenced by the initiators, monomers, transition metal/ligand complexes, temperature, pressure and the nature of the reaction medium. Depending on the initial conditions, ATRP can be performed in solution, suspension, emulsion, miniemulsion or dispersion.[6]

1.4 Components of the ATRP System

ATRP requires the use of monomer, initiator and a catalytic complex (composed of a transition metal coordinated with a ligand). Both solvent and temperature influence the concentration and solubility of all the components and for a successful ATRP, sometimes is necessary to use additives.

1.4.1 Monomers

It is possible to apply ATRP to a wide variety of monomers such as styrenics[16-17], (meth)acrylates[18-21], (meth)acrylamides[22], dienes[23] and acrylonitrile[17]. However, for the same catalyst each monomer leads to unique equilibrium and so the reaction conditions need to be adjusted (*e.g.* ligand, initiator, solvent and temperature) to afford a suitable concentration of propagating radicals and a proper radical deactivation rate in order to achieve the control over the polymerization.[6]

Although K_{ATRP} depends on other factors (not only on the monomer nature), two considerations can be generalized: (1) K_{ATRP} is lower for monosubstituted alkenes than for disubstituted (MMA >> MA); and (2) it decreases in the following order with the α-substituents: Ph<CN<C<C=O<COOR .[6]

1.4.2 Initiators

There is a wide variety of alkyl halides (R-X) initiators with (pseudo) halogen atom(s) available for ATRP. Initiators with α-carbonyl, phenyl, vinyl or cyano groups are efficient and their reactivity depends on the alkyl halide bond dissociation energy.[11] There are several studies to determine bond dissociation energies of initiators and how their structure affects both its own reactivity and the polymerization kinetic. The activity can be varied with the degree of the initiator substitution (primary < secondary < tertiary), with the leaving halogen atom (Cl < Br < I) and the stabilizing groups (-Ph ~ -COOR << - CN). [24]

The most used initiators are the bromine-substituted ones (Figure 1.1), however chlorine or iodine analogues can also be employed. The halogen atom play an important role in the first step of the polymerization (activation), since it must be transferred between the catalytic complex and the growing species to ensure the requirements of ATRP.[24]

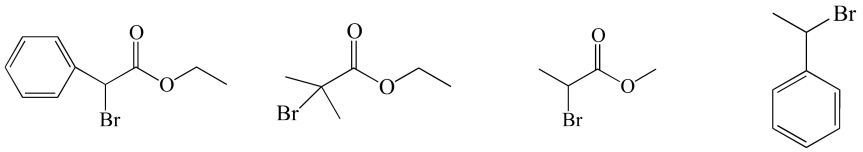

Figure 1.1 Bromine-functional initiators typically used in ATRP: α-bromophenylacetate (EBPA), α-bromoisobutyrate (EBIB), methylbromopropionate (MBP), 1-phenyl ethylbromide (PEBr)

Halogen terminated polymers as cholesteryl-2-bromoisobutyrate or bromo-telechelic poly(ethylene glycol)monomethyl ether) can also be used in ATRP reactions as initiators.[25] By choosing the ATRP initiator (or macroinitiator), the process might yield star, brush or hyperbranched structures. Additionally, halogenated initiators with different chemical groups (hydroxyl, cyano group, epoxides, alkene, and alkyne, azide, trichloro, or trialkoxysilyl groups, amino group, among others) can be used for further post-polymerization reactions (Figure 1.2).[5]

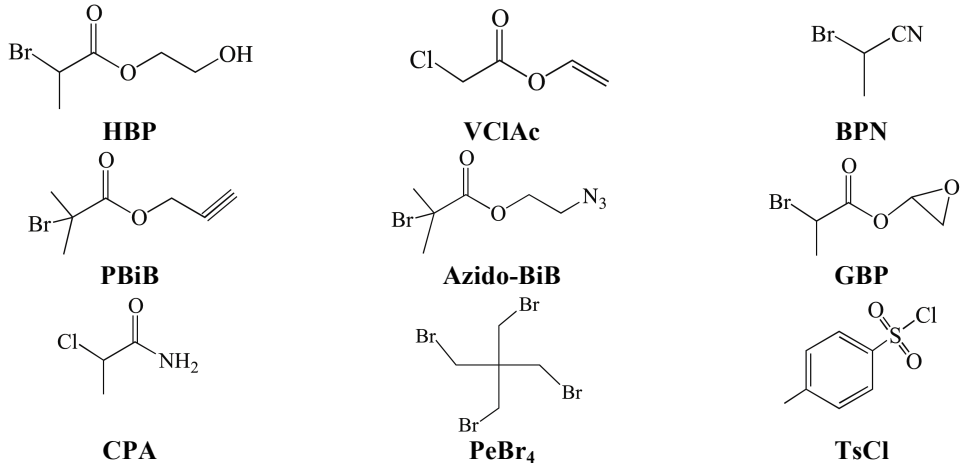

Figure 1.2 Initiators typically used in ATRP with different chemical groups: 2-hydroxyethyl 2-bromopropanoate (HBP), vinyl cloro acetate (VClAc), 2-bromopropionitrile(BPN), propargyl 2-bromoisobutyrate (PBiB), 2-azidoethyl 2-bromoisobutyrate (Azido-BiB), glycidol 2-bromopropionate (GBP), chloropropionamide (CPA), 2,2-dibromomethyl-1,3-dibromopropane (PeBr4), *p*-toluene sulfonyl chloride (TsCl)

It is also important to note that the choice of initiator with functional groups is a very convenient approach to afford polymer structures with pre-determined functionality. Additional details about the influence of the initiator structure in the rate constant of activation step are available in the literature.[26]

1.4.3 Catalysts and Ligands

The metallic catalyst plays a decisive role in the activation/deactivation of the propagating radicals. In the equilibrium, the complex must have a high association constant to halide ions, which should be able to form two valence states and the coordination sphere of the metal must be able to capture the halogen atom.

The metallic catalyst is the most important component in ATRP, since it determines the position of the atom transfer equilibrium and influences the dynamics between dormant and active species.[6] The main types of metal catalysts used in ATRP are: Cu, Mo, Mn, Ru, Fe, Co, Rh, Ni and Pd.[6] The ligand is required to perform the coordination with the metal catalysts, therefore modulating their redox activity and ensuring their solubilisation in the reaction mixture.

Copper complexes stabilized with nitrogen-based ligands (Figure 1.3) have been the most extensively studied catalysts for ATRP. There are also some application of phosphorous-based ligands, to complex with rhenium, iron, rhodium, nickel, and palladium.

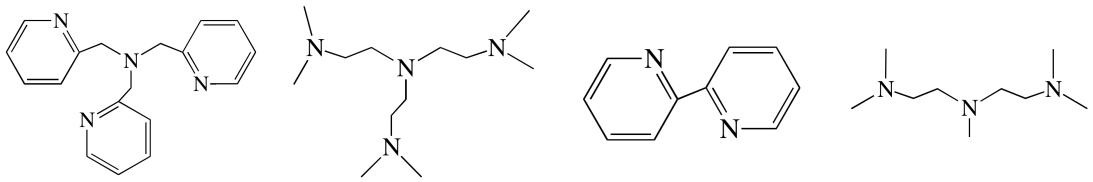

TPMA **Me_6TREN** **Bpy** **PMDETA**

Figure 1.3 Nitrogen-based ligands typically used in ATRP: tris(2-pyridylmethyl)amine (TPMA) , tris[2-(dimethylamino)ethyl]amine (Me_6TREN), 2,2'-bipyridine (Bpy) *N,N,N′,N″,N‴*-pentamethyldiethylenetriamine (PMDETA)

The effect of the ligand structures on the equilibrium constants has been amply studied in the literature.[26] The activity of the catalyst depends very strongly on: (1) the linking unit between the N atoms and the coordination angle; (2) the topology of the ligand (cyclic, linear or branched); (3) the nature of the N-ligand (aryl amine, aryl imine, alkyl imine, alkyl amine or pyridine) and (4) the steric bulkiness around the metal center.[5, 11]

1.4.4 Solvents

Generally ATRP can be carried out in bulk, solution or in a heterogeneous system (*e.g.* emulsion, miniemulsion or suspension).

For both homogeneous and heterogeneous systems, the right choice of solvents must take into account: (1) minimal radical chain transfer to the solvent; (2) minimal potential interactions between the solvent and the catalytic system; (3) minimal side reactions. Additionally, to obtain controlled polymerization in homogeneous conditions, it is necessary to ensure that monomer, polymer, initiator and catalytic complex are soluble in the selected solvent.[6]

Various polar and non-polar solvents such as benzene, toluene, anisole, diphenyl ether, ethyl acetate, acetone, dimethylformamide, ethylene carbonate, ethanol, water, carbon dioxide, ionic liquids, sulfolane and cyclopentyl methyl ether have been used in the polymerization of different monomers by ATRP.[6]

Horn and co-workers[27] studied the solvent effect on the activation, deactivation and equilibrium rate constants. The ATRP reaction was mediated by Cu(I)Br/1,1,4,7,10,10-Hexamethyltriethylenetetramine (HMTETA) at 25 ºC and the amount Cu(II) (deactivator species) were followed over time in 14 different solvents. The results revealed the importance of the solvent polarity in the magnitude of the activation rate. For solvents with higher polarity, it was observed a faster activation step, and slower deactivation step resulting in a higher K_{ATRP}.

The formation of hydrogen bonds and the presence of Lewis acid-base adducts cannot be neglected in ATRP reactions. For example, the redox potential is a function of solvent coefficients (*e.g* hydrogen bond donor/acceptor ability of solvent or polarizability) that affect K_{ATRP}. It has been observed that ATRP reactions increase their rate in the presence of water or polar organic solvents like DMSO, when compared to acetonitrile.[28] Additionally, some monomers (*e.g* methacrylamides and methacrylate esters) can complex with Lewis acids, which affects the monomer reactivity and the stereocontrol.[28-29]

1.5 ATRP: limitations, variations and "*greener*" strategies

The application of the classical ATRP method at an industrial scale was limited by several difficulties: oxygen sensibility of the reaction; amounts of catalytic complexes; process of polymer purification; and the use of expensive ligands. Moreover, the complex that mediates the ATRP processes is based on metals. Copper is the most used metal in ATRP.[30] The presence of metal in polymer products provides intense colour to the final materials and originates toxic materials for several polymer applications (*e.g.* metal has tendency to accumulate in the body, interact with enzymes or other biologic molecules and participate in redox reactions). [30]

The term "Green" has been used over the last years to qualify methods, techniques and procedures in chemistry, materials science and industry.[31] In polymer synthesis, the chemical processes imply the use of nontoxic and reusable reagents and solvents. The development of new technologies to lower energy consumption and the development of recycable or (bio)degradable polymeric materials, have recently called amply attention in the scientific community.[30]

Some strategies have already been used at the laboratory scale to remove the catalyst at the end of the polymerization, such as passing the polymer solution through a column with ion change resin or absorbent (alumina and silica) or extraction with water, ionic liquids or ligand solution with strong binding ability to copper ions.[31] When there is the possibility to use the catalyst in heterogeneous phase (supported ATRP), it can be an efficient laboratory alternative however, at the industrial level it creates some problems in the filtration process for large volumes of viscous polymer solution.

Many strategies have been implemented trying to mitigate those ATRP issues (beginning of section 1.5) including: (1) the use of Fe-based catalysts[25, 32-33]; (2) application of metal catalyst systems composed of heterogeneous zero valent metals in combination with low concentration of $CuBr_2$/L; (3) reduction of the amount of metal catalyst required[34-35]; (4) use of "green" solvents[36-39] and (5) low the reaction temperature[33].

The significant reduction of the copper amount could avoid the necessity of troublesome purification processes. The K_{ATRP} depends on both activator and deactivator concentrations and not on the total amount of metal catalyst used (Section 1.3). However, in practice, reducing the catalyst concentration to ppm levels could

lead to stop the reaction, due to low level of regeneration of Cu(I) species (activator) Considering this, new several ATRP variations have been developed (Figure 1.4) in which Cu(I) species could be continuously regenerated, from the "in situ" reduction of Cu(II) species, at low concentration, during the polymerization:

(1) Activators generated by electron transfer (AGET) ATRP: addition of reduction agents (*e.g.* sugars and ascorbic acid) to convert Cu(II) into Cu(I) *in situ*, in the beginning of the reaction. [40]

(2) Activators regenerated by electron transfer (ARGET) ATRP: possibility to adjust the AGET technique, in order to continuously regenerate Cu(I) during the reaction. A very low concentration of copper catalyst is used and the accumulated CuX_2/L is continuously reduced to regenerate Cu(I)X/L. [40]

(3) Initiators for continuous activator regeneration (ICAR) ATRP: uses conventional thermal radical initiators (*e.g.* AIBN) that react with Cu(II)/L to produce Cu(I)/L activator species.[5]

(4) Electrochemically mediated ATRP (e-ATRP): uses electrical current for the reduction process to (re)generate the activator species (Cu(I)/L), this is the most eco-friendly ATRP variation.[41]

(5) Supplemental activator and reducing agent (SARA) ATRP: uses zero valent metals (*e.g.* Cu, Fe, Zn or Mg) or inorganic sulphites that act not only as reducing agents but also participate in the supplemental activation of the dormant species (Cu(I)/L is still the main activator).[25, 32, 34, 36, 38-39, 42]

(6) Metal free ATRP: organic photoredox system that could be reducing species in the excited state and effectively catalyzes controlled radical polymerization processes. (*e.g.* phenothiazine derivatives: 10-methylphenothiazine)[43]

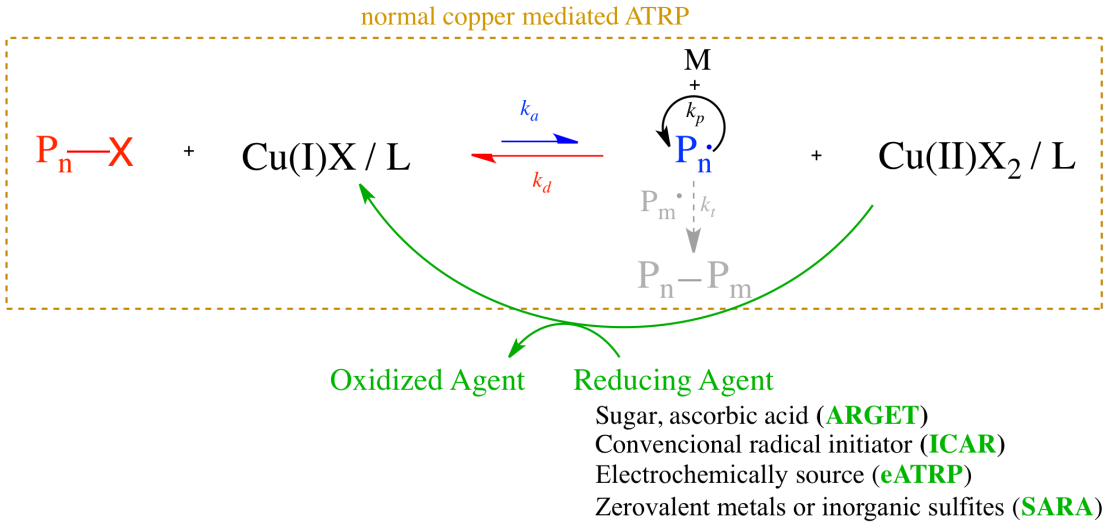

Figure 1.4 ATRP variation techniques

The work presented in this project aims to contribute to the development of new eco-friendly SARA-ATRP systems using "green" solvents as well as to the expansion of the technique to different monomer families.

1.5.1 Single Electron Transfer Living Radical Polymerization (SET–LRP)

Percec[7, 21] and co-workers, in an original publication, described the SET-LRP technique as a Cu(0)-catalyzed polymerization, and claimed a different mechanism for ATRP to explain the control over the polymerization. SET-LRP has been applied to the polymerization of a broad range of functional monomers (conjugated and non-conjugated) in homogeneous and heterogeneous conditions near room temperature.[7, 21, 44-45]

According to Percec's theory, the activation step in SET-LRP relies on a single electron transfer exclusively from the Cu(0) electron donor to the halide initiator electron acceptor, by an outer-sphere electron transfer process. As a result, Cu(I) is formed, and instantaneously disproportionates into Cu(II) and Cu(0), generating deactivation and regenerating the activator (auto-catalytic system), respectively (Figure 1.5). Cu(0) acts as major activator and no major activation occurs by Cu(I) species.[46] The high reactivity of Cu(0) and very small amounts of catalyst (ppm) lead to fast and controlled reactions in the presence of ligand and solvent. In this

explanation, the PRE mechanism previously mentioned in the case of ATRP does not exist in the SET-LRP because CuX_2/L is formed by decomposition of Cu(I)X/L and does not accumulate in the system, in the early stages of the polymerization. Since 2006 in, Matyjaszewski's and Percec's research gropus have published numerous papers supporting each of their own theory about the reaction mechanism.[2, 5-6, 21, 34, 47]

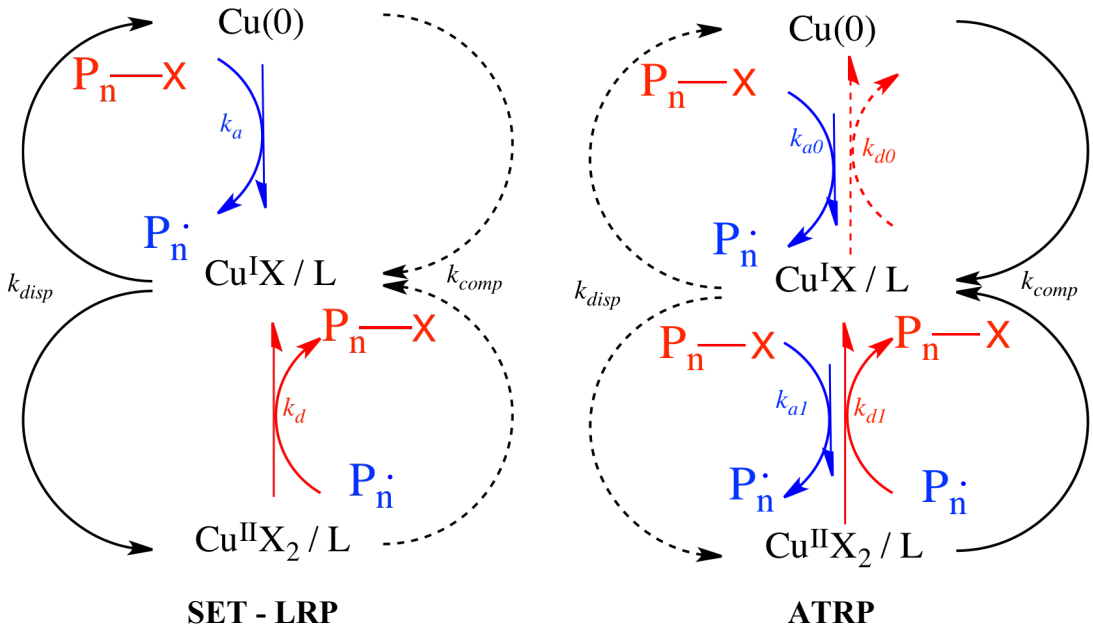

Figure 1.5 Copper-catalysed SET-LRP and SARA-ATRP mechanism

Percec[21], using Cu(0)-catalysed polymerization of vinyl chloride in water at room temperature, suggested that the formation of radical species on copper-catalysed RDRP is achieved by extremely active Cu(0) species and the polarity of the solvent interferes on the polymerization rate.

On the other hand, Matyjaszewski and his coworkers[47] studied the equilibrium between copper and copper/ligand complex in their different states and demonstrated that Cu(0) mechanism was similar to ARGET ATRP process, which involved a supplemental activator to direct activation of alkyl halides by Cu(0) and comproportionation (reducing agent) event during the polymerization. In this case, Cu(I) is the major activator and Cu(0) acts as a supplemental activator and reducing (SARA ATRP) agent of alkyl halides.[46]

In a recent publication Konkolewicz[48-49] covering different aspects concerning the use Cu(0), demonstrated that the reaction is mediated by SARA ATRP mechanism.

Table 1.1 SET-LRP and SARA ATRP - differences and similarities[46, 50]

	SET-LRP	SARA ATRP
Differences	Cu(0) is the main activator	Cu(I) is the main activator
	Outer sphere single electron transfer (OSET)	Inner sphere single electron transfer (ISET)
	Requires disproportionation solvents	Disproportionation and nondisproportionation solvents
Similarities	Cu(II) is the deactivator	
	Negligible deactivation by Cu(I)	
	The components are common (ligand and initiator)	
	Room temperature	
	Oxygen tolerant	
	High end-group functionality	

1.6 Green solvents

In chemical processes, solvents account for a large part of the environmental performance and the impact on safety and costs.[51] The development of efficient, "*greener*" and sustainable chemical procedures is one of the key issues in modern times. Alternative reaction media could reduce and replace harmful solvents that are currently used to have cleaner technologies.[52] The methods have evolved to: (1) substitution of hazardous solvents by some which have more environmental, healthy and safety properties (to increase the biodegradability and reduce the ozone depletion potential); (2) encourage the use of solvents produced from renewable resources ("bio-solvents") instead of fossil-based solvents; or (3) decrease the amount of organic compounds via an increase of green solvents such as ionic liquids, supercritical carbon dioxide or water. [30, 51]

1.6.1 Ionic liquids

Ionic liquids are mixtures formed by two salts that are in a liquid state below 100 °C. Throughout the last decades, ionic liquids are assumed as "green" solvents due to their negligible vapour pressure and high boiling point, which facilitates the recycling process.[53-55] In the 1990's, metal-free ionic liquids became an interesting subject and a combination of an organic cation (usually 1-alkyl-3-methylimidazolium cations, $[C_nmim]^+$) with anions (Cl^-, BH_4^-, PF_6^- or NTf_2^-) led to the preparation of a large

variety of ionic liquids with different physical properties (*e.g* melting point, solubility, viscosity, density, conductivity and refractivity). Ionic liquids have been utilized as catalysts, reagent or solvent for many chemical processes and can also be used in separation processes and electrolyte materials.[19, 52, 54, 56-58] The great advantage of using these compounds comes from the easy separation process from the final product and the possibility of its reuse in new processes due to its immiscibility with a range of compounds.[30-31, 52] Its use in polymerization reaction media is less interesting due to the necessity of using an organic solvent to recover the polymer, however they are interesting compounds as initiators, monomers and catalysts in polymer chemistry.[52]

When using ionic liquids it is important to consider their whole life cycle to evaluate their influence (positive/negative) on the *greenness* of the process.[52] Many authors[53, 59-60] have reported other factors that compromise the "*green*" nature of ionic liquids: the preparation methods (which are generally not considered or reported in the literature) require a large amount of salts and solvents to exchange the anions; toxicity; very poor biodegradability and high price. All of the above metioned disadvantages may hamper the industrial application of ionic liquids.

Despite the fact that substituted acrylates can be polymerized by controlled radical polymerization in ionic liquids,[19] the first controlled polymerization published in the literature was using 1-butyl-3-methylimidazolium hexafluorophosphate ([BMIM][PF_6]) as solvent in anionic polymerization of MMA.[61] Cu(I) mediated polymerizations using [BMIM]-[PF_6] were also reported in 2000 by Haddleton group[61] for MMA polymerization. The PMMA obtained had controlled structure and the catalyst was easily separated from the product and could be reused.[61] In addition, in ATRP processes, as published by Kubisa[58], [BMIM]-[PF_6] acts as an efficient plasticizer of the polymer, and it can interfere in the mechanism. Even in small amounts, [BMIM]-[PF_6] may have a favourable effect on ATRP process because the presence of the ionic liquid could avoid the use amine ligand with an iron or copper mediator (dibutylphosphonate anion was required for copper to become active).[58]

Years later (2005) Percec and co-workers[45] published a significant increase in the polymerization rate in the presence of [C_4MIM]-[PF_6] with Cu_2O/2,2'-bypyridine complex and phenoxybenzene-4,4'disulfonyl chloride. In general ionic liquids favor propagation rates of the reaction due to the formation of a complex between the growing radicals and the solvent.[52]

1.6.2 Water-based systems

Water is the most interesting solvent for industrial applications.[52] It is inexpensive, abundant, environmentally friendly and has high thermal capacity.[5, 52]

Polymerizations in water can be successfully carried out in homogeneous or in heterogeneous systems if the monomer is water-soluble or hydrophobic (*e.g* latexes in industrial scale process).[5]

The first ATRP process in homogeneous system was reported in 1998 by Matyjaszewski group.[62] 2-hydroxyethyl acrylate (HEA) at 90 ºC using a complex of CuBr/bpy and 2-bromopropionate or diethyl-2-methyl-2-bromomalonate as initiator, was polymerized. The PHEA was obtained with narrow molecular distribution up to 80% of conversion. In 1999, the polymerization of 2-phenoxyethyl methacrylate (MePEOMA) was carried out in water and it improved the polymerization rate comparing to the polymerization of the same monomer in bulk. [63-64] Additionally, it is known that ATRP reactions in aqueous systems are faster even at room temperature and are accelerated when the water amount is increased, even for polymerizations of hydrophobic monomers[31], most of the time due to presence of ionizable pendant groups in monomers.

There are also problems associated with ATRP reactions in water related to catalyst stability and the side reactions: (1) disproportionation of Cu(I) activator, (2) deactivation of Cu(II), (Cu(II)X/L) has tendency to dissociation, losing its halide ligand (Cu(II)/L) and (3) hydrolysis of the alkyl halide initiator .

Disproportionation of Cu(I) easily occurs in water and depends on the dielectric constant of the medium and water ability to solvate or coordinate to Cu(I) or Cu(II) ions.[30] Additional solvents (*e.g* DMSO, dimethylformamide (DMF) or acetonitrile) can be added[30], however the *greener* properties of the system will be reduced.

To improve the control over the polymerization and avoid the side reactions, large amounts of initial Cu(II)-based catalyst or extra halide salts can be added. In aqueous solutions 4-vinylpyridine (4VP) polymerization, it is necessary to add additional pyridinium salts[30] in order to prevent bimodal molecular weight of P4VP when bromide-based initiators are present. Other strategies include changing the used ligand (*e.g* PMDETA and Me_6TREN promote very fast disproportionation reaction and on the other hand HMTETA and TPMA are efficient ligands in aqueous media[31]).[31, 52] The selection of a suitable ligand that promotes high values of halidophilicity of the Cu(II) complex determines the concentration of deactivator

(Cu(II)X/L) in the system and the control of the polymerization (scheme 1.4).[30] In water, the hydrogen bonds that can easily be achieved between the solvent and the pendant groups of monomers (amine, amide, carboxylate group or pyridine moiety) promotes the participation of copper ATRP species in side reactions. One possible way to prevent this issue is to choose a suitable ligand that forms a stable complex with Cu(I) and Cu(II).

The polymerization of hydrophobic monomers can be successfully carried out in aqueous dispersed medium. The heterogeneous radical polymerization will be discussed in more detail in the next section (1.7).

1.7 Heterogeneous Polymerization: suspension, emulsion and miniemulsion

Aqueous dispersed polymerization systems are successfully carried out in suspension, dispersion, precipitation, emulsion, miniemulsion, microemulsion and inverse miniemulsion[65]

Since the first works of emulsion polymerization of styrene with 2,2,6,6-tetramethylpiperidinyl-l-oxy (TEMPO) derivatives in 1997 by Bon and co-workers,[66] several other RDRP techniques have been carried out in aqueous dispersed systems.

The several aqueous dispersed systems occur in a bi-phasic system usually with water in the continuous phase and the monomer/polymer in a fine dispersion in water.[67] They differ mostly from each other in (1) the initial state of the polymerization mixture; (2) in the mechanism of particle formation; (3) in the size of the polymer particles and (4) in the kinetics of the polymerization reaction[68]. The most relevant characteristics are summarized in table 1.2.

Table 1.2 The differences between the heterogeneous polymerization systems[67-68]

System	Particle Size		Size-distribution	Initiator	Continuous phase	Requires
	Initial	Polymer				
Suspension	> 1 μm	10 μm – 0.5 mm	Multi-disperse	Soluble in monomer phase	Water	
Emulsion	1-10 μm	50-500 nm	Mono-disperse	Soluble in water (hydrophobic are sometimes used)	Water	Monomer insoluble (or scarcely soluble) in water Surfactant
Miniemulsion	30-100 nm	10-50 nm	Mono-disperse	Water-soluble	Water	Surfactant Ultrasonic homogenization Co-stabilizer
Microemulsion	10-30 nm	20-40 nm	Mono-disperse	Water-soluble	Water	Surfactant and co-surfactant
Precipitation	50-300 nm		Mono-disperse	Soluble in reaction medium	Organic solvent	Polymer is insoluble in reaction medium
Dispersion	> 1 μm	1- 15 μm	Mono-disperse	Soluble in reaction medium	Organic solvent	Type of precipitation Suitable polymeric stabilizer soluble in reaction medium
Inverse emulsion	10^2-10^3 nm	≈ 1-10 μm	Mono-disperse	Water- or oil-soluble	Oil	

The suspension is the most known method in heterogeneous polymerizations.[67] The hydrophobic monomer is dispersed in continuous phase (water) and liquid droplets are formed with vigorous stirring. An initiator insoluble in water is added to start the polymerization inside the monomer droplets. Stabilizers, such as water soluble polymers (poly(*N*-vinylpyrrolidone) and poly(vinyl alcohol-*co*-vinyl acetate)) or insoluble inorganic salts (talc, calcium and magnesium carbonates, silicates and phosphates) are also present in small amounts to improve the dispersion, and prevent the coalescence of monomer droplets and/or adhesion of polymer particles, by forming a film at the droplets' surfaces to prevent the coalescence by steric effects.[68]

The diameter of the particles obtained is variable and depends on stirring, monomer/water volume ratio, stabilizer concentration, phase viscosity and the design of the reactor.[68] Additionally, the solubility properties of the polymer in the monomer interfere with the morphology of the final individual particles. If the polymer is soluble in its own monomer, the surface of particles is smooth and the texture is homogeneous (*e.g* poly(methyl methacrylate) and polystyrene), otherwise the surface is rough and the polymer obtained is porous (*e.g* poly(vinyl chloride) and polyacrylonitrile).[68]

The efficiency of ATRP in suspension was demonstrated for the poly(n-butyl methacrylate) (P*n*BMA) synthesis with 1-3 μm of polymer particle size. Non-ionic and cationic polymeric stabilizers and a highly hydrophobic ligand have been used.[69]

The process of emulsion is similar to a suspension as far as both use water insoluble monomers (*e.g.* styrene, acrylates, methacrylates), although water-soluble comonomers (*e.g.* acrylic/methacrylic acid) are often added to enhance the particle stability. However, in emulsion the addition of a surfactant (ionic or non-ionic) is crucial to obtain an emulsified system.[70]

The surfactant is composed by two phases, one hydrophobic and other hydrophilic, and it is able to stabilize the droplets if their concentration exceeds the critical micelle concentration[1] (C_M or c.m.c[71]). It is incorporated in the interface of the droplets, the monomer swollens its core and it gives stability by electrostatic effects (anionic and cationic surfactants), steric effects (non-ionic surfactants) or both (polyelectrolytes).[68]

In emulsion all the components are incorporated in the first step. The beginning of the polymerization occurs in continuous or organic phase given the kind of initiator used (hydrophilic or hydrophobic).[70] Mostly, the monomer is present in three forms: in large droplets, small amounts stabilized in surfactant micelles and molecularly dissolved in water (depending on the nature and concentration of monomer and surfactant). This is an important point since it affects the process of particle formation and the kinetics of the polymerization.[68] After the initiation process, the radicals in water propagate with small amounts of monomer dissolved in the aqueous phase (this phase is saturated with monomer). The aqueous oligoradicals become sufficiently hydrophobic (insoluble in the continuous phase) to be able to enter the micelles and

[1] Critical micelle concentration is the minimal concentration to all the surfactant molecules form micelles. Is the point at which micelles begin to form

continue the polymerization inside those. As long as monomer droplets are present in the system the homogeneous nucleation polymerization occurs.

Emulsion is largely applied to the polymerization of methacrylic ester, vinyl chloride, acrylamide, vinyl acetate, chloroprene or even for poly(acrylic ester) copolymers and polydiene-based synthetic rubbers. However, for hydrophobic monomers with high molecular weight (*e.g.* lauryl and stearyl methacrylate) the mass transfer for micelle/particle is very difficult. [67] The way to achieve the polymerization of very hydrophobic monomers in aqueous dispersed media with small size is to do a polymerization by miniemulsion, since the transport issues do not take place. [67]

The application of ATRP to emulsion could be very complex. To make it possible, a procedure based on emulsion and microemulsion simultaneously can be used in order to obtain polymers with narrow molecular weight distribution ($Đ$ = 1.2 to1.4).[67]

The process of miniemulsion is characterized by reducing the monomer droplets to sub-size micron (50-500 nm) through a mechanical strong force (ultrasonicator, for the miniemulsification of small quantities in a lab-scale batch process, or a high-pressure homogenizer, for larger scales[72]). The final product has the same particle size of an emulsion polymerization, however the particle nucleation mechanism is quite different.[70] At the beginning of the homogenization, the polydispersity of the droplets is still quite high, however it decreases and achieves a steady state through a constant fusion and fission process induced by the high shear.[72]

The droplets with narrow size distribution formed were regarded as a rather unstable dispersion state which lead to droplets growth for two mechanisms: growth by Ostwald ripening[2] and growth by collisions (and subsequent coalescence).[73] The suppression of both processes is important for the formulation of a stable miniemulsion.[73]

During ultrasonic homogenization (under nitrogen atmosphere or for a very short time[74]) the Ostwald ripening is reduced by the presence of an additional surfactant, so-called 'co-surfactant'. Co-surfactants or co-stabilizers are ultra-hydrophobic molecules with low molecular weight (*e.g.* hexadecane) or alcohols with long chain (*e.g.* hexadecanol) that are trapped in each droplet. Being so, this agent cannot be distributed in two phases. It limits the particle coalescence by forming a barrier at the surface and still prevents the Ostwald ripening by building up an osmotic pressure

[2] Ostwald ripening is the transfer of monomer (diffusion) from small to large droplets in order to reduce the total surface energy of the system

within the monomer droplets.[68] In other words lower Gibbs free energy of the droplet, decreases the driving force for diffusion. The choice of co-surfactants can be made taking into account the final properties of the product (*e.g* dyes, plasticizers, or cross-linkers).[72]

The unique advantage of miniemulsion is that polymerization occurs in locus (in the droplets) as in the suspension process. Ideally, each monomer droplet would have equal probability to nucleate and be converted into a polymer particle. It can also be be considered an isolated nanoreactor. Other additional features of this method are (1) the absence of micelles (characteristics of the emulsion) because all surfactant has been absorbed onto the large droplet-water interfacial area, (2) water and oil initiator can be used to form radicals and (3) it is also a powerful method to encapsulate materials (*e.g.* dye or pigment).[67-68]

St, *n*BA, MMA, vinyl acetate, vinyl 2-ethylhexanoate and numerous other copolymerizations were successfully carried out by miniemulsion.[68]

ATRP in miniemulsion was applied to *n*BMA, MMA, *n*BA and St combining different ligands (EHA_6TREN, dNbpy, tNtpyor BPMODA) or specific surfactant (cetyltrimethylammonium bromide (CTAB) or Brij 98) and initiator (VA-044 or EBiB).[67] The used ATRP based system in miniemulsion refers to the application of AGET ATRP with ascorbic acid as the reducing agent of Cu(II) complex to Cu(I). However, normal, reverse and simultaneous reverse and normal initiation (SR&NI) ATRP can be carried out in miniemulsion. [67]

In microemulsion the system is formed spontaneously by the presence of appropriate surfactants and co-surfactants without vigorous mechanical agitation. The system is characterized as isotropic and is optically transparent/translucent.[67] The polymerization can start in the continuous phase and the growing radicals formed will enter into the micelles to continue the polymerization.[67] Then, the nucleation occurs inside of the micelles due to mass transfer of monomer or by collision between particles.[67] Okubo and co-workers[75] polymerized *i*BMA with the initiator EBiB to obtain a controlled polymerization with monodispersed molecular weight distribution. In previous results Matyjaszewski[65] added the initiator EBiB after the system was emulsified in MMA and St polymerizations resulting a bimodal distribution of polymers.

The precipitation and the dispersion are two similar heterogeneous processes but usually the continuous phase is not water. The main solvents used include alkanes and

alcohol/water mixtures. Precipitation starts in the homogeneous phase but the polymer is insoluble in the reaction medium so it precipitates during the polymerization. On the other hand, in the dispersion the surfactant/stabilizer used is able to stabilize the particles in formation and it is a useful method to synthetize micron and submicron polymer particles.[67]

Matyjaszewski's group[76], in 2007, polymerized St in ethanol at 70 ºC with PVP as stabilizer and octylphenol ethoxylate. After initiating the nucleation, they added the deactivator ($CuBr_2$/TPMA) and obtained controlled polymerization by ATRP process. In the same year, Wan[77] published a ATRP of 4VP in ethanol/water at 60ºC. PEO-monomethylether 2-bromoisobutyrate was used as initiator and stabilizer and PMDETA as ligand. Particles with 30 nm and polymer with good controlled properties were obtained.

Inverse miniemulsion, instead of normal miniemulsion, is focused on the hydrophilic monomers dispersed in continuous hydrophobic phase and its major applications are related to bioapplications (*e.g.* drug delivery). For instance Averick[78] polymerized OEOMA copolymers using $CuBr_2$/TPMA and PEG-Br macroinitiator by inverse miniemulsion AGET ATRP (ascorbic acid as reducing agent), with cyclohexane as continuous phase.[79] With a biodegradable cross-linker, cationic nanogels with site-selected functionality were designed (protein−polymer hybrid) for the complexation and delivery of a pDNA that codes for a firefly luciferase protein and siRNA that targets a renilla luciferase mRNA for a dual luciferase reporter assay.

1.7.1 ATRP in aqueous dispersed media – focus on miniemulsion

ATRP was first developed in homogeneous systems for the synthesis of well-defined macromolecules such as linear (co)polymers, star (co)polymers or more complex architectures. However, to increase the potential of the method, it was fundamental to make it compatible with heterogeneous systems.[80] The ATRP in dispersed media can occur using organic solvents or supercritical CO_2 as continuous phase, but the solvent most widely used in these systems is water.[80]

To obtain a miniemulsion system, one fundamental process is the homogenization step to achieve monodisperse small droplets, by using an ultrasonicator.[73] Despite the major drawback of the miniemulsion being related to the high-energy input requirement in homogenization step, it is the most suitable method for implementation

of RDRP methods and consequently ATRP due to the aforementioned features of this method.

The multiphase nature of the ATRP in the miniemulsion leads to new challenges with the objective to identify an appropriate ligand and surfactant.

In order to establish the equilibrium and control the polymerization, the radical activator and the deactivator have to be in the organic phase.[68] Cu(II) species tend to extensively coordinate with the water molecule (*partitioning*) and the dissociation of the deactivator leads to formation of inactive Cu(II) complexes. This effect results in higher polymerization rates, loss of control, higher fraction of dead chains and broader molecular weight distribution.[81] In this sense, a suitable ligand should be chosen in order to retain the metal complex (at both oxidation states) into the organic phase.[68] Nonetheless, the ligands frequently used in homogeneous ATRP have been tested in miniemulsion, including bipyridyl and terpyridyl derivatives, picolyl amines and aliphatic amines, only ligands hydrophobic enough (Figure 1.6), such as picolyl amines, bipyridines, terpyridines and TREN-based ligands (with very hydrophobic substitutes) are soluble in the organic phase, and do not form water-soluble complexes and have shown to be more suitable for these polymerizations.[67-68]

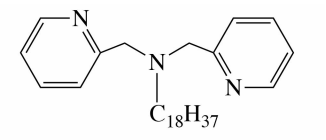

BPMODA

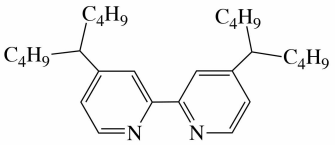

dNbpy

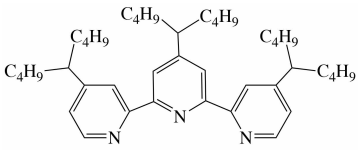

tNtpy

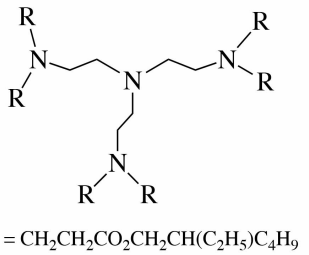

$R = CH_2CH_2CO_2CH_2CH(C_2H_5)C_4H_9$

EHA_6TREN

Figure 1.6 Typical ligands successfully used in ATRP miniemulsion: bis(2-pyridylmethyl)octadecylamine (BPMODA)4,4′-Dinonyl-2,2′-dipyridyl (dNbpy), 4,4',4"-tris(5-nonyl)-2,2':6',2"-terpyridine (tNtpy), tris(2-bis(3-(2-ethylhexoxy)-3-oxopropyl)aminoethyl)amine (EHA_6TREN)

Even with a hydrophobic ligand, the problems associated with the partition of copper species in the aqueous phase, in particular the deactivator, should not be negligible and may often occur. This effect can be augmented with the increase of the reaction temperature.[67]

In miniemulsion, the partitioning of Cu(I) and Cu(II) species can be easily evaluated by UV–vis spectroscopy by measuring periodically the absorbance in the 350-1100 nm.[82] For $CuBr_2$, the absorbance intensity at 957 nm.[83]

Generally, the surfactants used in dispersed media are responsible for the colloidal stability of the system.[67]

In ATRP miniemulsion systems, a good surfactant must have other characteristics: (1) do not interfere with the equilibrium between the active radicals and the dormant species, (2) enhance the partitioning ratio of the metal complexes in the organic phase and (3) reduce the diffusion rate of the metal complexes between the two phases.[67-68]

Generally, anionic and cationic surfactants allow the formation of monodisperse droplets between 30 and 200 nm, approximately; non-ionic oligomeric or polymeric surfactants are suitable for the formation of droplets in the range of 100 and 800 nm.[73]

The mostly used surfactants in ATRP are shown in Figure 1.7 and they are non-ionic, with hydrophilic-lipophilic balance (HLB) around 14 to 16 such as polyoxyethylene(20) oleyl ether (Brij 98), Tween 80 and poly(vinylalcohol) (PVA).[67]

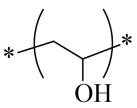

PVA

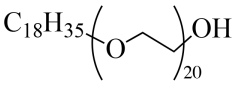

Brij 98

HLB = 15.3

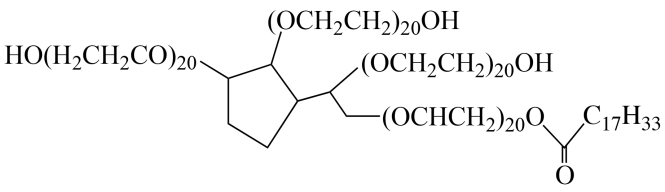

Tween 80

HLB = 15.0

Figure 1.7 Typical nonionic surfactants used in ATRP miniemulsion: poly(vinyl alcohol) (PVA), polyoxyethylene (20) oleyl ether (Brij 98), polyethylene glycol sorbitan monooleate (Tween 80)

The HLB is not the only property of the surfactant that interferes in the stabilization mechanism. The molecular weight, chemical nature of the hydrophobic or hydrophilic parts and the structural features of the hydrophilic moieties (such as degree of branching and chain length distribution) may also play an important role.[68] Additionally, regardless of ionic surfactants not interfering with the control of the polymerization, only non-ionic surfactants have been proven to be efficient to prevent the coagulation in stable latex.[68] Cationic surfactants (*e.g* cetyltrimethylammonium bromide (CTAB)) have been successfully used in controlled ATRP miniemulsion, however anionic surfactants (sodium dodecyl sulfate (SDS)) that are common for conventional emulsions, have the tendency to interact with the catalyst (especially Cu(II) complexes) and therefore no reports of their usage have been produced (Figure 1.8).[67]

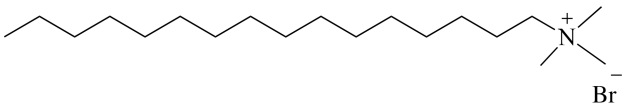

CTAB

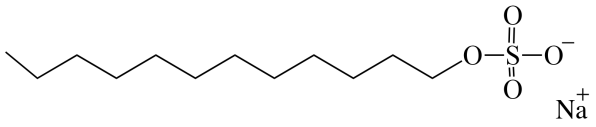

SDS

Figure 1.8 Typical ionic surfactants: cetrimonium bromide (CTAB) and sodium dodecyl sulfate (SDS)

Another important approach in ATRP miniemulsion systems is the use of reactive surfactants (*e.g.* poly(ethylene oxide)-*b*-polystyrene diblock copolymer (PEO-*b*-PSt-Br)), containing reactive double bonds and/or an initiating site, that are efficient for the stabilization of the latex particles, act as macroinitiators and avoid the possible surfactant migration from the latex upon film formation.[68]

1.8 References

1. Moad, G.; Rizzardo, E.; Thang, S. H., Toward Living Radical Polymerization, *Accounts of Chemical Research*, *41* (9), 1133-1142, 2008.
2. Matyjaszewski, K., General Concepts and History of Living Radical Polymerization. In *Handbook of Radical Polymerization*, Matyjaszewski, K.; Davis, T. P., Eds. John Wiley & Sons: 2002; pp 361-406.
3. Tsarevsky, N. V.; Matyjaszewski, K., "Green" Atom Transfer Radical Polymerization: From Process Design to Preparation of Well-Defined Environmentally Friendly Polymeric Materials, *Chemical Reviews*, *107* (6), 2270-2299, 2007.
4. Ebewele, R. O., Chain-Reaction (Addition) Polymerization. In *Polymer Science and Technology*, CRC Press: 2000.
5. Matyjaszewski, K., Atom Transfer Radical Polymerization (ATRP): Current Status and Future Perspectives, *Macromolecules*, *45* (10), 4015-4039, 2012.
6. Matyjaszewski, K.; Xia, J., Fundamentals of Atom Transfer Radical Polymerization. In *Handbook of Radical Polymerization*, Matyjaszewski, K.; Davis, T. P., Eds. John Wiley & Sons: 2002; pp 523-628.
7. Percec, V.; Tirrell, D. A., Living or controlled?, *Journal of Polymer Science Part A: Polymer Chemistry*, *38* (10), 1705-1705, 2000.
8. Matyjaszewski, K.; Tsarevsky, N. V., Macromolecular Engineering by Atom Transfer Radical Polymerization, *Journal of the American Chemical Society*, *136* (18), 6513-6533, 2014.
9. Allan, L. E. N.; Perry, M. R.; Shaver, M. P., Organometallic mediated radical polymerization, *Progress in Polymer Science*, *37* (1), 127-156, 2012.
10. Fischer, H., The Persistent Radical Effect: A Principle for Selective Radical Reactions and Living Radical Polymerizations, *Chemical reviews*, *101* (12), 3581-3610, 2001.
11. Braunecker, W. A.; Matyjaszewski, K., Controlled/living radical polymerization: Features, developments, and perspectives, *Progress in Polymer Science*, *32* (1), 93-146, 2007.
12. Kamigaito, M.; Ando, T.; Sawamoto, M., Metal-catalyzed living radical polymerization, *Chem Rev*, *101* (12), 3689-746, 2001.
13. Chiefari, J.; Chong, Y. K.; Ercole, F.; Krstina, J.; Jeffery, J.; Le, T. P. T.; Mayadunne, R. T. A.; Meijs, G. F.; Moad, C. L.; Moad, G.; Rizzardo, E.; Thang, S. H., Living Free-Radical Polymerization by Reversible Addition−Fragmentation Chain Transfer: The RAFT Process, *Macromolecules*, *31* (16), 5559-5562, 1998.
14. Moad, G.; Rizzardo, E.; Thang, S. H., Living Radical Polymerization by the RAFT Process – A Third Update, *Australian Journal of Chemistry*, *65* (8), 985-1076, 2012.
15. Matyjaszewski, K.; Paik, H.-j.; Zhou, P.; Diamanti, S. J., Determination of Activation and Deactivation Rate Constants of Model Compounds in Atom Transfer Radical Polymerization1, *Macromolecules*, *34* (15), 5125-5131, 2001.
16. Zhou, L. L.; Zhang, Z. B.; Cheng, Z. P.; Zhou, N. C.; Zhu, J.; Zhang, W.; Zhu, X. L., Fe(0) Powder/CuBr2-Mediated "Living"/Controlled Radical Polymerization of Methyl Methacrylate and Styrene at Ambient Temperature, *Macromolecular Chemistry and Physics*, *213* (4), 439-446, 2012.

17. Al-Harthi, M.; Sardashti, A.; Soares, J. B. P.; Simon, L. C., Atom transfer radical polymerization (ATRP) of styrene and acrylonitrile with monofunctional and bifunctional initiators, *Polymer*, *48* (7), 1954-1961, 2007.
18. Ando, T.; Kamigaito, M.; Sawamoto, M., Iron(II) Chloride Complex for Living Radical Polymerization of Methyl Methacrylate1, *Macromolecules*, *30* (16), 4507-4510, 1997.
19. Biedroń, T.; Kubisa, P., Atom-Transfer Radical Polymerization of Acrylates in an Ionic Liquid, *Macromolecular Rapid Communications*, *22* (15), 1237-1242, 2001.
20. Matyjaszewski, K.; Nakagawa, Y.; Jasieczek, C. B., Polymerization of n-Butyl Acrylate by Atom Transfer Radical Polymerization. Remarkable Effect of Ethylene Carbonate and Other Solvents, *Macromolecules*, *31* (5), 1535-1541, 1998.
21. Percec, V.; Guliashvili, T.; Ladislaw, J. S.; Wistrand, A.; Stjerndahl, A.; Sienkowska, M. J.; Monteiro, M. J.; Sahoo, S., Ultrafast synthesis of ultrahigh molar mass polymers by metal-catalyzed living radical polymerization of acrylates, methacrylates, and vinyl chloride mediated by SET at 25 degrees C, *J Am Chem Soc*, *128* (43), 14156-65, 2006.
22. Wever, D. A. Z.; Raffa, P.; Picchioni, F.; Broekhuis, A. A., Acrylamide Homopolymers and Acrylamide–N-Isopropylacrylamide Block Copolymers by Atomic Transfer Radical Polymerization in Water, *Macromolecules*, *45* (10), 4040-4045, 2012.
23. Yu, H. S., *Copper-mediated Atom Transfer Radical Polymerization of 1,3-Dienes*. University of Connecticut: 2014.
24. Ayres, N., Atom Transfer Radical Polymerization: A Robust and Versatile Route for Polymer Synthesis, *Polymer Reviews*, *51* (2), 138-162, 2011.
25. Cordeiro, R. A.; Rocha, N.; Mendes, J. P.; Matyjaszewski, K.; Guliashvili, T.; Serra, A. C.; Coelho, J. F. J., Synthesis of well-defined poly(2-(dimethylamino)ethyl methacrylate) under mild conditions and its co-polymers with cholesterol and PEG using Fe(0)/Cu(ii) based SARA ATRP, *Polymer Chemistry*, *4* (10), 3088-3097, 2013.
26. Tang, W.; Kwak, Y.; Braunecker, W.; Tsarevsky, N. V.; Coote, M. L.; Matyjaszewski, K., Understanding Atom Transfer Radical Polymerization: Effect of Ligand and Initiator Structures on the Equilibrium Constants, *Journal of the American Chemical Society*, *130* (32), 10702-10713, 2008.
27. Horn, M.; Matyjaszewski, K., Solvent Effects on the Activation Rate Constant in Atom Transfer Radical Polymerization, *Macromolecules*, *46* (9), 3350-3357, 2013.
28. Braunecker, W. A.; Tsarevsky, N. V.; Gennaro, A.; Matyjaszewski, K., Thermodynamic Components of the Atom Transfer Radical Polymerization Equilibrium: Quantifying Solvent Effects, *Macromolecules*, *42* (17), 6348-6360, 2009.
29. Lutz, J.-F.; Jakubowski, W.; Matyjaszewski, K., Controlled/Living Radical Polymerization of Methacrylic Monomers in the Presence of Lewis Acids: Influence on Tacticity, *Macromolecular Rapid Communications*, *25* (3), 486-492, 2004.
30. Tsarevsky, N. V.; Matyjaszewski, K., "Green" atom transfer radical polymerization: from process design to preparation of well-defined environmentally friendly polymeric materials, *Chemical reviews*, *107* (6), 2270-99, 2007.
31. Tsarevsky, N. V.; Matyjaszewski, K., Environmentally benign atom transfer radical polymerization: Towards “green” processes and materials, *Journal of Polymer Science Part A: Polymer Chemistry*, *44* (17), 5098-5112, 2006.
32. Mendonca, P. V.; Serra, A. C.; Coelho, J. F. J.; Popov, A. V.; Guliashvili, T., Ambient temperature rapid ATRP of methyl acrylate, methyl methacrylate and

styrene in polar solvents with mixed transition metal catalyst system, *European Polymer Journal*, *47* (7), 1460-1466, 2011.
33. Rocha, N.; Mendonca, P. V.; Mendes, J. P.; Simoes, P. N.; Popov, A. V.; Guliashvili, T.; Serra, A. C.; Coelho, J. F. J., Facile Synthesis of Well-Defined Telechelic Alkyne-Terminated Polystyrene in Polar Media Using ATRP With Mixed Fe/Cu Transition Metal Catalyst, *Macromolecular Chemistry and Physics*, *214* (1), 76-84, 2013.
34. Abreu, C. M. R.; Mendonca, P. V.; Serra, A. C.; Popov, A. V.; Matyjaszewski, K.; Guliashvili, T.; Coelho, J. F. J., Inorganic Sulfites: Efficient Reducing Agents and Supplemental Activators for Atom Transfer Radical Polymerization, *ACS Macro Letters*, *1* (11), 1308-1311, 2012.
35. Gois, J. R.; Konkolewicz, D.; Popov, A.; Guliashvili, T.; Matyjaszewski, K.; Serra, A. C.; Coelho, J., Improvement of the Control over SARA ATRP of 2-(Diisopropylamino)ethyl Methacrylate by Slow and Continuous Addition of Sodium Dithionite, *Polymer Chemistry*, in press, 2014.
36. Mendes, J. P.; Branco, F.; Abreu, C. M. R.; Mendonça, P. V.; Popov, A. V.; Guliashvili, T.; Serra, A. C.; Coelho, J. F. J., Synergistic Effect of 1-Butyl-3-methylimidazolium Hexafluorophosphate and DMSO in the SARA ATRP at Room Temperature Affording Very Fast Reactions and Polymers with Very Low Dispersity, *ACS Macro Letters*, *3* (6), 544-547, 2014.
37. Mendes, J. P.; Branco, F.; Abreu, C. M. R.; Mendonça, P. V.; Serra, A. C.; Popov, A. V.; Guliashvili, T.; Coelho, J. F. J., Sulfolane: an Efficient and Universal Solvent for Copper-Mediated Atom Transfer Radical (co)Polymerization of Acrylates, Methacrylates, Styrene, and Vinyl Chloride, *ACS Macro Letters*, *3* (9), 858-861, 2014.
38. Abreu, C. M. R.; Mendonca, P. V.; Serra, A. C.; Coelho, J. F. J.; Popov, A. V.; Guliashvili, T., Accelerated Ambient-Temperature ATRP of Methyl Acrylate in Alcohol-Water Solutions with a Mixed Transition-Metal Catalyst System, *Macromolecular Chemistry and Physics*, *213* (16), 1677-1687, 2012.
39. Abreu, C. M. R.; Serra, A. C.; Popov, A. V.; Matyjaszewski, K.; Guliashvili, T.; Coelho, J. F. J., Ambient temperature rapid SARA ATRP of acrylates and methacrylates in alcohol-water solutions mediated by a mixed sulfite/Cu(ii)Br2 catalytic system, *Polymer Chemistry*, *4* (23), 5629-5636, 2013.
40. Jakubowski, W.; Matyjaszewski, K., Activators Regenerated by Electron Transfer for Atom-Transfer Radical Polymerization of (Meth)acrylates and Related Block Copolymers, *Angewandte Chemie*, *118* (27), 4594-4598, 2006.
41. Magenau, A. J. D.; Strandwitz, N. C.; Gennaro, A.; Matyjaszewski, K., Electrochemically Mediated Atom Transfer Radical Polymerization, *Science*, *332* (6025), 81-84, 2011.
42. Zhang, Y.; Wang, Y.; Matyjaszewski, K., ATRP of Methyl Acrylate with Metallic Zinc, Magnesium, and Iron as Reducing Agents and Supplemental Activators, *Macromolecules*, *44* (4), 683-685, 2011.
43. Treat, N. J.; Sprafke, H.; Kramer, J. W.; Clark, P. G.; Barton, B. E.; Read de Alaniz, J.; Fors, B. P.; Hawker, C. J., Metal-Free Atom Transfer Radical Polymerization, *Journal of the American Chemical Society*, *136* (45), 16096-16101, 2014.
44. Percec, V.; Barboiu, B., "Living" Radical Polymerization of Styrene Initiated by Arenesulfonyl Chlorides and CuI(bpy)nCl, *Macromolecules*, *28* (23), 7970-7972, 1995.

45. Percec, V.; Grigoras, C., Catalytic effect of ionic liquids in the Cu2O/2,2′ - bipyridine catalyzed living radical polymerization of methyl methacrylate initiated with arenesulfonyl chlorides, *Journal of Polymer Science Part A: Polymer Chemistry*, *43* (22), 5609-5619, 2005.
46. Anastasaki, A.; Nikolaou, V.; Nurumbetov, G.; Wilson, P.; Kempe, K.; Quinn, J. F.; Davis, T. P.; Whittaker, M. R.; Haddleton, D. M., Cu(0)-Mediated Living Radical Polymerization: A Versatile Tool for Materials Synthesis, *Chemical reviews*, *116* (3), 835-877, 2016.
47. Matyjaszewski, K.; Tsarevsky, N. V.; Braunecker, W. A.; Dong, H.; Huang, J.; Jakubowski, W.; Kwak, Y.; Nicolay, R.; Tang, W.; Yoon, J. A., Role of Cu0 in Controlled/"Living" Radical Polymerization, *Macromolecules*, *40* (22), 7795-7806, 2007.
48. Konkolewicz, D.; Wang, Y.; Krys, P.; Zhong, M.; Isse, A. A.; Gennaro, A.; Matyjaszewski, K., SARA ATRP or SET-LRP. End of controversy?, *Polymer Chemistry*, *5* (15), 4396-4417, 2014.
49. Konkolewicz, D.; Wang, Y.; Zhong, M.; Krys, P.; Isse, A. A.; Gennaro, A.; Matyjaszewski, K., Reversible-Deactivation Radical Polymerization in the Presence of Metallic Copper. A Critical Assessment of the SARA ATRP and SET-LRP Mechanisms, *Macromolecules*, *46* (22), 8749-8772, 2013.
50. Boyer, C.; Corrigan, N. A.; Jung, K.; Nguyen, D.; Nguyen, T.-K.; Adnan, N. N. M.; Oliver, S.; Shanmugam, S.; Yeow, J., Copper-Mediated Living Radical Polymerization (Atom Transfer Radical Polymerization and Copper(0) Mediated Polymerization): From Fundamentals to Bioapplications, *Chemical reviews*, *116* (4), 1803-1949, 2016.
51. Capello, C.; Fischer, U.; Hungerbuhler, K., What is a green solvent? A comprehensive framework for the environmental assessment of solvents, *Green Chemistry*, *9* (9), 927-934, 2007.
52. Erdmenger, T.; Guerrero-Sanchez, C.; Vitz, J.; Hoogenboom, R.; Schubert, U. S., Recent developments in the utilization of green solvents in polymer chemistry, *Chemical Society Reviews*, *39* (8), 3317-3333, 2010.
53. Zhang, Q.; De Oliveira Vigier, K.; Royer, S.; Jerome, F., Deep eutectic solvents: syntheses, properties and applications, *Chemical Society Reviews*, *41* (21), 7108-7146, 2012.
54. Fukaya, Y.; Iizuka, Y.; Sekikawa, K.; Ohno, H., Bio ionic liquids: room temperature ionic liquids composed wholly of biomaterials, *Green Chemistry*, *9* (11), 1155-1157, 2007.
55. Dai, Y.; van Spronsen, J.; Witkamp, G.-J.; Verpoorte, R.; Choi, Y. H., Natural deep eutectic solvents as new potential media for green technology, *Analytica Chimica Acta*, *766*, 61-68, 2013.
56. Abbott, A. P.; Cullis, P. M.; Gibson, M. J.; Harris, R. C.; Raven, E., Extraction of glycerol from biodiesel into a eutectic based ionic liquid, *Green Chemistry*, *9* (8), 868-872, 2007.
57. Ferlin, N.; Courty, M.; Gatard, S.; Spulak, M.; Quilty, B.; Beadham, I.; Ghavre, M.; Haiß, A.; Kümmerer, K.; Gathergood, N.; Bouquillon, S., Biomass derived ionic liquids: synthesis from natural organic acids, characterization, toxicity, biodegradation and use as solvents for catalytic hydrogenation processes, *Tetrahedron*, *69* (30), 6150-6161, 2013.
58. Kubisa, P., Application of ionic liquids as solvents for polymerization processes, *Progress in Polymer Science*, *29* (1), 3-12, 2004.

59. Deetlefs, M.; Seddon, K. R., Assessing the greenness of some typical laboratory ionic liquid preparations, *Green Chemistry*, *12* (1), 17-30, 2010.
60. Abbott, A. P.; Boothby, D.; Capper, G.; Davies, D. L.; Rasheed, R. K., Deep Eutectic Solvents Formed between Choline Chloride and Carboxylic Acids: Versatile Alternatives to Ionic Liquids, *Journal of the American Chemical Society*, *126* (29), 9142-9147, 2004.
61. Carmichael, A. J.; Haddleton, D. M.; Bon, S. A. F.; Seddon, K. R., Copper() mediated living radical polymerisation in an ionic liquid, *Chemical Communications*, (14), 1237-1238, 2000.
62. Coca, S.; Jasieczek, C. B.; Beers, K. L.; Matyjaszewski, K., Polymerization of acrylates by atom transfer radical polymerization. Homopolymerization of 2-hydroxyethyl acrylate, *Journal of Polymer Science Part A: Polymer Chemistry*, *36* (9), 1417-1424, 1998.
63. Wang, X. S.; Armes, S. P., Facile Atom Transfer Radical Polymerization of Methoxy-Capped Oligo(ethylene glycol) Methacrylate in Aqueous Media at Ambient Temperature, *Macromolecules*, *33* (18), 6640-6647, 2000.
64. Wang, X. S.; F. Lascelles, S.; A. Jackson, R.; P. Armes, S., Facile synthesis of well-defined water-soluble polymers via atom transfer radical polymerization in aqueous media at ambient temperature, *Chemical Communications*, (18), 1817-1818, 1999.
65. Min, K.; Matyjaszewski, K., Atom Transfer Radical Polymerization in Microemulsion, *Macromolecules*, *38* (20), 8131-8134, 2005.
66. Bon, S. A. F.; Bosveld, M.; Klumperman, B.; German, A. L., Controlled Radical Polymerization in Emulsion, *Macromolecules*, *30* (2), 324-326, 1997.
67. Min, K.; Matyjaszewski, K., Atom transfer radical polymerization in aqueous dispersed media, *Central European Journal of Chemistry*, *7* (4), 657-674, 2009.
68. Qiu, J.; Charleux, B.; Matyjaszewski, K., Controlled/living radical polymerization in aqueous media: homogeneous and heterogeneous systems, *Progress in Polymer Science*, *26* (10), 2083-2134, 2001.
69. Limer, A.; Heming, A.; Shirley, I.; Haddleton, D., Living radical polymerisation in heterogeneous conditions—suspension polymerisation, *European Polymer Journal*, *41* (4), 805-816, 2005.
70. Cunningham, M. F., Living/controlled radical polymerizations in dispersed phase systems, *Progress in Polymer Science*, *27* (6), 1039-1067, 2002.
71. IUPAC. Compendium of Chemical Terminology, 2nd ed. (the "Gold Book"). Compiled by A. D. McNaught and A. Wilkinson. Blackwell Scientific Publications, Oxford (1997). XML on-line corrected version: http://goldbook.iupac.org (2006) created by M. Nic, J. Jirat, B. Kosata; updates compiled by A. Jenkins. ISBN 0-9678550-9-8. doi:10.1351/goldbook. Last update: 2014-02-24; version: 2.3.3. DOI of this term: doi:10.1351/goldbook.C01395.
72. Landfester, K., The Generation of Nanoparticles in Miniemulsions, *Advanced Materials*, *13* (10), 765-768, 2001.
73. Landfester, K.; Ramírez, L., Encapsulated magnetite particles for biomedical application, *Journal of Physics: Condensed Matter*, *15* (15), S1345-S1361, 2003.
74. Zetterlund, P. B.; Kagawa, Y.; Okubo, M., Controlled/Living Radical Polymerization in Dispersed Systems, *Chemical reviews*, *108* (9), 3747-3794, 2008.
75. Kagawa, Y.; Kawasaki, M.; Zetterlund, P. B.; Minami, H.; Okubo, M., Atom Transfer Radical Polymerization of iso-Butyl Methacrylate in Microemulsion with Cationic and Non-Ionic Emulsifiers, *Macromolecular Rapid Communications*, *28* (24), 2354-2360, 2007.

76. Min, K.; Matyjaszewski, K., Atom Transfer Radical Dispersion Polymerization of Styrene in Ethanol, *Macromolecules*, *40* (20), 7217-7222, 2007.
77. Wan, W.-M.; Pan, C.-Y., Atom Transfer Radical Dispersion Polymerization in an Ethanol/Water Mixture, *Macromolecules*, *40* (25), 8897-8905, 2007.
78. Averick, S. E.; Paredes, E.; Irastorza, A.; Shrivats, A. R.; Srinivasan, A.; Siegwart, D. J.; Magenau, A. J.; Cho, H. Y.; Hsu, E.; Averick, A. A.; Kim, J.; Liu, S.; Hollinger, J. O.; Das, S. R.; Matyjaszewski, K., Preparation of Cationic Nanogels for Nucleic Acid Delivery, *Biomacromolecules*, *13* (11), 3445-3449, 2012.
79. Zetterlund, P. B.; Thickett, S. C.; Perrier, S.; Bourgeat-Lami, E.; Lansalot, M., Controlled/Living Radical Polymerization in Dispersed Systems: An Update, *Chemical reviews*, *115* (18), 9745-9800, 2015.
80. Jennings, J.; He, G.; Howdle, S. M.; Zetterlund, P. B., Block copolymer synthesis by controlled/living radical polymerisation in heterogeneous systems, *Chemical Society Reviews*, *45* (18), 5055-5084, 2016.
81. Cunningham, M. F., Controlled/living radical polymerization in aqueous dispersed systems, *Progress in Polymer Science*, *33* (4), 365-398, 2008.
82. Kagawa, Y.; Zetterlund, P. B.; Minami, H.; Okubo, M., Atom Transfer Radical Polymerization in Miniemulsion: Partitioning Effects of Copper(I) and Copper(II) on Polymerization Rate, Livingness, and Molecular Weight Distribution, *Macromolecules*, *40* (9), 3062-3069, 2007.
83. Levere, M. E.; Nguyen, N. H.; Percec, V., No Reduction of CuBr2 during Cu(0)-Catalyzed Living Radical Polymerization of Methyl Acrylate in DMSO at 25 °C, *Macromolecules*, *45* (20), 8267-8274, 2012.

Part II

Synthesis Method

This chapter is a compilation of articles published in the scope of the PhD work.

Chapter 2

Sulfolane – an Efficient and Universal Solvent for Copper-Mediated Atom Transfer Radical (co)Polymerization of Acrylates, Methacrylates, Styrene and Vinyl Chloride.

This chapter is published in: **Mendes, J. P**.; Branco, F.; Abreu, C. M. R.; Mendonça, P. V.; Serra, A. C.; Popov, A. V.; Guliashvili, T.; Coelho, J. F. J., "*Sulfolane: an Efficient and Universal Solvent for Copper-Mediated Atom Transfer Radical (co)Polymerization of Acrylates, Methacrylates, Styrene, and Vinyl Chloride"*, *ACS Macro Letters***,** *3* (9), 858-861, 2014. A small part of this subchapter also contains information published in: Rocha, N.; Mendonca, P. V.; **Mendes, J. P**.; Simoes, P. N.; Popov, A. V.; Guliashvili, T.; Serra, A. C.; Coelho, J. F. J., "*Facile Synthesis of Well-Defined Telechelic Alkyne-Terminated Polystyrene in Polar Media Using ATRP With Mixed Fe/Cu Transition Metal Catalyst"*, Macromolecular Chemistry and Physics, 214 (1), 76-84, 2013.

2.1 Abstract

A very fast and controlled ATRP of acrylates, methacrylates, styrene and vinyl chloride is reported in a single dipolar aprotic solvent, sulfolane, with the use of ppm amount of the copper catalyst. The observed rates of polymerization (k_p^{app}) of the studied monomers are similar to those reported using DMSO and other polar solvents typically employed in single electron transfer (SET)-mediated ATRP processes. The possibility of the controlled synthesis of a diversity of block copolymers in sulfolane using a straightforward method is also demonstrated. As a proof-of-concept, ABA type block copolymers of polystyrene-*b*-poly(vinyl chloride)-*b*-polystyrene and poly(methyl acrylate)-*b*-poly(vinylchloride)-*b*-poly(methyl acrylate) were prepared for the first time using a RDRP method in a unique dipolar aprotic solvent. The quantitative preservation of halide chain-ends in the synthesized polymers was confirmed by ^{1}H NMR and MALDI-TOF analysis as well as by the complete shift of the SEC traces during polymeric macroinitiator chain extension experiments. The results presented in this work establish an innovative and robust system to afford a vast portfolio of (co)polymers in a single widely used industrial solvent.

2.2 Introduction

ATRP is a versatile, efficient and robust method that has opened unprecedented opportunities to synthesize (co)polymers with controlled molecular weight, composition, architecture, high chain-end functionality and $Đ$.[1] ATRP is mediated by a dynamic equilibrium between dormant alkyl halide chains and growing radicals, which is catalyzed by a transition metal/ligand complex.[2] Traditionally, metal catalyst concentration greater than 10000 parts per million (ppm) were required to perform normal ATRP reactions. Recently, new variations of ATRP systems have been developed, namely activators regenerated by electron transfer (ARGET) ATRP,[3] initiators for continuous activator regeneration (ICAR) ATRP,[4] electrochemically mediated (*e*-ATRP) ATRP[5] and supplemental activator and reducing agent (SARA) ATRP.[6-7] These new techniques allow the use of very low concentrations of metal catalyst (< 100 ppm), maintaining the control over the polymerization. Among these

methods, SARA ATRP has demonstrated to be a very attractive technique using heterogeneous[7-9] zero valent metal catalysts as both supplemental activator and reducing agent that can be easily removed from the reaction medium.[6-11] Also, Food and Drug Administration (FDA) approved inorganic sulfites, in combination with small amounts of soluble copper, proved to successfully mediate the SARA ATRP of several monomers in eco-friendly conditions.[12-16]

SARA ATRP has been used for the preparation of well-defined block copolymers in various solvents, such as water,[17] alcohol/water mixtures,[8, 13, 16, 18] and anisole.[15] However, due to solubility issues and system particularities, it is sometimes difficult to find appropriate solvents to perform copolymerization of a wide range of monomers using the same ATRP system without polymer isolation.

The SARA ATRP (originally called as SET living radical polymerization or SET-LRP) of activated and non-activated monomers catalyzed by copper complexes has become very popular method for the preparation of complex polymer architectures. It should be noted that the proposed mechanisms of SET-LRP and SARA ATRP processes are based on the same elemental microsteps,[19] the only difference being the identification of the major/minor contributing reactions.

DMSO has proven to be a suitable solvent for the SARA ATRP of MA[11] and MMA,[11] as well as for the non-activated monomer VC. For the polymerization of other relevant monomers such as St, DMSO is not an appropriate solvent due to the very poor solubility for polystyrene. Usually, St is polymerized in dimethylformamide (DMF),[7] toluene,[20] anisole[21] or in bulk.[22] Thus, the possibility of having a single universal solvent for the preparation of well-defined block copolymers able to polymerize a wide range of monomer families is highly desirable. Other disadvantage of using DMSO in ATRP reactions is the very low efficiency of universal ATRP initiators such as sulfonyl chloride derivatives (e.g.: tosyl chloride), due to their rapid reaction at room temperature.[23] Since the first report of ultrafast synthesis of high molar mass polymers mediated by SET-LRP in DMSO, the careful selection of solvent in addition to metal catalyst/monomer/initiator /polymer systems has become a very important issue for the successful control of ATRP polymerization.

Sulfolane (2,3,4,5-tetrahydrothiophene-1,1-dioxide) is a dipolar aprotic industrial solvent commonly used in organic synthesis, gas purification and oil refining.[24] This solvent is completely miscible with water and with most polar and several nonpolar solvents (except alkanes). It is also completely miscible with aromatic hydrocarbons

and can also dissolve polystyrene. Compared to other dipolar aprotic solvents, sulfolane presents several advantages, such as: high dipole moment, high relative permittivity and a high Hildebrand solubility parameter.[2, 8-9, 13, 24-25] Therefore, an elevated solvency power for the reactions involving polarizable intermediated (like in SET mediated reactions, for example) is expected when using sulfolane as the solvent. Sulfolane is also very stable towards various reactive organic and inorganic solvents and reagents and has the lowest penetration trough skin parameter (compared to other dipolar aprotic solvents).[24] While sulfolane is widely used in organic synthesis and step-growth polymerizations in place of DMSO, DMF or other solvents, this solvent has never been reported as a suitable solvent for the ATRP or related processes.

In this communication, we present for the first time the use of sulfolane as the single solvent for the successful Cu(0)-mediated SARA ATRP of MA, MMA, St and VC. Several reaction parameters were investigated in the polymerization of each monomer to allow good control. As a proof-of-concept, the reported system was used to prepare PMA-*b*-PVC-*b*-PMA and PS-*b*-PVC-*b*-PS block copolymers.

2.3 Experimental Section

2.3.1 Materials

Copper(II) bromide ($CuBr_2$) (+ 99 % extra pure, anhydrous; Acros), copper(II) chloride ($CuCl_2$) (max. 0.0008 % AS; Merck), zerovalent iron powder (Fe(0)) (99 %, ~ 70 mesh, Acros), metallic copper (Cu(0) wire) (≥ 99.9 %; Sigma-Aldrich), deuterated chloroform ($CDCl_3$) (+ 1 % tetramethylsilane (TMS); Euriso-top), deuterated tetrahydrofuran (THF-d_8) (99.5 %; Euriso-top), dimethyl sulfoxide (DMSO) (+ 99.8 % extra pure; Acros), sulfolane (+ 99 %; Acros), ethyl 2-bromoisobutyrate (EBiB) (98 %; Aldrich), p-toluenesulfonyl chloride (TsCl) (98 %; Merck), ethyl α-bromophenylacetate (EBPA) (97 %; Aldrich), bromoform ($CHBr_3$) (+ 99 % stabilized; Acros), tris(2-aminoethyl)amine (TREN) (96 %; Sigma-Aldrich), N,N,N′,N″,N″-pentamethyldiethylenetriamine (PMDETA) (99 %; Aldrich), 2,2′-bipyridine (bpy) (> 99 %, Acros) polystyrene (PS) standards (Polymer Laboratories), 2-(4-hydroxyphenylazo)benzoic acid (HABA) (99.5 %; Sigma-Aldrich) and 2,5-dihydroxybenzoic acid (DHB) (> 99 %; Sigma-Aldrich) were used as received. High-performance liquid chromatography (HPLC) grade THF (Panreac) was filtered (0.2 μm filter) under reduced pressure before use.

Methyl acrylate (MA) (99 % stabilized; Acros), methyl methacrylate (MMA) (99 % stabilized; Acros) and styrene (Sty) (+ 99 %; Sigma-Aldrich), were passed over a sand/alumina column before use to remove the radical inhibitors. Vinyl chloride (VC) (99 %) was kindly supplied by CIRES Lda, Portugal.

Me_6TREN was synthesized according to the procedure described in the literature.[26]

Metallic copper (Cu(0), d = 1 mm, Sigma Aldrich) was washed with nitric acid and subsequently rinsed with acetone and dried under a stream of nitrogen.

2.3.2 Techniques

The chromatographic parameters of the samples were determined using high performance size-exclusion chromatography (HPSEC); Viscotek (Viscotek TDAmax) with a differential viscometer (DV); right-angle laser-light scattering (RALLS) (Viscotek); low-angle laser-light scattering (LALLS) (Viscotek) and refractive index (RI) detectors. The column consisted of a PL 10 mm guard column (50 × 7.5 mm^2) followed by one Viscotek T200 column (6 μm), one MIXED-E PLgel column (3 μm) and one MIXED-C PLgel column (5 μm). A HPLC dual piston pump was set at a flow rate of 1 mL/min. The eluent, THF, was previously filtered through a 0.2 μm filter. The system was also equipped with an on-line degasser. The tests were done at 30 ºC using an Elder CH-150 heater. Before the injection (100 μL), the samples were filtered through a polytetrafluoroethylene (PTFE) membrane with 0.2 μm pore. The system was calibrated with narrow PS standards. The *dn/dc* was determined as 0.063 for PMA, 0.105 for PVC, 0.185 for PS and 0.089 for PMMA. The M_n^{SEC} and $Đ$ of the synthesized polymers and block copolymers were determined by multidetectors calibration using OmniSEC software version: 4.6.1.354.

400 MHz ^1H NMR spectra of the reaction mixture samples of MA, MMA and St polymerizations were recorded on a Bruker Avance III 400 MHz spectrometer, with a 5-mm TIX triple resonance detection probe, in $CDCl_3$ with TMS as an internal standard.

600 MHz ^1H NMR spectra of the reaction mixture samples of VC polymerization were recorded with a Varian VNMRS 600 MHz spectrometer, with a warm 3 mm PFG triple resonance indirect detection probe, in THF-d_8 with TMS as an internal standard. Monomer conversions were determined by integration of monomer and polymer peaks using MestRenova software version: 6.0.2-5475.

The PMA and PVC samples were dissolved in THF at a concentration of 10 mg/mL for the MALDI-TOF-MS analysis and DHB and HABA (0.05 M in THF) were used as matrices. The dried-droplet samples preparation technique was used to obtain a 1:1 ratio (sample/matrix); an aliquot of 1 μL of each sample was directly spotted on the MTP AnchorChip TM 600/384 TF MALDI target, BrukerDaltonik (Bremen Germany) and, before the sample dried, 1 μL of matrix solution in THF was added and the mixture was dried at room temperature, to allow matrix crystallization. External mass calibration was performed with a peptide calibration standard (PSCII) for the range 700-3000 (9 mass calibration points), 0.5 μL of the calibration solution and matrix previously mixed in an Eppendorf tube (1:2, v/v) were applied directly on the target and allowed to dry at room temperature. Mass spectra were recorded using an Autoflex III smartbeam 1 MALDI-TOF-MS mass spectrometer BrukerDaltonik (Bremen Germany) operating in the linear and reflectron positive ion mode. Ions were formed upon irradiation by a smartbeam laser using a frequency of 200 Hz. Each mass spectrum was produced by averaging 2500 laser shots collected across the whole sample spot surface by screening in the range m/z 500-13000 for PVC and in the range m/z 500-23000 for PMA. The laser irradiance was set to 35-40 % (relative scale 0-100) arbitrary units according to the corresponding threshold required for the applied matrix systems.

The ultraviolet-visible studies were performed with a Jasco V-530 spectrophotometer. The analyses were carried in the 350 – 1100 nm range at 30 ºC.

2.3.3 Procedures

2.3.3.1 Typical procedure for the $[Cu(0)]_0/[CuBr_2]_0/[Me_6TREN]_0$ = Cu(0) wire/0.1/1.1 catalyzed SARA ATRP of MA (DP = 222)

Cu(0) wire (590 mg) and a mixture of $CuBr_2$ (3.51 mg, 0.02 mmol), Me_6TREN (39.76 mg, 0.17 mmol) and sulfolane (1.58 mL) (previously bubbled with nitrogen for about 15 minutes) were placed in a Schlenk tube reactor. A mixture of MA (3.16 mL, 34.90 mmol) and EBiB (30.62 mg, 0.16 mmol) was added to the reactor that was sealed, by using a rubber septum, and frozen in liquid nitrogen. The Schlenk tube reactor containing the reaction mixture was deoxygenated with four freeze-vacuum-thaw cycles and purged with nitrogen. The reactor was placed in a water bath at 30 ºC with stirring (700 rpm). During the polymerization, different reaction mixture samples

were collected by using an airtight syringe and purging the side arm of the Schlenk tube reactor with nitrogen. The samples were analyzed by ^{1}H NMR spectroscopy to determine the monomer conversion and by SEC, to determine the average-number molecular weight (M_n^{SEC}) and dispersity ($Đ$) of the polymers.

2.3.3.2 Typical procedure for the $[Cu(0)]_0/[CuBr_2]_0/[bpy]_0$ = Cu(0) wire/0.1/2.2 catalyzed SARA ATRP of MMA (DP = 222)

For a typical polymerization of MMA, a mixture of Cu(0) wire (240 mg), $CuBr_2$ (3.16 mg, 0.014 mmol), bpy (46.38 mg, 0.30 mmol) and sulfolane (3.21 mL) (previously bubbled with nitrogen for about 15 minutes) was placed in a Schlenk tube reactor. A solution of EBPA (33.95 mg, 0.14 mmol) in MMA (3.21 mL, 30.0 mmol) was added to the reactor that was sealed, by using a rubber septum, and frozen in liquid nitrogen. The Schlenk tube reactor containing the reaction mixture was deoxygenated with four freeze-vacuum-thaw cycles and purged with nitrogen. The reactor was placed in a water bath at 40 ºC with stirring (700 rpm). During the polymerization, different reaction mixture samples were collected by using an airtight syringe and purging the side arm of the Schlenk tube reactor with nitrogen. The samples were analyzed by ^{1}H NMR spectroscopy to determine the monomer conversion and by SEC, to determine the M_n^{SEC} and $Đ$ of the polymers.

2.3.3.3 Typical procedure for the $[Cu(0)]_0/[CuBr_2]_0/[PMDETA]_0$ = Cu(0) wire/0/1.1 catalyzed ATRP of St (DP = 222)

A mixture of Cu(0) wire (335 mg), PMDETA (25.00 mg, 0.14 mmol) and sulfolane (1.66 mL) (previously bubbled with nitrogen for about 15 minutes) was placed in a Schlenk tube reactor. A solution of EBiB (25.27 mg, 0.13 mmol) in St (3.31 mL, 28.80 mmol) was added to the reactor that was sealed, by using a rubber septum, and frozen in liquid nitrogen. The Schlenk tube reactor containing the reaction mixture was deoxygenated with four freeze-vacuum-thaw cycles and purged with nitrogen. The reactor was placed in a water bath at 30 ºC with stirring (700 rpm). During the polymerization, different reaction mixture samples were collected by using an airtight syringe and purging the side arm of the Schlenk tube reactor with nitrogen. The samples were analyzed by ^{1}H NMR spectroscopy to determine the monomer conversion and by SEC, to determine the M_n^{SEC} and $Đ$ of the polymers.

2.3.3.4 Typical procedure for the $[Fe(0)]_0/[CuBr_2]_0/[Me_6TREN]_0$ = 1/0.1/1.1 catalyzed ATRP of Sty (DP = 125) in DMF.

The monomer (Sty) was purified in a sand/alumina column just before the reaction. A mixture of Fe(0) powder (11.7 mg, 0.209 mmol), $CuBr_2$ (4.7 mg, 0.021 mmol), Me_6TREN (53.0 mg, 0.230 mmol) and DMF (1.5 mL) (previously bubbled with nitrogen for about 15 minutes) was placed in a Schlenk tube reactor. A mixture of Sty (3.0 mL, 26.1 mmol) and EBiB (40.9 mg, 0.209 mmol) was added to the reactor that was sealed, by using a rubber septum, and frozen in liquid nitrogen. The Schlenk tube reactor containing the reaction mixture was deoxygenated with four freeze-vacuum-thaw cycles and purged with nitrogen. The Schlenk tube reactor was placed in an oil bath at 70 ºC with stirring (700 rpm). Different reaction mixture samples were collected during the polymerization by using an airtight syringe and purging the side arm of the Schlenk tube reactor with nitrogen. The samples were analyzed by ^1H NMR spectroscopy in order to determine the monomer conversion and by SEC, to determine de M_n^{SEC} and $Đ$ of the polymers.

2.3.3.5 Typical procedure for the $[Cu(0)]_0/[CuCl_2]_0/[PMDETA]_0$ = Cu(0) wire/0.1/1.1 catalyzed ATRP of St (DP = 222)

A mixture of $CuCl_2$ (2.30 mg, 0.013 mmol), PMDETA (24.73 mg, 0.14 mmol) and sulfolane (1.66 mL) (previously bubbled with nitrogen for about 15 minutes) was placed in a Schlenk tube reactor. A mixture of St (3.31 mL, 28.8 mmol) and $CHBr_3$ (34.73 mg, 0.13 mmol) was added to the reactor. Cu(0) wire (315 mg) was inserted in the reactor that was sealed, by using a rubber septum, and frozen in liquid nitrogen. The Schlenk tube reactor containing the reaction mixture was deoxygenated with four freeze-vacuum-thaw cycles and purged with nitrogen. The reactor was placed in an oil bath at 60 ºC with stirring (700 rpm). During the polymerization, different reaction mixture samples were collected by using an airtight syringe and purging the side arm of the Schlenk tube reactor with nitrogen. The samples were analyzed by ^1H NMR spectroscopy to determine the monomer conversion and by SEC, to determine the M_n^{SEC} and $Đ$ of the polymers.

2.3.3.6 Typical procedure for the $[Cu(0)]_0/[TREN]_0$ = Cu(0) wire/1 catalyzed SARA ATRP of VC (DP = 222)

A 50 mL Ace glass 8645#15 pressure tube, equipped with bushing and plunger valve, was charged with a mixture of $CHBr_3$ (86.43 mg, 0.33 mmol), TREN (50.19 mg, 0.33 mmol), Cu(0) wire (283 mg) and sulfolane (5 mL) (previously bubbled with nitrogen for about 15 min). The precondensed VC (5 mL, 72.8 mmol) was added to the tube. The exact amount of VC was determined gravimetrically. The tube was closed, submerged in liquid nitrogen and degassed through the plunger valve by applying reduced pressure and filling the tube with N_2 about 20 times. The valve was closed, and the tube reactor was placed in a water bath at 42 ºC with stirring (700 rpm). The reaction was stopped by plunging the tube into ice water. The tube was slowly opened, the excess of VC was distilled, and the mixture was precipitated into methanol. The polymer was separated by filtration and dried in a vacuum oven until constant weight was produced. The monomer conversion was determined gravimetrically. SEC was used for the determination of PVC´s M_n^{SEC} and $Đ$.

2.3.3.7 Typical procedure for chain extension of –Br terminated PMA

A PMA-Br macroinitiator obtained from a typical Cu(0)/$CuBr_2$/Me_6TREN-catalyzed SARA ATRP reaction was precipitated in water. The polymer was then dissolved in acetone, filtered through a sand/alumina column, to remove traces of the catalyst, and reprecipitated in water. The polymer was dried under vacuum until constant weight. MA (1.05 mL, 11.60 mmol) was added to the –Br terminated PMA macroinitiator (M_n^{SEC} = 4600 g.mol^{-1}; $Đ$= 1.16, 53.44 mg, 0.01 mmol) in a Schlenk tube reactor. A mixture of sulfolane (0.53 mL previously bubbled with nitrogen for about 15 min), Me_6TREN (2.94 mg, 0.01 mmol), and Cu(0) wire (233 mg) was added to the reactor that was sealed, by using a rubber septum, and frozen in liquid nitrogen. The Schlenk tube reactor containing the reaction mixture was deoxygenated with four freeze-vacuum-thaw cycles and purged with nitrogen. The Schlenk tube was placed in the water bath at 30 ºC with stirring (700 rpm) for 1.5 h.

2.3.3.8 Typical procedure for chain extension of –Br terminated PMMA

A PMMA-Br macroinitiator obtained from a typical Cu(0)/$CuBr_2$/Me_6TREN-catalyzed SARA ATRP reaction was precipitated in methanol. The polymer was then dissolved in THF, filtered through a sand/alumina column, to remove traces of the catalyst, and reprecipitated in methanol. The polymer was dried under vacuum until constant weight. (MMA (1.0 mL, 9.4 mmol) was added to the –Br terminated PMMA macroinitiator (M_n^{SEC} = 10 700 g.mol^{-1}; $Đ$= 1.05, 200.9 mg, 0.02 mmol) in a Schlenk tube reactor. A mixture of sulfolane (1.0 mL previously bubbled with nitrogen for about 15 min), bpy (6.45 mg, 0.04 mmol), and Cu(0) wire (230 mg) was added to the reactor that was sealed, by using a rubber septum, and frozen in liquid nitrogen. The Schlenk tube reactor containing the reaction mixture was deoxygenated with four freeze-vacuum-thaw cycles and purged with nitrogen. The Schlenk tube was placed in the water bath at 40 ºC with stirring (700 rpm) for 3.5 h.

2.3.3.9 Typical procedure for chain extension of –Br terminated PS

A PS-Br macroinitiator obtained from a typical Cu(0)/PMDETA catalyzed SARA ATRP reaction was precipitated in methanol. The polymer was then dissolved in THF, filtered through a sand/alumina column, to remove traces of the catalyst, and reprecipitated in methanol. St (0.55 mL, 4.8 mmol) was added to the –Br terminated PS macroinitiator (M_n^{SEC} = 3960 g.mol^{-1}; $Đ$= 1.36, 85.64 mg, 0.022 mmol) in a Schlenk tube reactor. A mixture of sulfolane (0.55mL previously bubbled with nitrogen for about 15 min), PMDETA (4.12 mg, 0.022 mmol) and Cu(0) wire (326 mg) was added to the reactor that was sealed, by using a rubber septum, and frozen in liquid nitrogen. The Schlenk tube reactor containing the reaction mixture was deoxygenated with four freeze-vacuum-thaw cycles and purged with nitrogen.The Schlenk tube reactor was placed in the oil bath at 60 ºC with stirring (700 rpm) for 7.5 h.

2.3.3.10 Typical procedure for the synthesis of PMA-*b*-PVC-*b*-PMA block copolymers by $[Cu(0)]_0/[Me_6TREN]_0$ = Cu(0) wire/1.1 catalyzed SARA ATRP

The α,ω-di(bromo)PVC macroinitiator was obtained from a typical Cu(0) wire/TREN catalyzed SARA ATRP reaction. After precipitation in methanol, the polymer was then dissolved in THF, filtered through a sand/alumina column, to remove traces of the catalyst, and reprecipitated in methanol again. The polymer was dried under vacuum until constant weight. A mixture of MA (3.0 mL, 33.3 mmol) and α,ω-di(bromo)PVC macroinitiator (M_n^{SEC} = 9100; $Đ$= 1.55; 505 mg, 0.056 mmol), previously dissolved in sulfolane (3.0 mL), was added to the recator.

Cu(0) wire (282 mg) and Me_6TREN (14.6 mg, 0.061 mmol) were added to the reactor that was sealed, by using a rubber septum, and frozen in liquid nitrogen. The Schlenk tube reactor was deoxygenated by five freeze-pump thaw cycles and purged with nitrogen. Then the reactor was placed in a water bath at 30 ºC with stirring (700 rpm). The reaction was stopped after 3 h and the mixture was analyzed by ^{1}H NMR spectroscopy in order to determine the MA conversion and by SEC, to determine the M_n^{SEC} and $Đ$ of the PMA-*b*-PVC-*b*-PMA block copolymer.

2.3.3.11 Typical procedure for the synthesis of PS-*b*-PVC-*b*-PS block copolymers by $[Cu(0)]_0/[PMDETA]_0$ = Cu(0) wire/1.1 catalyzed SARA ATRP

The α,ω-di(bromo)PVC macroinitiator was obtained from a typical Cu(0) wire/TREN catalyzed SARA ATRP reaction. After precipitation in methanol, the polymer was then dissolved in THF, filtered through a sand/alumina column, to remove traces of the catalyst, and reprecipitated in methanol. The polymer was dried under vacuum until constant weight. A mixture of St (3.0 mL, 26.1 mmol) and –Br terminated PVC macroinitiator (M_n^{SEC} = 9100; $Đ$= 1.55; 396 mg, 0.043 mmol), previously dissolved in sulfolane (3.0 mL), was added to the recator that was sealed, by using a rubber septum, and frozen in liquid nitrogen.

Cu(0) wire (2842 mg) and PMDETA (8.6 mg, 0.048 mmol) were added to the reactor. The Schlenk tube reactor was deoxygenated by five freeze-pump thaw cycles and purged with nitrogen. Then the reactor was placed in an oil bath at 60 ºC with stirring (700 rpm). The reaction was stopped after 16 h and the mixture was analyzed by ^{1}H

NMR spectroscopy in order to determine the St conversion and by SEC, to determine the M_n^{SEC} and $Đ$ of the PS-*b*-PVC-*b*-PS block copolymer.

2.3.3.12 Typical procedure for the synthesis of PMA-*b*-PVC-*b*-PMA block copolymers by "one-pot" $[Cu(0)]_0/[TREN]_0$ = Cu(0) wire/1 catalyzed SARA ATRP

A 50 mL Ace glass 8645#15 pressure tube, equipped with bushing and plunger valve, was charged with a mixture of $CHBr_3$ (230.14 mg, 0.87 mmol), TREN (133.16 mg, 0.87 mmol), Cu(0) wire (291.7 mg) and sulfolane (3.0 mL) (previously bubbled with nitrogen for about 15 min). The precondensed VC (3.0 mL, 43.7 mmol) was added to the tube. The exact amount of VC was determined gravimetrically. The tube was closed, submerged in liquid nitrogen and degassed through the plunger valve by applying reduced pressure and filling the tube with nitrogen about 20 times. The valve was closed, and the tube reactor was placed in a water bath at 42 °C with stirring (700 rpm). After 2 h, the reaction was stopped by plunging the tube into ice water. The tube was slowly opened and the excess VC was distilled. The monomer conversion were determined gravimetrically (62.2 %), and the M_n^{SEC} = 3900 and $Đ$= 1.69 were determined by SEC analysis in THF. A mixture of sulfolane (15.7 mL) and MA (15.7 mL, 174.8 mmol) was added to the same 50 mL Ace glass 8645#15 pressure tube (without any purification of the α,ω-di(bromo)PVC macroinitiator). The tube was closed, submerged in liquid nitrogen and degassed through the plunger valve by applying reduced pressure and filling the tube with nitrogen about 20 times. The valve was closed, and the tube reactor was placed in a water bath at 42 °C with stirring (700 rpm). The reaction was stopped after 1 h and the mixture was analyzed by ^{1}H NMR spectroscopy in order to determine the MA conversion and by SEC, to determine the M_n^{SEC} and $Đ$ of the PMA-*b*-PVC-*b*-PMA block copolymer.

2.3.3.13 UV-vis spectroscopic study of the catalytic systems

Cu(0) wire (l = 5 cm, d = 1 mm) and a magnetic stirrer were placed in a quartz UV-vis cell and purged with nitrogen. A mixture of $CuBr_2$ (4.2 mg, 19 μmol) and Me_6TREN (47.5 mg, 0.21 mmol) in the solvent (2.5 mL of DMSO or sulfolane) was bubbled with nitrogen for 20 min, to remove the oxygen. This solution was then added to the cuvette, which was sealed under nitrogen. The cuvette was placed in a

water bath at 30 ºC and several UV-vis spectra were recorded at different reaction times, in the 350 – 1100 nm range.

2.4 Results and discussion

Preliminary experiments were carried out for the SARA ATRP of MA catalyzed by Cu(0) wire in sulfolane (Table 2.1 and Figure 2.1).

Table 2.1 Kinetic data for the SARA ATRP of MA. Conditions: $[MA]_0/[EBiB]_0/[Cu(0)\ wire]_0/[CuBr_2]_0/[Me_6TREN]_0$=222/1/1/1.1. $[MA]_0$/[Sulfolane]= 2/1 (v/v);

Entry	$[MA]_0/[EBiB]_0/[Cu(0)\ wire^a]_0/[CuBr_2]_0/[Me_6TREN]_0$ (molar)	T (°C)	k_p^{app} (h^{-1})	Time (h)	Conv. (%)	M_n^{th} x10^{-3}	M_n^{SEC} x10^{-3}	$Đ$
1	222/1/Cu(0) wire /0/1.1	30	0.900	1.35	80.8	15.5	16.6	1.05
2	222/1/Cu(0) wire /0.1/1.1	30	0.557	1.30	71.6	13.7	17.0	1.10
3	100/1/Cu(0) wire /0/1.1	30	-	1.17	72.9	6.5	4.6	1.16
4	1100/1/Cu(0) wire /0/1.1	30	0.660	3.27	86.5	73.3	78.4	1.04
5	222/1/Cu(0) wire /0/1.1	30	1.048	1.50	74.05	14.9	17.9	1.07

[a] Cu(0) wire: d = 1 mm, l = 5 cm

For the purpose of comparison, DMSO was also used under the same reaction conditions because this solvent is often used in the SARA ATRP of the most studied model monomers MA, MMA and VC (by the so-called SET-LRP).[2, 6, 20] The results presented in Figure 2.1 show that the level of control achieved is similar for both solvents, affording the synthesis of PMA with very low $Đ$ (~ 1.05). The conversions reached are very high and the polymerization kinetics are of first-order with respect to monomer conversion.

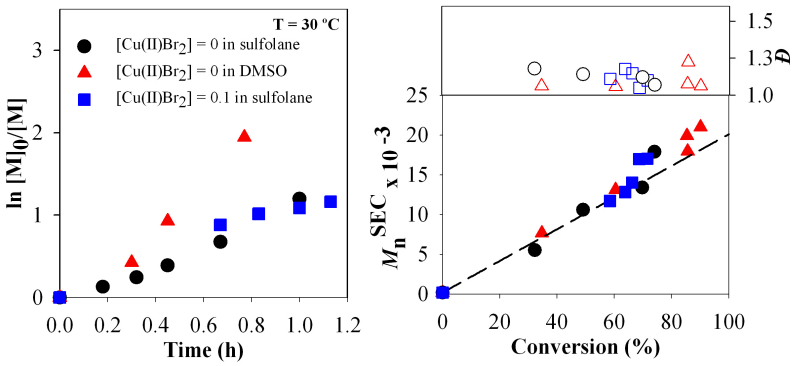

Figure 2.1 Kinetic plots of conversion and $\ln[M]_0/[M]$ *vs*. time (left) and plot of number-average molecular weights (M_n^{SEC}) and *Đ* *vs*. conversion (right) for the SARA ATRP of MA catalyzed by Cu(0) wire/$CuBr_2$/Me_6TREN in sulfolane (black circle and blue square symbols) or DMSO (red triangle symbols) at 30 °C. Conditions: $[MA]_0/[solvent]$ = 2/1 (v/v); $[MA]_0/[EBiB]_0$/Cu(0) wire/$[CuBr_2]/[Me_6TREN]_0$ = 222/1/Cu(0) wire/0 or 0.1/1.1 (molar); Cu (0): *d* = 1 mm, *l* = 5 cm.

The influence of the target DP was investigated (Table 2.1, entries 2-4). It is remarkable to note that even for DP = 1100, the *Đ* value of PMA is very low (1.04). This low value clearly indicates that in the system reported herein, the contribution of side reactions is minimal.

The reduction of $CuBr_2$/Me_6TREN by Cu(0) is known to be an important factor in the reaction kinetics.[2] The study of this process in sulfolane and DMSO by UV-vis spectroscopy is present in Figure 2.2. The concentration of Cu(II) species was mesured by the absorvance at the wavelength of 960 nm.[27]

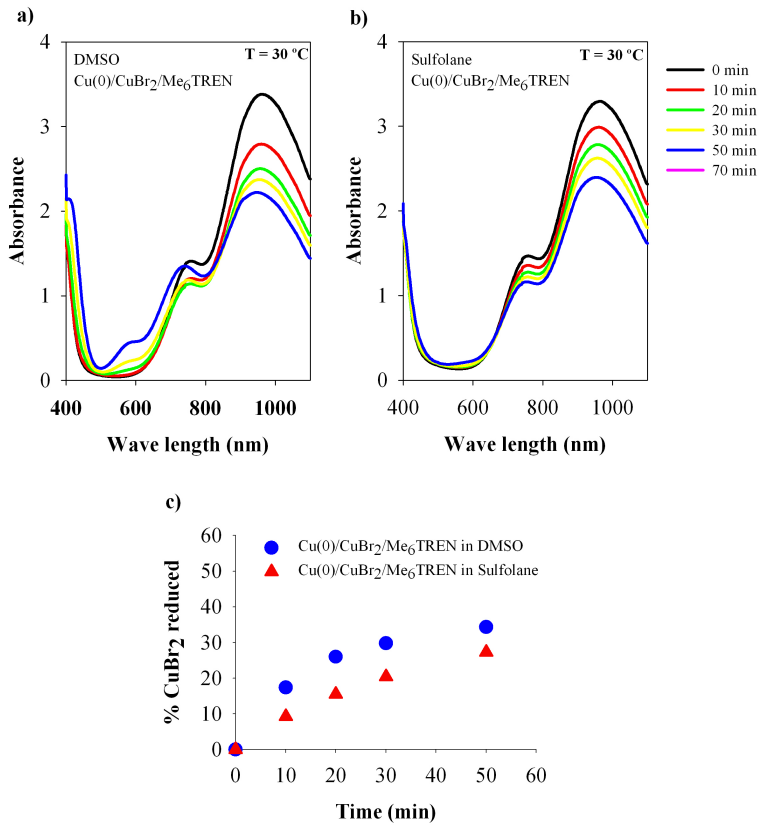

Figure 2.2 - Evolution of UV−vis spectra in comproportionation experiments at 30 ºC: (a) Cu(0) wire: *l* = 5 cm and *d* = 1 mm, $[CuBr_2]_0$ = 7.50 mM and $[Me_6TREN]_0$ = 82.5 mM in DMSO (2.5 mL); (b) Cu(0) wire: *l* = 5 cm and *d* = 1 mm, $[CuBr_2]_0$ = 7.50 mM and $[Me_6TREN]_0$ = 82.5 mM in sulfolane (2.5 mL); (c) Relative amount of $CuBr_2$ reduced during the comproportionation of Cu(0) and $CuBr_2$ in DMSO or sulfolane at 30 ºC. The values were determined by UV-vis spectroscopy.

With the previous result no major reactivity differences between both solvents are observed and the use of sulfolane as solvent was extended to the SARA ATRP of MMA, St and VC (Table 2.2, entries 1-12 and Figure 2.3). The necessary adjustments in the polymerization conditions were done regarding the initiator, ligand, ratio monomer/sulfolane and temperature taking into account the structure of each monomer.[6, 13, 20]

Table 2.2 - Kinetic data for the SARA ATRP of MMA, St and VC with $[Monomer]_0/[Sulfolane]= 2/1$ (v/v).

Entry	$[M]_0/[I]_0/[Cu(0)\ wire^a]_0/[CuX_2]_0/[L]_0$ (molar)	T (°C)	k_p^{app} (h^{-1})	Time (h)	Conv. (%)	M_n^{th} x10^{-3}	M_n^{SEC} x10^{-3}	$Đ$
1[b]	$[MMA]_0/[EBPA]_0/[Cu(0]_0/[CuBr_2]_0/[bpy]_0$ =222/1/Cu(0)/0/2.2	40	0.489	6.33	80.5	17.8	25.5	1.06
2[b]	$[MMA]_0/[EBPA]_0/[Cu(0)]_0/[CuBr_2]_0/ [bpy]_0$ =222/1/Cu(0)/0.1/2.2	40	0.410	4.05	87.0	18.9	21.9	1.10
3[b]	$[MMA]_0/[TsCl]_0/[Cu(0)]_0/[CuBr_2]_0/[bpy]_0$ =222/1/Cu(0)/0/2.2	40	0.161	7.62	76.6	16.9	25.8	1.21
4[b]	$[MMA]_0/[EBPA]_0/[Cu(0)]_0/[CuBr_2]_0/[bpy]_0$ = 80/1/Cu(0)/0/2.2	40	-	2.83	95.0	7.8	10.7	1.05
5	$[St]_0/[EBiB]_0/[Cu(0)]_0/[CuBr_2]_0/[PMDETA]_0$ =222/1/ Cu(0)/0/1.1	30	0.022	44.6	58.5	13.7	63.4	1.27
6	$[St]_0/[EBiB]_0/[Cu(0)]_0/[CuBr_2]_0/[PMDETA]_0$ =222/1/ Cu(0)/0/1.1	60	0.112	7.52	54.3	12.7	23.7	1.26
7	$[St]_0/[EBiB]_0/[Cu(0)]_0/[CuBr_2]_0/[PMDETA]_0$ =222/1/ Cu(0)/0/1.1	90	0.240	4.15	64.5	15.0	42.8	1.24
8	$[St]_0/[CHBr_3]_0/[Cu(0)]_0/[CuCl_2]_0/[PMDETA]_0$=222/1/Cu(0)/0.1/1.2	60	0.104	5.42	37.6	8.3	12.0	1.18
9[b]	$[VC]_0/[CHBr_3]_0/[Cu(0)]_0/[CuBr_2]_0/[TREN]_0$ =222/1/Cu(0)/0/1.1	42	0.141	6.5	62.5	12.1	16.9	1.48
10[b]	$[VC]_0/[CHBr_3]_0/[Cu(0)]_0/[CuBr_2]_0/[TREN]_0$ =222/1/Cu(0)/0/1.1	30	-	16.0	55.8	11.0	14.2	1.49
11[b]	$[VC]_0/[CHBr_3]_0/[Cu(0)]_0/[TREN]_0$ =100/1/Cu(0)/0/1.1	42	-	2.0	48.4	5.5	9.1	1.55
12[b]	$[VC]_0/[CHBr_3]_0/[Cu(0)]_0/[TREN]_0$ =50/1/Cu(0)/0/1.1	42	-	1.5	62.2	3.0	3.9	1.69

[a] Cu(0) wire: d = 1 mm, l = 5 cm; [b] $[monomer]_0/[solvent]= 1/1$

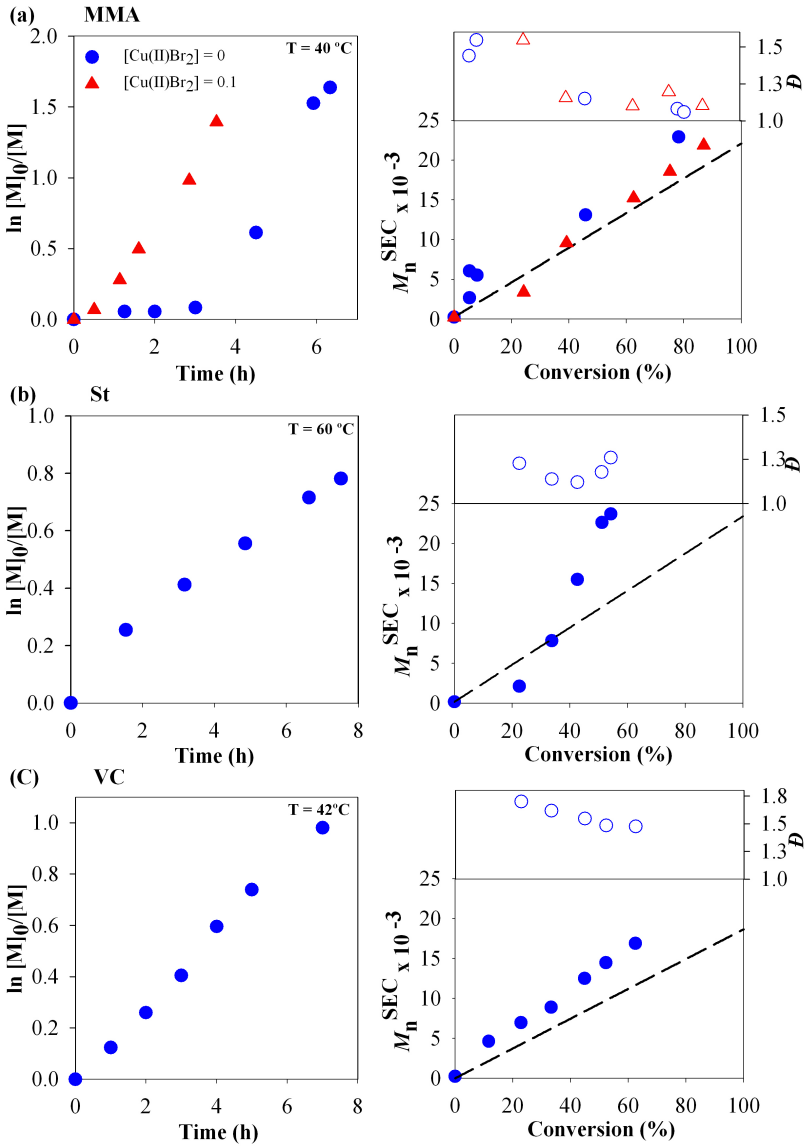

Figure 2.3 – Kinetic plots of conversion and ln[M]$_0$/[M] *vs*. time and plot of number-average molecular weights (M_n^{SEC}) and *Đ vs*. conversion for the SARA ATRP of (a) MMA, (b) St and (c) VC using Cu(0) wire as a supplemental activator and reducing agent in sulfolane. Conditions: (a) [MMA]$_0$/[EBPA]$_0$/Cu(0) wire/ [$CuBr_2$]$_0$/[bpy]$_0$ = 222/1/Cu(0) wire/0 (blue circle) or 0.1 (red triangle)/2.2 (molar), [MMA]$_0$/[Sulfolane] = 1/1 (v/v) and T = 40 ºC; (b) [St]$_0$/[EBiB]$_0$/Cu(0) wire/[PMDETA]$_0$ = 222/1/Cu(0) wire/1.1 (molar), [St]$_0$/[Sulfolane] = 2/1 (v/v) and T = 60 ºC; (c) [VC]$_0$/[$CHBr_3$]$_0$/[Cu(0) wire]$_0$/ [TREN]$_0$ = 222/1/ Cu(0) wire/1.1, [VC]$_0$/[Sulfolane] = 1/1and T = 42 ºC; Cu (0): *d* = 1 mm, *l* = 5 cm.

Figure 2.3 demonstrates the possibility of synthesizing poly(methyl methacrylate) (PMMA), PS and PVC with controlled molecular weights, by SARA ATRP in sulfolane. The rate of polymerization is of first-order with respect to the monomer conversion and the final *Đ* of the polymers is similar to the best values reported in the literature[6, 13, 20] for different monomers. In the case of MMA polymerization the induction period observed (Figure 2.3 (a)) was eliminated by adding $CuBr_2$ in the

beginning of the polymerization, in accordance with the previous results reported by our research group.[6]

The kinetic data obtained for the different monomers is particularly relevant for St (Figure 2.3 (b), Figure 2.4 and Table 2.2, entry 5-8).

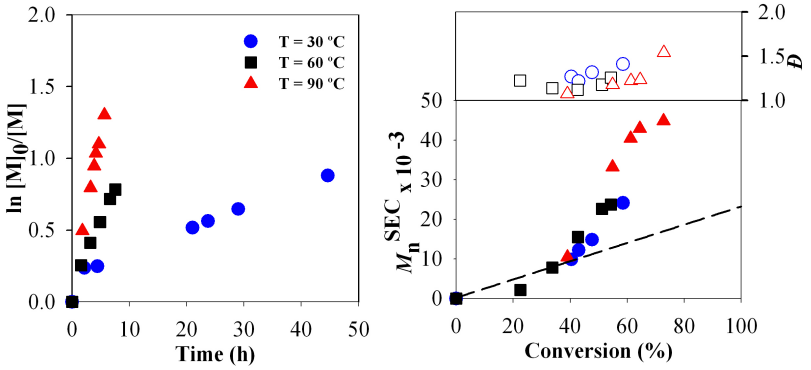

Figure 2.4 – (a) Kinetic plots of $\ln[M]_0/[M]$ *vs*. time and plot of number-average molecular weights (M_n^{SEC}) and *Đ vs*. conversion for the SARA ATRP of St using Cu(0) wire as supplemental activator and reducing agent in sulfolane at 30 ºC (blue circle symbols), 60 ºC (black square symbols) and 90 ºC (red triangle symbols) . Conditions: $[St]_0/[sulfolane]$ = 2/1 (v/v); $[St]_0/[EBiB]_0/Cu(0)wire /[PMDETA]_0$ = 222/1/Cu(0) wire/1.1 (molar); Cu (0): *d* = 1 mm, *l* = 5 cm.

According to kinetic data obtained by St polymerization an unusual plot M_n^{SEC} *vs* conversion was observed. This kinetic (Figure 2.3 (b)) was repeated and the same results were observed. Also, an additional kinetic using a ratio solvent/monomer of 1/1 (Figure 2.5) to evaluate the influence of this parameter in the reaction kinetic profile was carried out.

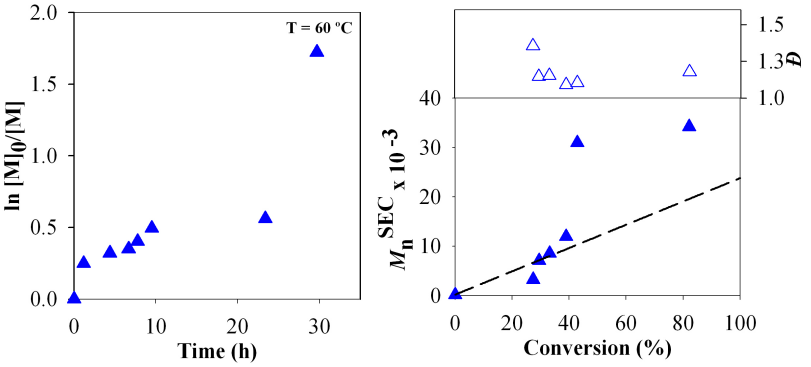

Figure 2.5 – Kinetic plots of conversion and $\ln[M]_0/[M]$ vs. time and plot of number-average molecular weights (M_n^{SEC}) and Đ vs. conversion for the SARA ATRP of St using Cu(0) wire as a supplemental activator and reducing agent in sulfolane. Conditions: $[St]_0/[EBiB]_0/Cu(0)$ wire/$[PMDETA]_0$ = 222/1/Cu(0) wire/1.1 (molar), $[St]_0/[$ Sulfolane] = 1/1 (v/v) and T = 60 ºC; Cu (0): d = 1 mm, l = 5 cm.

From the results presented in Figure 2.5 it is possible to conclude that the deviation of M_n^{SEC} is not related to solubility issues since the same profile was obtained in the case of the presence of more solvent. In a previous publication[9] the effect of temperature reaction in a Fe(0) and $CuBr_2/Me_6TREN$ mediated ATRP of Sty in DMF has been studied for the first time. The temperature reaction is particularly relevant knowing the very low conversions obtained for PS at room temperature.[6, 28] DMF was selected because of the high solubility of PS in this solvent. Figure 2.6 presents the M_n^{SEC} and $Đ$ of the PS that were obtained when the polymerization was carried out at 70 ºC and 90 ºC.

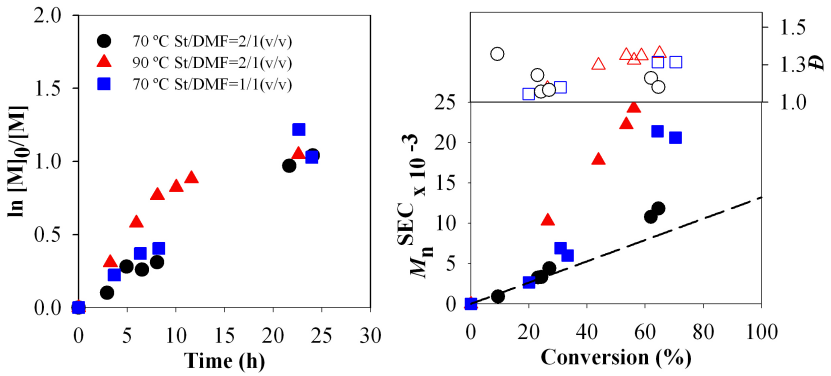

Figure 2.6 Kinetic plots of conversion and $\ln[M]_0/[M]$ *vs.* time and (b) plot of number average molecular weights (M_n^{SEC}) and $Đ$ *vs.* conversion for ATRP of St catalyzed with mixed catalyst system (Fe(0) and $CuBr_2/Me_6TREN$ at 70 ºC and 90 ºC in DMF. Conditions: $[St]_0/[EBiB]_0/[Fe(0)]_0/[CuBr_2]_0/[ligand]$ = 125/1/1/0.1/1.1 (molar); $[St]_0/[DMF]$ = 2/1 (v/v) and T = 70 ºC (circle black); $[St]_0/[DMF]$ = 2/1 (v/v) and T = 90ºC (triangle red); $[St]_0/[DMF]$ = 1/1 (v/v) and T = 70 ºC (square blue)

From Figure 2.6 the direct comparison of the kinetics data obtained at these two temperatures (70 ºC and 90 ºC) shows that an increase in the temperature leads to a very significant increase in the styrene conversion rate. However, in spite of the faster polymerization rates, the conversion is still limited to about 60%, with the disadvantage of causing broader molecular weight distribution than the one obtained for 70 ºC. In fact, very high temperatures are known to lead side reaction such as the loss of bromine chain-end functionality of even styrene thermal self-initiation.[29] Recently, another research group[28] has reproduced our previous results using a mixture of metal catalysts[6] and confirmed the low Sty polymerization rate at ambient temperature conditions. Figure 2.6 also highlights the fact the apparent initiator efficiency at 90 ºC is much lower than at 70 ºC. However, significant deviations seem

to occur at high monomer conversions, and an increase in the M_n^{SEC} values that seems to be more related to a non-ideal living behavior rather than to a real initiator efficiency. This conclusion is supported by a greater increase in *Đ* values when the apparent efficiency is lower. The selection of 70 ºC as the polymerization temperature seems to be a good compromise between the rate of polymerization and the *Đ* of the final products.

To evaluate the effect of DMF in this catalytic system, kinetic studies were carried out for ratios St/DMF=1/0 and Sty/DMF=1/1. In bulk conditions[9] (without DMF), the polymerization occurs slowly (k_p^{app} = 0.018 h^{-1}). This result is unexpected since the concentration of the monomer is higher, which could provide a faster reaction.

The solvent amount was increased for the ratio St/DMF=1/1 (Figure 2.6, blue square) and the results suggest that DMF plays an important role in the polymerization reaction (k_p^{app} = 0.048 h^{-1}) probably by decreasing the viscosity of the reaction medium as well as the $K_{ATRP}= k_{act}/k_{deact}$.

Comparing St/DMF polymerization kinetic results with Sty/sulfolane polymerization, similar data was obtained. Different issues could hamper its controlled synthesis, such as: low propagation rate compared to acrylates, thermal self-initiation, occurrence of irreversible termination reactions, vitrification and poor solubility of most catalysts.[9]

The results presented herein report the synthesis of PS under mild reaction conditions using a common solvent applied to other monomer families, which opens a portfolio of opportunities for the straightforward synthesis of block copolymers using PS segments.[9]

The structure of the obtained polymers was assessed by ^{1}H NMR and MALDI-TOF analysis (Figure 2.7-2.12).

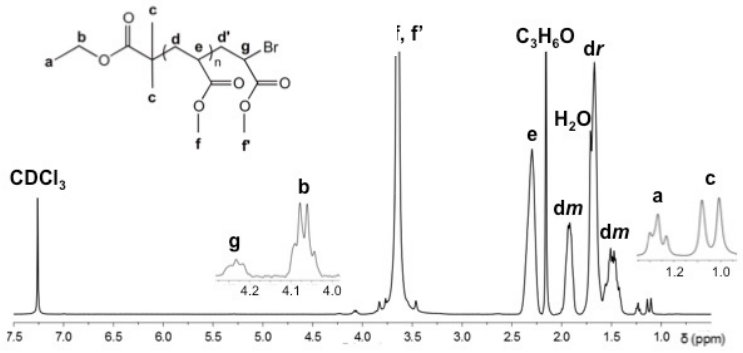

Figure 2.7 - ^{1}H NMR spectrum of PMA-Br (M_n^{SEC} = 15.9 x 10^3; *Đ* =1.08) in $CDCl_3$.

The structure of PMA was confirmed by ^{1}H NMR spectrum that is shown in Figure 2.7. The assignment of proton resonances was fulfilled according to the references: (e, g, f, f')[6, 20, 30-31], (a, b, c)[6, 32], (d*r*, d*m*)[6, 32-34]. The ^{1}H NMR spectrum reveals the resonance of the repeating unit CH_2-CH-CO_2Me: d (1.4-2.0 ppm), e (2.35-2.4 ppm) and f (3.6-3.75 ppm), respectively. The resonance of the terminal group CHBr-CO_2Me is also present at 4.2-4.35 ppm (g) and 3.75-3.85 ppm (f'), respectively. The initiator fragments (containing protons a, b and c) are revealed at 1.2-1.25 ppm, 4.05-4.1 ppm and 1.05-1.15 ppm.

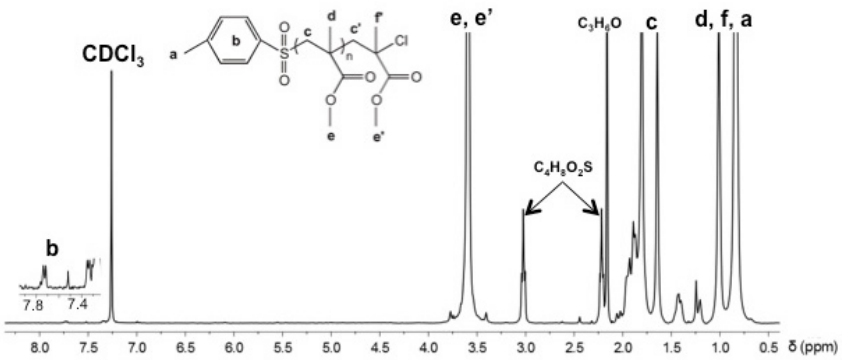

Figure 2.8 - ^{1}H NMR spectrum of PMMA-Br (M_n^{SEC} = 52500; $Đ$ =1.46) in $CDCl_3$.

^{1}H NMR technique was used to confirm the PMMA-Br structure and the spectrum is shown in Figure 2.8. The assignment of the proton resonances was fulfilled according to references: (a, b)[35], (c, d e, e', f)[36]. The ^{1}H NMR spectrum reveals the resonance of the repeating unit $CH_2CCH_3COOCH_3$: d (0.75-1.0 ppm) and e (3.5-3.75 ppm). The resonance of the terminal group is also present at 1.75-2.0 ppm. The initiator fragments are revealed through the resonance of protons at 1.25 ppm and 7.36 - 7.74 ppm respectively from the methyl and phenyl group.

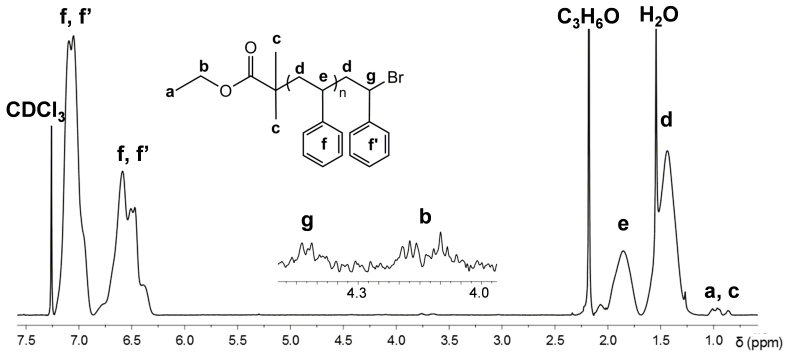

Figure 2.9 - ^{1}H NMR spectrum of PS-Br (M_n^{SEC} = 24.7 x 10^3; $Đ$ = 1.24) in $CDCl_3$.

The structure and the presence of the chain-end functionality of PS-Br polymer was evaluated by 400 MHz ^{1}H NMR spectroscopy. The initiator fragment is revealed by the appearance of the resonance peaks of protons a, b and c, at 0.90-1.05 ppm, 4.0-4.25 ppm and 0.7-0.9 ppm, respectively. The spectrum reveals the presence of the repeating unit CH_2-CHPh by the aromatic protons peaks at 6.25-7.5 ppm (f). The chain-end functionality is confirmed by the resonance of proton e, adjacent to bromine, at 4.35-4.5 ppm from CH_2-CHPhBr terminal group.[9]

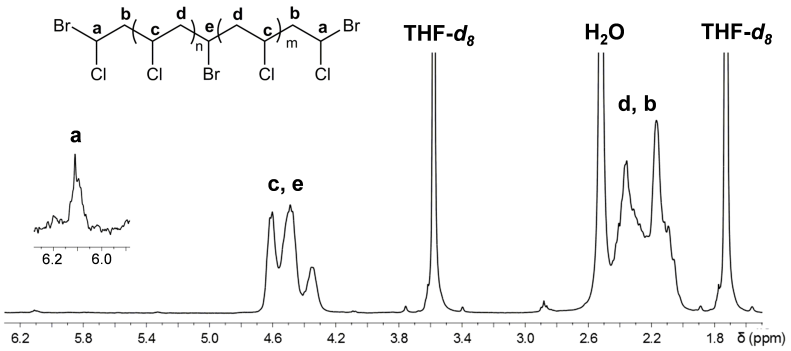

Figure 2.10 - The ^{1}H NMR spectrum of Br-PVC-Br (M_n^{SEC} = 9100; $Đ$ = 1.55) in THF-d_8.

The structure of α,ω-di(bromo)PVC was analyzed by 400 MHz ^{1}H NMR spectroscopy and the spectrum is shown in the Figure 2.10. The assignment of the proton resonances was realized according to the references: (a, d, e)[37] and (b, d)[25, 37]. The ^{1}H NMR spectrum reveals the resonance of the repeating unit CH_2-CHCl: 2.0-2.4 ppm (b) and 4.3-4.7 ppm (c). The resonance of the terminal group CH_2-CHClBr is also present at 2.0-2.7 ppm (d) and 6.05-6.15 ppm (e). The initiator fragments (a) is overlapped with the repeating unit signals in the range of 4.3-4.7

ppm.[37] Through the magnification of the region between 5.4 ppm and 6.5 ppm, it is possible to detect that only the diastereomeric –CHClBr (6.1 ppm) chain-ends were formed, since the signal from the diastereomeric $–CHBr_2$ at 6.0 ppm does not appear.[37]

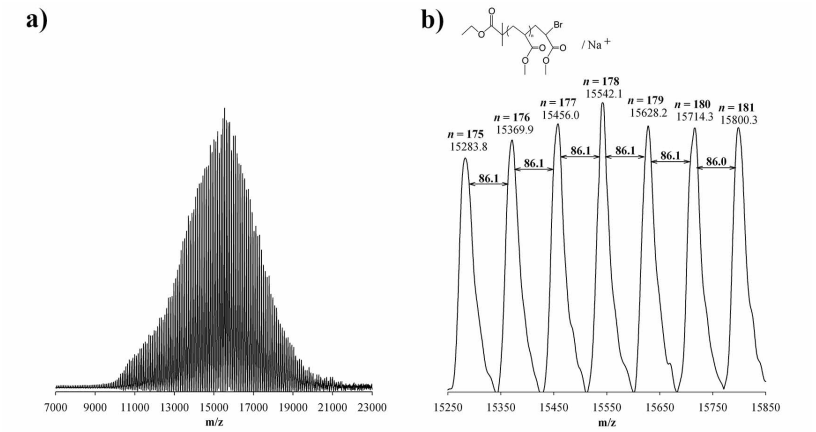

Figure 2.11 - a) MALDI-TOF-MS in the linear mode (using HABA as matrix) of PMA-Br (M_n^{SEC} = 15900, $Đ$ = 1.08); b) Enlargement of the MALDI-TOF-MS from m/z 15250 to 15850 of PMA-Br .

The MALDI-TOF-MS spectrum of PMA was acquired with two different matrices, HABA and DHB, but only HABA gave a clearly resolved spectrum (Figure 2.11 a) and b). MALDI-TOF-MS of PMA-Br with m/z ranging from 7000 to 23000 in linear mode is shown in Figure 2.10 a). Figure 2.11 b) shows the enlargement of the m/z 15250-15850 range. Importantly, the main peaks are separated by an interval corresponding to a monomer MA repeating unit (86.1 mass units). Figure 2.11 shows peaks that are attributed to a PMA-Br polymer chain, with ion formed of single alkali metal adduct $[R\text{-}(MA)_n\text{-}Br + Na^+]^+$, where R-Br is the initiator EBiB (15283.8 = 195.05 + 175 × 86.09 + 22.99, where 195.05, 86.09 and 22.99 correspond to the molar mass of EBiB, MA and Na^+, respectively).

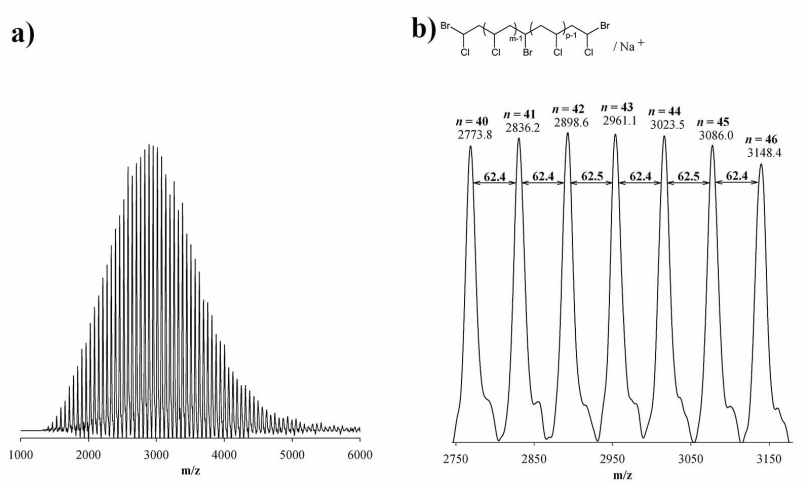

Figure 2.12 - a) MALDI-TOF-MS in the linear mode (using HABA as matrix) of Br-PVC-Br (M_n^{SEC} = 9100, $Đ$ = 1.55); b) Enlargement of the MALDI-TOF-MS from m/z 2750 to 3200 of Br-PVC-Br .

Again, for the MALDI-TOF-MS of Br-PVC-Br only HABA matrix allowed to obtain a clearly resolved spectrum (Figure 2.12 a) and b)). Figure 2.12 shows the enlargement of the m/z 2750-3200 range in linear mode. The higher peaks are separated by an interval that corresponds to a VC repeating unit (62.5 mass units). The peaks obtained from MALDI-TOF-MS analysis are attributed to a polymer chain $[Br\text{-}(PVC)_m\text{-}CHBr\text{-}(PVC)_p\text{-}Br + Na^+]^+$, where 'm + p' correspond to the degree of polymerization 'n' (2773.8 = 252.73 + 40 × 62.45 + 22.99, where 252.73, 62.45 and 22.99 correspond to the molar mass of initiator $CHBr_3$, VC and Na^+, respectively). The MALDI-TOF-MS confirmed the well-controlled PVC structure obtained using sulfolane as the solvent for the polymerization reactions.

The "living" nature of the polymers chain-ends was confirmed by carrying out successful chain extension experiments using PMA, PMMA and PS macroinitiators (Figure 2.13).

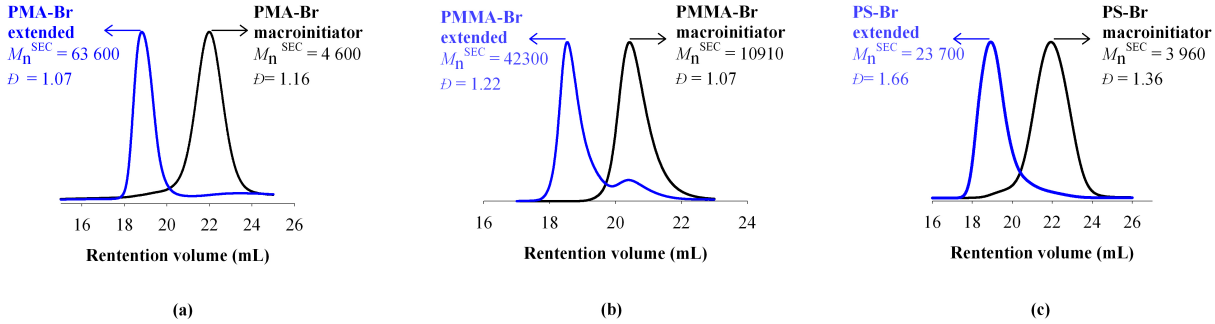

Figure 2.13 - Displacement of the SEC trace (RI signal) of a –Br-terminated (a) PMA (b) PMMA and (c) PS obtained by SARA ATRP (black line), towards high molecular weight values after a chain-extension experiment (blue line). Conditions: $[MA]_0/[solvent]$ = 2/1 (v/v); $[MA]_0/[EBiB]_0/Cu(0)$ wire /$[Me_6TREN]_0$= 222/1/ Cu(0) wire /1.1 (molar); $[MMA]_0/[solvent]$ = 2/1 $[MMA]_0/[EBPA]_0/Cu(0)wire/[PMDETA]_0$ = 222/1/Cu(0) wire/1.1 (molar); $[St]_0/[solvent]$ = 2/1 (v/v); $[St]_0/[EBiB]_0/Cu(0)$ wire/$[PMDETA]_0$ = 222/1/Cu(0) wire/1.1 (molar); Cu (0): d = 1 mm, l = 5 cm.

Figure 2.13 (a), (b) and (c) show the complete movement of the SEC traces of PMA-Br, PS-Br and PMMA-Br macroinitiators towards high molecular weights, resulting from the reinitiation of the –Br chain-ends using the respective monomers. The results presented in Figure 2.13 (c) are particularly relevant since they demonstrate the high chain-end functionality of the PS prepared by SARA ATRP in sulfolane.

As a proof-of-concept, macroinitiators of α,ω-di(bromo)PVC were used to afford block copolymers of PMA-*b*-PVC-*b*-PMA and PS-*b*-PVC-*b*-PS using Me_6TREN and PMDETA as ligands, respectively (Figure 2.14 (a)).

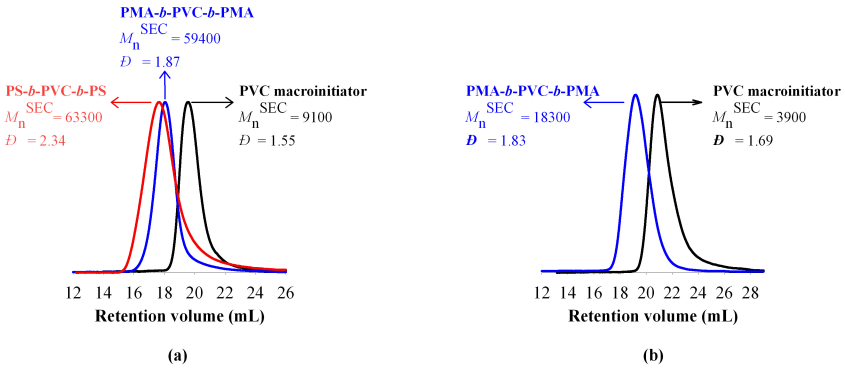

Figure 2.14 – (a) SEC traces of the Br-PVC-Br (conv.$_{VC}$ = 48.4%, M_n^{th} = 5500, M_n^{SEC} = 9100, Đ = 1.55) macroinitiator (black line), and the PMA-*b*-PVC-*b*-PMA (conv.$_{MA}$ = 86.5%, M_n^{th} = 53800, M_n^{SEC} = 59400, Đ = 1.87) (blue line) and PS-*b*-PVC-*b*-PS (conv.$_{St}$ = 57.5%, M_n^{th} = 45000, M_n^{SEC} = 63300, Đ = 2.34) block copolymers (red line). (b) SEC traces of the Br-PVC-Br (conv.$_{VC}$ = 62.2%, M_n^{th} = 3000, M_n^{SEC} = 3900, Đ = 1.69) macroinitiator (black line), and the PMA-*b*-PVC-*b*-PMA (conv.$_{MA}$ = 85.7%, M_n^{th} = 17800, M_n^{SEC} = 18300, Đ = 1.83) block copolymer (blue line) prepared by "one-pot" SARA ATRP chain extension.

Figure 2.14 (a) shows the movement of the low molecular weight PVC GPC trace (conv.$_{VC}$ = 48.4%, M_n^{th} = 5500, M_n^{SEC} = 9100, $Đ$ = 1.55) towards high molar mass PMA-*b*-PVC-*b*-PMA (conv.$_{MA}$ = 86.5%, M_n^{th} = 53800, M_n^{SEC} = 59400, $Đ$ = 1.87) and PS-*b*-PVC-*b*-PS (conv.$_{St}$ = 57.5%, M_n^{th} = 45000, M_n^{SEC} = 63300, $Đ$ = 2.34) block copolymers. Nevertheless, the movement is not complete either because the system is not optimized or due to the previously mentioned issues regarding the RDRP of styrene.

These results prove the "living" character of the PVC synthesized by this method and the possibility of using the reported system in the synthesis of unique block copolymers. It should be mentioned that to the best of our knowledge, the preparation of block copolymers containing PVC and PS blocks by sequential addition of the appropriated monomers by any RDRP method has never been reported.

In an attempt to push the potential of the system, the PMA-*b*-PVC-*b*-PMA was synthesized using the "one-pot" chain extension approach (Figure 2.14 (b)).

The SEC traces presented in Figure 2.14 (b) proves the remarkable advantage of using a single solvent to afford the controlled polymerization of different families of monomers. By using a straightforward procedure involving no purification steps, it is possible to afford well-controlled polymeric structures.

The structure of the block copolymers was confirmed by ^{1}H NMR (Fig 2.15 and 2.16) (^{1}H NMR results are independent of the reaction method used for the synthesis of the copolymers).

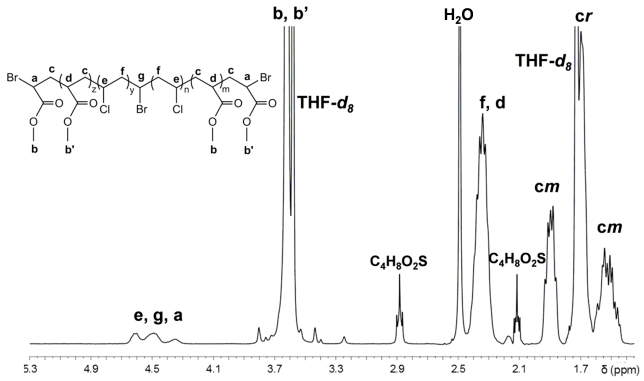

Figure 2.15 - The ^{1}H NMR spectrum of PMA-*b*-PVC-*b*-PMA block copolymer (M_n^{SEC} = 59400; $Đ$ = 1.87) in THF- d_8.

The PMA-*b*-PVC-*b*-PMA structure was studied by ^{1}H NMR spectroscopy and spectrum is presented in Figure 2.15. The presence of the PMA block is confirmed by the appearance of the signals: 3.5-3.7 ppm (f and f', 3H), 1.4-2.0 ppm (d) and 2.0-2.45 (e). The presence of the PVC block is confirmed by the signal at 4.3-4.7 ppm, corresponding to the resonance of the repeating unit CH_2-CHCl. The d*r* signal is overallaped with the THF-d_8 signal, which avoided the determination of the syndiotactic and isotactic diads (d*r* and d*m* respectively) fractions.

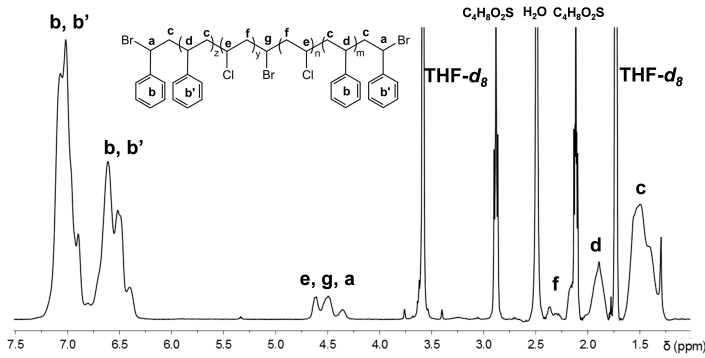

Figure 2.16 - ^{1}H NMR spectrum of PS-*b*-PVC-*b*-PS block copolymer (M_n^{SEC} = 63300; *Đ* = 2.34) in THF-d_8.

Figure 2.16 shows the ^{1}H NMR spectrum of the PS-*b*-PVC-*b*-PS block copolymer. The presence of the vinyl chloride repeating unit is revealed by the resonances of CH_2-CHCl: 2.0 -2.40 ppm (b), that is partially overlapped with the sulfolane and water signals, and 4.25-4.7 ppm (c). The styrene repeating unit is revealed by the resonance of the protons (d) at 1.25-2.0 ppm and (f) at 6.25-7.25 ppm.

2.5 Conclusions

The summarized results (Table 2.1 and 2.2) demonstrate that by adjusting the structure of the catalytic complexes and the initiator it is possible to afford a controlled polymerization of MA, MMA, St and VC by SARA ATRP in the same solvent-sulfolane. The presented values regarding k_p^{app}, conversion and *Đ* are in agreement with the best results reported in the literature for the polymerization processes of each monomer individually.[6, 13, 20]

The results presented herein establish an innovative and robust system to assess a vast portfolio of well-defined polymers and block copolymers using a common industrial solvent, and employing at the same time low amounts of soluble copper.

2.6 References

1. Matyjaszewski, K.; Tsarevsky, N. V., Macromolecular Engineering by Atom Transfer Radical Polymerization, *Journal of the American Chemical Society*, *136* (18), 6513-6533, 2014.
2. Guliashvili, T.; Mendonça, P. V.; Serra, A. C.; Popov, A. V.; Coelho, J. F. J., Copper-Mediated Controlled/"Living" Radical Polymerization in Polar Solvents: Insights into Some Relevant Mechanistic Aspects, *Chemistry – A European Journal*, *18* (15), 4607-4612, 2012.
3. Jakubowski, W.; Matyjaszewski, K., Activators Regenerated by Electron Transfer for Atom-Transfer Radical Polymerization of (Meth)acrylates and Related Block Copolymers, *Angewandte Chemie*, *118* (27), 4594-4598, 2006.
4. Matyjaszewski, K.; Jakubowski, W.; Min, K.; Tang, W.; Huang, J.; Braunecker, W. A.; Tsarevsky, N. V., Diminishing catalyst concentration in atom transfer radical polymerization with reducing agents, *Proceedings of the National Academy of Sciences*, *103* (42), 15309-15314, 2006.
5. Magenau, A. J. D.; Strandwitz, N. C.; Gennaro, A.; Matyjaszewski, K., Electrochemically Mediated Atom Transfer Radical Polymerization, *Science*, *332* (6025), 81-84, 2011.
6. Mendonca, P. V.; Serra, A. C.; Coelho, J. F. J.; Popov, A. V.; Guliashvili, T., Ambient temperature rapid ATRP of methyl acrylate, methyl methacrylate and styrene in polar solvents with mixed transition metal catalyst system, *European Polymer Journal*, *47* (7), 1460-1466, 2011.
7. Zhang, Y.; Wang, Y.; Matyjaszewski, K., ATRP of Methyl Acrylate with Metallic Zinc, Magnesium, and Iron as Reducing Agents and Supplemental Activators, *Macromolecules*, *44* (4), 683-685, 2011.
8. Cordeiro, R. A.; Rocha, N.; Mendes, J. P.; Matyjaszewski, K.; Guliashvili, T.; Serra, A. C.; Coelho, J. F. J., Synthesis of well-defined poly(2-(dimethylamino)ethyl methacrylate) under mild conditions and its co-polymers with cholesterol and PEG using Fe(0)/Cu(ii) based SARA ATRP, *Polymer Chemistry*, *4* (10), 3088-3097, 2013.
9. Rocha, N.; Mendonca, P. V.; Mendes, J. P.; Simoes, P. N.; Popov, A. V.; Guliashvili, T.; Serra, A. C.; Coelho, J. F. J., Facile Synthesis of Well-Defined Telechelic Alkyne-Terminated Polystyrene in Polar Media Using ATRP With Mixed Fe/Cu Transition Metal Catalyst, *Macromolecular Chemistry and Physics*, *214* (1), 76-84, 2013.
10. Abreu, C. M. R.; Mendonca, P. V.; Serra, A. C.; Coelho, J. F. J.; Popov, A. V.; Guliashvili, T., Accelerated Ambient-Temperature ATRP of Methyl Acrylate in Alcohol-Water Solutions with a Mixed Transition-Metal Catalyst System, *Macromolecular Chemistry and Physics*, *213* (16), 1677-1687, 2012.
11. Bortolamei, N.; Isse, A. A.; Magenau, A. J. D.; Gennaro, A.; Matyjaszewski, K., Controlled Aqueous Atom Transfer Radical Polymerization with Electrochemical Generation of the Active Catalyst, *Angew Chem Int Edit*, *50* (48), 11391-11394, 2011.

12. Mendes, J. P.; Branco, F.; Abreu, C. M. R.; Mendonça, P. V.; Popov, A. V.; Guliashvili, T.; Serra, A. C.; Coelho, J. F. J., Synergistic Effect of 1-Butyl-3-methylimidazolium Hexafluorophosphate and DMSO in the SARA ATRP at Room Temperature Affording Very Fast Reactions and Polymers with Very Low Dispersity, *ACS Macro Lett*, 544-547, 2014.
13. Abreu, C. M. R.; Serra, A. C.; Popov, A. V.; Matyjaszewski, K.; Guliashvili, T.; Coelho, J. F. J., Ambient temperature rapid SARA ATRP of acrylates and methacrylates in alcohol-water solutions mediated by a mixed sulfite/Cu(ii)Br2 catalytic system, *Polymer Chemistry*, *4* (23), 5629-5636, 2013.
14. Abreu, C. M. R.; Mendonca, P. V.; Serra, A. C.; Popov, A. V.; Matyjaszewski, K.; Guliashvili, T.; Coelho, J. F. J., Inorganic Sulfites: Efficient Reducing Agents and Supplemental Activators for Atom Transfer Radical Polymerization, *ACS Macro Letters*, *1* (11), 1308-1311, 2012.
15. Gois, J. R.; Rocha, N.; Popov, A. V.; Guliashvili, T.; Matyjaszewski, K.; Serra, A. C.; Coelho, J. F. J., Synthesis of well-defined functionalized poly(2-(diisopropylamino)ethyl methacrylate) using ATRP with sodium dithionite as a SARA agent, *Polymer Chemistry*, *5* (12), 3919-3928, 2014.
16. Gois, J. R.; Konkolewic, D.; Popov, A. V.; Guliashvili, T.; Matyjaszewski, K.; Serra, A. C.; Coelho, J. F. J., Improvement of the control over SARA ATRP of 2-(diisopropylamino)ethyl methacrylate by slow and continuous addition of sodium dithionite, *Polymer Chemistry*, *5* (16), 4617-4626, 2014.
17. Konkolewicz, D.; Krys, P.; Góis, J. R.; Mendonça, P. V.; Zhong, M.; Wang, Y.; Gennaro, A.; Isse, A. A.; Fantin, M.; Matyjaszewski, K., Aqueous RDRP in the Presence of Cu0: The Exceptional Activity of CuI Confirms the SARA ATRP Mechanism, *Macromolecules*, *47* (2), 560-570, 2014.
18. Mendonca, P.; Konkolewicz, D.; Averick, S.; Serra, A. C.; Popov, A.; Guliashvili, T.; Matyjaszewski, K.; Coelho, J., Synthesis of cationic poly((3-acrylamidopropyl) trimethylammonium chloride) by SARA ATRP in ecofriendly solvent mixtures, *Polym Chem*, *in press*, 2014.
19. Konkolewicz, D.; Wang, Y.; Krys, P.; Zhong, M.; Isse, A. A.; Gennaro, A.; Matyjaszewski, K., SARA ATRP or SET-LRP. End of controversy?, *Polym Chem*, in press., 2014.
20. Percec, V.; Guliashvili, T.; Ladislaw, J. S.; Wistrand, A.; Stjerndahl, A.; Sienkowska, M. J.; Monteiro, M. J.; Sahoo, S., Ultrafast Synthesis of Ultrahigh Molar Mass Polymers by Metal-Catalyzed Living Radical Polymerization of Acrylates, Methacrylates, and Vinyl Chloride Mediated by SET at 25 °C, *Journal of the American Chemical Society*, *128* (43), 14156-14165, 2006.
21. Tom, J.; Hornby, B.; West, A.; Harrisson, S.; Perrier, S., Copper(0)-mediated living radical polymerization of styrene, *Polym Chem*, *1* (4), 420-422, 2010.
22. Jakubowski, W.; Kirci-Denizli, B.; Gil, R. R.; Matyjaszewski, K., Polystyrene with Improved Chain-End Functionality and Higher Molecular Weight by ARGET ATRP, *Macromol Chem Phys*, *209* (1), 32-39, 2008.
23. Boyle, R. E., The Reaction of Dimethyl Sulfoxide and 5-Dimethylaminonaphthalene-1-sulfonyl Chloride, *J Org Chem*, *31* (11), 3880-3882, 1966.
24. Tilstam, U., Sulfolane: A Versatile Dipolar Aprotic Solvent, *Org Process Res Dev*, *16* (7), 1273-1278, 2012.
25. Abreu, C. M. R.; Mendonça, P. V.; Serra, A. C.; Coelho, J. F. J.; Popov, A. V.; Gryn'ova, G.; Coote, M. L.; Guliashvili, T., Reversible Addition–Fragmentation

Chain Transfer Polymerization of Vinyl Chloride, *Macromolecules*, *45* (5), 2200-2208, 2012.
26. Ciampolini, M.; Nardi, N., Five-Coordinated High-Spin Complexes of Bivalent Cobalt, Nickel, andCopper with Tris(2-dimethylaminoethyl)amine, *Inorganic Chemistry*, *5* (1), 41-44, 1966.
27. Wang, Y.; Soerensen, N.; Zhong, M.; Schroeder, H.; Buback, M.; Matyjaszewski, K., Improving the "Livingness" of ATRP by Reducing Cu Catalyst Concentration, *Macromolecules*, *46* (3), 683-691, 2013.
28. Zhou, L. L.; Zhang, Z. B.; Cheng, Z. P.; Zhou, N. C.; Zhu, J.; Zhang, W.; Zhu, X. L., Fe(0) Powder/CuBr2-Mediated "Living"/Controlled Radical Polymerization of Methyl Methacrylate and Styrene at Ambient Temperature, *Macromolecular Chemistry and Physics*, *213* (4), 439-446, 2012.
29. Matyjaszewski, K.; Xia, J., Atom Transfer Radical Polymerization, *Chemical reviews*, *101* (9), 2921-2990, 2001.
30. Anastasaki, A.; Nikolaou, V.; Nurumbetov, G.; Wilson, P.; Kempe, K.; Quinn, J. F.; Davis, T. P.; Whittaker, M. R.; Haddleton, D. M., Cu(0)-Mediated Living Radical Polymerization: A Versatile Tool for Materials Synthesis, *Chemical reviews*, *116* (3), 835-877, 2016.
31. Lligadas, G.; Ladislaw, J. S.; Guliashvili, T.; Percec, V., Functionally terminated poly(methyl acrylate) by SET-LRP initiated with CHBr3 and CHI3, *Journal of Polymer Science Part A: Polymer Chemistry*, *46* (1), 278-288, 2008.
32. Coelho, J. F. J.; Mendonça, P. V.; Popov, A. V.; Percec, V.; Gonçalves, P. M. O. F.; Gil, M. H., Synthesis of high glass transition temperature copolymers based on poly(vinyl chloride) via single electron transfer—Degenerative chain transfer mediated living radical polymerization (SET-DTLRP) of vinyl chloride in water, *Journal of Polymer Science Part A: Polymer Chemistry*, *47* (24), 7021-7031, 2009.
33. Coelho, J. F. J.; Carvalho, E. Y.; Marques, D. S.; Popov, A. V.; Goncalves, P. M.; Gil, M. H., Synthesis of Poly(lauryl acrylate) by Single-Electron Transfer/Degenerative Chain Transfer Living Radical Polymerization Catalyzed by Na2S2O4 in Water, *Macromolecular Chemistry and Physics*, *208* (11), 1218-1227, 2007.
34. Coelho, J. F. J.; Carvalho, E. Y.; Marques, D. S.; Popov, A. V.; Percec, V.; Gonçalves, P. M. F. O.; Gil, M. H., Synthesis of poly(ethyl acrylate) by single electron transfer-degenerative chain transfer living radical polymerization in water catalyzed by Na2S2O4, *Journal of Polymer Science Part A: Polymer Chemistry*, *46* (2), 421-432, 2008.
35. Gurr, P. A.; Mills, M. F.; Qiao, G. G.; Solomon, D. H., Initiator efficiency in ATRP: the tosyl chloride/CuBr/PMDETA system, *Polymer*, *46* (7), 2097-2104, 2005.
36. Gong, S.; Ma, H.; Wan, X., Atom transfer radical polymerization of methyl methacrylate induced by an initiator derived from an ionic liquid, *Polymer International*, *55* (12), 1420-1425, 2006.
37. Sienkowska, M. J.; Rosen, B. M.; Percec, V., SET-LRP of vinyl chloride initiated with CHBr3 in DMSO at 25 °C, *Journal of Polymer Science Part A: Polymer Chemistry*, *47* (16), 4130-4140, 2009.

Chapter 3

Getting faster: low temperature copper-mediated ATRP of methacrylates, acrylates, styrene and vinyl chloride in polar media using sulfolane/water mixtures

The results of these chapter are published in: **Mendes, J. P**.; Mendonca, P. V.; Maximiano, P.; Abreu, C. M. R.; Guliashvili, T.; Serra, A. C.; Coelho, J. F. J., *"Getting faster: low temperature copper-mediated SARA ATRP of methacrylates, acrylates, styrene and vinyl chloride in polar media using sulfolane/water mixtures"*, *RSC Advances*, *6* (12), 9598-9603, 2016

3.1 Abstract

Supplemental activator and reducing agent atom transfer radical polymerization of acrylates, methacrylates, styrene and vinyl chloride were successfully performed in sulfolane/water mixtures using ppm amounts of soluble copper. The catalytic effect of the presence of water in the reaction mixtures resulted in a notorious acceleration of the polymerization of the different monomers studied. The first-order kinetics with monomer conversion and the low *Đ* values of the polymers revealed the controlled features of the polymerization. As a proof-of-concept, an ABA block copolymer of PMA-*b*-PVC-*b*-PMA was prepared, also confirming the "living" character of the polymers. The results presented in this contribution, extend the importance of sulfolane as a universal industrial solvent for the SARA ATRP of a broad range of monomer families by significantly enhancing the polymerization rate, due to the selective addition of water to the solvent mixture. The incorporation of small amounts of water in the solvent mixture has also allowed the use of FDA-approved sulfites as the SARA agent, which was not possible using pure sulfolane as the polymerization solvent.

3.2 Introduction

RDRP methods have witnessed a remarkable development over the last two decades, since they allow the preparation of tailor-made polymers. ATRP, which is a metal-catalyzed RDRP, is one of the most studied methods due to its robustness, versatility, monomer tolerance and mild reaction conditions.[1] Important research efforts have been devoted to the reduction of the amount of metal complexes required to perform ATRP reactions. On this matter, different ATRP variations have been developed, lowering the required amount of catalyst to ppm levels to afford fast and controlled polymerizations. These methods include: activators regenerated by electron transfer (ARGET) ATRP,[2] initiators for continuous activator regeneration (ICAR) ATRP,[3] electrochemically mediated ATRP (e-ATRP)[2] and supplemental activator and reducing agent (SARA) ATRP.[4-5] From both environmental and industrial standpoints, the SARA ATRP is a very attractive technique since it can be performed using heterogeneous zerovalent metals[5-7] (easily removed from the reaction medium)

and FDA-approved inorganic sulfites as SARA agents.[8-11] These catalysts will then be used for the continuous regeneration of the activator species (e.g., Cu(I)X; X: halide) during the polymerization and will also participate on the direct activation of alkyl halides, to compensate for some termination reactions that might occur (Scheme 3.1).[12]

Several well-defined polymers and block copolymers have been synthesized using SARA ATRP in different solvents, such as water,[13] alcohol/water mixtures[7-8, 10, 14] and anisole.[8]

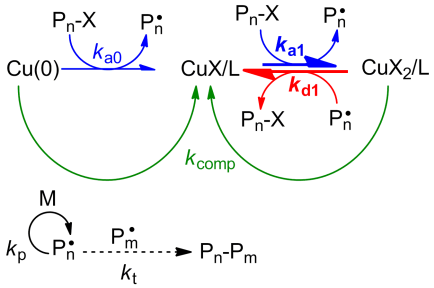

Scheme 3.1 General scheme mechanism of the Cu(0)/CuX_2/L-catalyzed SARA ATRP (L: ligand and X: halide).

Recently, our research group has studied the use of a dipolar aprotic industrial solvent, sulfolane, as a universal solvent for the SARA ATRP of acrylates, methacrylates, styrene and vinyl chloride.[15] The robustness of system was clearly demonstrated by the straightforward synthesis of PMA-*b*-PVC-*b*-PMA and PS-*b*-PVC-*b*-PS triblock copolymers. The use of this solvent for the controlled synthesis of macrostructures based on a wide range of monomer families by SARA ATRP provides an effective and easy route to access a vast portfolio of different block copolymers at a potential way to large scale production. The presence of water in solvent mixtures has been shown to significantly increase the rate of polymerization for the SARA ATRP of different monomers using either zero-valent metals[16] or sulfites,[8-10] while maintaining the controlled features of the polymerizations. This is due to the increase of the activity of Cu(I) complexes in more polar medium. The maximum water content is typically determined by the solubility of the polymer in the solvent mixtures (*e.g.*, ≈ 35 % for PMA) with DP = 222 in ethanol/water mixtures at 30 °C;[16] ≈ 5 % for poly(2-diisopropylamino)ethyl methacrylate) with DP = 50 in isopropanol/water mixtures at 40 °C).[8] In this work, we discuss the influence of water in sulfolane/water mixtures as the solvent for faster SARA ATRP reactions of

different monomers families, which can be advantageous in the case of a future industrial scale implementation of the method.

3.3 Experimental Section

3.3.1 Materials

Methyl acrylate (MA) (99 % stabilized; Acros), methyl methacrylate (MMA) (99 % stabilized; Acros) and styrene (St) (+ 99 %; Sigma-Aldrich), were passed over a sand/alumina column before use to remove the radical inhibitors.

Vinyl chloride (VC) (99 %) was kindly supplied by CIRES Lda, Portugal. Copper(II) bromide ($CuBr_2$) (+ 99 % extra pure, anhydrous; Acros), copper(II) chloride ($CuCl_2$) (max. 0.0008 % AS; Merck), zerovalent iron powder (Fe(0)) (99 %, ≈ 70 mesh, Acros), deuterated chloroform ($CDCl_3$) (+ 1 % tetramethylsilane (TMS); Euriso-top), deuterated tetrahydrofuran (THF-d8) (99.5 %; Euriso-top), sulfolane (+ 99 %; Acros), ethyl 2-bromoisobutyrate (EBiB) (98 %; Aldrich), p-toluenesulfonyl chloride (TsCl) (98 %; Merck), ethyl α-bromophenylacetate (EBPA) (97 %; Aldrich), bromoform ($CHBr_3$) (+ 99 % stabilized; Acros), tris(2-aminoethyl)amine (TREN) (96 %; Sigma-Aldrich), *N,N,N′,N″,N″*-pentamethyldiethylenetriamine (PMDETA) (99 %; Aldrich), 2,2′-bipyridine (bpy) (> 99 %, Acros) polystyrene (PSt) standards (Polymer Laboratories), 2-(4-hydroxyphenylazo)benzoic acid (HABA) (99.5 %; Sigma-Aldrich) and 2,5-dihydroxybenzoic acid (DHB) (> 99 %; Sigma-Aldrich) were used as received.

High-performance liquid chromatography (HPLC) grade THF (Panreac) was filtered (0.2 μm filter) under reduced pressure before use. *Tris*[2-(dimethylamino) ethyl] amine (Me_6TREN) was synthesized according to the procedure described in the literature.[17] Metallic copper (Cu(0), d = 1 mm, Sigma Aldrich) was washed with HCl in methanol and subsequently rinsed with acetone and dried under a stream of nitrogen following the literature procedures.[5] Purified water (Milli-Q®, Millipore, resistivity >18 MΩ.cm) was obtained by reverse osmosis.

3.3.2 Techniques

The chromatographic parameters of the samples were determined using high performance size exclusion chromatography HPSEC; Viscotek (Viscotek TDAmax) with a differential viscometer (DV); right-angle laser-light scattering (RALLS, Viscotek); low-angle laser-light scattering (LALLS, Viscotek) and refractive index (RI) detectors. The column set consisted of a PL 10 mm guard column (50 × 7.5 mm^2) followed by one Viscotek Tguard column (8 μm), one Viscotek T2000 column (6 μm), one Viscotek T3000 column (6 μm) and one Viscotek LT4000L column (7 μm). HPLC dual piston pump was set with a flow rate of 1 mL/min. The eluent (THF) was previously filtered through a 0.2 μm filter. The system was also equipped with an on-line degasser. The tests were done at 30 °C using an Elder CH-150 heater. Before the injection (100 μL), the samples were filtered through a polytetrafluoroethylene (PTFE) membrane with 0.2 μm pore. The system was calibrated with narrow PS standards. The *dn/dc* was determined as 0.063 for PMA, 0.068 for PMMA, 0.105 for PVC and 0.185 for PSt. M_n^{SEC} and $Đ$ of the synthesized polymers were determined by multidetectors calibration using the OmniSEC software version: 4.6.1.354.

400 MHz ^{1}H NMR spectra of reaction mixture samples were recorded on a Bruker Avance III 400 MHz spectrometer, with a 5-mm TIX triple resonance detection probe, in $CDCl_3$ with tetramethylsilane (TMS) as an internal standard or THF-d_8. The monomer conversion was determined by integration of monomer and polymer peaks using MestRenova software version: 6.0.2-5475.

3.3.3 Procedures

3.3.3.1 Typical procedure for the $[Cu(0)]_0/[CuBr_2]_0/[Me_6TREN]_0$ = Cu(0) wire/0.1/1.1 catalyzed SARA ATRP of MA in sulfolane/water = 90/10 (v/v)

Cu(0) wire (l = 5 cm) and a solution of $CuBr_2$ (3.506 mg, 0.016 mmol) and Me_6TREN (39.76 mg, 0.173 mmol) in sulfolane (1.42 mL) and water (157.9 μL) were placed in a Schlenk tube reactor. A mixture of MA (3.16 mL, 34.85 mmol) and EBiB (30.62 mg, 0.157 mmol) was added to the reactor that was sealed, by using a glass stopper, and frozen in liquid nitrogen. The Schlenk tube reactor containing the reaction mixture was deoxygenated with four freeze-vacuum-thaw cycles and purged with nitrogen. The reactor was placed in a water bath at 30 °C with stirring (700 rpm). During the

polymerization, different reaction mixture samples were collected by using an airtight syringe and purging the side arm of the Schlenk tube reactor with nitrogen. The samples were analyzed by ^{1}H NMR spectroscopy to determine the monomer conversion and by SEC, to determine M_n^{SEC} and $Đ$ of the polymers. The polymerizations of MMA and St were conducted following the same procedure and adjusting the reaction conditions (*e.g.*, temperature, catalyst nature, etc.)

3.3.3.2 Typical procedure for the $[Cu(0)]_0/[TREN]_0$ = Cu(0) wire/1 catalyzed SARA ATRP of VC

A 50 mL Ace glass 8645#15 pressure tube, equipped with bushing and plunger valve, was charged with a mixture of $CHBr_3$ (82.9 mg, 0.33 mmol), TREN (48.0 mg, 0.33 mmol), Cu(0) wire (l = 5), sulfolane (4.50 mL) and water (0.50 mL). The precondensed VC (5 mL, 72.8 mmol) was added to the tube. The exact amount of VC was determined gravimetrically. The tube was closed, placed in liquid nitrogen and degassed through the plunger valve by applying reduced pressure and filling the tube with N_2 about 20 times. The valve was closed, and the tube reactor was placed in a water bath at 42 °C with stirring (700 rpm). The reaction was stopped by plunging the tube into ice water. The tube was slowly opened, the excess of VC was distilled, and the mixture was precipitated into methanol. The polymer was separated by filtration and dried in a vacuum oven until constant weight to produce. The monomer conversion was determined gravimetrically. SEC was used for the determination of PVC´s M_n^{SEC} and $Đ$.

3.3.3.3 Typical procedure for the synthesis of PMA-*b*-PVC-*b*-PMA block copolymers by "one-pot" $[Cu(0)]_0/[TREN]_0$ = Cu(0) wire/1 catalyzed SARA ATRP

A 50 mL Ace glass 8645#15 pressure tube, equipped with bushing and plunger valve, was charged with a mixture of $CHBr_3$ (110.5 mg, 0.44 mmol), TREN (63.9 mg, 0.44 mmol), Cu(0) wire (l = 5), sulfolane (2.7 mL) and water (0.3 mL) . The precondensed VC (3.0 mL, 43.7 mmol) was added to the tube. The exact amount of VC was determined gravimetrically. The tube was closed, submerged in liquid nitrogen and degassed through the plunger valve by applying reduced pressure and filling the tube with nitrogen about 20 times. The valve was closed, and the tube reactor was placed

in a water bath at 42 °C with stirring (700 rpm). After 1.25 h, the reaction was stopped by plunging the tube into ice water. The tube was slowly opened and the excess VC was distilled. The monomer conversion was determined gravimetrically (47.3%), and the M_n^{SEC} = 7.8 x 103 and $Đ$ = 1.69 were determined by SEC analysis. A mixture of sulfolane (10.8 mL), water (1.2 mL) and MA (12 mL, 132.4 mmol) was added to the same 50 mL Ace glass 8645#15 pressure tube (without any purification of the α,ω-di(bromo)PVC macroinitiator). The tube was closed, submerged in liquid nitrogen and degassed through the plunger valve by applying reduced pressure and filling the tube with nitrogen about 20 times. The valve was closed, and the tube reactor was placed in a water bath at 42 °C with stirring (700 rpm). The reaction was stopped after 0.5 h and the mixture was analyzed by ^{1}H NMR spectroscopy in order to determine the MA conversion and by SEC, to determine the M_n^{SEC} and $Đ$ of the PMA-*b*-PVC-*b*-PMA triblock copolymer.

3.4 Results and discussion

Our research group[15] has reported for the first time the use of sulfolane as a universal solvent for the Cu(0)-mediated SARA ATRP of acrylates, methacrylates, St and VC. The results showed fast and controlled polymerizations, using low amounts of soluble copper for the SARA ATRP of MA, MMA, St and VC. It is known that the addition of water to a SARA ATRP solvent system leads to an increase of the reaction rate, which can also contribute to improve any process of polymer production in large scale.

The effect of water on the SARA ATRP of MA was firstly evaluated using different ratios sulfolane/water in order to find the optimal value that could afford the faster and yet controlled polymerizations. The results (Table 3.1) shows that the presence of water in the reaction mixture allowed the increase of the reaction rate in comparison to pure sulfolane (*e.g.*, 1.5 times faster for 10 % water content), as it was previously observed for other SARA ATRP systems. [15]

Table 3.1 Kinetic data for the Cu(0)-mediated SARA ATRP of MA in sulfolane/water mixtures. Conditions: $[MA]_0/[solvent]$ = 2/1 (v/v); $[MA]_0/[EBiB]_0/[Cu(0)\ wire]_0/[CuBr_2]_0/[Me_6TREN]_0$ = 222/1/1/0/1.1; T = 30 °C.

Entry	S/W[a] (v/v)	k_p^{app} (h^{-1})	Time (h)	Conv. (%)[b]	M_n^{th} x 10^{-3a}	M_n^{SEC} x 10^{-3a}	$Đ$
1	100/0	1.426	1.3	83	16.0	17.4	1.05
2	95/5	1.527	1.2	86	16.6	21.9	1.11
3	90/10	2.266	1.2	93	17.9	23.8	1.06
4	80/20	2.240	1.0	81	15.6	24.3	1.25
5	70/30	1.100	1.0	69	13.3	21.8	2.03
6	65/35	-	2.6	69	13.4	33.1	1.37

[a] Sulfolane/water [b] Maximum monomer conversion obtained in the reaction

Up to 20 % of water content in the solvent mixture, the rate of reaction was first-order with respect to monomer conversion and the molecular weights determined by SEC were in close agreement with the theoretical values (Figure 3.1). In addition, the resulting PMA presented very low dispersity ($Đ \leq 1.1$) throughout the reaction. Water contents of 30 % or higher were found to be not suitable for this particular sulfolane-based solvent mixture, since precipitation of the PMA (DP = 222) occurs, which ultimately hampered any control over the polymerization (Table B.1, entries 5-6).

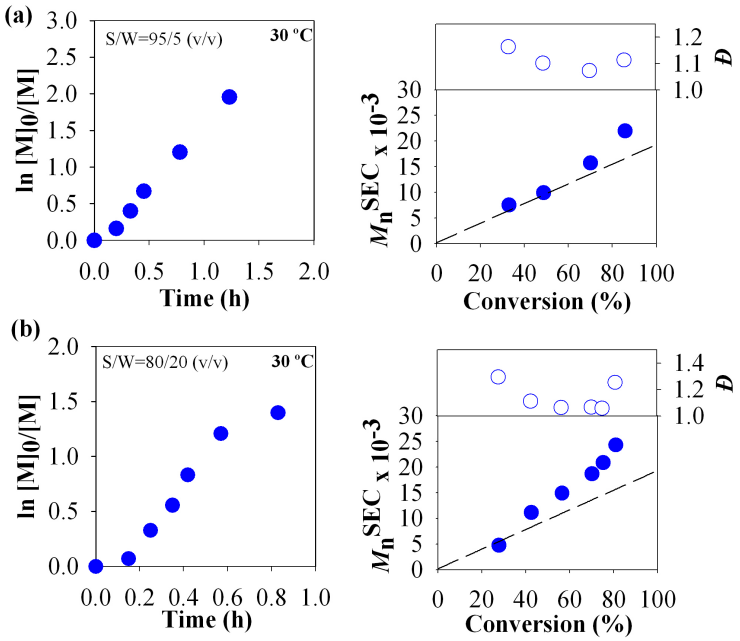

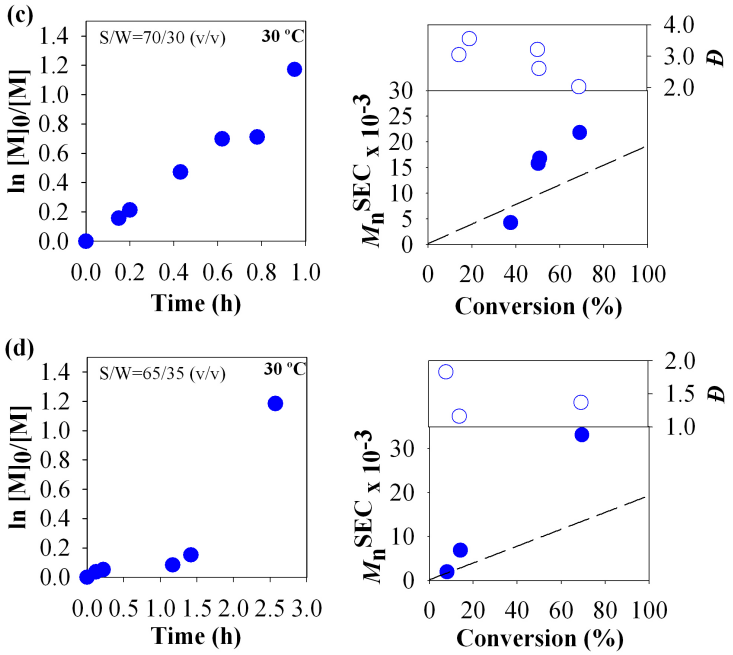

Figure 3.1 - Kinetic plots of (a) $\ln[M]_0/[M]$ *vs.* time and plot of number-average molecular weights (M_n^{SEC}) and $Đ$ *vs.* conversion for the SARA ATRP of MA using Cu(0) wire as supplemental activator and reducing agent in different sulfolane/water mixtures at 30 ºC. Conditions: $[MA]_0/[solvent]$ = 2/1 (v/v); $[MA]_0/[EBiB]_0/Cu(0)wire/[Me_6TREN]_0$ = 222/1/Cu(0) wire/1.1 (molar); Cu (0): d = 1 mm, l = 5 cm.

The kinetic data suggests that 10 % of water represents an interesting compromise between the rate of reaction and the control over the molecular weight of the polymers. Therefore, this value was selected for the following studies.

3.4.1 SARA ATRP of (meth)acrylates, styrene and vinyl chloride in sulfolane/water = 90/10 (v/v)

The use of the solvent mixture sulfolane/water = 90/10 (v/v) was investigated for the Cu(0)-catalyzed SARA ATRP of MA (section 3.4), MMA, St and VC (non-activated monomer) (Figure 3.2). The catalytic complexes and initiators were selected according to the structure of the monomers, in order to provide well-controlled polymerizations.[15]

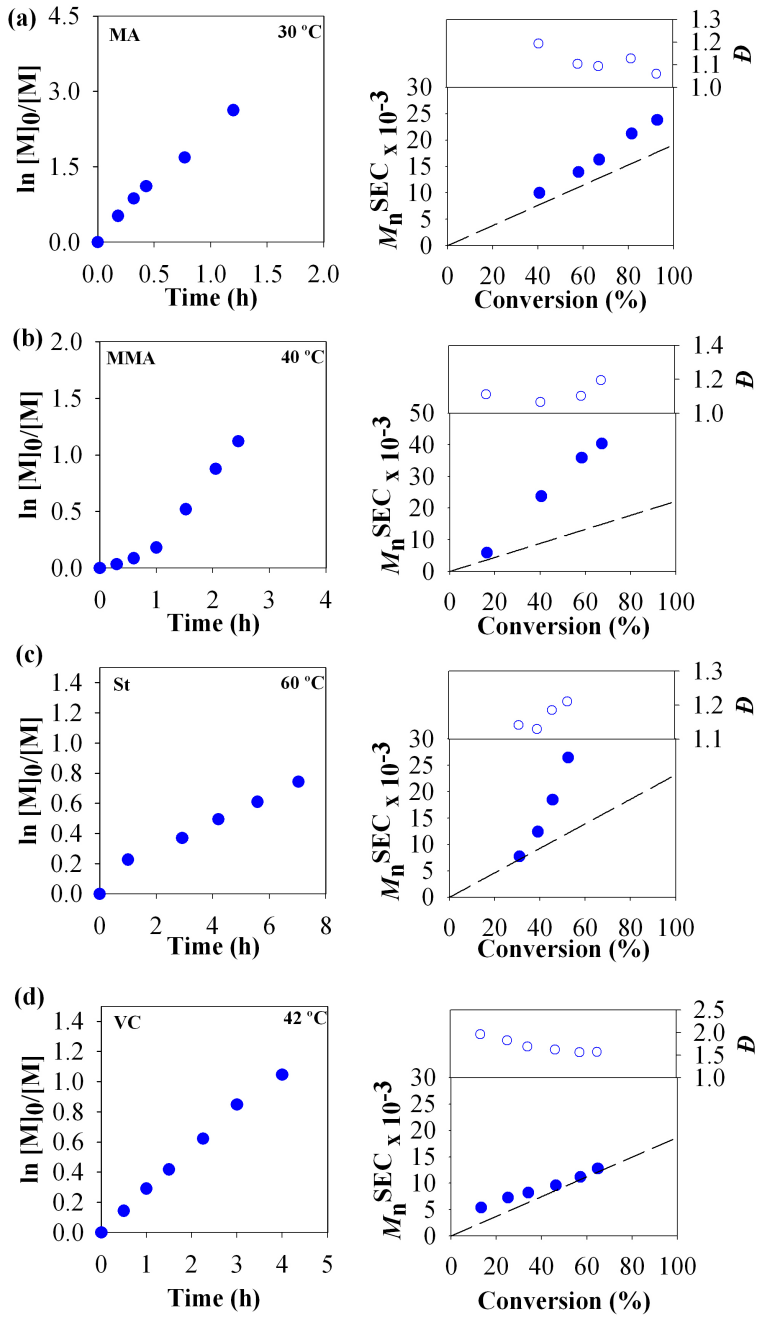

Figure 3.2 Kinetic plots of conversion and $\ln[M]_0/[M]$ *vs*. time and plot of number-average molecular weights (M_n^{SEC}) and $Đ$ (M_w/M_n) *vs*. conversion for the SARA ATRP of (a) MA, (b) MMA, (c) St and (d) VC using Cu(0) wire as the SARA agent in solvent sulfolane/water = 90/10 (v/v). Conditions: (a) $[MA]_0/[EBiB]_0$/Cu(0) wire/$[Me_6TREN]_0$ = 222/1/Cu(0) wire/1.1 (molar), $[MA]_0/[Solvent]$ = 2/1 (v/v) and T = 30 °C; (b) $[MMA]_0/[EBPA]_0$/Cu(0) wire/ $[CuBr_2]_0/[bpy]_0$ = 222/1/Cu(0) wire/0.1/2.2 (molar), $[MMA]_0/[Solvent]$ = 1/1 (v/v) and T = 40 °C; (c) $[St]_0/[EBiB]_0$/Cu(0) wire/$[PMDETA]_0$ = 222/1/Cu(0) wire/1.1 (molar), $[St]_0/[Solvent]$ = 2/1 (v/v) and T = 60 °C; (d) $[VC]_0/[CHBr_3]_0/[Cu(0)\ wire]_0/\ [TREN]_0$ = 222/1/ Cu(0) wire/1, $[VC]_0/[Solvent]$ = 1/1 and T = 42 °C; Cu (0): d = 1 mm, l = 5 cm

All the polymerizations were first-order with respect to monomer conversion and all the data obtained show the control over the reaction. Therefore they were in agreement with the ones previously reported for the polymerizations in anhydrous sulfolane.[15]

The rate of polymerization was considerably higher than the previously reported for MA, MMA and VC. However, it is interesting to notice that for St, the addition of 10 % of water in the reaction mixture did not influence the rate of polymerization. Nevertheless, the control over the PS molecular weight was good. Even though, these are encouraging results which suggest that the SARA ATRP method developed could be potentially used at an industrial scale. Faster reactions using industrial solvents will turn the large production much affordable. Therefore, it is strongly believed that the creation of industrially feasible ATRP methods for the production of common polymers will allow a wider use of the technique.

3.4.2 Influence of the catalytic system

In our previous report on the SARA ATRP in sulfolane,[15] it was demonstrated that the polymerization could not be performed using the $Na_2S_2O_4$ as the SARA agent, due to the insolubility of this compound. However, the use of $Na_2S_2O_4$ as a co-catalyst is a very interesting and safe alternative to the use of copper, since it is commonly used in some beverages (*e.g.*, wine). Previous results have shown that the addition of water to organic-based solvent mixtures provides a slow dissolution of $Na_2S_2O_4$ during the SARA ATRP, affording the continuous regeneration of Cu(I) activator species and a controlled polymerization.[9-10]

Table 3.2 - Molecular weight parameters of the PMA-Br prepared by SARA ATRP in sulfolane and sulfolane/water = 90/10 (v/v) at 30 °C, using different SARA agents. Reaction conditions: $[MA]_0/[EBiB]_0 = 222$; $[MA]_0/[solvent] = 2/1$ (v/v); $[Cu(0)]_0/[CuBr_2]_0/[Me_6TREN]_0$ = Cu(0) wire/0.1/1.1; $[Na_2S2O_4]_0/[CuBr_2]_0/[Me_6TREN]_0 = 1/0.1/0.2$.

Entry	S/W[b] (v/v)	SARA agent	k_p^{app} (h^{-1})	Time (h)	Conv. (%)	M_n^{th} x 10^{-3}	M_n^{SEC} x 10^{-3}	$Đ$
1	100/0	Cu(0)	1.002	1.3	72	13.8	17.0	1.1
2	90/10	Cu(0)	1.642	1.0	78	15.1	22.2	1.04
3[a]	100/0	$Na_2S_2O_4$	-	5.0	0	-	-	-
4	90/10	$Na_2S_2O_4$	1.348	1.0	77	14.8	20.4	1.12

[a] No polymerization occurred ; [b] Sulfolane/water

Table 3.2 (entry 4) shows that well-defined PMA could be obtained at high monomer conversion (DP = 222), in 1 h, when $Na_2S_2O_4$ was used as the SARA agent in a sulfolane/water = 90/10 (v/v) mixture. In addition, the polymerization rate was similar to the one obtained using Cu(0) as the SARA agent (Table 3.2, entry 2). These are very encouraging results, which clearly demonstrate the versatility of the SARA ATRP developed method.

3.4.3 Synthesis of a PMA-*b*-PVC-*b*-PMA triblock copolymer by "one-pot" SARA ATRP

One of the advantages of using RDRP methods is the possibility of designing complex polymeric structures, due to the high chain-end functionality of the resulting polymers. In this work, a α,ω-di(bromo)PVC (conv.$_{VC}$ = 47.3 %, M_n^{th} = 3.8 x 10^3, M_n^{SEC} = 7.8 x 10^3, $Đ$ = 1.69) obtained by bromoform-initiated SARA ATRP was used as a macroinitiator for the preparation of a PMA-*b*-PVC-*b*-PMA (conv.$_{MA}$ = 84.3%, M_n^{th} = 56.4 x 10^3, M_n^{SEC} = 36.3 x 10^3, $Đ$ = 1.48) triblock copolymer by "one-pot" SARA ATRP in sulfolane/water = 90/10 (v/v).

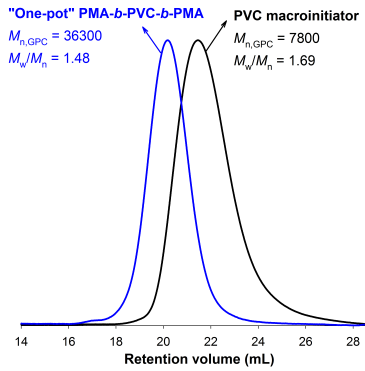

Figure 3.3 – SEC chromatograms of a α,ω-di(bromo)PVC (conv.$_{VC}$ = 47.3 %, M_n^{th} = 3.8 x 10^3, M_n^{SEC} = 7.8 x 10^3, $Đ$ = 1.69) macroinitiator (black line) and PMA-b-PVC-b-PMA triblock copolymer (conv.$_{MA}$ = 84.3%, M_n^{th} = 56.4 x 10^3, M_n^{SEC} = 36.3 x 10^3, $Đ$ = 1.48) (blue line), after "one-pot" chain extension by SARA ATRP in sulfolane/water = 90/10 (v/v).

The chromatograms shown in Figure 3.3 demonstrate a shift of the macroinitiator´s molecular weight distribution towards high molecular weight values (lower retention volume), with no increase of the dispersity of the block copolymer, confirming the retention of the chain-end functionality of the PVC prepared by SARA ATRP. Additionally, the structure of the well-defined PVC macroinitiator was confirmed by ^{1}H NMR spectroscopy (Figure 3.4).

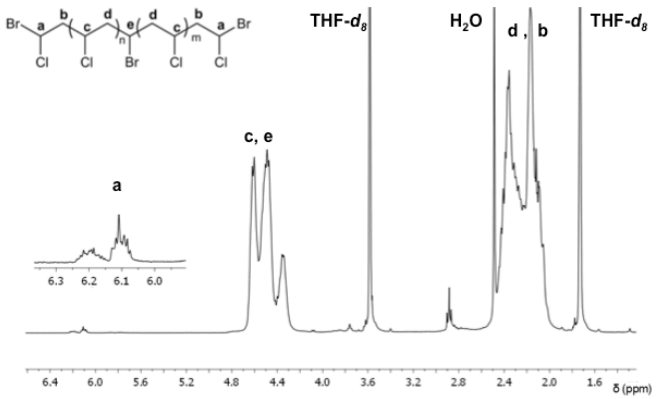

Figure 3.4 - ^{1}H NMR spectrum (solvent: THF-d_8) of a Br-PVC-Br (M_n^{SEC} = 7.8 x 10^3 ; $Đ$ = 1.69) sample obtained by SARA ATRP.

These results suggest that the SARA ATRP in sulfolane/water mixtures could be a very useful tool for the macromolecular engineering field. The structure of the block copolymer was confirmed by ^{1}H NMR analysis (Figure 3.5).

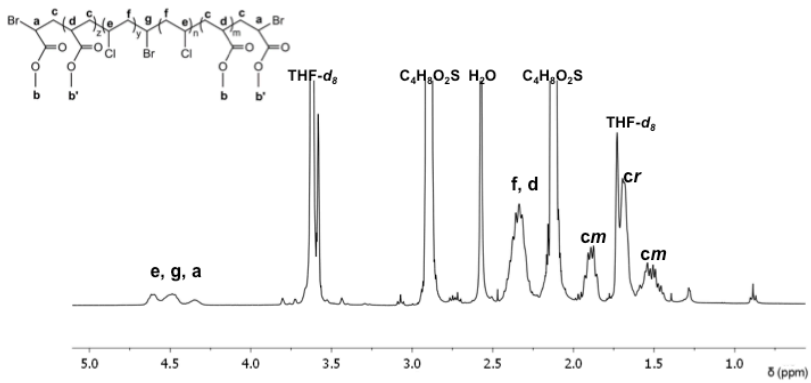

Figure 3.5^{1}H NMR spectrum (solvent: THF-d_8) of a purified PMA-*b*-PVC-*b*-PMA (M_n^{SEC} = 36.3 x 10^3, $Đ$ = 1.48) triblock copolymer obtained by "one-pot" SARA ATRP in sulfolane/water = 90/10 (v/v).

3.5 Conclusions

Well-defined (co)polymers derived from acrylates, methacrylates, styrene and vinyl chloride were synthesized through SARA ATRP in sulfolane/water mixtures using a low concentration of soluble copper. The addition of water to the reaction mixture was found to increase the polymerization rate compared to data published by our research group using pure sulfolane as the polymerization solvent. The reaction conditions used can be considered very attractive for a future industrial implementation of the technique, providing a convenient and robust method to afford a wide range of macromolecules.

3.6 References

1. Matyjaszewski, K.; Tsarevsky, N. V., Macromolecular Engineering by Atom Transfer Radical Polymerization, *Journal of the American Chemical Society*, *136* (18), 6513-6533, 2014.
2. Magenau, A. J. D.; Strandwitz, N. C.; Gennaro, A.; Matyjaszewski, K., Electrochemically Mediated Atom Transfer Radical Polymerization, *Science*, *332* (6025), 81-84, 2011.
3. Matyjaszewski, K.; Jakubowski, W.; Min, K.; Tang, W.; Huang, J.; Braunecker, W. A.; Tsarevsky, N. V., Diminishing catalyst concentration in atom transfer radical polymerization with reducing agents, *Proceedings of the National Academy of Sciences*, *103* (42), 15309-15314, 2006.
4. Mendonca, P. V.; Serra, A. C.; Coelho, J. F. J.; Popov, A. V.; Guliashvili, T., Ambient temperature rapid ATRP of methyl acrylate, methyl methacrylate and styrene in polar solvents with mixed transition metal catalyst system, *European Polymer Journal*, *47* (7), 1460-1466, 2011.
5. Zhang, Y.; Wang, Y.; Matyjaszewski, K., ATRP of Methyl Acrylate with Metallic Zinc, Magnesium, and Iron as Reducing Agents and Supplemental Activators, *Macromolecules*, *44* (4), 683-685, 2011.
6. Rocha, N.; Mendonca, P. V.; Mendes, J. P.; Simoes, P. N.; Popov, A. V.; Guliashvili, T.; Serra, A. C.; Coelho, J. F. J., Facile Synthesis of Well-Defined Telechelic Alkyne-Terminated Polystyrene in Polar Media Using ATRP With Mixed Fe/Cu Transition Metal Catalyst, *Macromolecular Chemistry and Physics*, *214* (1), 76-84, 2013.
7. Cordeiro, R. A.; Rocha, N.; Mendes, J. P.; Matyjaszewski, K.; Guliashvili, T.; Serra, A. C.; Coelho, J. F. J., Synthesis of well-defined poly(2-(dimethylamino)ethyl methacrylate) under mild conditions and its co-polymers with cholesterol and PEG using Fe(0)/Cu(ii) based SARA ATRP, *Polymer Chemistry*, *4* (10), 3088-3097, 2013.
8. Gois, J. R.; Rocha, N.; Popov, A. V.; Guliashvili, T.; Matyjaszewski, K.; Serra, A. C.; Coelho, J. F. J., Synthesis of well-defined functionalized poly(2-(diisopropylamino)ethyl methacrylate) using ATRP with sodium dithionite as a SARA agent, *Polymer Chemistry*, *5* (12), 3919-3928, 2014.

9. Gois, J. R.; Konkolewic, D.; Popov, A. V.; Guliashvili, T.; Matyjaszewski, K.; Serra, A. C.; Coelho, J. F. J., Improvement of the control over SARA ATRP of 2-(diisopropylamino)ethyl methacrylate by slow and continuous addition of sodium dithionite, *Polymer Chemistry*, *5* (16), 4617-4626, 2014.
10. Abreu, C. M. R.; Serra, A. C.; Popov, A. V.; Matyjaszewski, K.; Guliashvili, T.; Coelho, J. F. J., Ambient temperature rapid SARA ATRP of acrylates and methacrylates in alcohol-water solutions mediated by a mixed sulfite/Cu(ii)Br2 catalytic system, *Polymer Chemistry*, *4* (23), 5629-5636, 2013.
11. Abreu, C. M. R.; Mendonca, P. V.; Serra, A. C.; Popov, A. V.; Matyjaszewski, K.; Guliashvili, T.; Coelho, J. F. J., Inorganic Sulfites: Efficient Reducing Agents and Supplemental Activators for Atom Transfer Radical Polymerization, *ACS Macro Letters*, *1* (11), 1308-1311, 2012.
12. Guliashvili, T.; Mendonça, P. V.; Serra, A. C.; Popov, A. V.; Coelho, J. F. J., Copper-Mediated Controlled/"Living" Radical Polymerization in Polar Solvents: Insights into Some Relevant Mechanistic Aspects, *Chemistry – A European Journal*, *18* (15), 4607-4612, 2012.
13. Konkolewicz, D.; Krys, P.; Góis, J. R.; Mendonça, P. V.; Zhong, M.; Wang, Y.; Gennaro, A.; Isse, A. A.; Fantin, M.; Matyjaszewski, K., Aqueous RDRP in the Presence of Cu0: The Exceptional Activity of CuI Confirms the SARA ATRP Mechanism, *Macromolecules*, *47* (2), 560-570, 2014.
14. Mendonca, P.; Konkolewicz, D.; Averick, S.; Serra, A. C.; Popov, A.; Guliashvili, T.; Matyjaszewski, K.; Coelho, J., Synthesis of cationic poly((3-acrylamidopropyl) trimethylammonium chloride) by SARA ATRP in ecofriendly solvent mixtures, *Polymer Chemistry*, *in press*, 2014.
15. Mendes, J. P.; Branco, F.; Abreu, C. M. R.; Mendonça, P. V.; Serra, A. C.; Popov, A. V.; Guliashvili, T.; Coelho, J. F. J., Sulfolane: an Efficient and Universal Solvent for Copper-Mediated Atom Transfer Radical (co)Polymerization of Acrylates, Methacrylates, Styrene, and Vinyl Chloride, *ACS Macro Letters*, *3* (9), 858-861, 2014.
16. Abreu, C. M. R.; Mendonca, P. V.; Serra, A. C.; Coelho, J. F. J.; Popov, A. V.; Guliashvili, T., Accelerated Ambient-Temperature ATRP of Methyl Acrylate in Alcohol-Water Solutions with a Mixed Transition-Metal Catalyst System, *Macromolecular Chemistry and Physics*, *213* (16), 1677-1687, 2012.
17. Ciampolini, M.; Nardi, N., Five-Coordinated High-Spin Complexes of Bivalent Cobalt, Nickel, andCopper with Tris(2-dimethylaminoethyl)amine, *Inorganic Chemistry*, *5* (1), 41-44, 1966.

Chapter 4

Synergistic effect of 1-butyl-3-methylimidazolium hexafluorophosphate and DMSO in the SARA ATRP at room temperature affording very fast reactions and polymers with very low dispersity

The results of this work is published in: **Mendes, J. P**.; Branco, F.; Abreu, C. M. R.; Mendonça, P. V.; Popov, A. V.; Guliashvili, T.; Serra, A. C.; Coelho, J. F. J., *"Synergistic Effect of 1-Butyl-3-methylimidazolium Hexafluorophosphate and DMSO in the SARA ATRP at Room Temperature Affording Very Fast Reactions and Polymers with Very Low Dispersity", ACS Macro Letters*, 3 (6), 544-547, 2014.

4.1 Abstract

An unusual synergistic effect between 1-butyl-3-methylimidazolium hexafluorophosphate ([BMIM]-[PF_6]) and dimethyl sulfoxide (DMSO) mixtures is reported for the supplemental activator and reducing agent atom transfer radical polymerization (SARA ATRP) of methyl acrylate (MA) using a catalytic system composed by sodium dithionite ($Na_2S_2O_4$) and $CuBr_2$/Me_6TREN (Me_6TREN: *tris*[2-(dimethylamino)ethyl]amine) at room temperature. To the best of our knowledge, the use of ionic liquids (IL) has never been reported for the SARA ATRP. The kinetic data obtained for a broad range of target molecular weights revealed very fast polymerization rates, low dispersity values ($Đ$ < 1.05) and well-defined chain-end functionalities.

4.2 Introduction

Atom transfer radical polymerization (ATRP) is one the most efficient, versatile and robust reversible deactivation radical polymerization (RDRP) techniques.[1] This method allows the synthesis of polymers to have a vast range of specific functionalities with controlled molecular weight, architecture and topology.[2] ATRP is based on the use of a transition metal complex, which mediates a fast equilibrium between dormant and active species (Scheme 4.1).

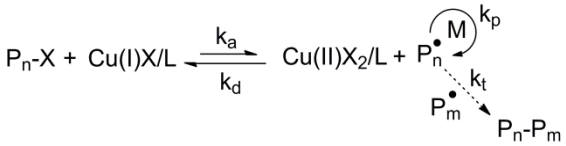

Scheme 4.1 General mechanism of ATRP.

Several transition metal complexes in combination with different ligands (typically nitrogen-based ligands) have been employed in ATRP,[3] being Cu-based the most used ones.[4] Aiming to reduce the amount of metal complexes required to control the polymerizations, several ATRP variations were proposed, such as: activators regenerated by electron transfer (ARGET) ATRP using inorganic or organic reducing

agents;[5-6] supplemental activator and reducing agent (SARA) ATRP involving the use of zero valent transition metals[3, 5, 7-9]or inorganic sulfites;[10-12] initiators for continuous activator regeneration (ICAR) ATRP employing conventional thermal radical initiators; and electrochemically mediated ATRP (*e*-ATRP) that uses electrical current for the reduction process.[13] The use of reducing agents allows the continuous regeneration of Cu(I) species during the polymerization, lowering the amount of catalyst to ppm levels. Ionic liquids (IL) are a class of "green solvents"[14-16] that present important advantages over several conventional and harmful organic solvents. Among those, one can stress the possibility of tailoring the properties of the IL by varying the structures of both cation and anion, excellent solubility of polar substrates, low volatility, recyclability and compatibility with various organic compounds. Since the pioneer works of Haddleton,[17] Kubisa[18] and Matyjaszewski,[19] several reports have been published using IL as solvents for ATRP.[16, 20-23] The results revealed interesting features of these solvents related to simplified separation of the polymer from the catalyst,[17, 19] controlled reactions in the absence of ligand, reduction of side reactions and catalytic effects.[20]

Here, we report a synergistic effect of dimethyl sulfoxide (DMSO) and 1-butyl-3-methylimidazolium hexafluorophosphate ([BMIM]-[PF_6]) in the SARA ATRP of methyl acrylate (MA) catalyzed by $Na_2S_2O_4$ and small amounts of $CuBr_2$/Me_6TREN (Me_6TREN: *tris*[2-(dimethylamino)ethyl]amine) deactivator complex at room temperature.

4.3 Experimental Section

4.3.1 Materials

Methyl acrylate (MA) (99 % stabilized; Acros) was passed over a sand/alumina column before use to remove the radical inhibitor. Pentaerythritol tetrakis(2-bromoisobutyrate) (4f-BiB, 97 %; Sigma-Aldrich), copper(II) bromide ($CuBr_2$, +99 % extra pure, anhydrous; Acros), sodium hydrosulfite also known as sodium dithionite ($Na_2S_2O_4$, 85 %, technical grade; Aldrich), ethyl 2-bromoisobutyrate (EBiB, 98 %; Aldrich), N,N,N',N'',N''-pentamethyldiethylenetriamine (PMDETA, 99 %; Aldrich), tetrabutylammonium hexafluorophosphate ($TBAPF_6$, 98 %, Sigma-Aldrich), Reichardt's dye (30) (90 %, Sigma-Aldrich), deuterated chloroform ($CDCl_3$, +1% tetramethylsilane (TMS); Euriso-top), dimethyl sulfoxide (DMSO, +99.8 % extra

pure; Acros), 1-butyl-3-methylimidazolium hexafluorophosphate ([BMIM]-[PF_6], > 98 %; TCI (Tokyo Chemical Industry Co. LTD)), polystyrene (PSt) standards (Polymer Laboratories), 2-(4-hydroxyphenylazo)benzoic acid (HABA, 99.5 %; Sigma Aldrich), 2,5-dihydroxybenzoic acid (DHB, > 99 %; Sigma Aldrich) were used as received. Tetrahydrofuran (THF, high-performance liquid chromatography (HPLC) grade; Panreac) was filtered (0.2 μm filter) under reduced pressure before use. Me_6TREN was synthesized according to the procedure described in the literature.[24]

4.3.2 Techniques

The chromatographic parameters of the samples were determined using high performance size-exclusion chromatography (HPSEC); Viscotek (Viscotek TDAmax) with a differential viscometer (DV); right-angle laser-light scattering (RALLS) (Viscotek); low-angle laser-light scattering (LALLS) (Viscotek) and refractive index (RI) detectors. The column set consisted in a PL 10 mm guard column (50 × 7.5 mm^2) followed by one Viscotek T200 column (6 μm), one MIXED-E PLgel column (3 μm) and one MIXED-C PLgel column (5 μm). A HPLC dual piston pump was set at a flow rate of 1 mL/min. The eluent, THF, was previously filtered through a 0.2 μm filter. The system was also equipped with an on-line degasser. The tests were done at 30 °C using an Elder CH-150 heater. Before the injection (100 μL), the samples were filtered through a polytetrafluoroethylene (PTFE) membrane with 0.2 μm pore. The system was calibrated with narrow polystyrene (PS) standards. The *dn/dc* of PMA was determined as 0.063. The number-average molecular weight (M_n^{SEC}) and dispersity (Đ) of synthesized polymers were determined by multidetectors calibration using OmniSEC software version: 4.6.1.354.

400 MHz ^{1}H NMR spectra of the reaction mixture samples were recorded on a Bruker Avance III 400 MHz spectrometer, with a 5-mm TIX triple resonance detection probe, in $CDCl_3$ with TMS as an internal standard. Conversion of the monomer was determined by integration of monomer and polymer peaks using MestRenova software version: 6.0.2-5475.

The PMA samples were dissolved in THF at a concentration of 10 mg/mL for the MALDI-TOF-MS analysis and DHB and HABA (0.05 M in THF) were used as matrices. The dried-droplet samples preparation technique was used to obtain a 1:1 ratio (sample/matrix); an aliquot of 1 μL of each sample was directly spotted on the

MTP AnchorChip TM 600/384 TF MALDI target, BrukerDaltonik (Bremen Germany) and, before the sample dried, 1 μL of matrix solution in THF was added and the mixture allowed to dry at room temperature, to allow matrix crystallization. External mass calibration was performed with a peptide calibration standard (PSCII) for the range 700-3000 (9 mass calibration points), 0.5 μL of the calibration solution and matrix previously mixed in an Eppendorf tube (1:2, v/v) were applied directly on the target and allowed to dry at room temperature. Mass spectra were recorded using an Autoflex III smartbeam 1 MALDI-TOF-MS mass spectrometer BrukerDaltonik (Bremen Germany) operating in the linear and reflectron positive ion mode. Ions were formed upon irradiation by a smartbeam laser using a frequency of 200 Hz. Each mass spectrum was produced by averaging 2500 laser shots collected across the whole sample spot surface by screening and in the range m/z 500-12500. The laser irradiance was set to 35-40% (relative scale 0-100) arbitrary units according to the corresponding threshold required for the applied matrix systems.

The UV/Vis studies were performed with a Jasco V-530 spectrophotometer. The analyses were carried out in the 350–1100 nm range at room temperature (rt).

4.4 Procedures

4.4.1.1 Typical Procedure for the $[Na_2S_2O_4]/[CuBr_2]/[Me_6TREN]$ = 1/0.1/0.1 catalyzed SARA ATRP of MA (DP=222) in [BMIM]-$[PF_6]$/DMSO = 50/50 (v/v)

In a typical SARA ATRP polymerization of MA, $Na_2S_2O_4$ (30.62 mg, 0.16 mmol) was placed in Schlenk reactor. A mixture of $CuBr_2$ (3.55 mg, 0.16 mmol), Me_6TREN (3.69 mg, 0.02 mmol) and DMSO (0.785 mL) was added to the reactor and after this a mixture of MA (3.14 mL, 34.8 mmol), EBiB (30.62 mg, 0.16 mmol) and [BMIM]-$[PF_6]$ (0.785 mL) was also added to the Schlenk that was sealed and frozen in liquid nitrogen. The Schlenk reactor containing the reaction mixture was deoxygenated with four freeze-vacuum-thaw cycles and purged with nitrogen. The reactor was placed in a water bath at 30 °C with stirring (700 rpm). During the polymerization, different reaction mixture samples were collected by using an airtight syringe and purging the side arm of the Schlenk reactor with nitrogen. The samples were analyzed by ^1H NMR spectroscopy to determine the monomer conversion and by SEC, to determine the M_n^{SEC} and $Đ$ of the polymers.

4.4.1.2 Chain extension experiment of –Br terminated PMA

A PMA-Br macroinitiator obtained with a typical $Na_2S_2O_4$/$CuBr_2$/Me_6TREN-catalyzed SARA ATRP reaction was precipitated in a cold hexane (ice bath). The polymer was then dissolved in THF and filtered through a sand/alumina column, to remove traces of the catalyst, and was reprecipitated in cold hexane. The polymer was dried under vacuum until constant weight. The purified monomer (MA) (4.18 mL, 46.5 mmol) was added to the –Br terminated PMA macroinitiator (M_n^{SEC} = 6.90 x 10^3; $Đ$ = 1.05 , 641 mg, 0.09 mmol) in a Schlenk reactor. A mixture of [BMIM]-[PF_6] (2.09 mL), DMSO (2.09 mL) (solvents previously bubbled with nitrogen for about 15 min), $Na_2S_2O_4$ (16.2 mg, 0.09 mmol), $CuBr_2$ (3.47 mg, 0.009 mmol) and Me_6TREN (3.58 mg, 0.009 mmol) was added to the reactor. The Schlenk was placed in the water bath at 30 °C with stirring (700 rpm) for 3h.

4.4.1.3 UV/Vis spectroscopy of $Na_2S_2O_4$/$CuBr_2$/Me_6TREN in [BMIM]-[PF_6]/DMSO = 50/50 (v/v)

$Na_2S_2O_4$ (50.0 mg, 0.250 mmol) were placed in a quartz UV/Vis cuvette, equipped with a magnetic stirrer, and purged with nitrogen. DMSO (1.25 mL), [BMIM]-[PF_6] (1.25 mL), $CuBr_2$ (5.6 mg, 0.025 mmol) and Me_6TREN (5.8 mg, 0.025 mmol) were mixed in a vial and bubbled with nitrogen for about 15 min to remove oxygen. This solution was then added to the UV/Vis cuvette which was sealed under nitrogen. The thermostated cuvette was placed in the spectrophotometer for spectra acquisition at specific times. The absorbance was measured at different times, in the 350-1100 nm range at room temperature.

4.4.1.4 Determination of E_T(30) in [BMIM]-[PF_6]/DMSO mixtures

Different [BMIM]-[PF_6] /DMSO mixtures (5.0 mL) were prepared and small amounts of Reichardt's dye 30 (0.138 mg) were added. These solutions were transferred placed into a UV/Vis cuvette and placed in the spectrophotometer for spectra acquisition. The absorbance was measured, in the 350-1100 nm range at room temperature. The E_T(30) values of different [BMIM]-[PF_6] mixtures were determined according to the expression $E_T(30) = 28591.5/\lambda_{abs,máx}(nm)$.[25]

4.5 Results and discussion

Preliminary experiments were performed using only [BMIM]-[PF_6] as solvent for the MA polymerization, but no polymer was formed. This result can be justified based on the partial solubilization of the $CuBr_2$/Me_6TREN complex and, most importantly, to the complete insolubility of the SARA agent ($Na_2S_2O_4$) in the [BMIM]-[PF_6], preventing the formation of Cu(I) activator species. With the introduction of DMSO as a co-solvent a controlled polymerization was observed. The kinetic plots of SARA ATRP carried out at room temperature in [BMIM]-[PF_6]/DMSO (ratio 5/95 and 50/50) catalyzed by $Na_2S_2O_4$/$CuBr_2$/Me_6TREN are presented in Figure 4.1 and Table 4.1 (entry 2 and 4), respectively.

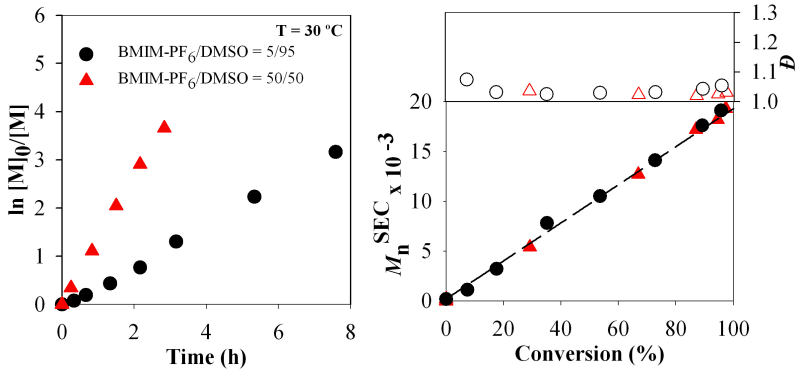

Figure 4.1 Kinetic plots of conversion and $\ln[M]_0/[M]$ *vs*. time and plots of number average molecular weights (M_n^{SEC}) and *Đ vs*. conversion for the SARA ATRP of MA catalyzed by $Na_2S_2O_4$/$CuBr_2$//Me_6TREN in [BMIM]-[PF_6]/DMSO = 5/95 (circle, black) and [BMIM]-[PF_6]/DMSO = 50/50 (triangle, red). Conditions: $[MA]_0/[solvent]$ = 2/1(v/v); $[MA]_0/[EBiB]_0/[Na_2S_2O_4]_0/[CuBr_2]_0/[Me_6TREN]_0$ = 222/1/1/0.1/0.1 (molar); T = 30 °C

The rate of polymerization (Figure 4.1) was first-order with respect to the concentration of monomer and the final conversion was close to 100%. The theoretical molecular weights were in very close agreement with M_n^{SEC} for the full range of monomer conversions, which indicates a quantitative initiation and an excellent control during the entire course of the polymerization (Figure 4.2).

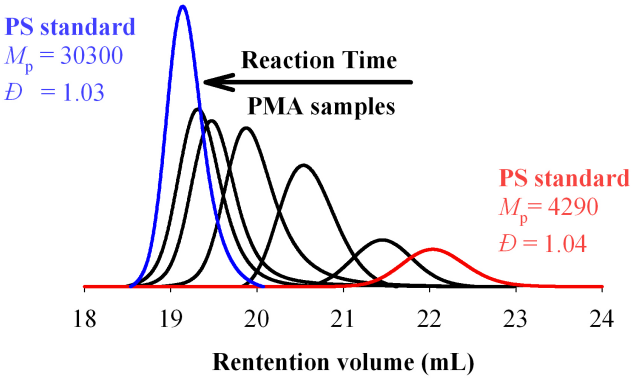

Figure 4.2 Chromatograms of PS standards (red and blue lines) and PMA samples (black lines) collected during the SARA ATRP of MA catalyzed by $Na_2S_2O_4$/$CuBr_2$/Me_6TREN in [BMIM]-[PF_6]/DMSO = 50/50. Conditions: $[MA]_0/[solvent]$ = 2/1 (v/v); $[MA]_0/[EBiB]_0/[Na_2S_2O_4]_0/[CuBr_2]_0/[Me_6TREN]_0$ = 222/1/1/0.1/0.1 (molar); T = 30 °C.

Interesting, for a ratio [BMIM]-[PF_6]/DMSO of 50/50 (Figure 4.1, Table 4.1 entry 4), the *Đ* data allowed us to draw the same conclusions as the ones obtained for a ratio of 5/95. However, the reaction rate was 3 times faster for the ratio 50/50 (6 times faster than the obtained for pure DMSO, Table 4.1 entry 1). In order to determine the optimal [BMIM]-[PF_6] to DMSO ratio in order to afford fast polymerization while maintaining the living characteristics of the system, different ratios were investigated (Figure 4.3, Table 4.1, entries 1 to 6).

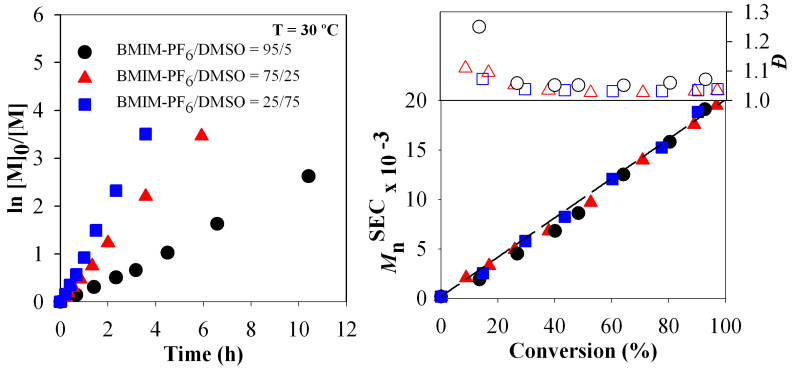

Figure 4.3 Kinetic plots of conversion and $\ln[M]_0/[M]$ *vs*. time and plots of number average molecular weights M_n^{SEC} and *Đ vs*. conversion for the SARA ATRP of MA catalyzed by $Na_2S_2O_4$/$CuBr_2$/Me_6TREN in [BMIM]-[PF_6]/DMSO = 95/5 (circle, black), [BMIM]-[PF_6]/DMSO = 75/25 (triangle, red) and [BMIM]-[PF_6]/DMSO = 25/75 (square, blue). Conditions: $[MA]_0/[solvent]$ = 2/1 (v/v); $[MA]_0/[EBiB]_0/[Na_2S_2O_4]_0/[CuBr_2]_0/[Me_6TREN]_0$ = 222/1/1/0.1/0.1 (molar); T = 30 °C.

Regardless of the solvent ratio studied (Figure 4.1 and 4.3, Table 4.1) the control over the SARA ATRP of MA was perfect because *Đ* was always below 1.07. Indeed, as we observed in Figure 4.4 the only observed difference was the overall polymerization rate, which as refereed above was faster for the ratio DMSO/[BMIM]-[PF_6] = 50/50.

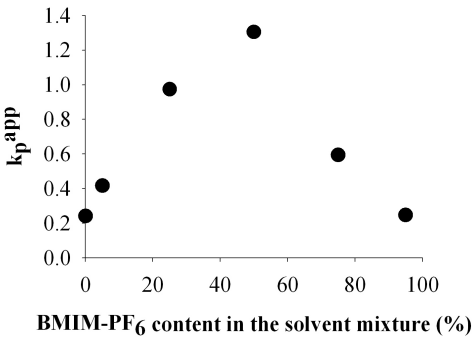

Figure 4.4 k_p^{app} values of the SARA ATRP of MA catalyzed by $Na_2S_2O_4$/$CuBr_2$/Me_6TREN in [BMIM]-[PF_6]/DMSO mixtures, for different contents of [BMIM]-[PF_6] in the reaction mixture. Conditions: $[MA]_0$/[solvent] = 2/1 (v/v); $[MA]_0/[EBiB]_0/[Na_2S_2O_4]_0/[CuBr_2]_0/[Me_6TREN]_0$ = 222/1/1/0.1/0.1 (molar); T = 30 °C

It is interesting to note that this ratio DMSO/[BMIM]-[PF_6] = 50/50 represents an optimum value for the mixture, which suggests that at this ratio a maximum of a synergistic effect between the two solvents is observed.

Considering the perfect miscibility of the [BMIM]-[PF_6] and DMSO for the different mixtures, it is believed that the polarity values of the mixture may play an important role in the kinetics of the polymerization. In this regard, it was reported that mixtures of [BMIM]-[PF_6] and tetraethylene glycol (TEG) exhibit unusual synergistic solvent effect, particularly a remarkable "hyperpolarity" for the mixture. In the presence of solvatochromic probes, as E_T(33), polarity of the medium is always higher in the mixtures than in pure solvents reaching a maximum value for equimolar mixtures of the two solvents.[25]

Using this analogy, absorbance spectra of Reichardt's dye (30) were collected in [BMIM]-[PF_6]/DMSO mixtures, and the results are present in Figure 4.5.

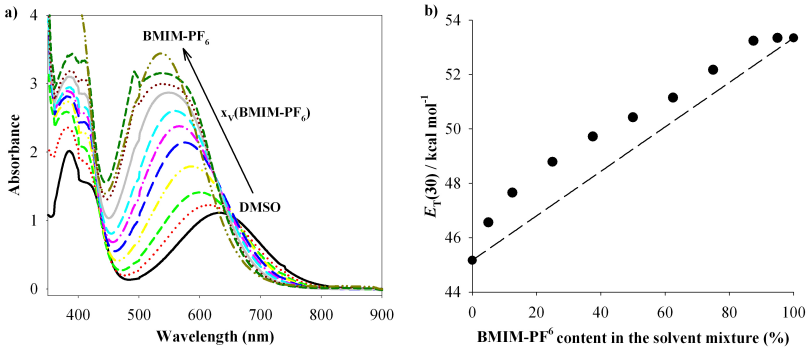

Figure 4.5 (a) UV-Vis spectra in different [BMIM]-[PF_6]/DMSO mixtures with Reichardt's dye 30 (50 μM); (b) Experimental $E_T(30)$ value in different [BMIM]-[PF_6]/DMSO mixtures (the dashed line represents the predicted $E_T(30)$).

Figure 4.5 showing that value of $E_T(30)$ for the different mixtures exceeds the value predicted by the simple mixture indicating that some synergistic effect occurs. On the other hand, the kinetic data using tetrabutylammonium hexafluorophosphate (TBA-PF_6) was determined in order to evaluate if the previous results were due to the [BMIM]-[PF_6] structure, or the speed up effect could be mainly due to the anion (PF_6) (Figure 4.6).

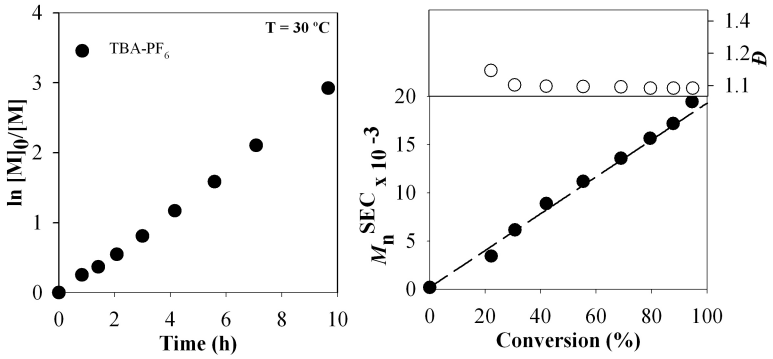

Figure 4.6 Kinetic plots of conversion and ln$[M]_0/[M]$ *vs*. time and plots of number average molecular weights (M_n^{SEC}) and *Đ vs*. conversion for the SARA ATRP of MA catalyzed by $Na_2S_2O_4$/TBA-PF_6/$CuBr_2$/Me_6TREN in DMSO. Conditions: $[MA]_0/[solvent]$ = 2/1 (v/v); $[MA]_0/[EBiB]_0/[Na_2S_2O_4]_0/[TBA\text{-}PF_6]_0/[CuBr_2]_0/[Me_6TREN]_0$ = 222/1/1/3/0.1/0.1 (molar); T = 30 °C.

Using ratio TBA-PF_6/DMSO (6/94) the obtained k_p^{app} was 0.295 h^{-1}. It is higher than using pure DMSO but much lower than the value obtained for a mixture [BMIM]-[PF_6] /DMSO (5/95) (0.417 h^{-1}).

The effect of the target molecular weight on the control over the polymerization is a critical parameter that should be evaluated, since it could lead to possible solubility

issues of the polymer in the reaction mixture. Therefore different targeted DP were investigated for the SARA ATRP of MA (Figure 4.7, Table 4.1 entries 4, 7 and 8) using a [BMIM]-[PF_6]/DMSO ratio of 50/50.

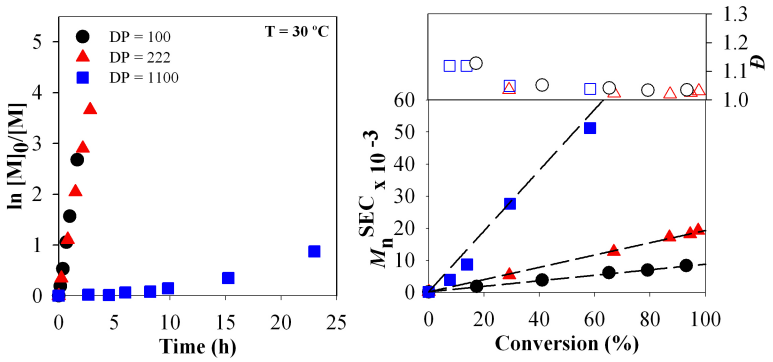

Figure 4.7 Kinetic plots of conversion and ln[M]$_0$/[M] *vs*. time and plots of number average molecular weights (M_n^{SEC}) and *Đ vs*. conversion for the SARA ATRP of MA catalyzed by $Na_2S_2O_4$/$CuBr_2$/Me_6TREN in [BMIM]-[PF_6]/DMSO = 50/50 (v/v) for different targeted DP values: (a) DP = 100; (b) DP = 222; (c) DP = 1100. Conditions: [MA]$_0$/[solvent] = 2/1 (v/v); [MA]$_0$/[EBiB]$_0$/[$Na_2S_2O_4$]$_0$/[$CuBr_2$]$_0$/[Me_6TREN]$_0$ = DP/1/1/0.1/0.1 (molar); T = 30 °C.

As expected, the polymerization rate was higher for lower DP values, due to the higher number of growing radicals. It is worthwhile to mention that even for the highest DP = 1100, the PMA dispersity values remained very low (*Đ* = 1.04). A 4-arm initiator was used to evaluate the potential of the polymerization method in the synthesis of 4-arm star PMA (Figure 4.8).

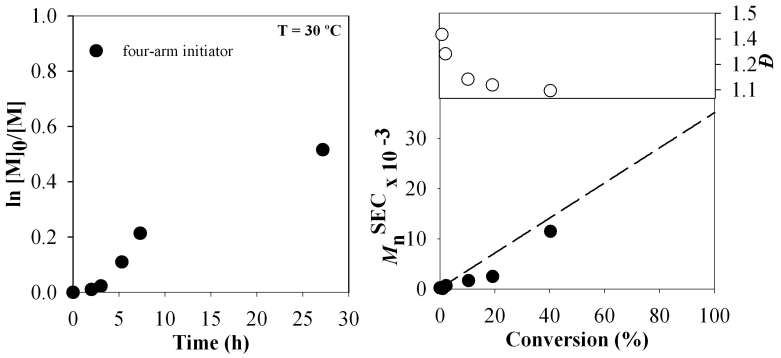

Figure 4.8 Kinetic plots of conversion and ln[M]$_0$/[M] *vs*. time and plots of number average molecular weights (M_n^{SEC}) and *Đ vs*. conversion for the SARA ATRP of MA initiated by a four-arm initiator and catalyzed by $Na_2S_2O_4$/$CuBr_2$/Me_6TREN, in [BMIM-PF_6]/DMSO = 50/50 (v/v) for a targeted DP of 400. Conditions: [MA]$_0$/[solvent] = 2/1 (v/v); [MA]$_0$/[4f-BiB]$_0$/[$Na_2S_2O_4$]$_0$/[$CuBr_2$]$_0$/[Me_6TREN]$_0$ = 400/1/1/0.4/0.4 (molar); T = 30 °C.

The results obtained in Figure 4.8 regarding the control of the polymerization were similar to the ones described for the monofunctional initiator. Again, the final dispersity obtained for the star-shaped PMA was very low ($Đ$ = 1.04). On this matter, it should be mentioned that the SEC apparatus used is equipped with multi-detectors (light scattering, viscosimeter and refractive index), which allows a very accurate determination of the molecular weights, without the use of common calibration curves[26] and the chromatograms of star-shaped PMA samples was comparing with chromatograms of PS standards (Figure 4.9)

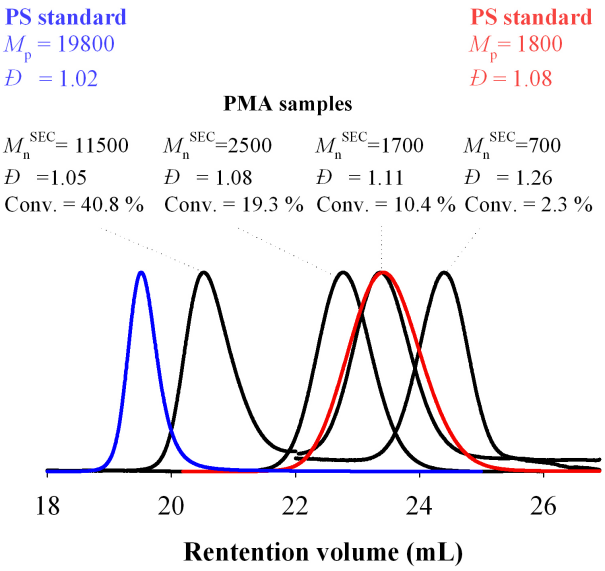

Figure 4.9 Chromatograms of PS standards (red and blue lines) and star-shaped PMA samples (black lines) collected during the SARA ATRP of MA catalyzed by $Na_2S_2O_4$/$CuBr_2$/Me_6TREN in [BMIM]-[FPF_6]/DMSO = 50/50 (v/v). Conditions: $[MA]_0/[solvent]$ = 2/1 (v/v); $[MA]_0/[4f\text{-}BiB]_0/[Na_2S_2O_4]_0/[CuBr_2]_0/[Me_6TREN]_0$ = 400/1/1/0.4/0.4 (molar); T = 30 °C

Table 4.1 summarizes the kinetic data obtained for SARA ATRP of MA in the presence of $Na_2S_2O_4$/$CuBr_2$/Me_6TREN in [BMIM]-[PF_6]/DMSO mixtures at 30 °C.

Table 4.1 Kinetic data for the SARA ATRP of MA in [BMIM]-[PF_6]/DMSO mixtures. Conditions: $[MA]_0/[solvent]$ = 2/1 (v/v); $[MA]_0/[EBiB]_0/[Na_2S_2O_4]_0/[CuBr_2]_0/[Me_6TREN]_0$ = 222/1/1/0.1/0.1; T = 30 °C

Entry	[BMIM]-[PF_6]/DMSO ratio	Targeted DP	k_p^{app} (h^{-1})	Time (h)	Conv. (%) [a]	M_n^{th} x 10^{-3} [a]	M_n^{SEC} x 10^{-3} [a]	Đ
1	0/100	222	0.242	14	97	18.7	20.7	1.04
2	5/95	222	0.417	7.5	96	18.5	19.1	1.05
3	25/75	222	0.974	3.6	97	18.7	20.20	1.04
4	50/50	222	1.305	2.8	98	18.8	19.3	1.03
5	75/25	222	0.595	5.9	97	18.7	19.5	1.03
6	95/5	222	0.248	10.5	93	17.9	19.1	1.07
7	50/50	100	1.588	1.7	93	8.20	8.30	1.04
8	50/50	1100	0.053	23	58	56,1	51,2	1.04

[a] Maximum monomer conversion obtained in the reaction

Independently of the [BMIM]-[PF_6]/DMSO ratio used, the polymer architecture or the target molecular weight, the reported system allowed the synthesis of well-defined PMA at room temperature with very low dispersity ($Đ$ < 1.1) below the reported values using the same IL.[18] The efficiency of initiation is always close 100 %.

The level of control obtained under the different polymerization conditions investigated should be a direct consequence of three main aspects: high propagation rates; absence of side reactions, and fast reduction of Cu(II) species to Cu(I). On this matter, the use of IL is known to decrease the activation energy involved in the propagation steps due to high polarity.[27] The increase in the rate of polymerization was postulated based on a complex formation between the growing radicals and the IL.[28] The hypothesis was later confirmed by showing that when chiral IL were used more isotactic sequences were formed.[21] In contrast, the termination rate decreases[18] due to higher viscosity limiting the diffusion of radicals.[27] In fact, for [BMIM]-[PF_6]/DMSO mixtures there was an exponential increase in the viscosity for contents of ionic liquid higher than 50 % (Figure 4.10).

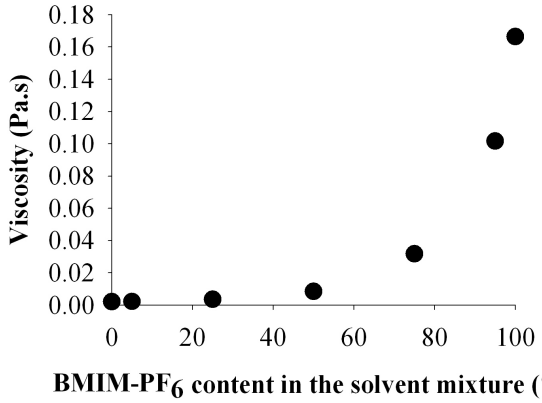

Figure 4.10 Viscosity as a function of the amount of [BMIM]-[PF_6] in the [BMIM]-[PF_6]/DMSO solvent mixture.

The reduction process of $CuBr_2$/Me_6TREN by $Na_2S_2O_4$ in [BMIM]-[PF_6]/DMSO (0/100, 25/75, 50/50) was also studied by UV-Vis spectroscopy (Figure 4.11) to provide more mechanistic insights.

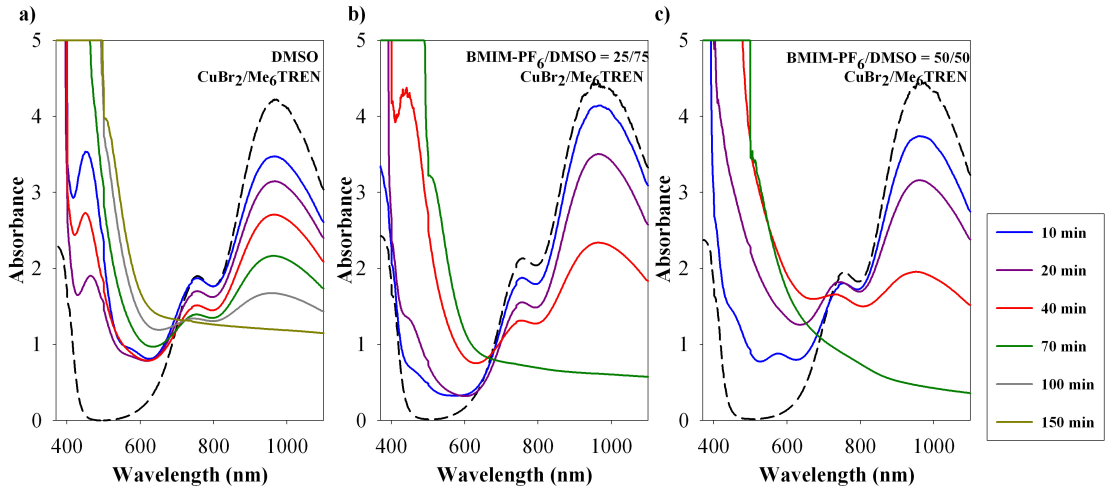

Figure 4.11 UV-Vis spectra of reduction of $CuBr_2$/Me_6TREN by $Na_2S_2O_4$ in a) pure DMSO, b) [BMIM]-[PF_6]/DMSO (25/75) and c) [BMIM]-[PF_6]/DMSO (50/50) at 30 °C.

The results revealed that the reduction of Cu(II) species into Cu(I) activators is faster for the mixture [BMIM]-[PF_6]/DMSO (50/50). This fact, along with the hyperpolarity effect observed for [BMIM]-[PF_6]/DMSO mixtures (Figure 4.4), can in part justify the maximum k_p value observed using [BMIM]-[PF_6]/DMSO (50/50) as the polymerization solvent. However, more detailed mechanistic studies will be needed to fully address the causes of this behaviour.

The "living" nature of the PMA-Br synthetized by the reported method was confirmed by doing a chain extension experiment (Figure 4.12), showing the complete movement of the macroiniatior SEC (M_n^{SEC} = 6.9 x 10^3, $Đ$ = 1.05) trace towards high molecular weight fractions.

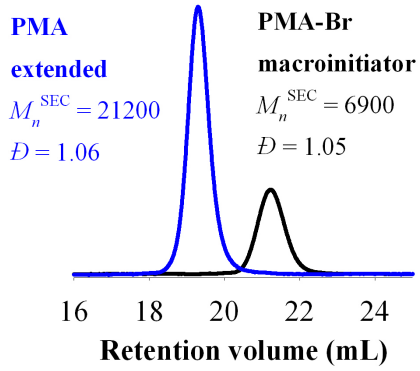

Figure 4.12 Chromatograms of the PMA before (black curve) and after the chain extension (blue curve) experiment.

The chemical structure of the PMA-Br (M_n^{SEC}= 6.9 x 10^3, $Đ$ = 1.05) synthesized by SARA ATRP in [BMIM]-[PF_6]/DMSO = 50/50 was analyzed by MALDI-TOF (Figures 4.13) and ^{1}H NMR spectroscopy (Figure 4.15). The results confirmed the expected structure and a high degree of chain-end functionality (92 %).

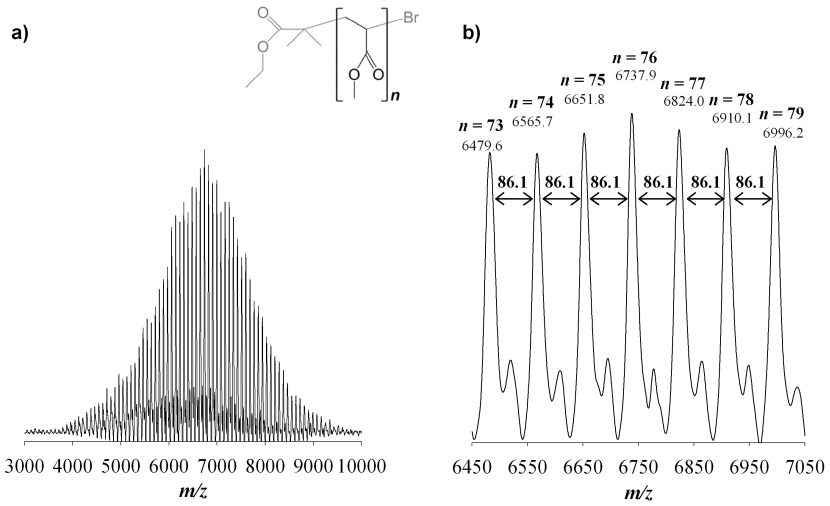

Figure 4.13 a) MALDI-TOF-MS in the linear mode (using HABA as matrix) of PMA-Br (M_n^{SEC} = 6.9 x 10^3, $Đ$ = 1.05) obtained by SARA ATRP of MA catalyzed by $Na_2S_2O_4$/$CuBr_2$/Me_6TREN, in [BMIM]-[PF_6]/DMSO = 50/50 (v/v). b) Enlargement of the MALDI-TOF-MS from m/z 6450 to 7050**.** Conditions: $[MA]_0$/[solvent] = 2/1 (v/v); $[MA]_0/[EBiB]_0/[Na_2S_2O_4]_0/[CuBr_2]_0/[Me_6TREN]_0$ = 222/1/1/0.1/0.1 (molar); T = 30 °C.

In the MALDI-TOF-MS experiment, both HABA and DHB were tested as matrices, but only the HABA matrix gave a clearly resolved spectrum (Figures 4.13). Figure 4.13 a) shows the MALDI-TOF-MS of PMA-Br in the linear mode with m/z ranging from 3000 to 10000. Enlargement of the m/z 6450-7050 range is presented in the Figure 4.13 b). It is important to note that the main peaks are separated by an interval corresponding to a MA repeating unit (86.1 mass unit). The highest peaks, presented in the Figures 4.13, are attributed to a polymer chain R-$(MA)_n$-Br, where R-Br is the initiator EBiB (6479.6 = 195.05 + 73×86.09, where 195.05 and 86.09 correspond, respectively, to the molar mass of EBiB and MA).

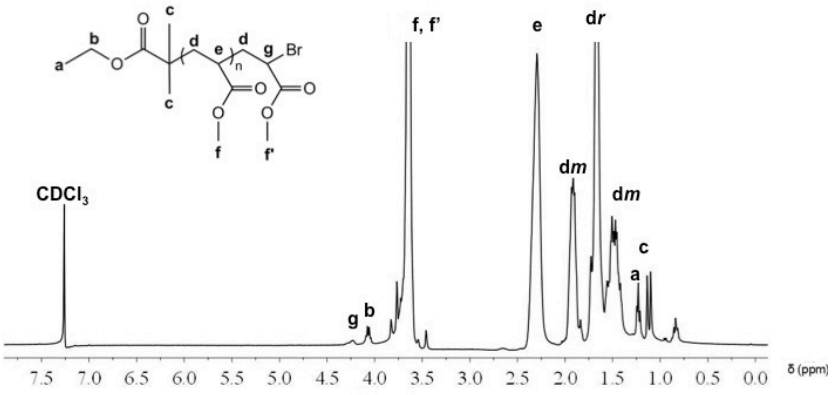

Figure 4.14 ^{1}H NMR spectrum, in $CDCl_3$, of PMA-Br obtained at high conversion ($M_{n,GPC}$ = 6900, Đ = 1.05, $M_{n,NMR}$ = 6600; active chain-end functionality = 92%). The PMA is atactic: [dr] = [dm] = 0.5.

In the ^{1}H NMR analysis the protons chemical shifts were assigned (Figure 4.14) according to the references: (e, g, f, f')[3, 29-30], (a, b, c)[3, 31], (d*r*, d*m*)[3, 32-35]. The spectrum reveals resonance at 1.7 ppm due to water trace in $CDCl_3$ that makes the signal of protons d*r* partially overlapped with the water signal. Chain-end functionality, in percentage, was calculated as follows: % funct. = [I(g)/(I(c)]/6 x 100%; where I(g) represents the integral of PMA terminal bromo chain-end –CH_2-CH_gBr-CO_2Me at 4.2-4.3 ppm and I(c) the integral of initiator fragment –$CH(CH_{c3})_2$-CO_2Et at 1.15-1.05 ppm. The molar mass of PMA polymer was also calculated from NMR results using the equation $M_{n,NMR} = ([I(e)/I(g)] + 1) \times MW_{MA} + MW_{EBiB}$, where I(e) represents the integral of the C-H proton of the PMA main chain –CH_2-CH_e-CO_2Me at 2.2-2.4 ppm and I(g) the integral of the active-end chain –CH_gBr at 4.2-4.3 ppm.

4.6 Conclusion

In conclusion, a synergistic effect of [BMIM]-[PF_6]/DMSO in the SARA ATRP of MA using $Na_2S_2O_4$/$CuBr_2$/Me_6TREN as the catalytic system is reported. The polymerization system allowed very fast polymerizations for a broad range of targeted molecular weights leading to polymers with very low dispersity values ($Đ < 1.1$).

Furthermore, for PMA, the system was robust and the polymer presented hight functionality which makes it possible to prepare a wide range of copolymers.

4.7 References

1. Matyjaszewski, K., Atom Transfer Radical Polymerization (ATRP): Current Status and Future Perspectives, *Macromolecules*, *45* (10), 4015-4039, 2012.
2. Ouchi, M.; Terashima, T.; Sawamoto, M., Transition Metal-Catalyzed Living Radical Polymerization: Toward Perfection in Catalysis and Precision Polymer Synthesis, *Chemical reviews*, *109* (11), 4963-5050, 2009.
3. Mendonca, P. V.; Serra, A. C.; Coelho, J. F. J.; Popov, A. V.; Guliashvili, T., Ambient temperature rapid ATRP of methyl acrylate, methyl methacrylate and styrene in polar solvents with mixed transition metal catalyst system, *European Polymer Journal*, *47* (7), 1460-1466, 2011.
4. Guliashvili, T.; Mendonça, P. V.; Serra, A. C.; Popov, A. V.; Coelho, J. F. J., Copper-Mediated Controlled/ "Living" Radical Polymerization in Polar Solvents: Insights into Some Relevant Mechanistic Aspects, *Chemistry – A European Journal*, *18* (15), 4607-4612, 2012.
5. Zhang, Y.; Wang, Y.; Matyjaszewski, K., ATRP of Methyl Acrylate with Metallic Zinc, Magnesium, and Iron as Reducing Agents and Supplemental Activators, *Macromolecules*, *44* (4), 683-685, 2011.
6. Jakubowski, W.; Min, K.; Matyjaszewski, K., Activators Regenerated by Electron Transfer for Atom Transfer Radical Polymerization of Styrene, *Macromolecules*, *39* (1), 39-45, 2005.
7. Abreu, C. M. R.; Mendonca, P. V.; Serra, A. C.; Coelho, J. F. J.; Popov, A. V.; Guliashvili, T., Accelerated Ambient-Temperature ATRP of Methyl Acrylate in Alcohol-Water Solutions with a Mixed Transition-Metal Catalyst System, *Macromolecular Chemistry and Physics*, *213* (16), 1677-1687, 2012.
8. Cordeiro, R. A.; Rocha, N.; Mendes, J. P.; Matyjaszewski, K.; Guliashvili, T.; Serra, A. C.; Coelho, J. F. J., Synthesis of well-defined poly(2-(dimethylamino)ethyl methacrylate) under mild conditions and its co-polymers with cholesterol and PEG using Fe(0)/Cu(ii) based SARA ATRP, *Polymer Chemistry*, *4* (10), 3088-3097, 2013.
9. Rocha, N.; Mendonca, P. V.; Mendes, J. P.; Simoes, P. N.; Popov, A. V.; Guliashvili, T.; Serra, A. C.; Coelho, J. F. J., Facile Synthesis of Well-Defined Telechelic Alkyne-Terminated Polystyrene in Polar Media Using ATRP With Mixed Fe/Cu Transition Metal Catalyst, *Macromolecular Chemistry and Physics*, *214* (1), 76-84, 2013.
10. Abreu, C. M. R.; Mendonca, P. V.; Serra, A. C.; Popov, A. V.; Matyjaszewski, K.; Guliashvili, T.; Coelho, J. F. J., Inorganic Sulfites: Efficient Reducing Agents and

Supplemental Activators for Atom Transfer Radical Polymerization, *ACS Macro Letters*, *1* (11), 1308-1311, 2012.
11. Abreu, C. M. R.; Serra, A. C.; Popov, A. V.; Matyjaszewski, K.; Guliashvili, T.; Coelho, J. F. J., Ambient temperature rapid SARA ATRP of acrylates and methacrylates in alcohol-water solutions mediated by a mixed sulfite/Cu(ii)Br2 catalytic system, *Polymer Chemistry*, *4* (23), 5629-5636, 2013.
12. Gois, J. R.; Rocha, N.; Popov, A.; Guliashvili, T.; Matyjaszewski, K.; Serra, A. C.; Coelho, J., Synthesis of Well-defined Functionalized Poly(2-(Diisopropylamino)ethyl Methacrylate) Using ATRP with Sodium Dithionite as a SARA Agent, *Polym. Chem.*, 2014.
13. Magenau, A. J. D.; Strandwitz, N. C.; Gennaro, A.; Matyjaszewski, K., Electrochemically Mediated Atom Transfer Radical Polymerization, *Science*, *332* (6025), 81-84, 2011.
14. G. Huddleston, J.; D. Rogers, R., Room temperature ionic liquids as novel media for 'clean' liquid-liquid extraction, *Chem. Commun.*, (16), 1765-1766, 1998.
15. Wheeler, C.; West, K. N.; Liotta, C. L.; Eckert, C. A., Ionic liquids as catalytic green solvents for nucleophilic displacement reactions, *Chem. Commun.*, (10), 887-888, 2001.
16. Erdmenger, T.; Guerrero-Sanchez, C.; Vitz, J.; Hoogenboom, R.; Schubert, U. S., Recent developments in the utilization of green solvents in polymer chemistry, *Chemical Society Reviews*, *39* (8), 3317-3333, 2010.
17. Carmichael, A. J.; Haddleton, D. M.; Bon, S. A. F.; Seddon, K. R., Copper() mediated living radical polymerisation in an ionic liquid, *Chemical Communications*, (14), 1237-1238, 2000.
18. Biedroń, T.; Kubisa, P., Atom-Transfer Radical Polymerization of Acrylates in an Ionic Liquid, *Macromolecular Rapid Communications*, *22* (15), 1237-1242, 2001.
19. Sarbu, T.; Matyjaszewski, K., ATRP of Methyl Methacrylate in the Presence of Ionic Liquids with Ferrous and Cuprous Anions, *Macromolecular Chemistry and Physics*, *202* (17), 3379-3391, 2001.
20. Percec, V.; Grigoras, C., Catalytic effect of ionic liquids in the Cu2O/2,2′-bipyridine catalyzed living radical polymerization of methyl methacrylate initiated with arenesulfonyl chlorides, *Journal of Polymer Science Part A: Polymer Chemistry*, *43* (22), 5609-5619, 2005.
21. Biedroń, T.; Kubisa, P., Radical polymerization in a chiral ionic liquid: Atom transfer radical polymerization of acrylates, *J. Polym. Sci., Part A: Polym. Chem.*, *43* (15), 3454-3459, 2005.
22. Ma, H.; Wan, X.; Chen, X.; Zhou, Q.-F., Reverse atom transfer radical polymerization of methyl methacrylate in room-temperature ionic liquids, *J. Polym. Sci., Part A: Polym. Chem.*, *41* (1), 143-151, 2003.
23. Biedroń, T.; Kubisa, P., Atom transfer radical polymerization of acrylates in an ionic liquid: Synthesis of block copolymers, *J. Polym. Sci., Part A: Polym. Chem.*, *40* (16), 2799-2809, 2002.
24. Ciampolini, M.; Nardi, N., Five-Coordinated High-Spin Complexes of Bivalent Cobalt, Nickel, andCopper with Tris(2-dimethylaminoethyl)amine, *Inorganic Chemistry*, *5* (1), 41-44, 1966.
25. Sarkar, A.; Trivedi, S.; Baker, G. A.; Pandey, S., Multiprobe Spectroscopic Evidence for “Hyperpolarity” within 1-Butyl-3-methylimidazolium Hexafluorophosphate Mixtures with Tetraethylene Glycol, *J. Phys. Chem. B*, *112* (47), 14927-14936, 2008.

26. Coelho, J. F. J.; Gonçalves, P. M. F. O.; Miranda, D.; Gil, M. H., Characterization of suspension poly(vinyl chloride) resins and narrow polystyrene standards by size exclusion chromatography with multiple detectors: Online right angle laser-light scattering and differential viscometric detectors, *Eur. Polym. J.*, *42* (4), 751-763, 2006.
27. Harrisson, S.; Mackenzie, S. R.; Haddleton, D. M., Pulsed Laser Polymerization in an Ionic Liquid: Strong Solvent Effects on Propagation and Termination of Methyl Methacrylate, *Macromolecules*, *36* (14), 5072-5075, 2003.
28. Harrisson, S.; Mackenzie, S. R.; Haddleton, D. M., Unprecedented solvent-induced acceleration of free-radical propagation of methyl methacrylate in ionic liquids, *Chem. Commun.*, (23), 2850-2851, 2002.
29. Lligadas, G.; Ladislaw, J. S.; Guliashvili, T.; Percec, V., Functionally terminated poly(methyl acrylate) by SET-LRP initiated with CHBr3 and CHI3, *Journal of Polymer Science Part A: Polymer Chemistry*, *46* (1), 278-288, 2008.
30. Percec, V.; Guliashvili, T.; Ladislaw, J. S.; Wistrand, A.; Stjerndahl, A.; Sienkowska, M. J.; Monteiro, M. J.; Sahoo, S., Ultrafast synthesis of ultrahigh molar mass polymers by metal-catalyzed living radical polymerization of acrylates, methacrylates, and vinyl chloride mediated by SET at 25 degrees C, *J Am Chem Soc*, *128* (43), 14156-65, 2006.
31. Hasneen, A.; Kim, S.; Paik, H.-j., Synthesis and characterization of low molecular weight poly(methyl acrylate)-b-polystyrene by a combination of ATRP and click coupling method, *Macromol. Res.*, *15* (6), 541-546, 2007.
32. Coelho, J. F. J.; Carvalho, E. Y.; Marques, D. S.; Popov, A. V.; Goncalves, P. M.; Gil, M. H., Synthesis of Poly(lauryl acrylate) by Single-Electron Transfer/Degenerative Chain Transfer Living Radical Polymerization Catalyzed by Na2S2O4 in Water, *Macromolecular Chemistry and Physics*, *208* (11), 1218-1227, 2007.
33. Coelho, J. F. J.; Mendonça, P. V.; Popov, A. V.; Percec, V.; Gonçalves, P. M. O. F.; Gil, M. H., Synthesis of high glass transition temperature copolymers based on poly(vinyl chloride) via single electron transfer−Degenerative chain transfer mediated living radical polymerization (SET-DTLRP) of vinyl chloride in water, *Journal of Polymer Science Part A: Polymer Chemistry*, *47* (24), 7021-7031, 2009.
34. Tabuchi, M.; Kawauchi, T.; Kitayama, T.; Hatada, K., Living polymerization of primary alkyl acrylates with t-butyllithium/bulky aluminum Lewis acids, *Polymer*, *43* (25), 7185-7190, 2002.
35. Coelho, J. F. J.; Carvalho, E. Y.; Marques, D. S.; Popov, A. V.; Percec, V.; Gonçalves, P. M. F. O.; Gil, M. H., Synthesis of poly(ethyl acrylate) by single electron transfer-degenerative chain transfer living radical polymerization in water catalyzed by Na2S2O4, *Journal of Polymer Science Part A: Polymer Chemistry*, *46* (2), 421-432, 2008.

Chapter 5

Ambient Temperature SARA ATRP for meth(acrylates), styrene and vinyl chloride using sulfolane/1-butyl-3-methylimidazolium hexafluorophosphate based mixtures

These results are published in: **Mendes, J. P.**; Góis, J. R.; Costa, J. R. C.; Maximiano, P.; Serra, A. C.; Guliashvili, T.; Coelho, J. F. J., "*Ambient temperature SARA ATRP for meth(acrylates), styrene, and vinyl chloride using sulfolane/1-butyl-3-methylimidazolium hexafluorophosphate-based mixtures", Journal of Polymer Science Part A: Polymer Chemistry*, *55* (8), 1322-1328, 2017.

5.1 Abstract

The SARA ATRP with catalytic system composed of Cu(0) and $CuBr_2$/Me_6TREN at room temperature using different sulfolane/co-solvent based mixtures is reported. Three different co-solvents were studied: 1-butyl-3-methylimidazolium hexafluorophosphate ([BMIM]-[PF_6]), water and tetraethylene glycol (TEG). The results revealed a synergistic effect between sulfolane and [BMIM]-[PF_6], which enhanced the polymerization rate several times while maintaining a stringent control over the polymerization. The catalytic system was used as proof-of-concept for the SARA-ATRP of MMA, St and VC. The addition of 10% of water (or TEG) to the sulfolane/[BMIM]-[PF_6] mixture resulted in fast polymerization rates. The results presented in this manuscript highlight the importance of the sulfolane as a universal industrial solvent for SARA-ATRP of different monomer families.

5.2 Introduction

ATRP is a very robust and efficient method for the synthesis of tailor made macromolecules.[1] This method is mediated by a dynamic equilibrium between active growing radicals and dormant species, which is catalyzed by a transition metal/ligand complex.[2] The continuous trend to diminish the amount of catalyst required to control the polymerization led to the development of different ATRP variations, namely: activators regenerated by electron transfer (ARGET) ATRP,[3] initiators for continuous activator regeneration (ICAR) ATRP,[4] electrochemically mediated (*e*-ATRP) ATRP,[5] and supplemental activator and reducing agent (SARA) ATRP.[6-8] These techniques enable the use of catalyst concentration below 100 ppm, while traditional approaches required values above 10000 ppm. SARA ATRP is a very versatile technique that can be carried out using heterogeneous zero valent metal catalyst or inorganic sulfites that act as both supplemental activators and reducing agents.

DMSO has been used for the SARA-ATRP of MA[9], MMA[9] and VC[9]. Several authors have been published using ionic liquid as solvents for ATRP, and their rate-accelerating effect has been reported.[10-12]

An unusual synergetic effect of DMSO and [BMIM]-[PF_6] for the SARA-ATRP of MA has been recently reported by our research group, which enabled very fast

polymerization rates for a broad range of targeted molecular weights, with a very stringent control over the dispersity during the entire course of the polymerizations.[13] In a further contribution[14], a synergetic effect is observed in the mixtures of [BMIM]-[PF_6] and glycols which was explored to access the "flash" polymerization of MA reaching almost full conversion in only 11 min (for target DP = 222).

Aiming to avoid some important limitations of using DMSO as solvent for ATRP methods (e.g the poor solubility of styrene), sulfolane was introduced in the ATRP arena as a "universal" and industrial solvent for SARA-ATRP of meth(acrylate)s, St and VC[15-16].

The development of sulfolane mixtures as solvents that could enhance the SARA-ATRP polymerization rates is highly desirable to expand the use of this convenient solvent that enables the straightforward synthesis of block copolymers using different monomer families. In this chapter, the SARA-ATRP using a catalytic system of $CuBr_2$/M_6TREN and Cu(0) is explored in different sulfolane based mixtures.

5.3 Experimental Section

5.3.1 Materials

Copper(II) bromide ($CuBr_2$) (+ 99 % extra pure, anhydrous; Acros), metallic copper (Cu(0) wire, diameter 1 mm) (≥ 99.9 %; Sigma-Aldrich), deuterated chloroform ($CDCl_3$) (+ 1 % tetramethylsilane (TMS); Euriso-top), deuterated tetrahydrofuran (THF-d_8) (99.5 %; Euriso-top), dimethyl sulfoxide (DMSO) (+ 99.8 % extra pure; Acros), sulfolane (+ 99 %; Acros), 1-butyl-3-methylimidazolium hexafluorophosphate ([BMIM]-[PF_6]) (> 98 %; TCI (Tokyo Chemical Industry Co. LTD)), ethyl 2-bromoisobutyrate (EBiB) (98 %; Aldrich), ethyl α-bromophenylacetate (EBPA) (97 %; Aldrich), bromoform ($CHBr_3$) (+ 99 % stabilized; Acros), tris(2-aminoethyl)amine (TREN) (96 %; Sigma-Aldrich), *N,N,N′,N″,N″*-pentamethyldiethylenetriamine (PMDETA) (99 %; Aldrich), 2,2′-bipyridine (bpy) (> 99 %, Acros), triethylene glycol (TEG, 99%; Acros) and polystyrene (PSt) standards (Polymer Laboratories) were used as received. High-performance liquid chromatography (HPLC) grade THF (Panreac) was filtered (0.2 μm filter) under reduced pressure before use.

Methyl acrylate (MA) (99 % stabilized; Acros), methyl methacrylate (MMA) (99 % stabilized; Acros) and styrene (St) (+ 99 %; Sigma-Aldrich), were passed over a

column filled with basic alumina to remove inhibitor prior to use. Vinyl chloride (VC) (99 %) was kindly supplied by CIRES Lda, Portugal. Me_6TREN was synthesized according to the procedure described in the literature.[17]

Metallic copper (Cu(0), d = 1 mm, Sigma Aldrich) was washed with nitric acid and subsequently rinsed with acetone and dried under a stream of nitrogen.

5.3.2 Techniques

The chromatographic parameters of the samples were determined using high performance size-exclusion chromatography (HPSEC); Viscotek (Viscotek TDAmax) with a differential viscometer (DV); right-angle laser-light scattering (RALLS) (Viscotek); low-angle laser-light scattering (LALLS) (Viscotek) and refractive index (RI) detectors. The column set consisted in a PL 10 mm guard column (50 × 7.5 mm^2) followed by two MIXED-B PL gel columns (300 x 7.5 mm^2, 10 μm).

The column set consisted of a PL 10 mm guard column (50 x7.5 mm^2) followed by one Viscotek Tguard column (8 μm), one Viscotek T2000 column (6 μm), one Viscotek T3000 column (6 μm), and one Viscotek LT4000L column (7 μm). A dual piston pump was set at a flow rate of 1.0 mL/min. The eluent, THF, was previously filtered through a 0.2 μm filter. The system was also equipped with an on-line degasser. The tests were done at 30 °C using an Elder CH-150 heater. Before the injection (100 μL), the samples were filtered through a polytetrafluoroethylene (PTFE) membrane with 0.2 μm pore. The system was calibrated with narrow PS standards. The *dn/dc* of PMA was determined as 0.063. The $M_{n,}^{SEC}$ and $Đ$ of synthesized polymers were determined by multidetectors calibration using OmniSEC software version: 4.6.1.354.

400 MHz ^{1}H NMR spectra of the reaction mixture samples were recorded on a Bruker Avance III 400 MHz spectrometer, with a 5-mm TIX triple resonance detection probe, in $CDCl_3$ with TMS as an internal standard. Conversion of the monomer was determined by integration of monomer and polymer peaks using MestRenova software version: 6.0.2-5475.

The UV/Vis studies were performed with a Jasco V-530 spectrophotometer. The analyses were carried out in the 350–1100 nm range at room temperature.

The solvent polarity parameter, $E_T(30)$ was determined in different [BMIM]-[PF_6] /sulfolane mixtures (5.0 mL) by adding small amounts of Reichardt's dye 30 (0.138

mg). These solutions were then added to the UV/Vis cuvette and placed in the spectrophotometer for spectra acquisition. The absorbance was measured, in the 350-1100 nm range, at room temperature. The $E_T(30)$ values of different mixtures were determined according to the expression: $E_T(30) = 28591.5/\lambda_{abs,máx}(nm)$.[13]

5.3.3 Procedures

5.3.3.1 Typical procedure for the $[Cu(0)]_0/[CuBr_2]_0/[Me_6TREN]_0$ = Cu(0) wire/0.1/1.1 catalyzed SARA ATRP of MA (DP = 222)

Cu(0) wire (590 mg) and a mixture of $CuBr_2$ (3.51 mg, 0.02 mmol), Me_6TREN (39.76 mg, 0.17 mmol) and solvent mixture (1.58 mL) (previously bubbled with nitrogen for about 15 minutes) were placed in a Schlenk tube reactor. A mixture of MA (3.16 mL, 34.90 mmol) and EBiB (30.62 mg, 0.16 mmol) was added to the reactor that was sealed, with a rubber septum, and frozen in liquid nitrogen. The Schlenk tube reactor containing the reaction mixture was deoxygenated with four freeze-vacuum-thaw cycles and purged with nitrogen. The reactor was placed in a water bath at 30 ºC with stirring (700 rpm). During the polymerization, different reaction mixture samples were collected by using an airtight syringe and purging the side arm of the Schlenk tube reactor with nitrogen. The samples were analyzed by ^{1}H NMR spectroscopy to determine the monomer conversion and by SEC, to determine M_n^{SEC} and $Đ$ of the polymers.

5.3.3.2 Typical procedure for the $[Cu(0)]_0/[CuBr_2]_0/[bpy]_0$ = Cu(0) wire/0.1/2.2 catalyzed SARA ATRP of MMA (DP = 222)

For a typical polymerization of MMA, a mixture of Cu(0) wire (240 mg), $CuBr_2$ (3.15 mg, 0.014 mmol), bpy (46.38 mg, 0.30 mmol) and the solvente mixture (3.21 mL) (previously bubbled with nitrogen for about 15 minutes) were placed in a Schlenk tube reactor. A solution of EBPA (32.81 mg, 0.14 mmol) in MMA (3.21 mL, 30.0 mmol) was added to the reactor that was sealed, with a rubber septum, and frozen in liquid nitrogen. The Schlenk tube reactor containing the reaction mixture was deoxygenated with four freeze-vacuum-thaw cycles and purged with nitrogen. The reactor was placed in a water bath at 40 ºC with stirring (700 rpm). During the polymerization, different reaction mixture samples were collected by

using an airtight syringe and purging the side arm of the Schlenk tube reactor with nitrogen. The samples were analyzed by ^{1}H NMR spectroscopy to determine the monomer conversion and by SEC, to determine the M_n^{SEC} and $Đ$ of the polymers.

5.3.3.3 Typical procedure for the $[Cu(0)]_0/[CuBr_2]_0/[PMDETA]_0$ = Cu(0) wire/0/1.1 catalyzed ATRP of St (DP = 222)

A mixture of Cu(0) wire (335 mg), PMDETA (25.00 mg, 0.14 mmol) and the solvent mixture (1.66 mL) (previously bubbled with nitrogen for about 15 minutes) were placed in a Schlenk tube reactor. A solution of EBiB (25.31 mg, 0.13 mmol) in St (3.31 mL, 28.80 mmol) was added to the reactor that was sealed, with a rubber septum, and frozen in liquid nitrogen. The Schlenk tube reactor containing the reaction mixture was deoxygenated with four freeze-vacuum-thaw cycles and purged with nitrogen. The reactor was placed in a water bath at 30 ºC with stirring (700 rpm). During the polymerization, different reaction mixture samples were collected by using an airtight syringe and purging the side arm of the Schlenk tube reactor with nitrogen. The samples were analyzed by ^{1}H NMR spectroscopy to determine the monomer conversion and by SEC, to determine the M_n^{SEC} and $Đ$ of the polymers.

5.3.3.4 Typical procedure for chain extension of PMA-Br

A PMA-Br macroinitiator was obtained from a typical Cu(0)/$CuBr_2$/Me_6TREN-catalyzed SARA ATRP reaction with [BMIM]-[PF_6] /solvent ratio of 25/75 (v/v) after precipitation in water. The polymer was then dissolved in acetone, filtered through a sand/alumina column, to remove traces of the copper catalys and precipitated again in water. The PMA-Br was dried under vacuum until constant weight (M_n^{SEC} = 16,000; $Đ$= 1.06). The PMA-Br macroinitiator (236.6 mg, 0.01 mmol) was dissolved in 1.51 mL of sulfolane (previously bubbled with nitrogen for about 15 min) in a Schlenk tube reactor. A mixture of MA (0.74 mL, 8.13 mmol), $CuBr_2$ (1 mg, 0.004 mmol), Me_6TREN (3.74 mg, 0.02 mmol), [BMIM]-[PF_6] (554 μL) and Cu(0) wire (500 mg) was added to the reactor that was sealed, by using a rubber septum, and frozen in liquid nitrogen. The Schlenk tube reactor containing the reaction mixture was deoxygenated with four freeze-vacuum-thaw cycles, purged with nitrogen and placed in a water bath at 30 ºC with stirring (700 rpm). The reaction was stopped after 24h and the mixture was analyzed by SEC.

5.3.3.5 UV/Vis spectroscopy of Cu(0) wire/$CuBr_2$/Me_6TREN in mixtures of DMSO/BMIM-PF_6 and Sulfolane/[BMIM]-[PF_6] = 100/0, 75/25, 50/50 and 25/75 (v/v)

Cu(0) wire was placed in a quartz UV/Vis cuvette, equipped with a magnetic stirrer, and purged with nitrogen. The solvent mixture (2.5 mL) of DMSO / [BMIM]-[PF_6] or sulfolane / [BMIM]-[PF_6] in different proportions, $CuBr_2$ (2.234 mg, 0.01 mmol) and Me_6TREN (66.26 mg, 0.288 mmol) were mixed in a vial and bubbled with nitrogen for about 15 min to remove oxygen. This solution was then added to the UV/Vis cuvette, which was sealed under nitrogen. The cuvette was placed in a water bath at 30 ºC and in a stirrer plate, and placed in the spectrophotometer for spectra acquisition at specific times. The absorbance was measured at different times, in the 350-1100 nm range at room temperature.

5.4 Results and discussion

The unusual synergistic effect between [BMIM]-[PF_6] and DMSO mixtures for the SARA ATRP of MA using a catalytic system of $Na_2S_2O_4$ and $CuBr_2$/Me_6TREN at room temperature was recently reported by our research group.[13] In comparison to pure DMSO, the addition of this ionic liquid to the solvent mixture induces very fast reactions maintaining stringent control over the molecular weight distribution throughout the polymerization. With the same purpose, herein, the effect of [BMIM]-[PF_6] in the solvent mixtures was evaluated using the catalytic complex of $CuBr_2$/M_6TREN and Cu(0) as SARA agent. Two different solvents were used: DMSO and sulfolane.

The kinetic results presented in Table 5.1 and Figure 5.1 suggest that the use of [BMIM]-[PF_6] as a co-solvent promotes faster reactions in comparison to pure sulfolane or DMSO, with a stringent control over the molecular weight distribution and $Đ$ ($Đ$ < 1.12). All polymerizations proceed following a first order kinetics relative to the monomer, reaching 80% conversion in less than 1 hour. The evolution of M_n is linear with monomer conversion, with a very good agreement between the M_n^{th} and M_n^{SEC}, which indicates an excellent control throughout the polymerization.

Table 5.1 Kinetic data for the SARA ATRP of MA using DMSO or sulfolane/[BMIM]-[PF_6] solvent mixture. Conditions: $[MA]_0/[EBiB]_0/[Cu(0)\ wire]_0/[CuBr_2]_0/[Me_6TREN]_0$=222/1/Cu(0) wire/0.1/1.1 (molar); $[MA]_0$/[solvent mixture]$_0$= 2/1 (v/v), Cu (0): d = 1 mm, l = 5 cm, T = 30 ºC.

Entry	DMSO/[BMIM]-[PF_6] (v/v)	DMSO/[BMIM]-[PF_6] (mol/mol)	k_p^{app} (h^{-1})	M_n^{SEC} *	$Đ$*	Conv. (%)*	Time (h)*
1	100/0	100/0	1.550	17060	1.07	73	0.87
2	75/25	89.77/10.23	3.488	19000	1.12	86	0.78
3	50/50	74.35/25.65	2.927	14750	1.11	80	0.78
4	25/75	48.93/51.07	2.512	18140	1.04	85	0.67
	Sulfolane /[BMIM]-[PF_6] (v/v)	**Sulfolane /[BMIM]-[PF_6] (mol/mol)**					
5	100/0	100/0	0.7784	11753	1.06	50	0.88
6	75/25	85.88/14.12	2.6498	16500	1.05	74	0.65
7	50/50	66.78/33.22	1.743	16300	1.06	78	1.07
8	25/75	39.92/60.08	1.496 ($k_{p,2}$)	18600	1.05	96	1.00

(*) values obtained from the last point of the kinetic study.

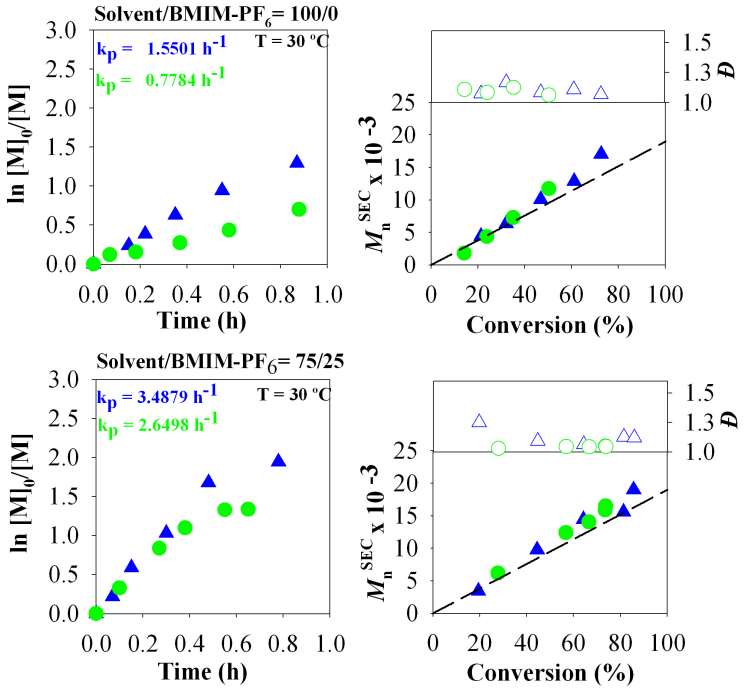

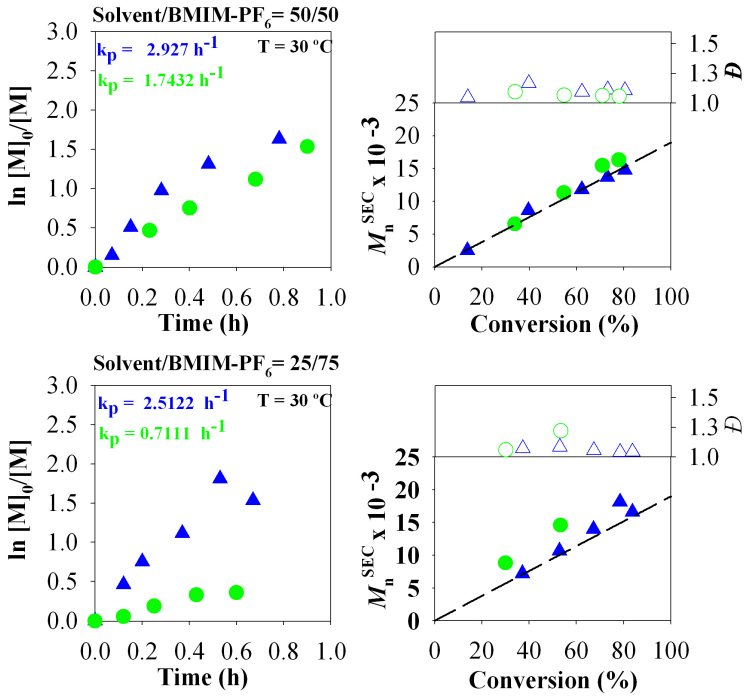

Figure 5.1 Kinetic plots of ln[M]$_0$/[M] *vs*. time and plot of number-average molecular weights (M_n^{SEC}) and $Đ$ (M_w/M_n) *vs*. conversion for the SARA ATRP of MA using Cu(0) wire as supplemental activator and reducing agent in DMSO (blue symbols) or sulfolane (green symbols)/ [BMIM]-[PF_6] mixtures at 30 ºC. Conditions: [MA]$_0$/[solvent mixture] = 2/1 (v/v); [MA]$_0$/[EBiB]$_0$/Cu(0)wire/[$CuBr_2$]/[Me_6TREN]$_0$ = 222/1/Cu(0) wire/0.1/1.1 (molar); Cu (0): d = 1 mm, l = 5 cm.

The results presented in Figure 5.2 suggest that the ratio of [BMIM]-[PF_6] in the solvent mixture plays an important role in the polymerization kinetics.

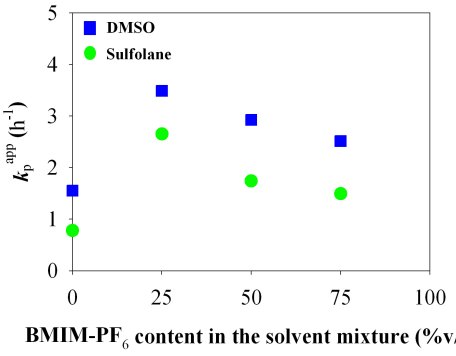

Figure 5.2 k_p^{app} values for SARA ATRP of MA catalyzed by Cu(0)/$CuBr_2$/Me_6TREN in sulfolane/[BMIM[-[PF_6] (green symbols) and DMSO/[BMIM]-[PF_6] (blue symbols) mixtures.

The results reveal that the reactions with a [BMIM]-[PF_6] amount of 25% in sulfolane or DMSO (v/v) exhibited the higher polymerization rates (*e.g.* 3.4 and 2.3 times faster than in pure sulfolane and DMSO, respectively). This result is particularly interesting

since, for similar experiments of SARA ATRP of MA catalyzed by $Na_2S_2O_4/CuBr_2/Me_6TREN$ in [BMIM]-[PF_6]/DMSO mixtures, the highest polymerization rate was obtained for a ionic liquid content of 50%,[13] which indicates the importance of SARA agent on the kinetics of the polymerization. Furthermore, the results also indicate that when DMSO was used as cosolvent in the SARA ATRP of MA mediated by Cu(0), the rate of polymerization is always higher when compared to sulfolane mixtures, which corroborates the previously reported results.[15]

5.4.1 Absorption spectra of Reichardt's dye (30)

In a previous study[13] our research group demonstrated that [BMIM]-[PF_6] / DMSO mixtures may present a synergistic solvent effect due to an increase of the total solvent polarity parameter, $E_T(30)$, when compared to the simple contribution of the mixture elements. Taking into account the kinetic data presented in Figure 5.2 for sulfolane, the absorbance spectra of Reichardt's dye (30) were collected in several [BMIM]-[PF_6] /sulfolane mixtures (Figure 5.3) to understand the possible effect of the ionic liquid in the polarity of the solvent mixture. The $E_T(30)$ values for the different solvent mixtures were found to always exceed the value predicted by the simple mixture, which confirms a synergistic polarity effect between sulfolane and [BMIM]-[PF_6].

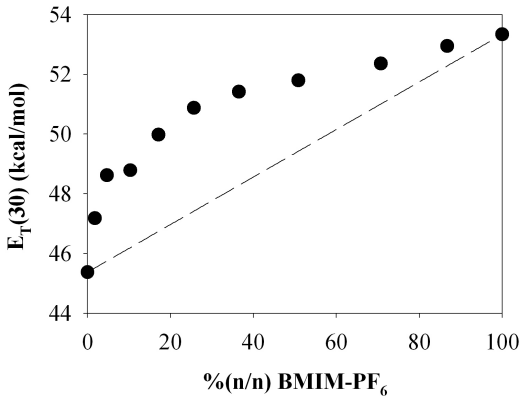

Figure 5.3 Experimental $E_T(30)$ value in different [BMIM]-[PF_6]/sulfolane mixtures (the dashed line represents the predicted $E_T(30)$).

5.4.2 Comproportionation studies in the solvent mixtures

The SARA agent (Cu(0)) is responsible for the *in situ* reduction of $CuBr_2$/Me_6TREN to Cu(I)X activation species. The use of different [BMIM]-[PF_6] percentages (v/v) was found to have a strong impact on the polymerization rates using either DMSO or sulfolane. Therefore, the reduction of $CuBr_2$/Me_6TREN by Cu(0) was studied in both sulfolane and DMSO reaction mixtures by UV−vis spectroscopy (Figure 5.4).

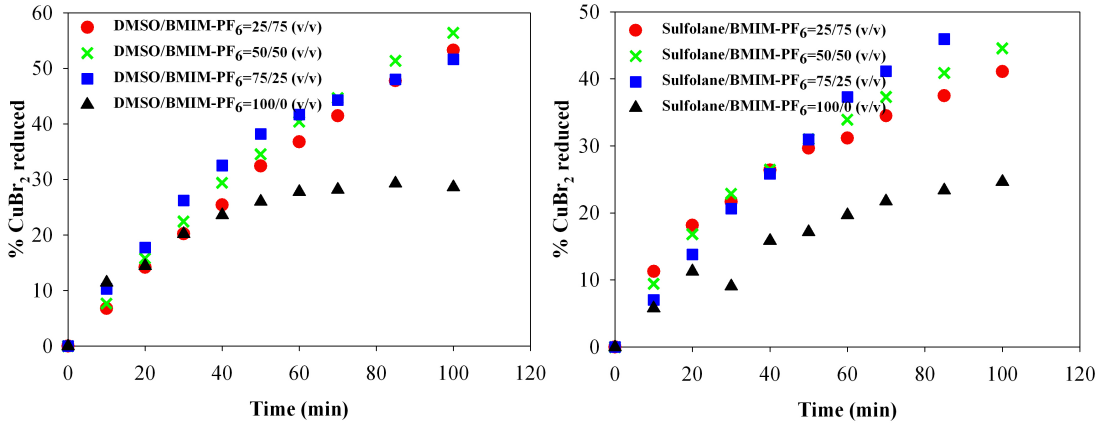

Figure 5.4 Percentage of $CuBr_2$ reduced during the comproportionation of Cu(0) and $CuBr_2$ in DMSO/[BMIM]-[PF_6] or sulfolane/[BMIM]-[PF_6] at 30 ºC. The values were determined by UV-vis spectroscopy.

For both solvents, the use of ionic liquid (IL) as cosolvent lead to a faster copper reduction, which indicates the formation of a higher concentration of Cu(I)X species (Figure 5.1) and consequently faster polymerization rates. For DMSO mixtures, when [BMIM]-[PF_6] is used as cosolvent in a content of 25 % (v/v), the reduction of copper is faster since the early stages of the polymerization, which is in agreement with the kinetic results previously presented. However, for sulfolane mixtures (sulfolane/ [BMIM]-[PF_6] = 75/25 (v/v)), this faster reduction is only observed after 50 min of reaction. It is known that the comproportionation is related to the difference of redox potential of Cu(II)/Cu(I) and Cu(I)/Cu(0) in each solvent.[18] Also, polarity, solvation and coordination activity have a strong effect on the reduction of Cu(II) to Cu(I). The data presented in Figure 5.4 clearly indicates that synergist effect regarding the polarity of the solvent mixtures (DMSO/ [BMIM]-[PF_6] and Sulfolane/ [BMIM]-[PF_6]) has a notorious effect on the comproportionation, being the rate always higher than the obtained for the pure solvent (DMSO and Sulfolane). These results might be explained by a bigger stabilization of Cu(I)Br/L in [BMIM]-[PF_6] and its mixtures

with DMSO and sulfolane. [19] However, further mechanistic studies are needed to fully understand the obtained results.

5.4.3 Effect of TEG and water in the sulfolane mixtures

The solvent polarity plays an important role in the polymerization kinetics. A recent study revealed an unusual increase in polarity, when DMSO/[BMIM]-[PF_6]/glycol mixtures are used in the SARA ATRP of MA which allows very fast and controlled polymerizations.[14] Furthermore, the presence of water in the sulfolane reactions also contributes to an increase of the rate of polymerization catalyzed by zero-valent metals[16]. Here, we investigated the influence of both TEG and water in the SARA ARTP of MA with Cu(0) and $CuBr_2$/Me_6TREN catalytic system at room temperature (Table 5.2).

To evaluate the influence of glycol and water in the solvent mixture that provided the fastest polymerization of MA (DMSO or sulfolane with 25% of [BMIM]-[PF_6]) polymerizations containing 10 % of water or TEG as cosolvent mixture were carried out (Table 5.2).

Table 5.2 Kinetic data for the SARA ATRP of MA using sulfolane/[BMIM]-[PF_6] solvent mixture. Conditions: $[MA]_0/[EBiB]_0/[Cu(0)\ wire]_0/[CuBr_2]/[Me_6TREN]_0$=222/1/Cu(0) wire/0.1/1.1 (molar); $[MA]_0$/[solvent mixture]= 2/1 (v/v), Cu (0): d = 1 mm, l = 5 cm, T = 30 ºC.

Entry	Solvent mixture (%)		Co-Solvent (%)		k_p^{app} (h^{-1})	M_n^{SEC} x10^{-3}*	Đ*	Conv. (%)*	Time (h)
1[a]	Sulfolane	100	-	-	1.003	17.10	1.10	72	1.30
2[b]	Sulfolane	90	water	10	1.642	22.00	1.04	78	1.00
3	Sulfolane / [BMIM]-[PF_6] (ratio 1:1 (v/v))	100	-	-	1.743	16.30	1.06	78	1.07
4	Sulfolane / [BMIM]-[PF_6] (ratio 1:1 (v/v))	90	water	10	2.317	15.70	1.06	86	1.13
5	Sulfolane / [BMIM]-[PF_6] (ratio 1:1 (v/v))	90	TEG	10	2.428	15.40	1.06	87	0.90
6	[BMIM]-[PF_6]	50	TEG	50	1.788	17.40	1.07	85	1.28
7	[BMIM]-[PF_6]	45	TEG water	45 10	1.617	16.10	1.12	79	1.00

([a]) and ([b]) Kinetic data reported in references 9 and 10 respectively ; (*) values obtained from the last sample from the kinetic study.

From Table 5.2 it is possible to observe that for the SARA ATRP of MA with Cu(0), the addition of a small percentage of water to the reaction mixture (10 %) increases the polymerization rate (~1.6 times) maintaining the level of control ($Đ \leq 1.10$) (Table 5.2, entry 1 to 4).

A similar result is observed when TEG is used as cosolvent (Table 5.2, entry 5). No significant differences were observe in the k_p^{app} value for the reactions that occur in the presence of 10 % of water or TEG (Table 5.2, entry 4 and 5) using the mixture sulfolane/[BMIM]-[PF_6]. It is worth to note that the presence of TEG with the ionic liquid is also important to enhance the solubility of the catalytic system ($CuBr_2$/Me_6TREN, which is insoluble in the ionic liquid) and consequently increase the control over the polymerization, (Table 5.2, entry 6). Nevertheless, it was also observed that the simultaneous presence of water and TEG (Table 5.2, entry 7) promotes faster reactions while maintaining the living characteristics of the system. This result suggests that the dramatic increase of polymerization rate reported in the presence of TEG[14] may be more associated to an effect related to the $Na_2S_2O_4$ dissociation.

5.4.4 SARA ATRP of MMA, St and VC in a mixture of sulfolane/[BMIM]-[PF_6]

As a proof of concept, herein, the use of a solvent mixture sulfolane/[BMIM]-[PF_6]= 75/25 was extended for SARA ATRP of MMA, St and VC using Cu(0) as SARA agent. The reaction conditions, catalytic complexes and initiators were selected considering the structure of the monomers, aiming to have good controlled polymerizations (Table 5.3).[15]

Table 5.3 Kinetic data for the SARA ATRP of MMA, Sty and VC using sulfolane/ [BMIM]-[PF_6]=75/25 (v/v) as solvent mixture at T = 40 ºC (MMA), 60 ºC (Sty) and 42 ºC (VC); Cu (0): *d* = 1 mm, *l* = 5 cm.

Entry	$[M]_0/[I]_0$	M/ S (v/v)	$[Cu(0)]_0/[CuBr_2]_0/[ligand]_0$	Time (h)	Conv. (%)	M_n^{th} x10^{-3}	M_n^{SEC} x10^{-3}	*Đ*
1	$[MMA]_0/[EBPA]_0$ = 222/1	1/1	$[Cu(0)]_0/[CuBr_2]_0/[Bpy]_0$ = Cu(0) wire /0.1/2.2	2.2	89	19.1	26.8	1.03
2	$[St]_0/[EBiB]_0$ =222/1	2/1	$[Cu(0)]_0/[CuBr_2]_0/[PMDETA]_0$ = Cu(0) wire /0/1.1	5.0	64	14.8	29.4	1.43
3	$[St]_0/[EBiB]_0$ =222/1	1/2	$[Cu(0)]_0/[CuBr_2]_0/[PMDETA]_0$ = Cu(0) wire /0/1.1	23.4	51	11.3	4.57	1.06
4	$[VC]_0/[CHBr_3]_0$ =222/1	1/1	$[Cu(0)]_0/[CuBr_2]_0/[TREN]_0$ = Cu(0) wire /0/1.1	6.0	55	10.4	22.8	1.82
5	$[VC]_0/[CHBr_3]_0$ =222/1	1/2	$[Cu(0)]_0/[CuBr_2]_0/[TREN]_0$ = Cu(0) wire /0/1.1	15.4	60	11.2	18.3	1.87

The results demonstrate the possibility of synthesizing PMMA, with controlled molecular weights by SARA ATRP in a sulfolane/[BMIM]-[PF_6] mixture (75/25 (v/v)) (Table 5.3, entry 1 and Figure 5.5).

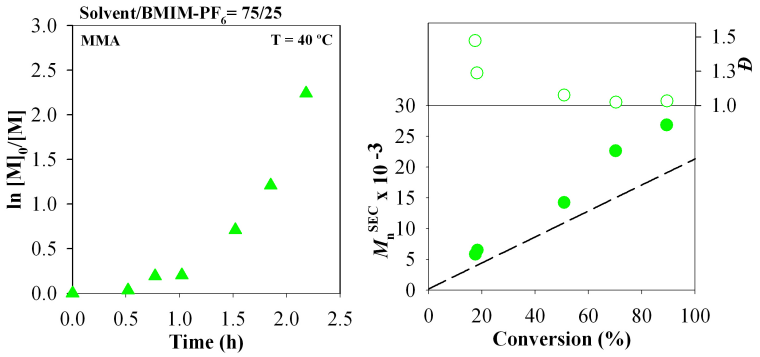

Figure 5.5 Kinetic plots of $\ln[M]_0/[M]$ *vs*. time and plot of number-average molecular weights (M_n^{SEC}) and $Đ$ (M_w/M_n) *vs*. conversion for the SARA ATRP of MMA using Cu(0) wire as supplemental activator and reducing agent in sulfolane/[BMIM]-[PF_6]=75/25(v/v) mixture at 40 ºC. Conditions: $[MMA]_0/[\text{solvent mixture}] = 1/1$ (v/v); $[MMA]_0/[EBPA]_0/Cu(0)\text{wire}/[CuBr_2]/[bpy]_0 = 222/1/Cu(0)$ wire/0.1/2.2 (molar); Cu (0): d = 1 mm, l = 5 cm.

The MMA polymerization follows a linear first order kinetics, the evolution of M_n is linear with monomer conversion and the $Đ \leq 1.1$. However, it was observed an induction period of 30 minutes (Figure 5.5) which retards the polymerization and reduces the polymerization rate when compared to the reactions carried out in only sulfolane.[15] For St and VC polymerizations, the addition of IL does not result in the enhancement of the polymerization rate compared to the previous reported results (Table 5.3, entry 2 to 5).[15]

5.4.5 ^{1}H NMR analysis

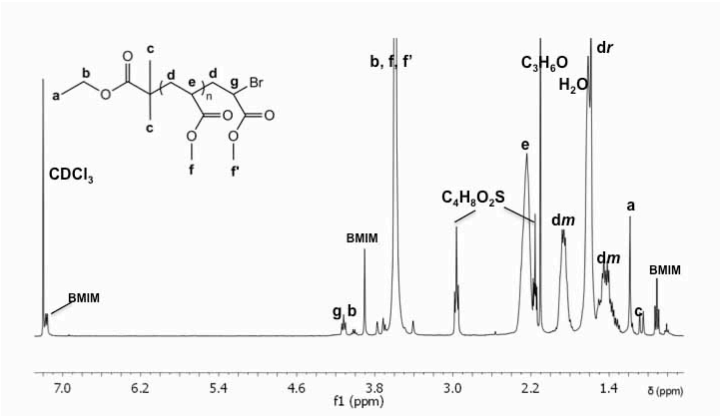

Figure 5.6 ^{1}H NMR spectrum of purified PMA-Br (M_n^{SEC} = 16.0 x 10^3; $Đ$ =1.06) in $CDCl_3$. Reaction conditions: $[MA]_0/[EBiB]_0/[Cu(0)\text{ wire}]_0/[CuBr_2]_0/[Me_6TREN]_0$=222/1/Cu(0) wire/0.1/1.1 (molar); $[MA]_0/[\text{solvent mixture}]$= 2/1 (v/v), sulfolane/[BMIM]-[PF_6]=75/25 (v/v), T = 30 ºC.

The structure of PMA synthesized through the reported method, in a mixture of sulfolane/[BMIM]-[PF_6] of 75/25 (v/v), was confirmed by ^{1}H NMR spectroscopy (Figure 5.6). The characeristic peaks of the MA repeating unit at 1.4-2.0 ppm (**d, d*r*, d*m***), 2.35-2.4 ppm (**e**) and 3.6-3.75 ppm (**f, f'**) are in agreement with the data reported in the literature.[9, 20-25] The presence of the active chain-end (g) at 4.3 ppm and the initiator fragments (a, b and c) arround 1.2, 4.1 and 1.10 ppm, respectivelly[23, 26] allows the determination of the bromine chain-end functionality of the PMA prepared (95 %).

The structure of the obtained polymers (PMMA, PS and PVC) was assessed by ^{1}H NMR analysis (Figure 5.7 – 5.9).

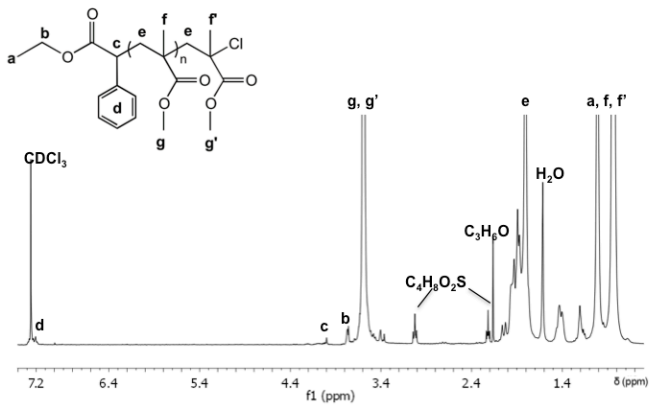

Figure 5.7 ^{1}H NMR spectrum of PMMA-Br (M_n^{SEC} = 24.7 x 10^3; $Đ$ =1.02) in $CDCl_3$.

^{1}H NMR technique was used to confirm the PMMA-Br structure and the spectrum is shown in Figure 5.7. The assignment of the proton resonances was carried out according to references: (a, b, c, d e, f, f', g, g')[15]. The ^{1}H NMR spectrum reveals the resonance of the repeating unit $CH_2CCH_3COOCH_3$: f (0.75-1.0 ppm) and g (3.5-3.75 ppm). The resonance of the terminal group is also present at 1.75-2.0 ppm.

The initiator fragments are revealed through the resonance of protons at 3.76 - 4.00 ppm and 7.2 ppm respectively from the ethyl and phenyl group.

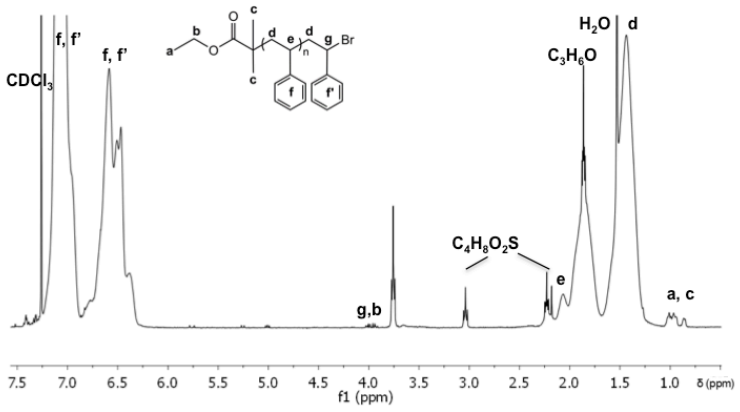

Figure 5.8 ^{1}H NMR spectrum of PS-Br (M_n^{SEC} =39.5 x 10^3; $Đ$ =1.33) in $CDCl_3$.

The structure and the presence of the chain-end functionality of PS-Br polymer was evaluated by ^{1}H NMR spectroscopy (Figure 5.8). The initiator fragment is revealed by the appearance of the resonance peaks of protons a, b and c, at 0.90-1.05 ppm, 4.0-4.25 ppm and 0.7-0.9 ppm, respectively. The spectrum reveals the presence of the repeating unit CH_2-CHPh by the aromatic protons peaks at 6.25-7.5 ppm (f). The chain-end functionality is confirmed by the resonance of proton and, adjacent to bromine, at 4.35-4.5 ppm from CH_2-CHPhBr terminal group.[27]

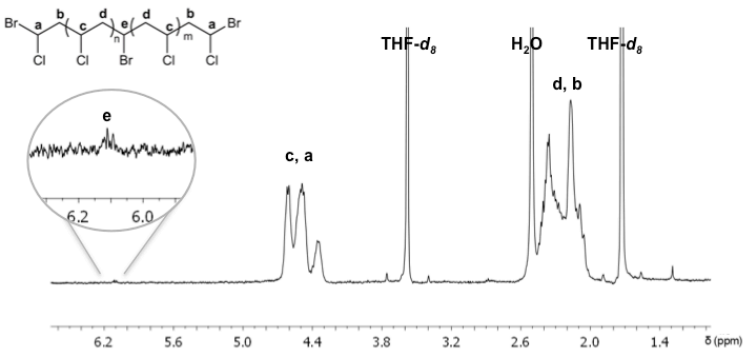

Figure 5.9 The ^{1}H NMR spectrum of Br-PVC-Br (M_n^{SEC} = 9100; $Đ$ = 1.55) in THF-d_8.

The structure of α,ω-di(bromo)PVC was analyzed by 400 MHz ^{1}H NMR spectroscopy and the spectrum is shown in the Figure 5.9 . The assignment of the proton resonances was done according to the references: (a, d, e)[28] and (b, d).[28-29] The ^{1}H NMR spectrum reveals the resonance of the repeating unit CH_2-CHCl: 2.0-2.4 ppm (b) and 4.3-4.7 ppm (c). The resonance of the terminal group CH_2-CHClBr is also present at 2.0-2.7 ppm (d) and 6.05-6.15 ppm (e). The initiator fragments (a) is overlapped with the repeating unit signals in the range of 4.3-4.7 ppm.[28]

5.4.6 Reinitiation experiment

The "living" nature of the PMA synthesized by this method was also confirmed through a chain extension experiment. Figure 5.10 shows the complete movement of the SEC trace of the PMA macroinitiator (M_n^{SEC}= 16,000, $Đ$ = 1.06) towards high molecular weight fractions maintaining the low $Đ$ values (M_n^{SEC}= 45,000, $Đ$ = 1.30). The low molecular weight shoulder observed in the SEC trace of the extended polymer indicates the presence of PMA dead chains (~7.4 %). This result is in agreement with the chain-end functionalization determined by ^{1}H NMR.

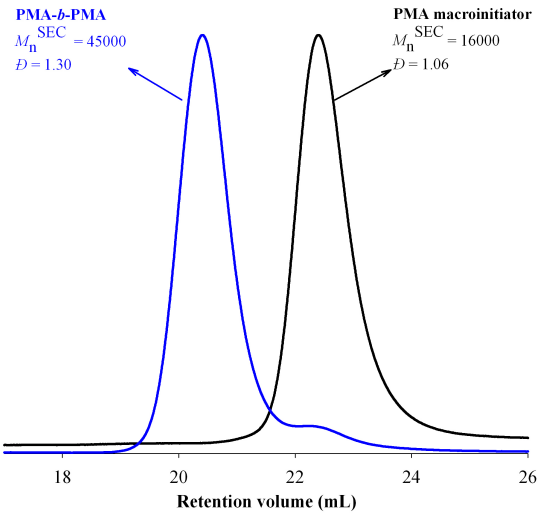

Figure 5.10 Displacement of the SEC trace (RI signal) of a –Br-terminated PMA, obtained by SARA ATRP (black line), towards high molecular weight values after a chain-extension experiment (blue line) using the solvent mixture sulfolane/[BMIM]-[PF_6]= 75/25 (v/v). Conditions: $[MA]_0$/[solvent mixture] = 1/1 (v/v); $[MA]_0$/[PMA-Br]$_0$/Cu(0) wire/$[Me_6TREN]_0$= 550/1/ Cu(0) wire/1.1 (molar); Cu (0): d = 1 mm, l = 5 cm.

5.5 Conclusions

In conclusion, the results presented herein suggest that the use of [BMIM]-[PF_6] as co-solvent promote faster reactions in comparison to pure sulfolane, using $CuBr_2$/M_6TREN as catalytic complex and Cu(0) as SARA agent. The reduction of copper is faster when [BMIM]-[PF_6] is used as cosolvent in a content of 25 % (v/v) and a synergistic effect is also observed between sulfolane and [BMIM]-[PF_6].

The addition of 10 % (v/v) of water or TEG to the sulfolane/[BMIM]-[PF_6] mixtures promotes faster reactions while maintaining a stringent control over the polymerization.

5.6 References

1. Matyjaszewski, K.; Tsarevsky, N. V., Macromolecular Engineering by Atom Transfer Radical Polymerization, *Journal of the American Chemical Society*, *136* (18), 6513-6533, 2014.
2. Guliashvili, T.; Mendonça, P. V.; Serra, A. C.; Popov, A. V.; Coelho, J. F. J., Copper-Mediated Controlled/"Living" Radical Polymerization in Polar Solvents: Insights into Some Relevant Mechanistic Aspects, *Chemistry – A European Journal*, *18* (15), 4607-4612, 2012.
3. Jakubowski, W.; Matyjaszewski, K., Activators Regenerated by Electron Transfer for Atom-Transfer Radical Polymerization of (Meth)acrylates and Related Block Copolymers, *Angewandte Chemie*, *118* (27), 4594-4598, 2006.
4. Matyjaszewski, K.; Jakubowski, W.; Min, K.; Tang, W.; Huang, J.; Braunecker, W. A.; Tsarevsky, N. V., Diminishing catalyst concentration in atom transfer radical polymerization with reducing agents, *Proceedings of the National Academy of Sciences*, *103* (42), 15309-15314, 2006.
5. Magenau, A. J. D.; Strandwitz, N. C.; Gennaro, A.; Matyjaszewski, K., Electrochemically Mediated Atom Transfer Radical Polymerization, *Science*, *332* (6025), 81-84, 2011.
6. Konkolewicz, D.; Wang, Y.; Zhong, M.; Krys, P.; Isse, A. A.; Gennaro, A.; Matyjaszewski, K., Reversible-Deactivation Radical Polymerization in the Presence of Metallic Copper. A Critical Assessment of the SARA ATRP and SET-LRP Mechanisms, *Macromolecules*, *46* (22), 8749-8772, 2013.
7. Anastasaki, A.; Nikolaou, V.; Nurumbetov, G.; Wilson, P.; Kempe, K.; Quinn, J. F.; Davis, T. P.; Whittaker, M. R.; Haddleton, D. M., Cu(0)-Mediated Living Radical Polymerization: A Versatile Tool for Materials Synthesis, *Chemical reviews*, *116* (3), 835-877, 2016.
8. Anastasaki, A.; Nikolaou, V.; Haddleton, D. M., Cu(0)-mediated living radical polymerization: recent highlights and applications; a perspective, *Polymer Chemistry*, *7* (5), 1002-1026, 2016.
9. Percec, V.; Guliashvili, T.; Ladislaw, J. S.; Wistrand, A.; Stjerndahl, A.; Sienkowska, M. J.; Monteiro, M. J.; Sahoo, S., Ultrafast Synthesis of Ultrahigh Molar Mass Polymers by Metal-Catalyzed Living Radical Polymerization of Acrylates, Methacrylates, and Vinyl Chloride Mediated by SET at 25 °C, *Journal of the American Chemical Society*, *128* (43), 14156-14165, 2006.
10. Biedroń, T.; Kubisa, P., Atom-Transfer Radical Polymerization of Acrylates in an Ionic Liquid, *Macromolecular Rapid Communications*, *22* (15), 1237-1242, 2001.
11. Sarbu, T.; Matyjaszewski, K., ATRP of Methyl Methacrylate in the Presence of Ionic Liquids with Ferrous and Cuprous Anions, *Macromolecular Chemistry and Physics*, *202* (17), 3379-3391, 2001.
12. Carmichael, A. J.; Haddleton, D. M.; Bon, S. A. F.; Seddon, K. R., Copper() mediated living radical polymerisation in an ionic liquid, *Chemical Communications*, (14), 1237-1238, 2000.
13. Mendes, J. P.; Branco, F.; Abreu, C. M. R.; Mendonça, P. V.; Popov, A. V.; Guliashvili, T.; Serra, A. C.; Coelho, J. F. J., Synergistic Effect of 1-Butyl-3-methylimidazolium Hexafluorophosphate and DMSO in the SARA ATRP at Room Temperature Affording Very Fast Reactions and Polymers with Very Low Dispersity, *ACS Macro Letters*, 544-547, 2014.

14. Costa, J. R. C.; Mendonça, P. V.; Maximiano, P.; Serra, A. C.; Guliashvili, T.; Coelho, J. F. J., Ambient Temperature "Flash" SARA ATRP of Methyl Acrylate in Water/Ionic Liquid/Glycol Mixtures, *Macromolecules*, *48* (19), 6810-6815, 2015.
15. Mendes, J. P.; Branco, F.; Abreu, C. M. R.; Mendonça, P. V.; Serra, A. C.; Popov, A. V.; Guliashvili, T.; Coelho, J. F. J., Sulfolane: an Efficient and Universal Solvent for Copper-Mediated Atom Transfer Radical (co)Polymerization of Acrylates, Methacrylates, Styrene, and Vinyl Chloride, *ACS Macro Letters*, *3* (9), 858-861, 2014.
16. Mendes, J. P.; Mendonca, P. V.; Maximiano, P.; Abreu, C. M. R.; Guliashvili, T.; Serra, A. C.; Coelho, J. F. J., Getting faster: low temperature copper-mediated SARA ATRP of methacrylates, acrylates, styrene and vinyl chloride in polar media using sulfolane/water mixtures, *RSC Advances*, *6* (12), 9598-9603, 2016.
17. Ciampolini, M.; Nardi, N., Five-Coordinated High-Spin Complexes of Bivalent Cobalt, Nickel, andCopper with Tris(2-dimethylaminoethyl)amine, *Inorganic Chemistry*, *5* (1), 41-44, 1966.
18. Tsarevsky, N. V.; Braunecker, W. A.; Matyjaszewski, K., Electron transfer reactions relevant to atom transfer radical polymerization, *Journal of Organometallic Chemistry*, *692* (15), 3212-3222, 2007.
19. Electrochemistry in Ionic Liquids. Torriero, A. A. J. E., Ed. 2015; Vol. Volume 2: Applications, p 398.
20. Coelho, J. F. J.; Carvalho, E. Y.; Marques, D. S.; Popov, A. V.; Goncalves, P. M.; Gil, M. H., Synthesis of Poly(lauryl acrylate) by Single-Electron Transfer/Degenerative Chain Transfer Living Radical Polymerization Catalyzed by Na2S2O4 in Water, *Macromolecular Chemistry and Physics*, *208* (11), 1218-1227, 2007.
21. Coelho, J. F. J.; Carvalho, E. Y.; Marques, D. S.; Popov, A. V.; Percec, V.; Gonçalves, P. M. F. O.; Gil, M. H., Synthesis of poly(ethyl acrylate) by single electron transfer-degenerative chain transfer living radical polymerization in water catalyzed by Na2S2O4, *Journal of Polymer Science Part A: Polymer Chemistry*, *46* (2), 421-432, 2008.
22. Coelho, J. F. J.; Mendonça, P. V.; Popov, A. V.; Percec, V.; Gonçalves, P. M. O. F.; Gil, M. H., Synthesis of high glass transition temperature copolymers based on poly(vinyl chloride) via single electron transfer—Degenerative chain transfer mediated living radical polymerization (SET-DTLRP) of vinyl chloride in water, *Journal of Polymer Science Part A: Polymer Chemistry*, *47* (24), 7021-7031, 2009.
23. Mendonca, P. V.; Serra, A. C.; Coelho, J. F. J.; Popov, A. V.; Guliashvili, T., Ambient temperature rapid ATRP of methyl acrylate, methyl methacrylate and styrene in polar solvents with mixed transition metal catalyst system, *European Polymer Journal*, *47* (7), 1460-1466, 2011.
24. Tabuchi, M.; Kawauchi, T.; Kitayama, T.; Hatada, K., Living polymerization of primary alkyl acrylates with t-butyllithium/bulky aluminum Lewis acids, *Polymer*, *43* (25), 7185-7190, 2002.
25. Lligadas, G.; Ladislaw, J. S.; Guliashvili, T.; Percec, V., Functionally terminated poly(methyl acrylate) by SET-LRP initiated with CHBr3 and CHI3, *Journal of Polymer Science Part A: Polymer Chemistry*, *46* (1), 278-288, 2008.
26. Hasneen, A.; Kim, S.; Paik, H.-j., Synthesis and characterization of low molecular weight poly(methyl acrylate)-b-polystyrene by a combination of ATRP and click coupling method, *Macromol. Res.*, *15* (6), 541-546, 2007.
27. Rocha, N.; Mendonca, P. V.; Mendes, J. P.; Simoes, P. N.; Popov, A. V.; Guliashvili, T.; Serra, A. C.; Coelho, J. F. J., Facile Synthesis of Well-Defined

Telechelic Alkyne-Terminated Polystyrene in Polar Media Using ATRP With Mixed Fe/Cu Transition Metal Catalyst, *Macromolecular Chemistry and Physics*, *214* (1), 76-84, 2013.
28. Sienkowska, M. J.; Rosen, B. M.; Percec, V., SET-LRP of vinyl chloride initiated with CHBr3 in DMSO at 25 °C, *Journal of Polymer Science Part A: Polymer Chemistry*, *47* (16), 4130-4140, 2009.
29. Abreu, C. M. R.; Mendonça, P. V.; Serra, A. C.; Coelho, J. F. J.; Popov, A. V.; Gryn'ova, G.; Coote, M. L.; Guliashvili, T., Reversible Addition–Fragmentation Chain Transfer Polymerization of Vinyl Chloride, *Macromolecules*, *45* (5), 2200-2208, 2012.

Chapter 6

Cyclopentyl Methyl Ether: a New Green Co-Solvent for Supplemental Activator and Reducing Agent Atom Transfer Radical Polymerization

The results of this work are published in: Maximiano, P.; **Mendes, J. P**.; Mendonça, P. V.; Abreu, C. M. R.; Guliashvili, T.; Serra, A. C.; Coelho, J. F. J., *"Cyclopentyl methyl ether: A new green co-solvent for supplemental activator and reducing agent atom transfer radical polymerization"*, *Journal of Polymer Science Part A: Polymer Chemistry***,** *53* (23), 2722-2729, 2015.

6.1 Abstract

A new green solvent, cyclopentyl methyl ether (CPME), is used for the first time in solvent mixtures for the successful SARA ATRP of both activated and non-activated monomers. The SARA ATRP of MA, glycidyl methacrylate (GMA), St and VC in CPME-based mixtures is studied and presents similar features to those reported in the literature using other SARA ATRP systems. Moreover, CPME-based mixtures are suitable solvents for the controlled SARA ATRP of MA using different SARA agents, such as Fe(0), Cu(0) or $Na_2S_2O_4$. The chemical structure and the retention of the chain-end functionality of the polymers is confirmed by ^{1}H NMR and MALDI-TOF analyses and the preparation of a well-defined PMA-*b*-PVC-*b*-PMA triblock copolymer. The method reported here presents an additional improvement in the search for new ecofriendly ATRP systems.

6.2 Introduction

RDRP methods are very effective techniques that allow the preparation of tailor-made polymers with targeted molecular weight, architecture, chain-end functionality and more importantly with low *Đ*.[1] ATRP is one of the most robust and versatile RDRP techniques, which has been employed for the polymerization of a wide range of monomers.[2-3] In ATRP, the fine control over the molecular weight of the polymers is provided by a metal-catalyzed (transition metal complexes with appropriate ligands) dynamic equilibrium between growing radicals ($P_n^{\bullet}$) and alkyl halide dormant species (P_n–X).[4] However, the main issue associated with the original ATRP technique is the use of a high concentration of metal catalyst required to guarantee the equilibrium, typically higher than 1000 parts per million (ppm), which can be problematic from both contamination of polymer and environmental standpoints. Therefore, new ATRP variation techniques[5-8] have been developed aiming to reduce the total amount of metal used to successfully mediate the polymerizations without losing their main features.[9-10] SARA ATRP is one of the most recent developed ATRP variations and it is considered to be a very attractive technique since it allows the use of a low concentration of soluble catalyst (e.g., 100 ppm[8]). With this approach, zero valent metals[8, 11-15] or FDA-approved inorganic sulfites[16-20] have been successfully used as

SARA agents. The role of these species is to continuously regenerate the activator (e.g., CuX; X: halide) by deactivator reduction (e.g., CuX_2) and to slowly generate growing radicals by supplemental activation (Scheme 6.1).[4]

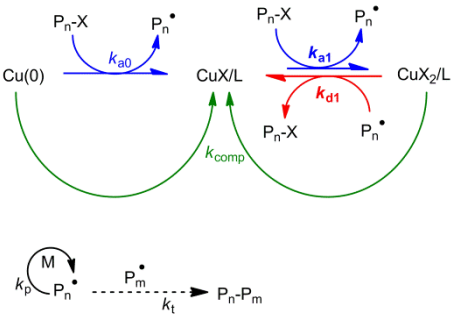

Scheme 6.1 General mechanism of the Cu(0)/CuX_2/L-catalyzed SARA ATRP (L: ligand and X: halide).

Besides the concerns about the amount of metal catalyst used in the polymerization, current research efforts on ATRP are also focused on the use of alternative ecofriendly solvents to the traditional organic ones used, such as DMF,[15] DMSO[21] or THF,[22] which present high concern when considering pharmaceutical usages.[23] Recently, our research group has demonstrated the possibility of using the industrial solvent sulfolane, which is a more acceptable solvent, as universal solvent for the preparation of a wide range of polymers by SARA ATRP.[20] This strategy aims to potentiate the implementation of ATRP at an industrial scale, as well as to provide harmless reaction conditions for the preparation of polymers for the biomedical field. On this matter, it is worth to notice that the SARA ATRP of acrylates, methacrylates and acrylamides has also been successfully performed in alcohol/water mixtures[11-13, 18-19] or even aqueous medium.[13, 24]

In the search of new ecofriendly solvents, the attention was turned to CPME (Figure 6.1), an ethereal solvent which has emerged as a green alternative to similar solvents (e.g., THF). This feature is a direct consequence of unique properties, such as high hydrophobicity, relative stability under both acidic and basic conditions and low formation of peroxides as by products.[25] In addition, CPME reveals negative skin sensitization,[26] presents no genotoxicity and no mutagenicity,[27] and it is approved by the Toxic Substances Control Act (TSCA) and the European List of Notified Chemical Substances (ELINCS). Due to the above mentioned advantages, CPME has been employed as a green process solvent for organic synthesis.[28] Despite being already used as solvent for radical reactions,[29] CPME has never been reported in ATRP reactions (or ATRP variations). The use of CPME in place of DMSO and/or

THF in controlled radical polymerization (including ATRP) of VC is very challenging. This is because DMSO and THF are the only known best solvents for homogeneous and hererogeneous living polymerizations of VC and the replacement of above solvents with less toxic and recyclable CPME is very attractive.

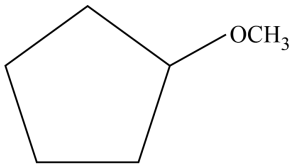

Ecofriendly, high hydrophobicity, negative skin sensitization, no mutagenicity and no genotoxicity

Figure 6.1 Chemical structure of cyclopentyl methyl ether and some of its "green" aspects.

In this work, CPME-based mixtures were used for the first time as solvents for the SARA ATRP of different monomer families: (meth)acrylates, St and VC. The three most studied SARA agents (Cu(0), Fe(0) and $Na_2S_2O_4$) were tested and allowed the preparation of well-defined PMA. In addition, an unique PMA-*b*-PVC-*b*-PMA block copolymer was prepared using this SARA ATRP developed system.

6.3 Experimental Section

6.3.1 Materials

Methyl acrylate (MA, Acros, 99% stabilized), glycidyl methacrylate (GMA, Sigma-Aldrich, 97% stabilized) and St were passed through a sand/alumina column before use in order to remove the radical inhibitor. $CuBr_2$ (Acros, 99+% extra pure, anhydrous), deuterated chloroform ($CDCl_3$) (Euriso-top, +1% TMS), DMF (Sigma-Aldrich, +99.8%), CPME (Sigma-Aldrich, inhibitor-free, anhydrous, +99.9%), DMSO (Acros, 99.8+% extra pure), ethyl α-bromoisobutyrate (EBiB) (Sigma-Aldrich, 98%), bromoform ($CHBr_3$) (+ 99 % stabilized; Acros), ethanol (EtOH, Panreac, 99.5%), PS standards (Polymer Laboratories), iron powder (Fe(0) (Acros, 99%, ~70 mesh), 2-(4-hydroxyphenylazo)benzoic acid (HABA) (Sigma–Aldrich, 99.5%), 2,5-dihydroxybenzoic acid (DHB) (Sigma–Aldrich, >99%), *N*,*N*,*N*′,*N*″,*N*″-pentamethyldiethylenetriamine (PMDETA, Aldrich, 99%), tris(2-aminoethyl)amine (TREN) (96 %; Sigma-Aldrich), 2,2'-bipyridine (bpy) (Sigma-Aldrich, +99.8%) and sodium dithionite ($Na_2S_2O_4$, 85 %, technical grade; Aldrich) were used as received.

Metallic copper (Cu(0), d = 1 mm, Sigma Aldrich) was washed with HCl in methanol and subsequently rinsed with methanol and dried under a stream of nitrogen following the literature procedures.[30]

Purified water (Milli-Q®, Millipore, resistivity >18 MΩ.cm) was obtained by reverse osmosis.

THF (Panreac, HPLC grade) was filtered under reduced pressure before use.

Tris[2-(dimethylamino)ethyl]amine (Me_6TREN)[31] and tris(2-pyridylmethyl)amine (TPMA)[32] were synthesized according to the procedures described in the literature.

VC (99 %) was kindly supplied by CIRES Lda, Portugal.

6.3.2 Techniques

The chromatographic parameters of the samples were determined using high performance size exclusion chromatography HPSEC; Viscotek (Viscotek TDAmax) with a differential viscometer (DV); right-angle laser-light scattering (RALLS, Viscotek); low-angle laser-light scattering (LALLS, Viscotek) and refractive index (RI) detectors. The column set consisted of a PL 10 mm guard column (50 × 7.5 mm^2) followed by one Viscotek T200 column (6 μm), one MIXED-E PLgel column (3 μm) and one MIXED-C PLgel column (5 μm). HPLC dual piston pump was set with a flow rate of 1 mL/min. The eluent (THF) was previously filtered through a 0.2 μm filter. The system was also equipped with an on-line degasser. The tests were done at 30 °C using an Elder CH-150 heater. Before the injection (100 μL), the samples were filtered through a polytetrafluoroethylene (PTFE) membrane with 0.2 μm pore. The system was calibrated with narrow PS standards. The *dn/dc* was determined as 0.063 mL/g for PMA, 0.105 mL/g for PVC, 0.087 mL/g for PGMA and 0.185 mL/g for PS. M_n^{SEC} and $Đ$ of the synthesized polymers were determined by multidetectors calibration using the OmniSEC software version: 4.6.1.354.

400 MHz ^1H NMR spectra of reaction mixture samples were recorded on a Bruker Avance III 400 MHz spectrometer, with a 5-mm TIX triple resonance detection probe, in $CDCl_3$ with tetramethylsilane (TMS) as an internal standard. Conversions of the monomer were determined by integration of monomer and polymer signals using MestRenova software version: 6.0.2-5475.

For the MALDI-TOF-MS analysis, the PMA samples were dissolved in THF at a concentration of 10 mg/mL. DHB and HABA (0.05 M in THF) were used as matrix.

The dried-droplet sample preparation technique was used to obtain 1:1 ratio (sample/matrix); an aliquot of 1 μL of each sample was directly spotted on the MTP AnchorChip TM 600/384 TF MALDI target, Bruker Daltonik (Bremen Germany) and, before the sample dry, 1 μL of matrix solution in THF was added and allowed to dry at room temperature, to allow matrix crystallization. External mass calibration was performed with a peptide calibration standard (PSCII) for the range 700-3000 (9 mass calibration points), 0.5 μL of the calibration solution and matrix previously mixed in an Eppendorf tube (1:2, v/v) were applied directly on the target and allowed to dry at room temperature. Mass spectra were recorded using an Autoflex III smartbeam1 MALDI-TOF-MS mass spectrometer Bruker Daltonik (Bremen, Germany) operating in the linear and reflection positive ion mode. Ions were formed upon irradiation by a smartbeam laser using a frequency of 200 Hz. Each mass spectrum was produced by averaging 2500 laser shots collected across the whole sample spot surface by screening in the range m/z 500-10000. The laser irradiance was set to 35-40% (relative scale 0-100) arbitrary units according to the corresponding threshold required for the applied matrix systems.

6.3.3 Procedures

6.3.3.1 Typical procedure for the $[Cu(0)]_0/[CuBr_2]_0/[Me_6TREN]_0$ = Cu(0) wire/0.1/1.1 catalyzed SARA ATRP of MA

Cu(0) wire (5 cm, 450 mg) and a solution of $CuBr_2$ (3.506 mg, 0.016 mmol) and Me_6TREN (39.76 mg, 0.173 mmol) in CPME (1.1 mL), water (31.6 μL) and ethanol (0.44 mL) were placed in a Schlenk tube reactor. A mixture of MA (3.16 mL, 34.85 mmol) and EBiB (30.62 mg, 0.157 mmol) was added to the reactor that was sealed, using a glass stopper, and frozen in liquid nitrogen. The Schlenk tube reactor containing the reaction mixture was deoxygenated with four freeze-vacuum-thaw cycles and purged with nitrogen. The reactor was placed in a water bath at 30 ºC with stirring (700 rpm). During the polymerization, different reaction mixture samples were collected by using an airtight syringe and purging the side arm of the Schlenk tube reactor with nitrogen. The samples were analyzed by ^{1}H NMR spectroscopy to determine the monomer conversion and by SEC, to determine M_n^{SEC} and $Đ$ of the polymers.

6.3.3.2 Typical procedure for the $[Fe(0)]_0/[CuBr_2]_0/[Me_6TREN]_0$ = Cu(0) wire/0.1/1.1 catalyzed SARA ATRP of MA

Fe(0) powder (8.77 mg, 0.16 mmol) and a solution of $CuBr_2$ (3.506 mg, 0.016 mmol) and Me_6TREN (39.76 mg, 0.17 mmol) in CPME (1.1 mL), water (31.6 μL) and ethanol (0.44 mL) were placed in a Schlenk tube reactor. A mixture of MA (3.16 mL, 34.85 mmol) and EBiB (30.62 mg, 0.157 mmol) was added to the reactor that was sealed, using a glass stopper, and frozen in liquid nitrogen. The Schlenk tube reactor containing the reaction mixture was deoxygenated with four freeze-vacuum-thaw cycles and purged with nitrogen. The reactor was placed in a water bath at 30 ºC with stirring (700 rpm). During the polymerization, different reaction mixture samples were collected by using an airtight syringe and purging the side arm of the Schlenk tube reactor with nitrogen. The samples were analyzed by ^{1}H NMR spectroscopy to determine the monomer conversion and by SEC, to determine M_n^{SEC} and $Đ$ of the polymers.

6.3.3.3 Typical procedure for the $[Na_2S_2O_4)]_0/[CuBr_2]_0/[Me_6TREN]_0$ = Cu(0) wire/0.1/0.5 catalyzed SARA ATRP of MA

$Na_2S_2O_4$ (27.3 mg, 0.16 mmol) and a solution of $CuBr_2$ (3.506 mg, 0.016 mmol) and Me_6TREN (18.07 mg, 0.079 mmol) in CPME (1.1 mL), water (31.6 μL) and ethanol (0.44 mL) were placed in a Schlenk tube reactor. A mixture of MA (3.16 mL, 34.85 mmol) and EBiB (30.62 mg, 0.157 mmol) was added to the reactor that was sealed, using a glass stopper, and frozen in liquid nitrogen. The Schlenk tube reactor containing the reaction mixture was deoxygenated with four freeze-vacuum-thaw cycles and purged with nitrogen. The reactor was placed in a water bath at 30 ºC with stirring (700 rpm). During the polymerization, different reaction mixture samples were collected by using an airtight syringe and purging the side arm of the Schlenk tube reactor with nitrogen. The samples were analyzed by ^{1}H NMR spectroscopy to determine the monomer conversion and by SEC, to determine M_n^{SEC} and $Đ$ of the polymers.

6.3.3.4 Typical procedure for the $[Cu(0)]_0/[CuBr_2]_0/[PMDETA]_0$ = Cu(0) wire/0/1.1 catalyzed SARA ATRP of St

A mixture of Cu(0) wire (5 cm, 450 mg), PMDETA (24.73 mg, 0.14 mmol), CPME (1.2 mL) and DMF (0.5 mL) was placed in a Schlenk tube reactor. A solution of EBiB (25.31 mg, 0.13 mmol) in St (3.30 mL, 28.81 mmol) was added to the reactor that was sealed, by using a glass stopper, and frozen in liquid nitrogen. The Schlenk tube reactor containing the reaction mixture was deoxygenated with four freeze-vacuum-thaw cycles and purged with nitrogen. The reactor was placed in a oil bath at 60 ºC with stirring (700 rpm). During the polymerization, different reaction mixture samples were collected by using an airtight syringe and purging the side arm of the Schlenk tube reactor with nitrogen. The samples were analyzed by ^{1}H NMR spectroscopy to determine the monomer conversion and by SEC, to determine the M_n^{SEC} and $Đ$ of the polymers.

6.3.3.5 Typical procedure for the $[Fe(0)]_0/[CuBr_2]_0/[TPMA]_0$ = 1/0/1.1 catalyzed SARA ATRP of GMA

A mixture of Fe(0) (5.3 mg, 0.1mmol), TPMA (30.36 mg, 0.1 mmol), CPME (1.0 mL) and DMF (0.4 mL) was placed in a Schlenk tube reactor. A solution of EBiB (18.54 mg, 0.10 mmol) in GMA (2.88 mL, 21.10 mmol) was added to the reactor that was sealed, by using a glass stopper, and frozen in liquid nitrogen. The Schlenk tube reactor containing the reaction mixture was deoxygenated with four freeze-vacuum-thaw cycles and purged with nitrogen. The reactor was placed in a water bath at 30 ºC with stirring (700 rpm). During the polymerization, different reaction mixture samples were collected by using an airtight syringe and purging the side arm of the Schlenk tube reactor with nitrogen. The samples were analyzed by ^{1}H NMR spectroscopy to determine the monomer conversion and by SEC, to determine the M_n^{SEC} and $Đ$ of the polymers.

6.3.3.6 Typical procedure for the $[Cu(0)]_0/[CuBr_2]_0/[TREN]_0$ = Cu(0) wire/0.1/1.1 catalyzed SARA ATRP of VC

A 50 mL Ace glass 8645#15 pressure tube, equipped with bushing and plunger valve, was charged with a mixture of $CHBr_3$ (86.43 mg, 0.33 mmol), TREN (55.03 mg, 0.36 mmol), $CuBr_2$ (7.34 mg, 0.033 mmol), Cu(0) wire (5 cm, 450 mg), CPME (3.5 mL) and DMSO (1.5 mL) (previously bubbled with nitrogen for about 15 min). The precondensed VC (5 mL, 72.8 mmol) was added to the tube. The exact amount of VC was determined gravimetrically. The tube was closed, placed in liquid nitrogen and degassed through the plunger valve by applying reduced pressure and filling the tube with N_2 about 20 times. The valve was closed, and the tube reactor was placed in a water bath at 42 ºC with stirring (700 rpm). The reaction was stopped by plunging the tube into ice water. The tube was slowly opened, the excess of VC was distilled, and the mixture was precipitated into methanol. The polymer was separated by filtration and dried in a vacuum oven until constant weight was observed. The monomer conversion was determined gravimetrically. GPC was used for the determination of PVC´s M_n^{SEC} and $Đ$.

6.3.3.7 Typical procedure for the synthesis of PMA-*b*-PVC-*b*-PMA block copolymer by "one-pot" $[Cu(0)]_0/[CuBr_2]_0/[TREN]_0$ = Cu(0) wire/0.1/1.1 catalyzed SARA ATRP

A 50 mL Ace glass 8645#15 pressure tube, equipped with bushing and plunger valve, was charged with a mixture of $CHBr_3$ (115.07 mg, 0.44 mmol), TREN (73.24 mg, 0.48 mmol), $CuBr_2$ (9.76 mg, 0.044 mmol), Cu(0) wire (5 cm, 450 mg), CPME (2.1 mL) and DMSO (0.9 mL) (previously bubbled with nitrogen for about 15 min). The precondensed VC (3.0 mL, 43.7 mmol) was added to the tube. The exact amount of VC was determined gravimetrically. The tube was closed, submerged in liquid nitrogen and degassed through the plunger valve by applying reduced pressure and filling the tube with nitrogen about 20 times. The valve was closed, and the tube reactor was placed in a water bath at 42 °C with stirring (700 rpm). After 10 h, the reaction was stopped by plunging the tube into ice water. The tube was slowly opened and the excess VC was distilled. The monomer conversion was determined gravimetrically (61.8%), and the M_n^{SEC} = 6100 and $Đ$ = 1.57 were determined by GPC

analysis in THF. A mixture of CPME (8.4 mL), DMSO (3.6 mL) and MA (12 mL, 132.4 mmol) was added to the same 50 mL Ace glass 8645#15 pressure tube (without any purification of the α,ω-di(bromo)PVC macroinitiator). The tube was closed, submerged in liquid nitrogen and degassed through the plunger valve by applying reduced pressure and filling the tube with nitrogen about 20 times. The valve was closed, and the tube reactor was placed in a water bath at 42 °C with stirring (700 rpm). The reaction was stopped after 32 h and the mixture was analyzed by ^{1}H NMR spectroscopy in order to determine the MA conversion and by SEC, to determine the M_n^{SEC} and $Đ$ of the PMA-*b*-PVC-*b*-PMA block copolymer.

6.4 Results and discussion

6.4.1 Influence of the solvent mixture composition

There are several reports on the controlled polymerization of MA (used as model monomer).[4, 11, 16-17, 21, 30] In this study, the SARA ATRP of MA was investigated using the catalytic system of Cu(0)/$CuBr_2$/Me_6TREN.[4, 20, 24, 30] Preliminary experiments using just CPME as the polymerization solvent were not successful due the insolubility of several catalytic complexes in this solvent ($CuBr_2$/ligand; ligand: Me_6TREN, TPMA, bpy, PMDETA or TREN). Alternatively, CPME was mixed with DMSO, which is a common solvent used in the controlled polymerization of MA.[21] Several CPME/DMSO ratios were tested and the minimum amount of DMSO required for the complete dissolution of the $CuBr_2$/Me_6TREN complex was found to be 30% (v/v). The kinetic results showed that the SARA ATRP of MA in CPME/DMSO = 70/30 (v/v) was extremely well-controlled ($Đ \leq 1.1$) at a reasonable polymerization rate (Figure 6.2), proving the usefulness of the CPME as a green solvent for the SARA ATRP of MA.

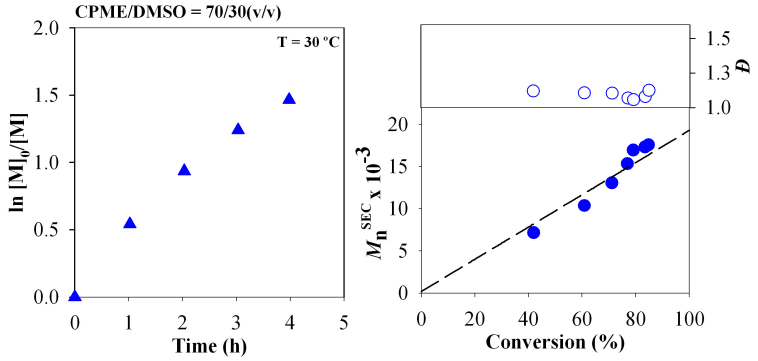

Figure 6.2 Kinetic plots of conversion and ln[M]$_0$/[M] *vs.* time (triangle) and plot of number-average molecular weights (M_n^{SEC}) and *Đ vs.* monomer conversion (circle) for the SARA ATRP of MA in CPME/DMSO = 70/30 (v/v) at 30 °C. Reaction conditions: [MA]$_0$/[solvent] = 2/1 (v/v); [MA]$_0$/[EBiB]$_0$/Cu(0)/[$CuBr_2$]$_0$/[Me_6TREN]$_0$= 222/1/Cu(0) wire/0.1/1.1.

Aiming to achieve a complete harmless reaction solvent mixture, DMSO was replaced by the EtOH, which has been also used for the SARA ATRP of different monomers.[11, 13, 17] In this case, the addition of a small amount of water was also required to allow a complete dissolution of the catalytic complex. The optimum value of the water content was found to be 2% (v/v), based on a compromise between the solubility of the catalytic system and the miscibility of the solvents, since CPME and water are not miscible. Figure 6.3 shows that this ecofriendly SARA ATRP system provided a stringent control over the *Đ* throughout the entire reaction, and the theoretical molecular weights were in close agreement to the experimental ones.

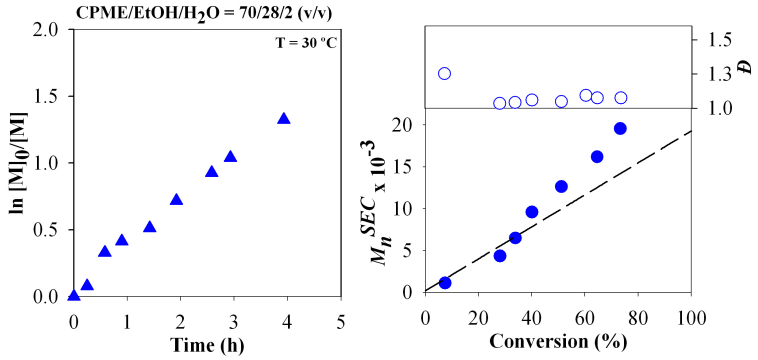

Figure 6.3 Kinetic plots of conversion and ln[M]$_0$/[M] *vs.* time (triangle) and plot of number-average molecular weights (M_n^{SEC}) and *Đ vs.* monomer conversion (circle) for the SARA ATRP of MA in CPME/EtOH/H_2O = 70/28/2 (v/v/v) at 30 °C. Reaction conditions: [MA]$_0$/[solvent] = 2/1 (v/v); [MA]$_0$/[EBiB]$_0$/Cu(0)/[$CuBr_2$]$_0$/[Me_6TREN]$_0$= 222/1/Cu(0) wire/0.1/1.1.

In the last two CMPE systems (Figure 6.2 and Figure 6.3) it was observed the similar polymerization rate. The structure of the well-defined Br-terminated PMA (obtained in both cases) was confirmed by ^{1}H NMR spectroscopy (Figure 6.4) and MALDI-TOF (Figure 6.5).

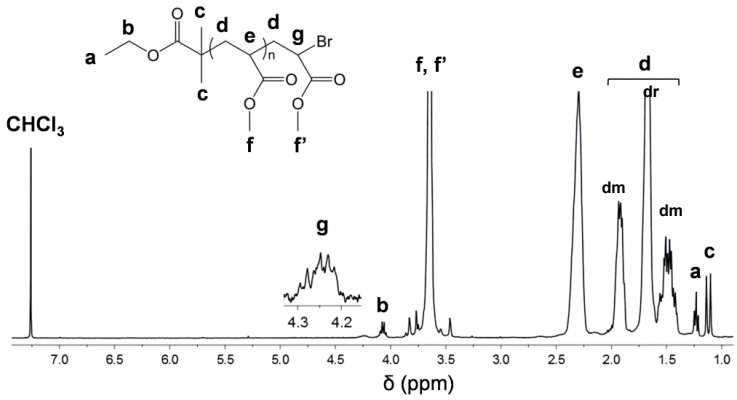

Figure 6.4 ^{1}H NMR spectrum of a PMA sample (M_n^{SEC} = 10 600 ; $Đ$ = 1.28) obtained by SARA ATRP in CPME/EtOH/H_2O = 70/28/2 (v/v/v) at 30 °C.

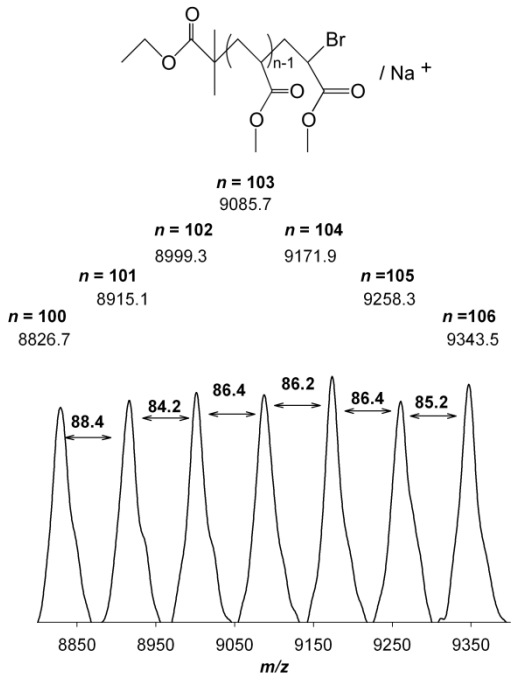

Figure 6.5 Enlargement of the MALDI-TOF-MS from m/z 8800 to 9400 in the linear mode (using HABA as matrix) of PMA-Br (M_n^{SEC} = 10600, $Đ$ =1.28).

6.4.2 Influence of the catalytic system

The viability of the new reaction solvent mixture (CPME/EtOH/H_2O) was investigated using the most common SARA agents: Cu(0),[4, 13, 24] Fe(0)[8, 11-12, 14] and $Na_2S_2O_4$.[16-19] Besides the use of an ecofriendly solvent mixture, the use of these SARA agents is very attractive considering the preparation of polymers for biomedical applications. On this matter, it is worth noting that the zero valent metals can be easily removed from the reaction medium after the polymerization (iron is also a very biocompatible metal), while $Na_2S_2O_4$ is a FDA-approved compound. The polymerization rate was in the same order when either Cu(0) or Fe(0) were used as SARA agents (Figure 6.6).

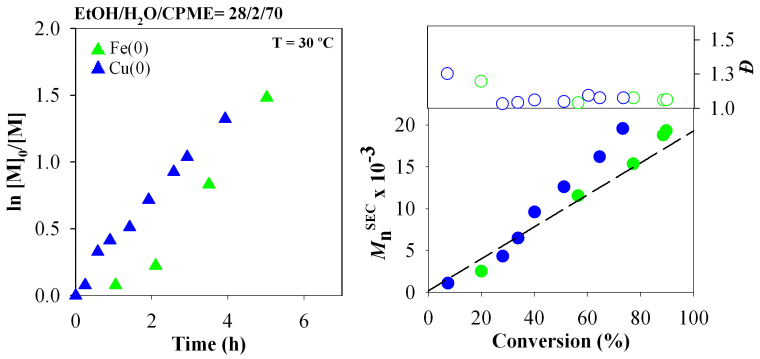

Figure 6.6 Kinetic plots of conversion and ln$[M]_0/[M]$ *vs.* time (triangle) and plot of number-average molecular weights (M_n^{SEC}) and $Đ$ *vs*. monomer conversion (circle) for the SARA ATRP of MA in CPME/EtOH/H_2O = 70/28/2 (v/v/v) at 30 °C, using different SARA agents. Reaction conditions: $[MA]_0$/[solvent] = 2/1 (v/v); $[MA]_0/[EBiB]_0$/SARA agent/$[CuBr_2]_0/[Me_6TREN]_0$= 222/1/Cu(0) wire (blue) or Fe(0) powder (green)/0.1/1.1.

In the case of $Na_2S_2O_4$, the polymerization was considerably slower (Table 6.1), most probably due to the very low solubility of $Na_2S_2O_4$ in the reaction solvent mixture. A similar behavior has been observed when DMSO was used as the polymerization solvent.[16] Nevertheless, the results also show that regardless the SARA agent used, the polymerization system allowed an excellent control over the molecular weight of PMA (Figure 6.6 and Table 6.1). This observation suggests that the SARA ATRP is a very robust and versatile technique for the preparation of well-defined polymers under different experimental conditions near room temperature.

.

Table 6.1 Molecular weight parameters of the PMA-Br prepared by SARA ATRP in CPME/EtOH/H_2O = 70/28/2 (v/v/v) at 30 °C, using different SARA agents. Reaction conditions: $[MA]_0/[EBiB]_0$ = 222; $[MA]_0$/[solvent] = 2/1 (v/v); [Fe(0) or Cu(0)]/$[CuBr_2]_0/[Me_6TREN]_0$ = Cu(0) wire or Fe(0) powder/0.1/1.1; $[Na_2S_2O_4]/[CuBr_2]_0/[Me_6TREN]_0$ = 1/0.1/0.5

Entry	SARA agent	k_p^{app} (h^{-1})	Time (h)	Conv. (%)	M_n^{SEC} x 10^{-3}	$Đ$
1	Cu(0)	0.332	3.9	73	19.6	1.08
2	Fe(0)	0.344	5.0	77	15.4	1.08
3	$Na_2S_2O_4$	0.194	7.9	42	4.7	1.01

6.4.3 Influence of the degree of polymerization

The targeted degree of polymerization (DP) has a major role in the rate of reaction due to different concentration of radicals during the polymerization. In addition, the control over the polymerization and the maximum monomer conversion that can be achieved could be compromised for high targeted DP values. In this work, the targeted DP of MA was investigated in the range of 100-1000 in order to evaluate the robustness of the SARA ATRP using a CPME-based mixture. As expected, the rate of polymerization decreased with the increase of the targeted DP (Figure 6.7). The solvent mixture used (CPME/EtOH/H_2O = 70/28/2 (v/v/v)) allowed the preparation of very well-defined PMA ($Đ \approx 1.1$) and high monomer conversion, for the range of DPs studied, suggesting that the SARA ATRP system developed is quite robust.

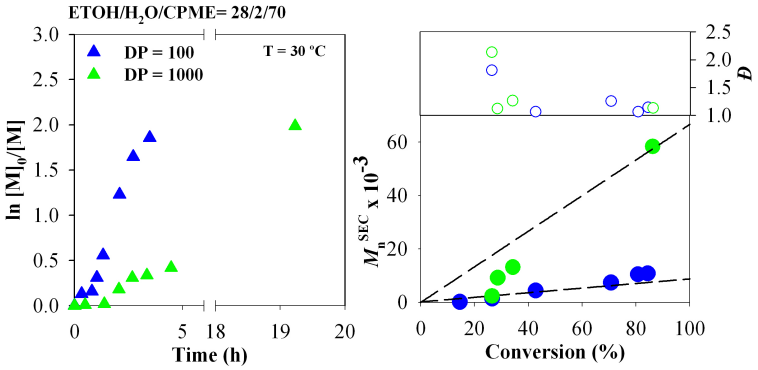

Figure 6.7 Kinetic plots of conversion and $\ln[M]_0/[M]$ *vs.* time (triangle) and plot of number-average molecular weights (M_n^{SEC}) and $Đ$ *vs.* monomer conversion (cirdcle) for the SARA ATRP of MA in CPME/EtOH/H_2O = 70/28/2 (v/v/v) at 30 °C, for different targeted DP values. Reaction conditions: $[MA]_0$/[solvent] = 2/1 (v/v); $[MA]_0/[EBiB]_0/Cu(0)/[CuBr_2]_0/[Me_6TREN]_0$= DP/Cu(0) wire/0.1/1.1.

6.4.4 Polymerization of styrene, vinyl chloride and glycidyl methacrylate

The application of the new solvent mixture developed for the SARA ATRP technique was extended to the polymerization of three relevant monomers: St, GMA and VC. The CPME-based mixtures were ajusted for each polymerization. DMF was used as co-solvent for St and GMA polymerization and DMSO was chosen for the polymerization of VC. The catalytic complexes and initiators were also adjusted according to the structure of the monomers, in order to provide well-controlled polymerizations.[20, 33]

Figure 6.8 shows the kinetic data obtained for the polymerization of St in a CPME/DMF = 70/30 (v/v) mixture.

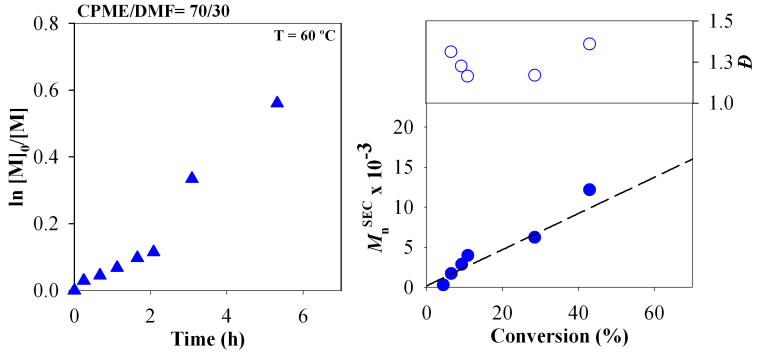

Figure 6.8 Kinetic plots of conversion and ln[M]$_0$/[M] *vs.* time (triangle) and plot of number-average molecular weights (M_n^{SEC}) and *Đ vs.* monomer conversion (circle) for the SARA ATRP of St in CPME/DMF = 70/30 (v/v) at 60 °C. Reaction conditions: [St]$_0$/[solvent] = 2/1 (v/v); [St]$_0$/[EBiB]$_0$/Cu(0)/[$CuBr_2$]$_0$/[PMDETA]$_0$= 222/1/Cu(0) wire/0.1/1.1.

The polymerization (Figure 6.8) was the first-order with respect to monomer conversion and both the reaction rate and the control over the molecular weight were in the same range of previous results reported by our group on the Fe(0)-catalyzed SARA ATRP of St in DMF.[15] Additionally, the present work allowed the polymerization of St at a lower temperature (60 °C) than the usual value (> 70 °C) reported in the literature.[15, 34-37] This fact could potentially contribute to the decrease of the well-known side reactions occurring for the St polymerization at high temperatures, such as the loss of the chain-end functionality or monomer self-initiation.[38] The chemical structure of the PS prepared by SARA ATRP was confirmed by ^{1}H NMR analysis (Figure 6.9) and the "living" character of the polymer was evaluated by a self-extension experiment (Figure 6.10).

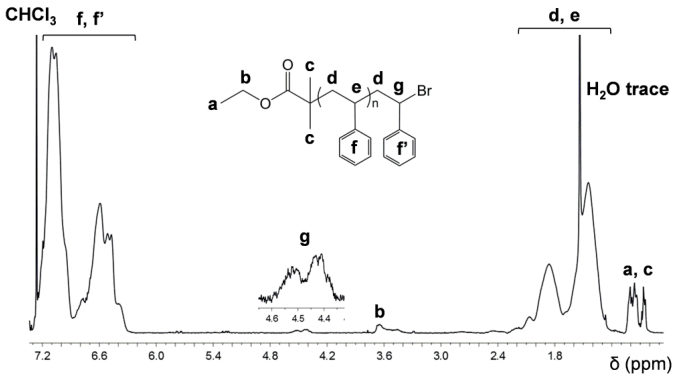

Figure 6.9 ^{1}H NMR spectrum of a PS sample ($M_n^{|SEC}$ = 3800 ; $Đ$ =1.14; conversion = 27 %; functionality = 90 %) obtained by SARA ATRP; solvent: $CDCl_3$

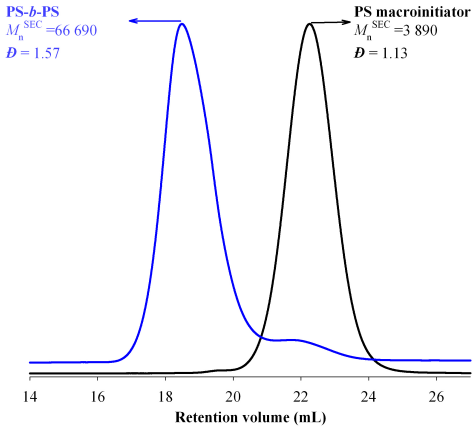

Figure 6.10 SEC chromatograms of a PS-Br macroinitiator (black line) and self-extended PS (blue line) by SARA ATRP.

The presence of the epoxide ring in the structure of GMA makes this monomer very attractive for the preparation of useful polymeric structures, through post-polymerization ring-opening reactions. GMA-based polymers have been employed in several areas, such as adhesives, drug-delivery or coatings, among others, proving the versatility and economical value of this monomer.[39-41] The polymerization of GMA by SARA ATRP was recently reported by our research group using a mixed-metal catalytic system in toluene/DMF mixtures.[33] In this work, it was possible to replace the harmful toluene by the ecofriendly CPME, with very promising results in terms of $Đ$ (Table 6.2, entry 2)).

In addition, the polymerization was considerably faster than the previously reported,[33] with monomer reaching relatively high conversion (70%) after 1.2 h of reaction. The structure of PGMA was confirmed by ^{1}H NMR (Figure 6.11).

Table 6.2 Molecular weight parameters of the PS-Br, PGMA-Br and Br-PVC-Br prepared by SARA ATRP in CPME-based mixtures.

Entry	Monomer	Solvent (v/v)	$[M]_0/[I]_0$[d]	Time (h)	Conv. (%)	M_n^{SEC} x 10^{-3}	$Đ$
1	St[a]	CPME/DMF = 70/30	222	3	28	6.2	1.17
2	GMA[b]	CPME/DMF = 70/30	222	1.2	70	17.5	1.27
3	VC[c]	CPME/DMSO = 70/30	222	7.5	37	6.7	1.58
4	VC[c]	CPME/DMSO = 70/30	100	10	62	6.1	1.57

[a] Reaction conditions: $[St]_0/[solvent]$ = 2/1 (v/v); $[St]_0/[EBiB]_0/[Cu(0)]_0/[CuBr_2]_0/[PMDETA]_0$=222/1/Cu(0) wire/0.1/1.1; T = 60 °C.

[b] Reaction conditions: $[GMA]_0/[solvent]$ = 2/1 (v/v); $[GMA]_0/[EBiB]_0/[Fe(0)]_0/[CuBr_2]_0/[TPMA]_0$= 222/1/1/0.1/1.1; T = 30 °C

[c] Reaction conditions: $[VC]_0/[solvent]$ = 1/1 (v/v); $[VC]_0/[CHBr_3]_0/[Cu(0)]_0/[CuBr_2]_0/[TREN]_0$ = DP/1/Cu(0) wire/0.1/1.1; T = 42 °C.

[d] M: monomer; I: initiator (EBiB for St and GMA and $CHBr_3$ for VC)

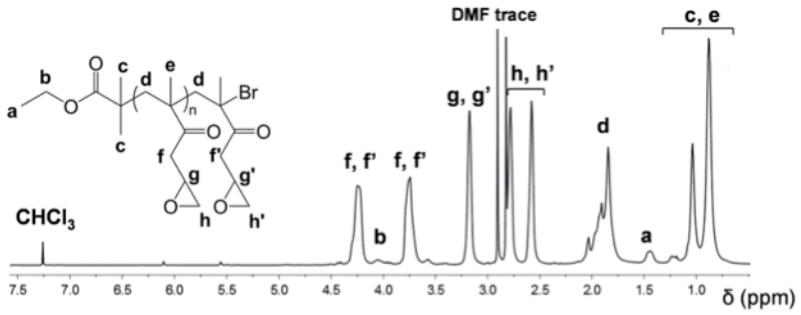

Figure 6.11 ^{1}H NMR spectrum of a PGMA sample (M_n^{SEC} = 46600; $Đ$ = 1.39) obtained by SARA ATRP; solvent: $CDCl_3$

The use of a CPME/DMSO = 70/30 (v/v) mixture for the SARA ATRP of VC (non-activated monomer) allowed the preparation well-defined structures (Table 6.2, entries 3–4)). Similar results were obtained using a previously reported SARA ATRP system in sulfolane.[20] This observation corroborates the versatility and robustness of the SARA ATRP technique for both activated and non-activated monomers. In addition, a α,ω-di(bromo)PVC ($conv._{VC}$ = 61.8%, M_n^{th} = 5000, M_n^{SEC} = 6100, $Đ$ =

1.57, see Figure 6.12) obtained by bromoform-initiated SARA ATRP was used as a macroinitiator for the preparation of a PMA-*b*-PVC-*b*-PMA (conv.$_{MA}$ = 77.3%, M_n^{th} = 39400, M_n^{SEC} = 40700, $Đ$ = 1.49) triblock copolymer by "one-pot" SARA ATRP in CPME/DMSO = 70/30 (v/v).

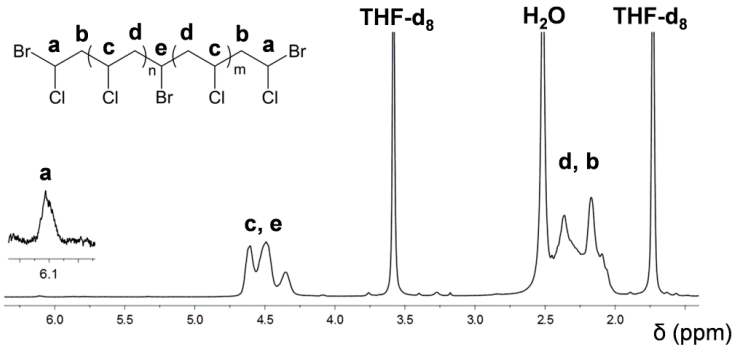

Figure 6.12 ^{1}H NMR spectrum of a PVC sample (M_n^{SEC} = 6100; $Đ$ =1.57) obtained by SARA ATRP; solvent: d_8-THF.

The chromatograms shown in Figure 6.13 demonstrate a shift of the macroinitiator molecular weight distribution towards high molecular weight values (lower retention volume), with no increase of the dispersity of the block copolymer.

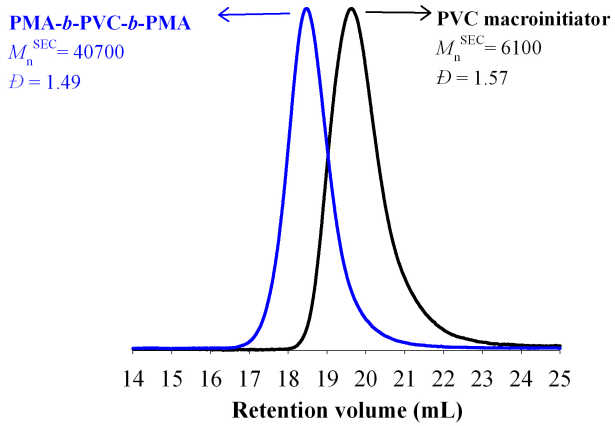

Figure 6.13 SEC chromatograms of a α,ω-di(bromo)PVC (conv.$_{VC}$ = 61.8%, M_n^{th} = 5000, M_n^{SEC} = 6100, $Đ$ = 1.57) macroinitiator (black line) and PMA-*b*-PVC-*b*-PMA (conv.$_{MA}$ = 77.3%, M_n^{th} = 39400, M_n^{SEC} = 40700, $Đ$ = 1.49) triblock copolymer (blue line), after "one-pot" chain extension by SARA ATRP in CPME/DMSO = 70/30 (v/v).

These results suggest that the PVC prepared by SARA ATRP, using this system, is able to retain enough chain-end functionality to allow the preparation of copolymeric structures, which is of extreme importance for the macromolecular engineering field. The structure of the block copolymer was confirmed by ^{1}H NMR analysis (Figure 6.14).

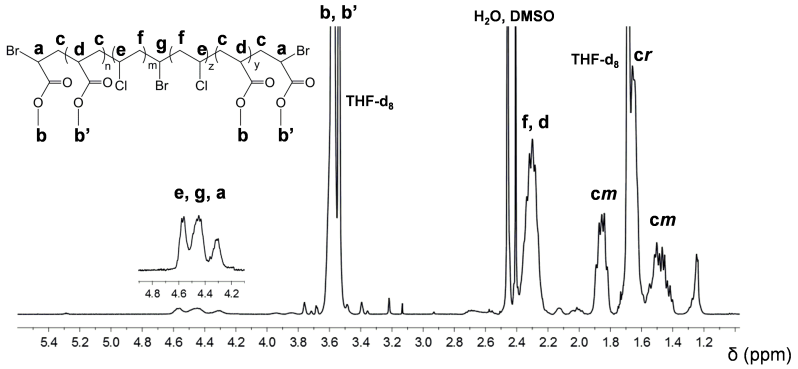

Figure 6.14 ^{1}H NMR of a purified PMA-*b*-PVC-*b*-PMA (M_n^{SEC} = 40700, $Đ$ = 1.49) triblock copolymer obtained by "one-pot" SARA ATRP in CPME/DMSO = 70/30 (v/v); solvent: d_8-THF.

6.5 Conclusions

The use of environmentally-attractive CPME in solvent mixtures for the Cu(0)-catalyzed SARA ATRP of several monomer families was demonstrated. Well-defined PMA, PGMA, PS and PVC were obtained using several experimental conditions. In addition, the biocompatible Fe(0) or $Na_2S_2O_4$ were successfully used as SARA agents to mediate the MA polymerization. As a proof-of-concept, the SARA ATRP system developed was also used for the preparation of a PMA-*b*-PVC-*b*-PMA triblock copolymer. Besides the ecofriendly nature of both CPME and SARA agents used, the SARA ATRP technique can be of particular interest due to the low concentration of soluble metal catalyst employed. Therefore, the strategy presented here could be useful for the preparation of well-defined materials for biomedical applications.

6.6 References

1. Braunecker, W. A.; Matyjaszewski, K., Controlled/living radical polymerization: Features, developments, and perspectives, *Progress in Polymer Science*, *32* (1), 93-146, 2007.
2. Kamigaito, M.; Ando, T.; Sawamoto, M., Metal-Catalyzed Living Radical Polymerization, *Chemical reviews*, *101* (12), 3689-3746, 2001.
3. Matyjaszewski, K.; Xia, J., Atom Transfer Radical Polymerization, *Chemical reviews*, *101* (9), 2921-2990, 2001.
4. Guliashvili, T.; Mendonça, P. V.; Serra, A. C.; Popov, A. V.; Coelho, J. F. J., Copper-Mediated Controlled/"Living" Radical Polymerization in Polar Solvents: Insights into Some Relevant Mechanistic Aspects, *Chemistry – A European Journal*, *18* (15), 4607-4612, 2012.
5. Jakubowski, W.; Matyjaszewski, K., Activators Regenerated by Electron Transfer for Atom-Transfer Radical Polymerization of (Meth)acrylates and Related Block Copolymers, *Angewandte Chemie International Edition*, *45* (27), 4482-4486, 2006.
6. Magenau, A. J. D.; Strandwitz, N. C.; Gennaro, A.; Matyjaszewski, K., Electrochemically Mediated Atom Transfer Radical Polymerization, *Science*, *332* (6025), 81-84, 2011.
7. Matyjaszewski, K.; Jakubowski, W.; Min, K.; Tang, W.; Huang, J.; Braunecker, W. A.; Tsarevsky, N. V., Diminishing catalyst concentration in atom transfer radical polymerization with reducing agents, *Proceedings of the National Academy of Sciences*, *103* (42), 15309-15314, 2006.
8. Zhang, Y.; Wang, Y.; Matyjaszewski, K., ATRP of Methyl Acrylate with Metallic Zinc, Magnesium, and Iron as Reducing Agents and Supplemental Activators, *Macromolecules*, *44* (4), 683-685, 2011.
9. Tsarevsky, N. V.; Matyjaszewski, K., "Green" Atom Transfer Radical Polymerization: From Process Design to Preparation of Well-Defined Environmentally Friendly Polymeric Materials, *Chem. Rev.*, *107* (6), 2270-2299, 2007.
10. Pintauer, T.; Matyjaszewski, K., Atom transfer radical addition and polymerization reactions catalyzed by ppm amounts of copper complexes, *Chemical Society Reviews*, *37* (6), 1087-1097, 2008.
11. Abreu, C. M. R.; Mendonca, P. V.; Serra, A. C.; Coelho, J. F. J.; Popov, A. V.; Guliashvili, T., Accelerated Ambient-Temperature ATRP of Methyl Acrylate in Alcohol-Water Solutions with a Mixed Transition-Metal Catalyst System, *Macromolecular Chemistry and Physics*, *213* (16), 1677-1687, 2012.
12. Cordeiro, R. A.; Rocha, N.; Mendes, J. P.; Matyjaszewski, K.; Guliashvili, T.; Serra, A. C.; Coelho, J. F. J., Synthesis of well-defined poly(2-(dimethylamino)ethyl methacrylate) under mild conditions and its co-polymers with cholesterol and PEG using Fe(0)/Cu(ii) based SARA ATRP, *Polymer Chemistry*, *4* (10), 3088-3097, 2013.
13. Mendonca, P. V.; Konkolewicz, D.; Averick, S. E.; Serra, A. C.; Popov, A. V.; Guliashvili, T.; Matyjaszewski, K.; Coelho, J. F. J., Synthesis of cationic poly((3-acrylamidopropyl)trimethylammonium chloride) by SARA ATRP in ecofriendly solvent mixtures, *Polymer Chemistry*, *5* (19), 5829-5836, 2014.
14. Mendonca, P. V.; Serra, A. C.; Coelho, J. F. J.; Popov, A. V.; Guliashvili, T., Ambient temperature rapid ATRP of methyl acrylate, methyl methacrylate and styrene in polar solvents with mixed transition metal catalyst system, *European Polymer Journal*, *47* (7), 1460-1466, 2011.

15. Rocha, N.; Mendonca, P. V.; Mendes, J. P.; Simoes, P. N.; Popov, A. V.; Guliashvili, T.; Serra, A. C.; Coelho, J. F. J., Facile Synthesis of Well-Defined Telechelic Alkyne-Terminated Polystyrene in Polar Media Using ATRP With Mixed Fe/Cu Transition Metal Catalyst, *Macromolecular Chemistry and Physics*, *214* (1), 76-84, 2013.
16. Abreu, C. M. R.; Mendonca, P. V.; Serra, A. C.; Popov, A. V.; Matyjaszewski, K.; Guliashvili, T.; Coelho, J. F. J., Inorganic Sulfites: Efficient Reducing Agents and Supplemental Activators for Atom Transfer Radical Polymerization, *ACS Macro Letters*, *1* (11), 1308-1311, 2012.
17. Abreu, C. M. R.; Serra, A. C.; Popov, A. V.; Matyjaszewski, K.; Guliashvili, T.; Coelho, J. F. J., Ambient temperature rapid SARA ATRP of acrylates and methacrylates in alcohol-water solutions mediated by a mixed sulfite/Cu(ii)Br2 catalytic system, *Polymer Chemistry*, *4* (23), 5629-5636, 2013.
18. Gois, J. R.; Konkolewic, D.; Popov, A. V.; Guliashvili, T.; Matyjaszewski, K.; Serra, A. C.; Coelho, J. F. J., Improvement of the control over SARA ATRP of 2-(diisopropylamino)ethyl methacrylate by slow and continuous addition of sodium dithionite, *Polymer Chemistry*, *5* (16), 4617-4626, 2014.
19. Gois, J. R.; Rocha, N.; Popov, A. V.; Guliashvili, T.; Matyjaszewski, K.; Serra, A. C.; Coelho, J. F. J., Synthesis of well-defined functionalized poly(2-(diisopropylamino)ethyl methacrylate) using ATRP with sodium dithionite as a SARA agent, *Polymer Chemistry*, *5* (12), 3919-3928, 2014.
20. Mendes, J. P.; Branco, F.; Abreu, C. M. R.; Mendonça, P. V.; Serra, A. C.; Popov, A. V.; Guliashvili, T.; Coelho, J. F. J., Sulfolane: an Efficient and Universal Solvent for Copper-Mediated Atom Transfer Radical (co)Polymerization of Acrylates, Methacrylates, Styrene, and Vinyl Chloride, *ACS Macro Letters*, *3* (9), 858-861, 2014.
21. Percec, V.; Guliashvili, T.; Ladislaw, J. S.; Wistrand, A.; Stjerndahl, A.; Sienkowska, M. J.; Monteiro, M. J.; Sahoo, S., Ultrafast Synthesis of Ultrahigh Molar Mass Polymers by Metal-Catalyzed Living Radical Polymerization of Acrylates, Methacrylates, and Vinyl Chloride Mediated by SET at 25 °C, *J. Am. Chem. Soc.*, *128* (43), 14156-14165, 2006.
22. Ye, J.; Narain, R., Water-Assisted Atom Transfer Radical Polymerization of N-Isopropylacrylamide: Nature of Solvent and Temperature, *J. Phys. Chem. B*, *113* (3), 676-681, 2009.
23. Prat, D.; Hayler, J.; Wells, A., A survey of solvent selection guides, *Green Chem.*, *16* (10), 4546-4551, 2014.
24. Konkolewicz, D.; Krys, P.; Góis, J. R.; Mendonça, P. V.; Zhong, M.; Wang, Y.; Gennaro, A.; Isse, A. A.; Fantin, M.; Matyjaszewski, K., Aqueous RDRP in the Presence of Cu0: The Exceptional Activity of CuI Confirms the SARA ATRP Mechanism, *Macromolecules*, *47* (2), 560-570, 2014.
25. Watanabe, K.; Yamagiwa, N.; Torisawa, Y., Cyclopentyl Methyl Ether as a New and Alternative Process Solvent, *Org. Process Res. Dev.*, *11* (2), 251-258, 2007.
26. Watanabe, K., The Toxicological Assessment of Cyclopentyl Methyl Ether (CPME) as a Green Solvent, *Molecules*, *18* (3), 3183-3194, 2013.
27. Antonucci, V.; Coleman, J.; Ferry, J. B.; Johnson, N.; Mathe, M.; Scott, J. P.; Xu, J., Toxicological Assessment of 2-Methyltetrahydrofuran and Cyclopentyl Methyl Ether in Support of Their Use in Pharmaceutical Chemical Process Development, *Org. Process Res. Dev.*, *15* (4), 939-941, 2011.
28. SAKAMOTO, S., Contribution of Cyclopentyl Methyl Ether (CPME) to Green Chemistry, *Chim. Oggi Chem.*, *31* (6), 24-27, 2013.

29. Kobayashi, S.; Kuroda, H.; Ohtsuka, Y.; Kashihara, T.; Masuyama, A.; Watanabe, K., Evaluation of cyclopentyl methyl ether (CPME) as a solvent for radical reactions, *Tetrahedron*, *69* (10), 2251-2259, 2013.
30. Zhang, Y.; Wang, Y.; Peng, C.-h.; Zhong, M.; Zhu, W.; Konkolewicz, D.; Matyjaszewski, K., Copper-Mediated CRP of Methyl Acrylate in the Presence of Metallic Copper: Effect of Ligand Structure on Reaction Kinetics, *Macromolecules*, *45* (1), 78-86, 2011.
31. Ciampolini, M.; Nardi, N., Five-Coordinated High-Spin Complexes of Bivalent Cobalt, Nickel, andCopper with Tris(2-dimethylaminoethyl)amine, *Inorganic Chemistry*, *5* (1), 41-44, 1966.
32. Britovsek, G. J. P.; England, J.; White, A. J. P., Non-heme Iron(II) Complexes Containing Tripodal Tetradentate Nitrogen Ligands and Their Application in Alkane Oxidation Catalysis, *Inorg. Chem.*, *44* (22), 8125-8134, 2005.
33. Catalao, F.; Gois, J. R.; Trino, A. S. M.; Serra, A. C.; Coelho, J. F. J., Facile synthesis of well-controlled poly(glycidyl methacrylate) and its block copolymers via SARA ATRP at room temperature, *Polym. Chem.*, *6* (10), 1875-1882, 2015.
34. Jakubowski, W.; Kirci-Denizli, B.; Gil, R. R.; Matyjaszewski, K., Polystyrene with improved chain-end functionality and higher molecular weight by ARGET ATRP, *Macromol. Chem. Phys.*, *209* (1), 32-39, 2008.
35. Jakubowski, W.; Matyjaszewski, K., Activators Regenerated by Electron Transfer for Atom-Transfer Radical Polymerization of (Meth)acrylates and Related Block Copolymers, *Angewandte Chemie*, *118* (27), 4594-4598, 2006.
36. Lutz, J. F.; Matyjaszewski, K., Nuclear magnetic resonance monitoring of chain-end functionality in the atom transfer radical polymerization of styrene, *J. Polym. Sci. Pol. Chem.*, *43* (4), 897-910, 2005.
37. Tom, J.; Hornby, B.; West, A.; Harrisson, S.; Perrier, S., Copper(0)-mediated living radical polymerization of styrene, *Polym. Chem.*, *1* (4), 420-422, 2010.
38. Matyjaszewski, K.; Xia, J. H., Atom transfer radical polymerization, *Chem. Rev.*, *101* (9), 2921-2990, 2001.
39. Han, T. L.; Kumar, R. N.; Rozman, H. D.; Noor, M. A. M., GMA grafted sago starch as a reactive component in ultra violet radiation curable coatings, *Carbohydr Polym.*, *54* (4), 509-516, 2003.
40. Hagit, A.; Soenke, B.; Johannes, B.; Shlomo, M., Synthesis and Characterization of Dual Modality (CT/MRI) Core−Shell Microparticles for Embolization Purposes, *Biomacromolecules*, *11* (6), 1600-1607, 2010.
41. Papakonstantinou, A. E.; Eliades, T.; Cellesi, F.; Watts, D. C.; Silikas, N., Evaluation of UDMA's potential as a substitute for Bis-GMA in orthodontic adhesives, *Dent. Mater.*, *29* (8), 898-905, 2013.

Chapter 7

Miniemulsion SARA ATRP of butyl acrylate and styrene mediated by sodium dithionite

The results of this paper were submitted for publication.

7.1 Abstract

The SARA ATRP of butyl acrylate (*n*BA) and St using miniemulsion is reported for the first time. The polymerization was carried out in the presence of $CuBr_2$ based catalytic systems using EHA_6TREN or BPMODA* as ligands and sodium dithionite ($Na_2S_2O_4$) as SARA agent. The kinetic data revealed a controlled polymerization for both monomers, with a stringent control over the molecular weight distribution ($Đ \leq$ 1.2). The reaction conditions were optimized to afford the control over the polymerization and to increase the final monomer conversion. The presence of active chain end was confirmed by ^1H NMR spectroscopy and self-chain extension reactions. The results presented in this chapter demonstrate the possibility of using the SARA ATRP with $Na_2S_2O_4$ in miniemulsion conditions in order to obtain well-defined P*n*BA and PS with narrow molecular weight distributions.

7.2 Introduction

RDRP methods have provided a very relevant tool box for the synthesis of polymers with controlled architecture, morphology, topology, chain-end functionalities and narrow molecular distributions.[1] Among the different RDRP methods, ATRP is the most used to afford a wide range of (co)polymers with different functionalities.[2-5] This method is based on the fast equilibrium between dormant species and active radical species mediated by a transition-metal complex.[6] It has been a long time challenge for researchers working on ATRP to develop strategies to turn the process viable at industrial scale. For this purpose two major subjects have been intensively studied: the decrease in the concentration of metal catalyst complex and the use of environmental friendly solvents. The former was achieved by developing several ATRP variations, such as: activators regenerated by electron transfer (ARGET)[7-9], initiators for continuous activator regeneration (ICAR)[10], supplementary activator and reducing agent (SARA) ATRP[6, 11-21], electrochemically mediated ATRP (*e*ATRP)[22-24], and photochemically mediated ATRP[25-27]. Our research group has introduced the use of inorganic sulphites, in particular sodium dithionite ($Na_2S_2O_4$) as a SARA agent.[16] By this way it is sufficient to use very little amounts of soluble copper catalyst to

achieve controlled polymerizations.[16, 28] The synthesis of (co)polymers based on poly(2-(diisopropylamino)ethyl methacrylate) (PDPA) through SARA ATRP with Na_2S_2O4 in isopropanol/water mixtures was recently proposed.[29] It was found that the slow and continuous addition of the inorganic sulphite is crucial for the control over the polymerization.[30]

Another viable approach is the development of technologies involving the use of ATRP in aqueous dispersed media to reduce and/or replace harmful volatile organic compounds (VOC)s in the reaction medium.[31] Water is the most interesting solvent for industrial applications.[31] It is environmentally friendly, has high thermal capacity and it is inexpensive.[31-32] In addition, water ensures a good heat removal (particularity relevant for high exothermic polymerization) during the polymerization and allows the preparation of polymers with high molecular weight, while maintaining a low medium viscosity.[33] The success of the ATRP process using heterogeneous medium relies on the compliance of several critical issues, such as: the catalyst complex should remain in the monomer phase[34] to control the polymerization; the complex metal/ligand must be stable; and the reduction of Cu(II) to Cu(I) should be fast and efficient.

Aqueous dispersed ATRP systems were successfully carried out in suspension, dispersion, precipitation, emulsion, microemulsion, inverse miniemulsion, and miniemulsion.[35] Using the latter, St, *n*BA, MMA, vinyl acetate, vinyl 2-ethylhexanoate and numerous copolymerizations were successfully carried out by ATRP, using different type of ligands (tris(2-bis(3-(2-ethylhexoxy)-3-oxopropyl)aminoethyl) amine (EHA_6TREN), 4,4'-Di-5-nonyl-2,2'-bipyridine (dNbpy), 4,4',4''-tris(5-nonyl)-2,2':6',2''-terpyridine (tNtpy) or N,N-bis(2-pyridylmethyl)octadecylamine (BPMODA)), specific surfactants (*e.g*. Brij 98, sodium dodecyl sulfate (SDS)[36] or reactive surfactants[37]) and initiators (VA-044 or ethyl α-bromoisobutyrate (EBiB)).[34,38] Regarding reducing agents, the most common one reported is ascorbic acid (AA) that efficiently regenerate Cu (I) species from Cu(II).[39-42] Recently, Matyjaszewski and co-workers reported the synthesis of high molecular weight P*n*BA ($M_n^{SEC} > 700\ 000$) with relatively low $Đ$ ($Đ \sim 1.39$) using a more active ligand (N′,N″-dioctadecyl-N′,N″-bis[2-(4-methoxy-3,5dimethyl) pyridylmethyl] ethane-1,2-diamine (DOD-BPED*)), ascorbic acid and only 50 ppm of $CuBr_2$.[42]

Herein, it is reported for the first time the miniemulsion process of SARA ATRP of *n*BA and styrene using $Na_2S_2O_4$. For comparison purposes, AA was also used under the same reaction conditions.

7.3 Experimental Section

7.3.1 Materials

*n*BA (99 % stabilized; Acros) and St (+ 99 %; Sigma-Aldrich) were passed over a basic alumina column before use to remove the radical inhibitors. Copper(II) bromide ($CuBr_2$) (+ 99 % extra pure, anhydrous; Acros), iron powder (Fe(0)) (99 %, ~ 70 mesh, Acros), deuterated chloroform ($CDCl_3$) (+ 1 % tetramethylsilane (TMS); Euriso-top), ethyl 2-bromoisobutyrate (EBiB) (98 %; Aldrich), *tris*(2-aminoethyl)amine (TREN) (96 %; Sigma-Aldrich), polystyrene (PSt) standards (Polymer Laboratories), $Na_2S_2O_4$ (>87%; Merck), $NaHCO_3$ (Fisher Chemical), sodium hydroxide (Fisher Chemical), cetyltrimethylammonium bromide (PTC) (Sigma-Aldrich), 6-o-palmitoyl-l-ascorbic acid (AA_{org}) (99%, Sigma-Aldrich), (n-hexadecyl)tri-n-butylphosphonium bromide (98%; Alfa Aesar), Copper(II) 2-ethylhexanoate (Alfa Aesar) 1-octadecylamine (98%; Alfa Aesar), 2-cloromethyl-3,5-dimethyl-4-methoxypyridine, HCl (98%; Alfa Aesar), AA (Aldrich), Brij 98 (M_n ~1150 , Aldrich), sodium dodecyl sulfate (SDS) (+99%, Sigma-Aldrich), hexadecane (Merck), 2-ethylhexylacrylate (98%, Aldrich), tetrahydrofuran (THF) (+99.8%, Sigma-Aldrich), dimethylformamide (DMF) (+99.8%, Sigma-Aldrich) and toluene (Labsolve) were used as received.

For size exclusion chromatography (SEC) analysis DMF (HPLC grade; Panreac) and THF (HPLC grade; Panreac) were filtered (0.2 μm filter) under reduced pressure before use.

EHA_6TREN[43] and BPMODA*[44] were synthesized according to the procedures described in the literature.

7.3.2 Techniques

The chromatographic parameters of P*n*BA samples were determined using a size exclusion chromatography (SEC) setup from Viscotek (Viscotek TDAmax) with a refractive index (RI) detector (Knauer K-2301). The column set consisted of a PL 10-

μL guard column (50 x 7.5 mm^2), followed by two MIXED-B PL columns (300 x 7.5mm^2, 10 μL). The HPLC pump was set with a flow rate of 1 mL/min and the analyses were carried out at 60 ºC using an Elder CH-150 heater. The eluent was DMF, containing 0.3% of LiBr. Before injection (100 μL), the samples were filtered through a polytetrafluoroethylene (PTFE) membrane with 0.2 μm pore size. The system was calibrated with PMMA standards. The M_n^{SEC} and $Đ$ of synthesized polymers were determined by conventional calibration using OmniSEC software version: 4.6.1.354.

The chromatography parameters of PS samples were determined using SEC setup from Viscotek (Viscotek TDAmax) equipped with a differential viscometer (DV) and right-angle laser-light scattering (RALLS, Viscotek), low-angle laser-light scattering (LALLS, Viscotek) and refractive index (RI) detectors. The column set consisted of a PL 10 mm guard column (50 × 7.5 mm^2) followed by one Viscotek T200 column (6 μm), one MIXED-E PLgel column (3 μm) and one MIXED-C PLgel column (5 μm). A dual piston pump was set with a flow rate of 1 mL/min. The eluent (THF) was previously filtered through a 0.2 μm filter. The system was also equipped with an on-line degasser. The tests were performed at 30 ºC using an Elder CH-150 heater. Before the injection (100 μL), the samples were filtered through a polytetrafluoroethylene (PTFE) membrane with 0.2 μm pore. The system was calibrated with narrow PS standards.

400 MHz ^{1}H NMR spectra of the the P*n*BA and PS samples were recorded on a Bruker Avance III 400 MHz spectrometer, with a 5-mm TIX triple resonance detection probe, in $CDCl_3$ with TMS as an internal standard. The integrations polymer peaks were determined using MestRenova software version: 6.0.2-5475.

7.3.3 Procedures

7.3.3.1 Typical procedure for SARA ATRP of *n*BA in miniemulsion catalyzed by $[Na_2S_2O_4]_0/[CuBr_2]_0/[BPMODA^*]_0$ = 0.2/0.4/0.4 (DP = 200)

The organic phase was prepared by dissolving $CuBr_2$ (10.46 mg, 0.05 mmol) and BPMODA* (26.59 mg, 0.05 mmol) in *n*BA (3.36 mL, 23 mmol) over 30 min at 60 ºC. The solution was cooled to room temperature and EBiB (17.2 μL, 0.12 mmol) and hexadecane (139.7 μl, 0.5 mmol) were added. In an ice bath, 12 mL of an aqueous solution of Brij 98 (5 mM) was mixed with the organic phase and subject to

sonication (QSonic Sonicator with a cycle at 70% during 1 min). The stable miniemulsion was introduced into a Schlenk tube reactor, that was sealed by using a rubber septum, purged with nitrogen for 30 min and placed in an oil bath at 80 ºC with stirring (700 rpm). 408 µL of an aqueous stock solution of $Na_2S_2O_4$ (50 mM) and $NaHCO_3$ (14 mM) (previously bubbled with nitrogen) were injected into the miniemulsion using a syringe pump at a feed rate of 0.233 mL/min to start the polymerization. During the polymerization, samples were collected by using an airtight syringe. The samples were dried in a vacuum oven to determine the monomer conversion gravimetrically, and then dissolved in DMF for SEC analysis, to determine the average-number molecular weight (M_n^{SEC}) and dispersity ($Đ$) of the polymers.

7.3.3.2 Typical procedure for SARA ATRP of St in miniemulsion catalyzed by $[Na_2S_2O_4]_0/[CuBr_2]_0/[BPMODA^*]_0$ = 0.2/0.4/0.4 (DP = 200)

The organic phase was prepared by dissolving $CuBr_2$ (12.87 mg, 0.06 mmol) and BPMODA* (32.72 mg, 0.06 mmol) in St (3.30 mL, 0.029 mol) over 30 min at 60 ºC. The solution was cooled down to room temperature and EBiB (21.1 µL, 0.14 mmol) and hexadecane (139.7 µl, 0.5 mmol) were added. In an ice bath 12 mL of an aqueous solution of Brij 98 (5 mM) was mixed with the organic phase and subject to sonication (QSonic Sonicator with a cycle at 70% during 1 min). The stable miniemulsion was introduced into a Schlenk tube reactor, that was sealed by using a rubber septum, purged with nitrogen for 30 min and placed in a oil bath at 80 ºC with stirring (700 rpm). 502 µL of an aqueous stock solution of $Na_2S_2O_4$ (57 mM) and $NaHCO_3$ (14 mM) (previously bubbled with nitrogen) were injected into the miniemulsion using a syringe pump at a feed rate of 0.233 mL/min to start the polymerization. During the polymerization, different samples were collected by using an airtight syringe. The samples were dried in a vacuum oven to determine the monomer conversion gravimetrically, and then dissolved in THF for SEC analysis, to determine the average-number molecular weight (M_n^{SEC}) and dispersity ($Đ$) of the polymers.

7.3.3.3 Typical procedure for chain extension of P*n*BA- Br

The P*n*BA-Br macroinitiator obtained by SARA ATRP in miniemulsion (M_n^{SEC} = 3.80 x 10^3; $Đ$=1.10) (98.8 mg, 0.03 mmol) was dried, dissolved in 2.24 mL of CPME at room temperature and then added to the *n*BA (2.24 mL, 15.6 mmol) in a Schlenk tube reactor. Cu(0) wire (5 cm) and a mixture of $CuBr_2$ (2.9 mg, 0.01 mmol), Me_6TREN (6.0 mg, 0.03 mmol) and DMF (200 μL previously bubbled with nitrogen) were added to the reactor that was sealed and frozen in liquid nitrogen. The Schlenk tube reactor containing the reaction mixture was deoxygenated with four freeze-vacuum-thaw cycles, purged with nitrogen and placed in a water bath at 30 ºC with stirring (700 rpm). The reaction was stopped after 24h and the mixture was analyzed by SEC.

7.3.3.4 Typical procedure for chain extension of PS–Br

A PS-Br macroinitiator obtained from a typical ATRP miniemulsion was dried, dissolved in THF and precipitated in methanol. The polymer was then dissolved in THF, filtered through a sand/alumina column to remove traces of the copper catalyst, precipitated again in methanol and dried under vaccum.

The PS-Br macroinitiator (M_n^{SEC} = 10.0 x10^3; $Đ$ = 1.03) (165 mg, 0.02 mmol) was dissolved in DMF (1.65 mL previously bubbled with nitrogen for about 15 min) at 40 ºC in a Schlenk tube reactor. The St (1.65 mL, 14.4 mmol), $CuBr_2$ (0.9 mg, 0.004 mmol) Me_6TREN (10.4 mg, 0.045 mmol) and Fe(0) (2.3 mg, 0.04 mmol) were added to the reactor that was sealed and frozen in liquid nitrogen. The Schlenk tube reactor containing the reaction mixture was deoxygenated with four freeze-vacuum-thaw cycles, purged with nitrogen and placed in a oil bath at 70 ºC with stirring (700 rpm). The reaction was stopped after 48h and the mixture was analyzed by SEC.

7.4 Results and discussion

Sodium dithionite is an inexpensive and environmentally friendly compound that was recently reported by our research group as an efficient SARA ATRP agent for the polymerization of different monomers families in several solvents, such as: DMSO,[16] alcohol/water mixtures[28-30] and pure water.[45] $Na_2S_2O_4$ acts as a powerful reducing agent for X-Cu^{II}/L species and also as a supplemental activator to generate radicals from halogen chain ends. It was found that in homogeneous systems, $Na_2S_2O_4$ is able to mediate the polymerization up to high monomer conversions, while maintaining a stringent control over the process.[16, 28, 30, 45] In this contribution, this promising catalytic system is studied in the miniemulsion polymerization of *n*BA and St.

7.4.1 Influence of ligand structure

The structure of the ligand plays an important role in the miniemulsion ATRP.[46] The polymerization occurs in the organic phase, which requires the ligand to be sufficiently hydrophobic to avoid the excessive partitioning of copper species into the aqueous phase. BPMODA is the most reported ligand in miniemulsion-based ATRP.[47] It was found that the addition of electron donating groups to the structure of BPMODA (to form BPMODA*) (Figure 7.1) increases the K_{ATRP} value from 10^{-7} up to 10^{-5}, and allows to conduct a controlled heterogeneous polymerization under reduced concentrations of copper catalyst.[44]

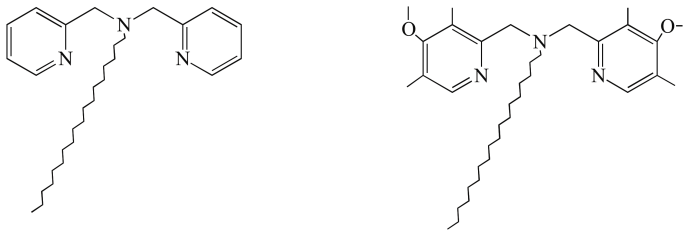

BPMODA **BPMODA***

Figure 7.1 Structure of bis(2-pyridylmethyl) octadecylamine (BPMODA) and bis[2-(4-methoxy-3,5-dimethyl)pyridylmethyl]octadecylamine (BPMODA*) ligands.

Matyjaszewski's research group[48] reported the synthesis of the EHA_6TREN ligand, a nitrogen-based tetradentate ligand synthesized from the Michael addition reaction of 2-ethylhexylacrylate with tris(2-aminoethyl) amine (TREN), for the homopolymerization of *n*BA in a miniemulsion system using simultaneous reverse

and normal initiation (SRNI) ATRP processes. This ligand was also employed in reverse ATRP miniemulsion systems.[48-50] Both ligands have a good solubility in the *n*BA and are capable of bringling the copper catalyst to the organic phase. In this work, miniemulsion polymerizations of *n*BA were carried out using both BPMODA* and EHA_6TREN ligands and the kinetic results are shown in Figure 7.2. The reaction components and concentrations were set according to similar studies reported in the literature.[44] Brij98 is a non-ionic surfactant and it was chosen to avoid electrostatic repulsion with the charged species of $Na_2S_2O_4$ dissolution products (dithionite ions).

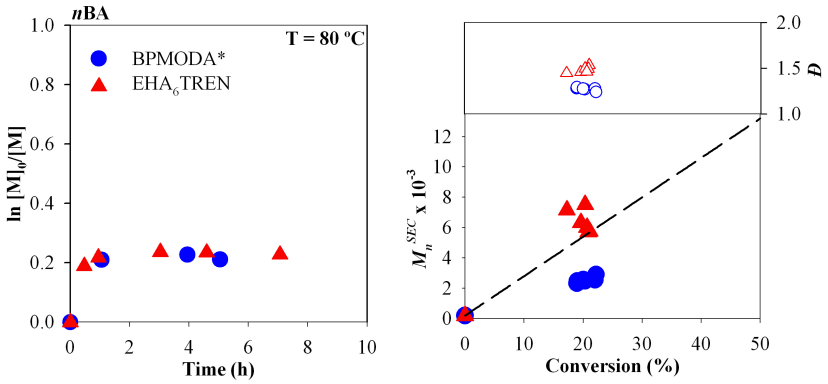

Figure 7.2 Kinetic plots of conversion and $\ln[M]_0/[M]$ *vs*. time (left) and plot of number-average molecular weights (M_n^{SEC}) and $Đ$ *vs*. conversion (right) for ATRP of *n*BA in miniemulsion catalyzed by $Na_2S_2O_4$ in the presence of EHA_6TREN (triangle red symbols) or BPMODA* (round blue symbols) at 80 °C. Conditions: $[Brij98]_0/[Hexadecane]_0$ = 2.3/3.6 % *vs* *n*BA; $[nBA]_0/[EBiB]_0/[CuBr_2]_0/[ligand]/[Na_2S_2O_4]_0$ = 200/1/0.4/0.4/0.2 (mol).

As can be seen by the kinetic results of these first experiments (Figure 7.2), regardless the ligand used (BPMODA* or EHA_6TREN), the controlled polymerization of *n*BA via SARA ATRP using $Na_2S_2O_4$ in miniemulsion can be obtained. Further proof of the control over the process is shown by the low $Đ$ values obtained throughout the polymerization. In both cases after 1 h of reaction, the monomer reaches 20% of conversion with M_n values closed to the theoretical values, and $Đ$ values of 1.28 and 1.45 for BPMODA* and EHA_6TREN, respectively. For comparison the ATRP miniemulsion using AA and BPMODA* reveled the same data as reported in the literature (Figure 7.3).[44] The major difference between the ATRP miniemulsion mediated by AA and $Na_2S_2O_4$, when BPMODA* is used, concerns the rate of polymerization and monomer conversion which are lower in the presence of $Na_2S_2O_4$.

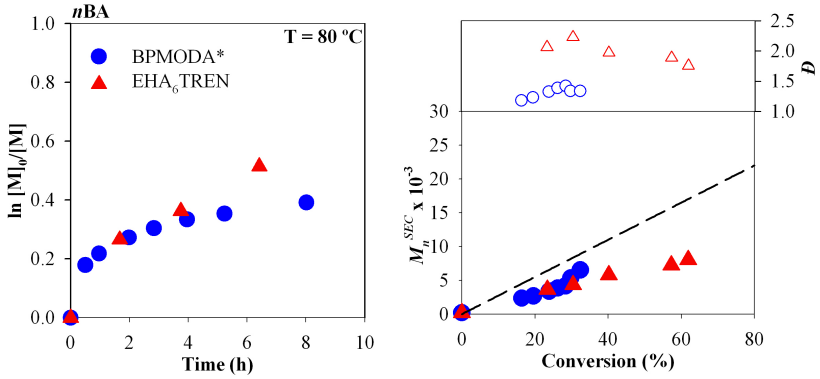

Figure 7.3 Kinetic plots of conversion and ln[M]$_0$/[M] *vs*. time (left) and plot of number-average molecular weights (M_n^{SEC}) and *Đ vs*. conversion (right) for ATRP of *n*BA in miniemulsion catalyzed by AA in the presence of EHA_6TREN (triangle red symbols) or BPMODA* (round blue symbols) at 80 °C. Conditions: [Brij*98*]$_0$/[Hexadecane]$_0$=2.3/3.6 % *vs* *n*BA; [*n*BA]$_0$/[EBiB]$_0$/[AA]/[$CuBr_2$]/ [EHA_6TREN]$_0$=200/1/0.2/0.4/0.4 (mol) and [*n*BA]$_0$/[EBiB]$_0$/[AA]/[$CuBr_2$]/[BPMODA*]$_0$ = 200/1/0.2/0.4/0.4 (mol).

7.4.2 Effect of the deactivator concentration

For the success of the ATRP miniemulsion it is mandatory the presence of both radical activator (Cu^I species) and deactivator (Cu^{II} species) in the organic phase where the polymerization occurs. For this, the choice of a suitable ligand and the concentration of the catalytic complex in the organic phase is crucial to ensure that the copper complexs does not diffuse out of the organic phase.

In order to understand the effect of the initial deactivator concentration, and minimize the possible loss of the Cu^{II} species to the aqueous phase, two similar reactions were performed using different molar ratios of the $CuBr_2$/ligand complex to the initiator (0.4 and 1.0). The kinetic results of the homopolymerization of *n*BA (Figure 7.4), suggest that an increase of the deactivator ratio (while maintaining the SARA agent concentration) has no direct impact in the polymerization rate but increases the monomer conversion up to 32% and narrows down the MW distribution (*Đ* ~ 1.15). An important observation is the extremely fast polymerization rate at the beginning of the polymerization resulting in P*n*BA with higher *Đ (Đ~1.4)*, followed by a plateau region in which the polymerization conversion remains almost constant, but *Đ* was reduced up to 1.15. Such result might be related to an inefficient $S_2O_4^{2-}$ diffusion inside the organic phase.

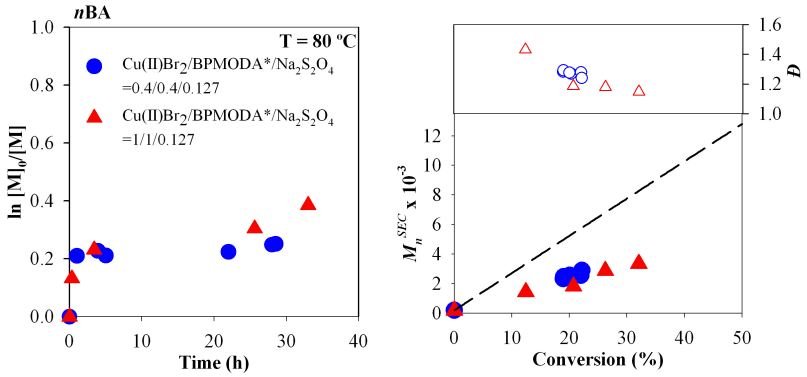

Figure 7.4 Kinetic plots of conversion and $\ln[M]_0/[M]$ *vs*. time (left) and plot of number-average molecular weights (M_n^{SEC}) and *Đ* *vs*. conversion (right) for ATRP of *n*BA in miniemulsion catalysed by $Na_2S_2O_4$/$CuBr_2$/BPMODA* with $CuBr_2$/BPMODA* = 0.4/0.4 (round blue symbols) or 1/1 (triangle red symbols) at 80 °C. Conditions: $[Brij98]_0/[Hexadecane]_0$ = 2.3/3.6 % *vs* *n*BA; $[nBA]_0/[EBiB]_0/[CuBr_2]/[BPMODA^*]_0/[Na_2S_2O_4]$ = 200/1/1/1/0.127 (mol) or $[nBA]_0/[EBiB]_0/[CuBr_2]_0/[BPMODA^*]_0/[Na_2S_2O_4]_0$ = 200/1/0.4/0.4/0.127 (mol).

7.4.3 Effect of $Na_2S_2O_4$ concentration

The $SO_2^{-\bullet}$ radical anion species resulting from dithionite ion dissolution are a powerful reducing agent. An excessive amount of the radical anions at the beginning of the reaction may increase the termination reactions associated with the high rate of activator (re)generation[30] of Cu^IBr/L. This hypothesis was confirmed by carrying out the polymerizations using a continuous feeding of $Na_2S_2O_4$ that revealed the possibility of enhancing the polymerization rate and diminish the *Đ* at the same time.[30] In this sense, the concentration and the molar ratio of the SARA agent are very important factors to conduct a controlled polymerization. Therefore, in an attempt to optimize the miniemulsion polymerization of *n*BA, leading to the reduction of the metal catalyst concentration, the amounts of $CuBr_2$ and $Na_2S_2O_4$ were reduced significantly (Figure 7.5). The polymerizations followed the above described general procedures and the ratios of metal catalyst/SARA agent were adjusted accordingly.

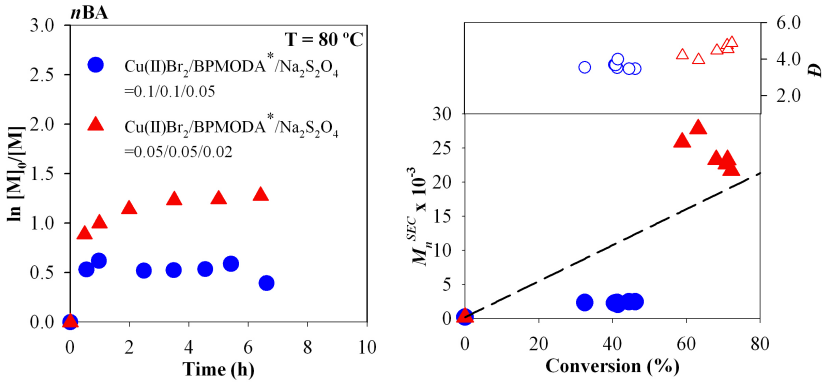

Figure 7.5 Kinetic plots of conversion and ln[M]$_0$/[M] *vs*. time (left) and plot of number-average molecular weights (M_n^{SEC}) and *Đ vs*. conversion (right) for ATRP of *n*-BA in miniemulsion catalyzed by $Na_2S_2O_4$/$CuBr_2$/BPMODA* = 0.05/0.1/0.1 (blue symbols) or 0.02/0.05/0.05 (red symbols) at 80 °C. Conditions: [Brij*98*]$_0$/[Hexadecane]$_0$ = 2.3/3.6 % *vs n*-BA; [*n*-BA]$_0$/ [EBiB]$_0$/ [$CuBr_2$]/ [BPMODA*]$_0$/ [$Na_2S_2O_4$] = 200/1/0.1/0.1/0.05 (mol) or [*n*-BA]$_0$/ [EBiB]$_0$ /[$CuBr_2$]$_0$/ [BPMODA*]$_0$/ [$Na_2S_2O_4$]$_0$/ = 200/1/0.05/0.05/0.02 (mol).

The kinetic results presented in Figure 7.5 reveal that a reduction of the molar ratio $CuBr_2/Na_2S_2O_4$ to 0.1/0.05 and 0.05/0.02 respectively leads to uncontrolled polymerizations with very high *Đ* values (*Đ* < 2.0) which might be associated with the loss of the catalytic complex to the aqueous phase.

As mentioned above, the initial concentration of the SARA agent is a crucial factor to mediate the ATRP polymerization. It should provide a fast rate of activator re(generator) while the concentrations of radicals should remain low to avoid the loss of the end functionality through termination[30]. In an attempt to increase the *n*BA conversion, the initial molar ratio of [EBiB]/[$Na_2S_2O_4$] was varied from 1/0.127 to 1/0.244. The aqueous solution of $Na_2S_2O_4$ (1% w/w) was totally added in one step, under N_2 atmosphere, immediately after the homogenization of the reaction mixture.

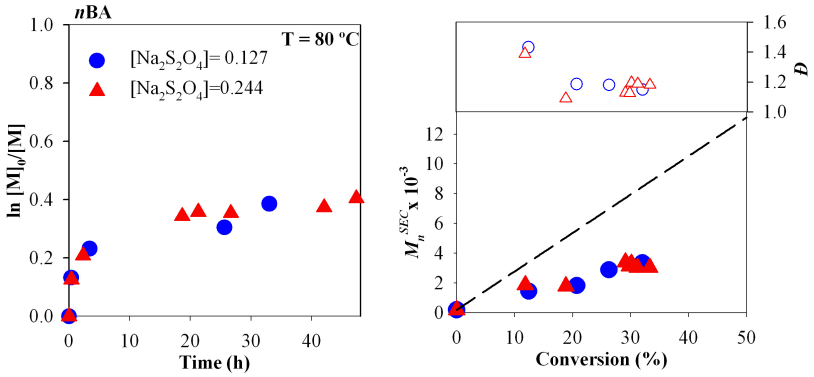

Figure 7.6 Kinetic plots of conversion and ln[M]$_0$/[M] *vs*. time (left) and plot of number-average molecular weights (M_n^{SEC}) and *Đ vs*. conversion (right) for ATRP of *n*BA in miniemulsion catalysed by $Na_2S_2O_4$/$CuBr_2$/BPMODA* with [$Na_2S_2O_4$]= 0.127 (blue symbols) or [$Na_2S_2O_4$]= 0.244 (red symbols) at 80 °C. Conditions: [Brij*98*]$_0$/[Hexadecane]$_0$ = 2.3/3.6 % *vs* *n*BA; [*n*BA]$_0$/[EBiB]$_0$/[$CuBr_2$]$_0$/[BPMODA*]$_0$/[$Na_2S_2O_4$]$_0$/ = 200/1/1/1/(0.127 or 0.244) (mol).

The kinetic results presented in Figure 7.6, suggest no relevant variations on the polymerization rate, monomer conversion and molecular parameters of the resultant polymers. Despite the low *Đ* values that indicate a controlled reaction, the maximum monomer conversion achieved remains around 33 %. A similar result was obtained when the $Na_2S_2O_4$ solution was successively added during the course of the polymerization, in both step-by-step injection (Figure 7.7) or continuous feeding (Figure 7.8).

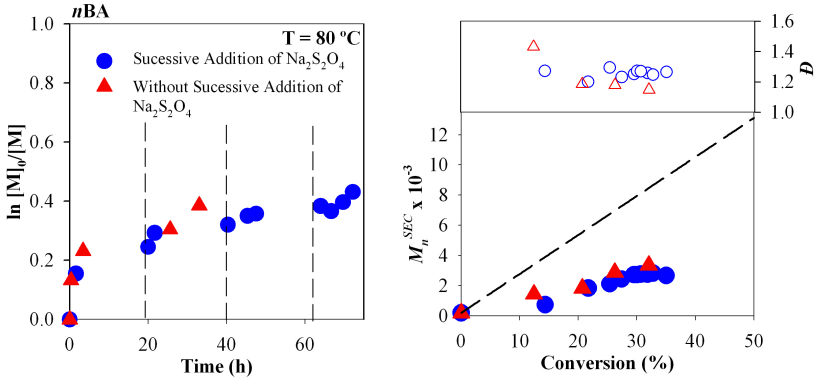

Figure 7.7 Kinetic plots of conversion and $\ln[M]_0/[M]$ *vs*. time (left) and plot of number-average molecular weights (M_n^{SEC}) and *Đ* (M_w/M_n) *vs*. conversion (right) for ATRP of *n*BA in miniemulsion catalyzed by $Na_2S_2O_4/CuBr_2/BPMODA^*$ = 0.12/1/1 at 80 °C with successive addition of $Na_2S_2O_4$ (blue symbols). Conditions: $[Brij98]_0/[Hexadecane]_0$ = 2.3/3.6 % vs *n*BA; $[nBA]_0/[EBiB]_0/[CuBr_2]_0/[BPMODA^*]_0/[Na_2S_2O_4]_0$ = 200/1/1/1/ 0.12 (mol).

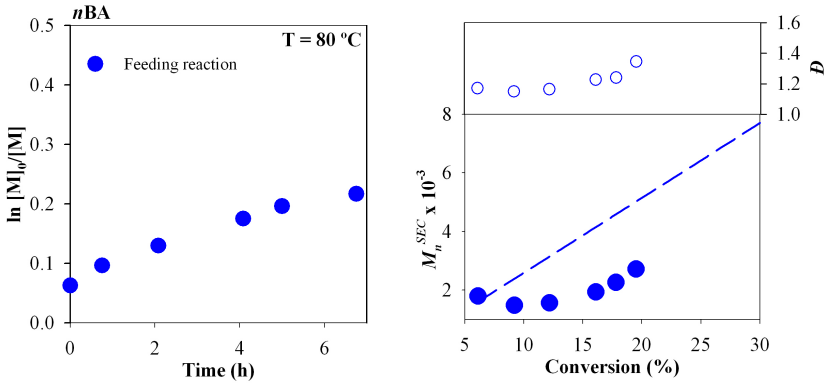

Figure 7.8 Kinetic plots of conversion and $\ln[M]_0/[M]$ *vs*. time (left) and plot of number-average molecular weights (M_n^{SEC}) and *Đ vs*. conversion (right) for ATRP of *n*BA in miniemulsion catalyzed by $Na_2S_2O_4$ at 80 °C. Conditions: $[Brij98]_0/[Hexadecane]_0$ = 2.3/3.6 % vs *n*BA; $[nBA]_0/[EBiB]_0/[CuBr_2]_0/[BPMODA^*]_0/[Na_2S_2O_4]_0$ = 200/1/0.4/0.4/0.2(mol). 400 µl of an aqueous solution of $Na_2S_2O_4$ (57 mM) was injected into the reaction medium using a syringe pump at a rate of 1 $\mu L.min^{-1}$.

In fact, in the feeding reaction, the addition of excessive amounts of $Na_2S_2O_4$ causes emulsion destabilization and phase separation which leads to uncontrolled polymerization, as evidenced by the increase of *Đ* (Figure 7.8). These results suggest that the low monomer conversion obtained is neither directly associated with the initial concentration of the SARA agent nor the addition method.

A summary of the experiments performed to optimize the miniemulsion ATRP of *n*Ba is shown in Table 7.1.

The main conclusion of the data in Table 7.1 is that miniemulsion SARA ATRP of *n*Ba in the presence of $Na_2S_2O_4$, can yield well controlled polymers (with very low *Đ* values) but is mostly limited to low monomer conversions. Similar results were observed for different DP, 50, 100 and 200 respectively (Table 7.1, entry 21-23).

Table 7.1 Kinetic data of miniemulsion polymerization of *n*BA with [*n*BA]/[EBiB] = DP/1, $[Brij98]_0/[Hexadecane]_0$ = 2.3/3.6 % *vs n*BA at T = 80 ºC.

Entry	DP	$Na_2S_2O_4$	AA	BPMODA*	EHA_6TREN	$CuBr_2$	Time (h)	Conv. (%)	$M_n^{th}x10^3$	M_n^{SEC} $x10^3$	*Đ*
1	200	-	0.06	0.8	-	0.4	6.2	32	8,28	6,42	1.19
2	200	-	0.06	-	0.4	0.2	7.2	43	11,0	7,27	1.68
3	200	-	0.06	-	0.4	0.4	6.4	40	5,82	10,77	1.97
4	200	-	0.03	0.4	-	0.4	6.4	26	6,73	5,31	1.50
5	200	-	0.13	0.3	-	0.3	6.3	33	5,70	4,60	1.29
6	200	-	0.2	0.4	-	0.4	5.2	30	7,91	5,33	1.34
7	200	0.2	-	-	0.4	0.4	7.0	20	5,34	7,52	1.50
8	200	0.13	-	-	0.4	0.7	6.4	46	10,43	8,12	1.78
9	200	0.2	-	0.4	-	0.4	5.1	19	4.84	2.47	1.29
10	200	0.13	-	1	-	1	3.4	21	5,39	1,83	1.19
11	200	0.24	-	1	-	1	2.3	19	4,79	1,79	1.09
12	200	0.27	-	1	-	1	5.4	17	3,73	1,86	1.22
13	200	0.21	-	0.8	-	0.8	5.0	22	4,45	2,51	1.17
14	200	0.24	-	1	-	1	2.1	21	2,82	1,55	1.44
15	200	0.12	-	0.9	-	0.9	20	22	5,09	1,84	1.20
16	200	0.2	-	0.4	-	0.4	7.6	19	4,97	2,41	1.17
17	200	0.13	-	0.3	-	0.3	7.2	33	5,68	5,06	1.27
18	200	0.05	-	0.1	-	0.1	5.6	44	11,83	2,46	3.46
19	200	0.02	-	0.05	-	0.05	5.0	71	17,37	23,29	4.54
20	200	0.22	-	0.4	-	0.4	6.8	16	4,30	1,06	1.47
21	200	0.2	-	1	-	1	5.0	22	4.5	2.5	1.17
22	100	0.2	-	1	-	1	2.1	21	2.8	1.6	1.26
23	50	0.2	-	1	-	1	2.2	20	1.2	2.1	1.27

In an attempt to increase the monomer conversion, which might be associated with the concentration of $S_2O_4^{2-}$ and $SO_2^{\bullet-}$ species inside the droplets, different reaction additives were studied: a phase-transfer catalyst (PTC)[51] (Figure 7.9); the use of copper(II) 2-ethylhexanoate as deactivator in combination with the use of additional solvents (chloroform or toluene) to increase the solubility of the catalytic system in the organic phase (Table 7.2); a common conventional anionic surfactant (SDS) typically used in emulsion (Figure 7.10).

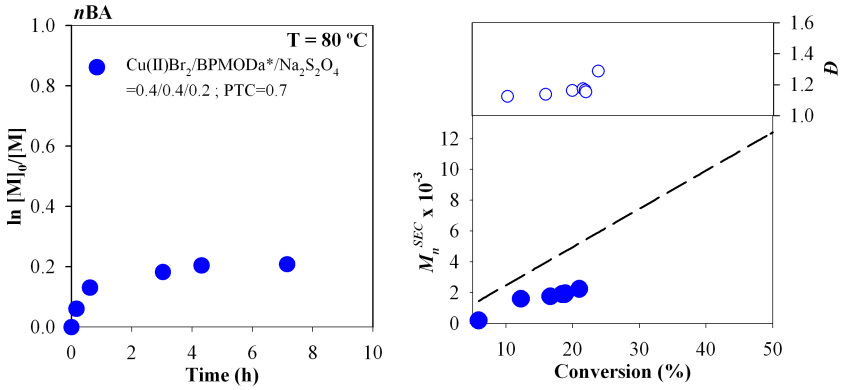

Figure 7.9 Kinetic plots of conversion and $\ln[M]_0/[M]$ *vs*. time (left) and plot of number-average molecular weights (M_n^{SEC}) and *Đ vs*. conversion (right) for ATRP of *n*BA in miniemulsion catalyzed by $Na_2S_2O_4$ at 80 °C in the presence of PTC. Conditions: $[Brij98]_0/[Hexadecane]_0$ = 2.3/3.6 % *vs* *n*BA; $[nBA]_0/[EBiB]_0/[CuBr_2]_0/[BPMODA^*]_0/[Na_2S_2O_4]_0/[PTC]_0$ = 200/1/0.4/0.4/0.2 /0.7 (mol).

Table 7.2 Kinetic data of the influence of copper(II) 2-ethylhexanoate chloroform and toluene in miniemulsion polymerization of *Ba* with $[nBA]_0/[EBiB]_0$=200/1; $[Brij98]_0/[Hexadecane]_0$ = 2.3/3.6 % *vs nBA* at T=80 ºC.

Entry	$Na_2S_2O_4$ (molar)	BPMODA* (molar)	Deactivator (molar)	Time (h)	Conv. (%)	$M_n^{th} x10^3$	$M_n^{SEC} x10^3$	Đ
1	0.2	0.4	0.4[a]	2	79	20.4	>50.0	-[b]
2[d]	0.2	0.4	0.4[c]	18	14	3.6	1.8	1.07
3[e]	0.2	0.4	0.4[c]	18	24	6.2	4.0	1.31

[a] Copper(II) 2-ethylhexanoate ; [b] Out of limits of calibration curve; [c]$CuBr_2$; [d] Chloroform and [e] toluene as additional solvent to increase the solubility

The results suggest that none of the systems were able to increase monomer conversion but in all cases a controlled polymerization is observed.

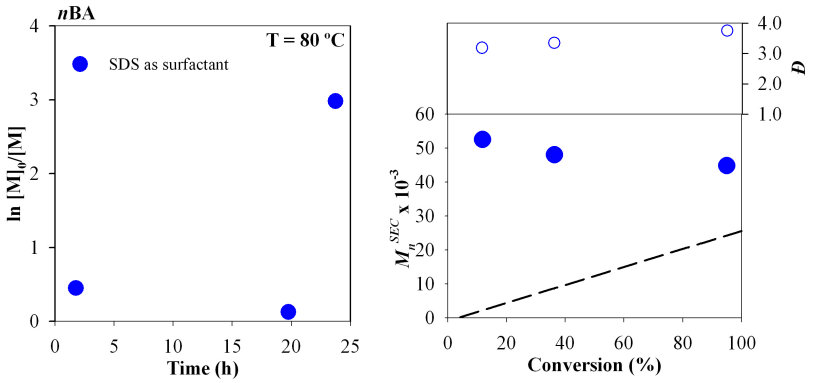

Figure 7.10 Kinetic plots of conversion and ln[M]$_0$/[M] *vs*. time (left) and plot of number-average molecular weights (M_n^{SEC}) and *Đ vs*. conversion (right) for ATRP of *n*BA in miniemulsion catalyzed by $Na_2S_2O_4$ at 80 °C. Conditions: [SDS]$_0$/[Hexadecane]$_0$ = 2.3/3.6 % *vs n*BA; [*n*BA]$_0$/[EBiB]$_0$/[$CuBr_2$]$_0$/[BPMODA*]$_0$/[$Na_2S_2O_4$]$_0$ = 200/1/0.4/0.4/0.2(mol).

Furthermore, the use of additional solvents contributes to a phase separation throughout the reaction, and, when compared to the miniemulsions carried out with Brij*98,* the use of a charged surfactant (SDS) led to uncontrolled polymerizations, with *Đ* > 3.0, probably due to the SDS propensity to interact with the copper catalyst (especially Cu(II) complexes) and with dithionite used species.[34] Additionally, the organic soluble ascorbic acid (6-o-palmitoyl-l-ascorbic acid, AA_{org}) was used as a SARA agent in substitution of AA, in an attempt to understand its role in the ARTP reaction, however, no improvement was observed when compared to AA (Figure 7.11).

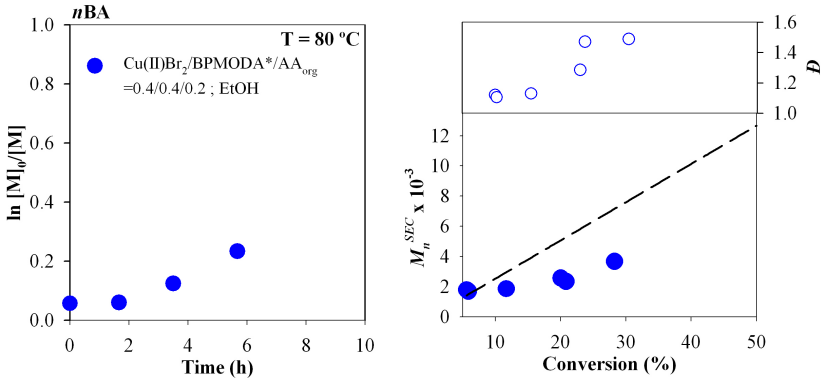

Figure 7.11 Kinetic plots of conversion and ln[M]$_0$/[M] *vs*. time (left) and plot of number-average molecular weights (M_n^{SEC}) and *Đ vs*. conversion (right) for ATRP of *n*BA in miniemulsion catalyzed by 6-o-palmitoyl-l-ascorbic acid (dissolved in ethanol) at 80 °C. Conditions: [Brij*98*]$_0$/[Hexadecane]$_0$ = 2.3/3.6 % *vs n*BA; [*n*BA]$_0$/[EBiB]$_0$/[$CuBr_2$]$_0$/[BPMODA*]$_0$[AA_{org}]$_0$/ = 200/1/0.4/0.4/0.2 (mol).

7.4.4 St Polymerization

As a proof-of-concept, the SARA ATRP miniemulsion mediated by $Na_2S_2O_4$ was extended to St (Table 7.3).

Table 7.3 – Kinetic data of miniemulsion polymerization of St with [St]/[EBiB] = 200/1, [Brij*98*]$_0$/[Hexadecane]$_0$ = 2.3/3.6 % *vs* St at T = 80 ºC.

Entry	$Na_2S_2O_4$ (molar)	BPMODA* (molar)	$CuBr_2$ (molar)	Time (h)	Conv. (%)	$M_n^{th} x10^3$	$M_n^{SEC} x10^3$	Đ
1	0.11	1	1	42	24	5.07	4.8	1.11
2	0.2	0.4	0.4	2.2	13	1.97	1.80	1.05

Despite the low monomer conversions that are in agreement with the *n*Ba polymerization results, the obtained PS presents a very narrow MW distribution ($Đ \geq$ 1.05) which is a very promising result taking in consideration the challenge nature of the St monomer (Figure 7.12).

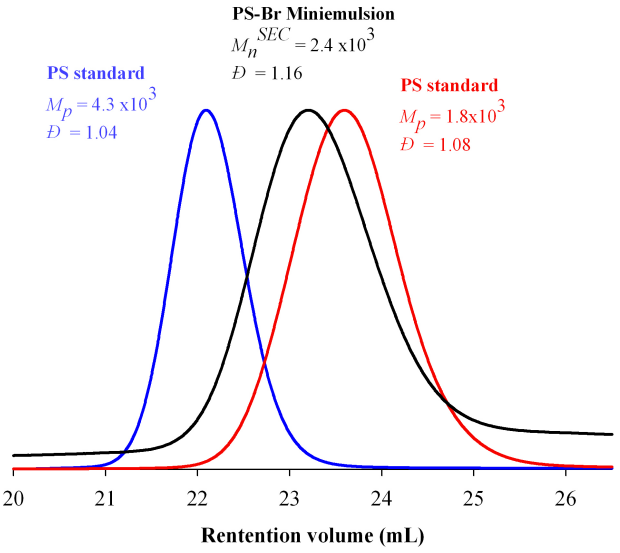

Figure 7.12 Chromatograms of PS standard (red and blue lines) and PS sample obtained by ATRP of St in miniemulsion (black lines) catalysed by $Na_2S_2O_4/CuBr_2$/BPMODA* = 0.2/0.4/0.4. Conditions: [Brij*98*]$_0$/[Hexadecane]$_0$ = 2.3/3.6 % vs St [St]$_0$/[EBiB]$_0$/[$Na_2S_2O_4$]$_0$/[$CuBr_2$]$_0$/[BPMODA*]$_0$ = 200/1/0.2 /0.4/0.4 (mol); T = 80 °C.

7.4.5 Evaluation of chain-end functionality

The presence of active-chain ends and the chemical structure of the P*n*BA-Br (M_n^{SEC} = 5.0 x 10^3; $Đ$ =1.2) and PS-Br (M_n^{SEC} = 4.78 x 10^3; $Đ$=1.11) were confirmed by ^{1}H NMR spectroscopy (Figures 7.13 and 7.14 respectively).

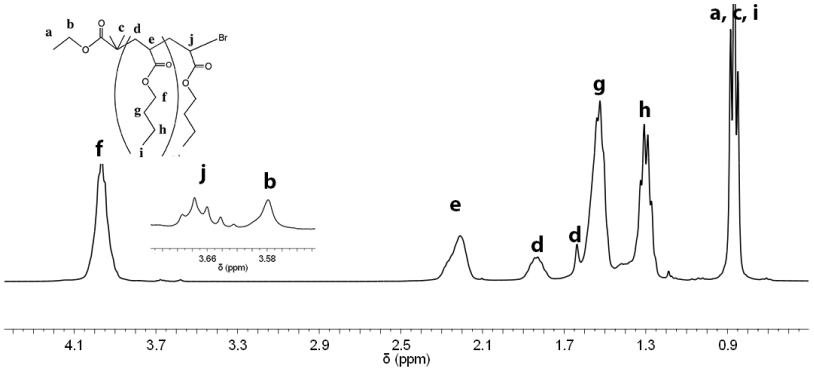

Figure 7.13 ^{1}H NMR spectrum of P*n*BA-Br (M_n^{SEC} = 5.0 x 10^3; $Đ$ = 1.2) in $CDCl_3$.

The proton chemical shifts in the ^{1}H NMR spectrum of the pure P*n*BA-Br (Figure 7.12) were assigned according to literature,[52] i.e., the signals of three methylene group in main chain at 3.97 ppm ($OCH_2CH_2CH_2CH_3$, **f**), 1.52 ppm ($OCH_2CH_2CH_2CH_3$, **g**) and 1.30 ppm ($OCH_2CH_2CH_2CH_3$, **h**) and end methyl group at 0.87 ppm ($OCH_2CH_2CH_2CH_3$, **i**). The methine protons of repeating unit are shows at 2.21 ppm (**e**) and the methylene (**d**) reveals both meso protons at 1.83, 1.31-1.51 ppm and recemo protons at 1.64 ppm. The initiator fragments (containing protons **a**, **b** and **c**) appears at 0.71 ppm and 3.58 ppm. The chain-end functionality is confirmed by the resonance of proton adjacent to bromine (**j**) at 3.68 ppm and allows the determination of the bromine chain-end functionality of the P*n*BA prepared (33 %).

The ^{1}H NMR spectrum of Ps-Br obtained by miniemulsion ATRP is presented in Figure 7.14.

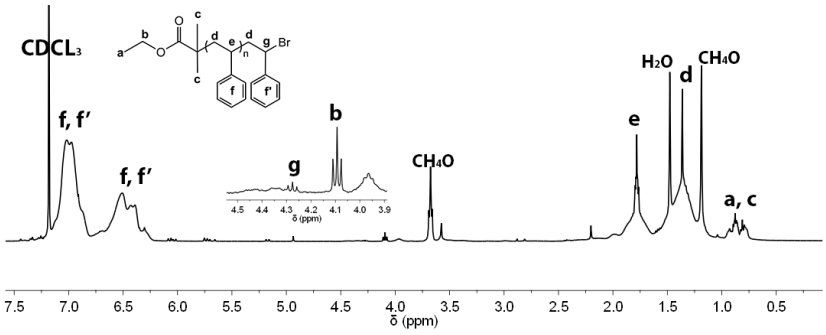

Figure 7.14 ^{1}H NMR spectrum of PS-Br (M_n^{SEC} = 4.78 x 10^3; $Đ$ =1.11) in $CDCl_3$.

In Figure 7.14 the initiator fragment is revealed by the appearance of the resonance peaks of protons at 0.80-1.00 ppm (**CH_3**CH_2OCOC**(CH_3)$_2$**, **a** and **c**) and 4.1 ppm (CH_3**CH_2**$OCOC(CH_3)_2$, **b**). The spectrum reveals the presence of the repeating unit of methine protons at 2.20 ppm (CH_2-**CH**Ph, **e**), methylene protons at 1.48 ppm (**CH_2**-CHPh, **d**) and the aromatic protons peaks at 6.25-7.5 ppm (CH_2-CH**Ph**, **f**). The chain-end functionality is confirmed by the resonance of proton adjacent to bromine terminal group at 4.2-4.3 ppm (CH_2-**CH**PhBr).[12]

The "livingness" of the P*n*BA-Br and PS–Br obtained through the miniemulsion method, were demonstrated by caring out a chain extension reaction in a homogeneous medium. Both polymers were able to reinitiate as confirmed by an increase in the molecular weight (Table 7.4).

Table 7.4 – Kinetic data of chain extension reaction in a homogeneous medium for of the P*n*BA-Br and PS–Br obtained through the miniemulsion method

Entry	Macroinitiator	M_n^{SEC} x10^3	*Đ*	Copolymer	M_n^{SEC} x10^3	*Đ*	Dead chains
1	P*n*BA-Br[a]	2.10	1.25	P*n*BA-*b*- P*n*BA[c]	15.0	3.4	81%
2	PS–Br[b]	9.90	1.10	PS-*b*- PS[d]	110.6	1.30	62%

[a] Conditions of P*n*BA miniemulsion: $[Brij98]_0/[Hexadecane]_0$ = 2.3/3.6 % *vs* *n*BA; $[nBA]_0/[EBiB]_0/[Na_2S_2O_4]/[CuBr_2]/$ $[BPMODA^*]_0$ = 200/1/0.2/0.4/0.4 (mol); T=80 ºC.

[b] Conditions of PS miniemulsion: $[Brij98]_0/[Hexadecane]_0$ = 2.3/3.6 % *vs* St; $[St]_0/[EBiB]_0/[Na_2S_2O_4]/[CuBr_2]/[$ $BPMODA^*]_0$ = 200/1/0.1/1/1 (mol); T=80 ºC

[c] Conditions of P*n*BA-*b*- P*n*BA chain-extension experiment: $[nBA]_0/[CPME]_0$ = 1/1 (v/v) and 200 µL of DMF; $[nBA]_0/[PnBA]_0/[Cu(0)]_0/[CuBr_2]_0/[Me_6TREN]_0$= 350/1/Cu(0) wire/0.5/1 (mol); T=30 ºC

[d] Conditions of PS chain-extension experiment: $[St]_0/[DMF]$ = 1/1 (v/v); $[St]_0/[EBiB]_0/[Fe(0)]_0/[CuBr_2]_0/[Me_6TREN]_0$= 350/1/1/0.1/1.1 (mol); T = 70 ºC.

The movement of the SEC trace of the P*n*BA-Br and PS-Br macroinitiator towards high molecular weights is shown in Figure 7.15 and 7.16.

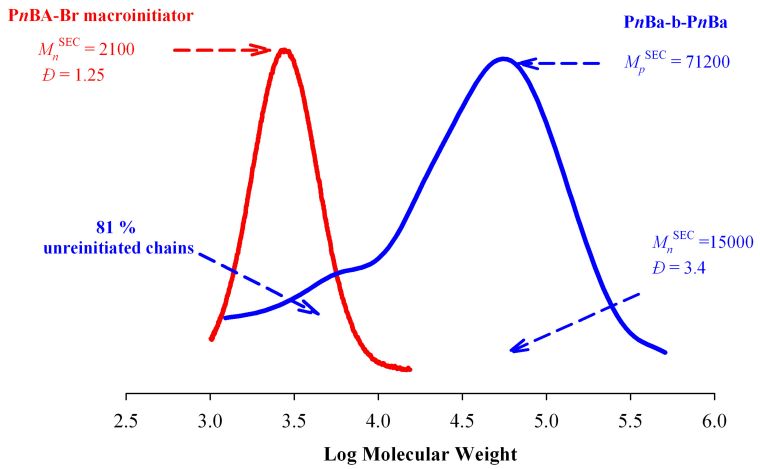

Figure 7.15 - Movement of the SEC trace (RI signal) of a –Br-terminated P*n*Ba, obtained by ATRP in miniemulsion (left, red line), towards high molecular weight values after a chain-extension experiment (right, blue line). Conditions of miniemulsion experiment: $[Brij98]_0/[Hexadecane]_0$ = 2.3/3.6 % vs *n*Ba; $[nBa]_0/[EBiB]_0/[Na_2S_2O_4]/[Cu(II)Br_2]/[BPMODA^*]_0$ = 200/1/0.2/0.4/0.4 (mol); T=80 ºC. Condition of chain-extension experiment : $[nBA]_0/[EtOH]$ = 1/1 (v/v); $[nBA]_0/[PnBA\text{-}Br]_0/[Cu(0)]_0/[Cu(II)Br_2]_0/[Me_6TREN]_0$=600/1/ Cu(0) wire/0.5/1 (mol); T = 30 ºC.

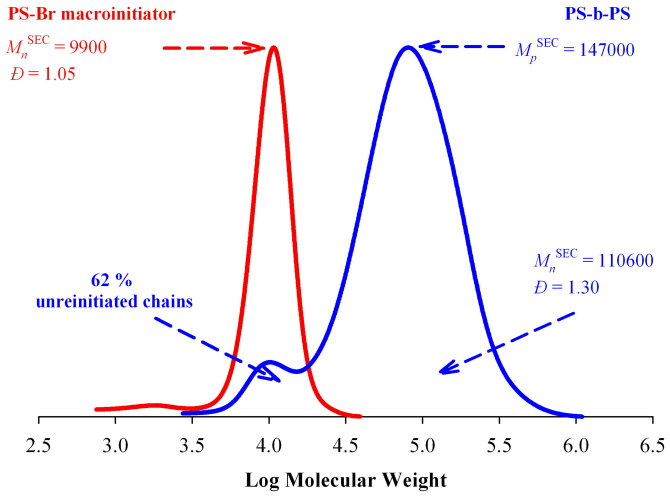

Figure 7.16 Movement of the SEC trace (RI signal) of a –Br-terminated PS, obtained by ATRP in miniemulsion (left, blue line), towards high molecular weight values after a chain-extension experiment (right, red line). Conditions: $[Brij98]_0/[Hexadecane]_0$ = 2.3/3.6 % vs St; $[St]_0/[EBiB]_0/[Na_2S_2O_4]/[CuBr_2]/[BPMODA^*]_0$ = 200/1/0.1/1/1 (mol); T=80 ºC. Condition of chain-extension experiment : $[St]_0/[DMF]$ = 1/1 (v/v); $[St]_0/[EBiB]_0/[Fe(0)]_0/[CuBr_2]_0/[Me_6TREN]_0$= 350/1/1/0.1/1.1 (mol); T = 70 ºC.

In Figure 7.15 the low molecular weight shoulder present in the SEC trace of the P*S-b-* P*S* copolymer shown the presence of PS dead chains (~62 %). However, these results are particularly relevant since that demonstrate the high chain-end functionality of the PS prepared by miniemulsion.

The results presented herein established an innovative system to polymerize P*n*BA and PS using a heterogeneous systems under SARA ATRP conditions.

The polymerization system reported does not allow to achieve very high monomer conversion (~20-30%), which is most probably associated to the dithionite diffusion inside the monomer droplets. Although, the polymerization system leads to polymers with very low dispersity values ($Đ < 1.1$).

7.5 Conclusions

The miniemulsion ATRP of *n*BA and St using $Na_2S_2O_4$ as SARA agent was reported for the first time. The use of one inorganic sulfite in heterogeneous SARA ATRP polymerizations results in the synthesis of well-defined polymers with very narrow molecular weight distributions. The low monomer conversions obtained even after the adjustment of several reaction parameters, could be mostly related with an inefficient diffusion of the SARA agent to the organic phase. Nevertheless, the ^{1}H NMR spectrum of the resultant polymers and the reinitiation experiments confirmed the high degree of chain end functionality and the ”living” character of the system.

7.6 References

1. Braunecker, W. A.; Matyjaszewski, K., Controlled/living radical polymerization: Features, developments, and perspectives, *Progress in Polymer Science*, *32* (1), 93-146, 2007.
2. Golas, P. L.; Matyjaszewski, K., Marrying click chemistry with polymerization: expanding the scope of polymeric materials, *Chemical Society Reviews*, *39* (4), 1338-1354, 2010.
3. Lee, H.-i.; Pietrasik, J.; Sheiko, S. S.; Matyjaszewski, K., Stimuli-responsive molecular brushes, *Progress in Polymer Science*, *35* (1–2), 24-44, 2010.
4. Gao, H.; Matyjaszewski, K., Synthesis of functional polymers with controlled architecture by CRP of monomers in the presence of cross-linkers: From stars to gels, *Progress in Polymer Science*, *34* (4), 317-350, 2009.
5. Davis, K. A.; Matyjaszewski, K., *Advances in Polymer Science*, *159*, 2002.
6. Guliashvili, T.; Mendonça, P. V.; Serra, A. C.; Popov, A. V.; Coelho, J. F. J., Copper-Mediated Controlled/“Living” Radical Polymerization in Polar Solvents: Insights into Some Relevant Mechanistic Aspects, *Chemistry – A European Journal*, *18* (15), 4607-4612, 2012.
7. Kwak, Y.; Magenau, A. J. D.; Matyjaszewski, K., ARGET ATRP of Methyl Acrylate with Inexpensive Ligands and ppm Concentrations of Catalyst, *Macromolecules*, *44* (4), 811-819, 2011.

8. Jakubowski, W.; Matyjaszewski, K., Activators Regenerated by Electron Transfer for Atom-Transfer Radical Polymerization of (Meth)acrylates and Related Block Copolymers, *Angewandte Chemie International Edition*, *45* (27), 4482-4486, 2006.
9. Jakubowski, W.; Min, K.; Matyjaszewski, K., Activators Regenerated by Electron Transfer for Atom Transfer Radical Polymerization of Styrene, *Macromolecules*, *39* (1), 39-45, 2005.
10. Matyjaszewski, K.; Jakubowski, W.; Min, K.; Tang, W.; Huang, J.; Braunecker, W. A.; Tsarevsky, N. V., Diminishing catalyst concentration in atom transfer radical polymerization with reducing agents, *Proceedings of the National Academy of Sciences*, *103* (42), 15309-15314, 2006.
11. Cordeiro, R. A.; Rocha, N.; Mendes, J. P.; Matyjaszewski, K.; Guliashvili, T.; Serra, A. C.; Coelho, J. F. J., Synthesis of well-defined poly(2-(dimethylamino)ethyl methacrylate) under mild conditions and its co-polymers with cholesterol and PEG using Fe(0)/Cu(ii) based SARA ATRP, *Polymer Chemistry*, *4* (10), 3088-3097, 2013.
12. Rocha, N.; Mendonca, P. V.; Mendes, J. P.; Simoes, P. N.; Popov, A. V.; Guliashvili, T.; Serra, A. C.; Coelho, J. F. J., Facile Synthesis of Well-Defined Telechelic Alkyne-Terminated Polystyrene in Polar Media Using ATRP With Mixed Fe/Cu Transition Metal Catalyst, *Macromolecular Chemistry and Physics*, *214* (1), 76-84, 2013.
13. Wang, Y.; Zhong, M.; Zhu, W.; Peng, C.-H.; Zhang, Y.; Konkolewicz, D.; Bortolamei, N.; Isse, A. A.; Gennaro, A.; Matyjaszewski, K., Reversible-Deactivation Radical Polymerization in the Presence of Metallic Copper. Comproportionation–Disproportionation Equilibria and Kinetics, *Macromolecules*, *46* (10), 3793-3802, 2013.
14. Peng, C.-H.; Zhong, M.; Wang, Y.; Kwak, Y.; Zhang, Y.; Zhu, W.; Tonge, M.; Buback, J.; Park, S.; Krys, P.; Konkolewicz, D.; Gennaro, A.; Matyjaszewski, K., Reversible-Deactivation Radical Polymerization in the Presence of Metallic Copper. Activation of Alkyl Halides by Cu0, *Macromolecules*, *46* (10), 3803-3815, 2013.
15. Zhong, M.; Wang, Y.; Krys, P.; Konkolewicz, D.; Matyjaszewski, K., Reversible-Deactivation Radical Polymerization in the Presence of Metallic Copper. Kinetic Simulation, *Macromolecules*, *46* (10), 3816-3827, 2013.
16. Abreu, C. M. R.; Mendonca, P. V.; Serra, A. C.; Popov, A. V.; Matyjaszewski, K.; Guliashvili, T.; Coelho, J. F. J., Inorganic Sulfites: Efficient Reducing Agents and Supplemental Activators for Atom Transfer Radical Polymerization, *ACS Macro Letters*, *1* (11), 1308-1311, 2012.
17. Abreu, C. M. R.; Mendonça, P. V.; Serra, A. C.; Coelho, J. F. J.; Popov, A. V.; Guliashvili, T., Accelerated Ambient-Temperature ATRP of Methyl Acrylate in Alcohol–Water Solutions with a Mixed Transition-Metal Catalyst System, *Macromolecular Chemistry and Physics*, *213* (16), 1677-1687, 2012.
18. Zhang, Y.; Wang, Y.; Matyjaszewski, K., ATRP of Methyl Acrylate with Metallic Zinc, Magnesium, and Iron as Reducing Agents and Supplemental Activators, *Macromolecules*, *44* (4), 683-685, 2011.
19. Mendonca, P. V.; Serra, A. C.; Coelho, J. F. J.; Popov, A. V.; Guliashvili, T., Ambient temperature rapid ATRP of methyl acrylate, methyl methacrylate and styrene in polar solvents with mixed transition metal catalyst system, *European Polymer Journal*, *47* (7), 1460-1466, 2011.
20. Wang, Y.; Zhang, Y.; Parker, B.; Matyjaszewski, K., ATRP of MMA with ppm Levels of Iron Catalyst, *Macromolecules*, *44* (11), 4022-4025, 2011.

21. Magenau, A. J. D.; Kwak, Y.; Matyjaszewski, K., ATRP of Methacrylates Utilizing CuIIX2/L and Copper Wire, *Macromolecules*, *43* (23), 9682-9689, 2010.
22. Magenau, A. J. D.; Strandwitz, N. C.; Gennaro, A.; Matyjaszewski, K., Electrochemically Mediated Atom Transfer Radical Polymerization, *Science*, *332* (6025), 81-84, 2011.
23. Bortolamei, N.; Isse, A. A.; Magenau, A. J.; Gennaro, A.; Matyjaszewski, K., Controlled aqueous atom transfer radical polymerization with electrochemical generation of the active catalyst, *Angewandte Chemie*, *123* (48), 11593-11596, 2011.
24. Magenau, A. J. D.; Bortolamei, N.; Frick, E.; Park, S.; Gennaro, A.; Matyjaszewski, K., Investigation of Electrochemically Mediated Atom Transfer Radical Polymerization, *Macromolecules*, *46* (11), 4346-4353, 2013.
25. Tasdelen, M. A.; Uygun, M.; Yagci, Y., Photoinduced controlled radical polymerization in methanol, *Macromolecular Chemistry and Physics*, *211* (21), 2271-2275, 2010.
26. Mosnáček, J.; Ilčíková, M. t., Photochemically mediated atom transfer radical polymerization of methyl methacrylate using ppm amounts of catalyst, *Macromolecules*, *45* (15), 5859-5865, 2012.
27. Konkolewicz, D.; Schröder, K.; Buback, J.; Bernhard, S.; Matyjaszewski, K., Visible Light and Sunlight Photoinduced ATRP with ppm of Cu Catalyst, *ACS Macro Letters*, *1* (10), 1219-1223, 2012.
28. Abreu, C. M. R.; Serra, A. C.; Popov, A. V.; Matyjaszewski, K.; Guliashvili, T.; Coelho, J. F. J., Ambient temperature rapid SARA ATRP of acrylates and methacrylates in alcohol-water solutions mediated by a mixed sulfite/Cu(ii)Br2 catalytic system, *Polymer Chemistry*, *4* (23), 5629-5636, 2013.
29. Gois, J. R.; Rocha, N.; Popov, A. V.; Guliashvili, T.; Matyjaszewski, K.; Serra, A. C.; Coelho, J. F. J., Synthesis of well-defined functionalized poly(2-(diisopropylamino)ethyl methacrylate) using ATRP with sodium dithionite as a SARA agent, *Polymer Chemistry*, *5* (12), 3919-3928, 2014.
30. Gois, J. R.; Konkolewicz, D.; Popov, A.; Guliashvili, T.; Matyjaszewski, K.; Serra, A. C.; Coelho, J., Improvement of the Control over SARA ATRP of 2-(Diisopropylamino)ethyl Methacrylate by Slow and Continuous Addition of Sodium Dithionite, *Polymer Chemistry*, in press, 2014.
31. Erdmenger, T.; Guerrero-Sanchez, C.; Vitz, J.; Hoogenboom, R.; Schubert, U. S., Recent developments in the utilization of green solvents in polymer chemistry, *Chemical Society Reviews*, *39* (8), 3317-3333, 2010.
32. Matyjaszewski, K., Atom Transfer Radical Polymerization (ATRP): Current Status and Future Perspectives, *Macromolecules*, *45* (10), 4015-4039, 2012.
33. Cunningham, M. F., Controlled/living radical polymerization in aqueous dispersed systems, *Progress in Polymer Science*, *33* (4), 365-398, 2008.
34. Min, K.; Matyjaszewski, K., Atom transfer radical polymerization in aqueous dispersed media, *Central European Journal of Chemistry*, *7* (4), 657-674, 2009.
35. Min, K.; Matyjaszewski, K., Atom Transfer Radical Polymerization in Microemulsion, *Macromolecules*, *38* (20), 8131-8134, 2005.
36. Teo, V. L.; Davis, B. J.; Tsarevsky, N. V.; Zetterlund, P. B., Successful Miniemulsion ATRP Using an Anionic Surfactant: Minimization of Deactivator Loss by Addition of a Halide Salt, *Macromolecules*, *47* (18), 6230-6237, 2014.
37. Kaczorowski, M.; Rokicki, G., Reactive surfactants – chemistry and applications Part I. Polymerizable surfactants, *Polimery*, *61* (11-12), 745-882, 2016.

38. Qiu, J.; Charleux, B.; Matyjaszewski, K., Controlled/living radical polymerization in aqueous media: homogeneous and heterogeneous systems, *Progress in Polymer Science*, *26* (10), 2083-2134, 2001.
39. Jennings, J.; He, G.; Howdle, S. M.; Zetterlund, P. B., Block copolymer synthesis by controlled/living radical polymerisation in heterogeneous systems, *Chemical Society Reviews*, *45* (18), 5055-5084, 2016.
40. Zetterlund, P. B.; Thickett, S. C.; Perrier, S.; Bourgeat-Lami, E.; Lansalot, M., Controlled/Living Radical Polymerization in Dispersed Systems: An Update, *Chemical reviews*, *115* (18), 9745-9800, 2015.
41. Matyjaszewski, K.; Tsarevsky, N. V., Macromolecular Engineering by Atom Transfer Radical Polymerization, *Journal of the American Chemical Society*, *136* (18), 6513-6533, 2014.
42. Elsen, A. M.; Burdyńska, J.; Park, S.; Matyjaszewski, K., Activators Regenerated by Electron Transfer Atom Transfer Radical Polymerization in Miniemulsion with 50 ppm of Copper Catalyst, *ACS Macro Letters*, *2* (9), 822-825, 2013.
43. Gromada, J.; Spanswick, J.; Matyjaszewski, K., Synthesis and ATRP Activity of New TREN-Based Ligands, *Macromolecular Chemistry and Physics*, *205* (5), 551-566, 2004.
44. Elsen, A. M.; Burdyńska, J.; Park, S.; Matyjaszewski, K., Active Ligand for Low PPM Miniemulsion Atom Transfer Radical Polymerization, *Macromolecules*, *45* (18), 7356-7363, 2012.
45. Abreu, C. M. R.; Fu, L.; Carmali, S.; Serra, A. C.; Matyjaszewski, K.; Coelho, J. F. J., Aqueous SARA ATRP using inorganic sulfites, *Polymer Chemistry*, *8* (2), 375-387, 2017.
46. Li, M.; Matyjaszewski, K., Reverse Atom Transfer Radical Polymerization in Miniemulsion, *Macromolecules*, *36* (16), 6028-6035, 2003.
47. Oh, J. K., Recent advances in controlled/living radical polymerization in emulsion and dispersion, *Journal of Polymer Science Part A: Polymer Chemistry*, *46* (21), 6983-7001, 2008.
48. Li, M.; Min, K.; Matyjaszewski, K., ATRP in Waterborne Miniemulsion via a Simultaneous Reverse and Normal Initiation Process, *Macromolecules*, *37* (6), 2106-2112, 2004.
49. Simms, R. W.; Cunningham, M. F., Compartmentalization of Reverse Atom Transfer Radical Polymerization in Miniemulsion, *Macromolecules*, *41* (14), 5148-5155, 2008.
50. Simms, R. W.; Cunningham, M. F., High Molecular Weight Poly(butyl methacrylate) by Reverse Atom Transfer Radical Polymerization in Miniemulsion Initiated by a Redox System, *Macromolecules*, *40* (4), 860-866, 2007.
51. Percec, V.; Popov, A. V.; Ramirez-Castillo, E.; Coelho, J. F. J.; Hinojosa-Falcon, L. A., Phase transfer catalyzed single electron transfer–degenerative chain transfer mediated living radical polymerization (PTC-SET–DTLRP) of vinyl chloride catalyzed by sodium dithionite and initiated with iodoform in water at 43 °C, *Journal of Polymer Science Part A: Polymer Chemistry*, *43* (4), 779-788, 2005.
52. Coelho, J. F. J.; Carvalho, E. Y.; Marques, D. S.; Popov, A. V.; Percec, V.; Gil, M. H., Influence of the isomeric structures of butyl acrylate on its single-electron transfer-degenerative chain transfer living radical polymerization in water Catalyzed by Na2S2O4, *Journal of Polymer Science Part A: Polymer Chemistry*, *46* (19), 6542-6551, 2008.

Part III

Application

Chapter 8

Poly(ethylene glycol)-block-poly(4-vinyl pyridine) as a versatile block copolymer to prepare nanoaggregates of superparamagnetic iron oxide nanoparticles

This chapter is focused on the potential of copolymers synthesized during the PhD work. This chapter is published in Rocha, N.; **Mendes, J**.; Duraes, L.; Maleki, H.; Portugal, A.; Geraldes, C. F. G. C.; Serra, A.; Coelho, J., "*Poly(ethylene glycol)-block-poly(4-vinyl pyridine) as a versatile block copolymer to prepare nanoaggregates of superparamagnetic iron oxide nanoparticles"*, *Journal of Materials Chemistry B***,** *2* (11), 1565-1575, 2014.

8.1 Abstract

This work reports a very efficient method to prepare aqueous dispersions of superparamagnetic iron oxide nanoparticles (SPIONs), independently on their original coating nature (hydrophilic or hydrophobic), using an amphiphilic block copolymer, poly(ethylene glycol)-block-poly(4-vinyl pyridine) (*m*PEG-*b*-P4VP). The high dispersion ability is due to the strong direct interaction of hydrophobic P4VP segments with ironoxide species based on complexation properties of pyridine ring. Well-defined blockcopolymers of different compositions and molecular weights were prepared by ATRP and their aqueous self-assembly was compared taking into account the methodology used for the process (titration and solvent exchange). The addition of ionic species during titration is found to have a significant effect on the size and type of nanostructures formed, depending on the block copolymers molecular design. When the same self-assembly methodologies are applied in the presence of SPIONs, a similar trend in the type of nanostructures that are formed is observed. The magnetic resonance imaging (MRI) performance of the hybrid SPIONs nanoaggregates is further evaluated, showing high r_2/r_1 relaxivity ratios, which makes these materials potentially effective T_2-weighted MRI contrast agents.

8.2 Introduction

The encapsulation of inorganic species by the self-assembly of amphiphilic block copolymers is a powerful technique for the preparation of inorganic-based nanoparticles having controlled structures and properties. [1-2] RDRP methods [3-4] are a powerful tool for preparing tailor-made telechelic polymers and related amphiphilic block copolymers that have well controlled molecular weights, composition and architecture, under mild reaction conditions.[5-9] In the presence of inorganic species, the self-assembly of amphiphilic block copolymers can be used to afford hybrid nanoparticles that possess controlled nanostructured morphology. [10]

The coating of magnetic nanoparticles with polymers has often been assumed to be an efficient means of avoiding agglomeration on the basis of electrostatic or static repulsion.[11-12] This process enhances the particle stability that is of great importance when, for instance, the magnetic nanoparticles are intended to be used in biomedical

applications[13-19] This aspect is critical for the determination of blood circulation pathway, since the biodistribution of nanoparticles depends on their hydrodynamic sizes and their stability.[18]

Block copolymers have been regarded as an efficient means to prepare size-controlled and aqueous-stable clusters of magnetic nanoparticles, as long as they include, at least, one hydrophilic block for steric stabilization and one anchoring block with affinity for the nanoparticles.[20-22] The possibility of preparing block copolymer with an efficient control of their molecular structure through RDRP methodologies may be of great significance to control the final structure of the magnetic nanoparticles aggregates. In fact, depending on the block copolymer molecular design and on the self-assembly conditions, in the presence of the magnetic nanoparticles, it has been shown that it is possible to obtain nanoaggregates of different morphological properties, such as aggregation number, size and shape, and, therefore, of different magnetic performance. [21, 23-24]

For the preparation of stable superparamagnetic iron oxide nanoparticles (SPIONs) agglomerates by co-micellization in the presence of block copolymers, the selection of the anchoring segment has been mainly based on the surface's chemical nature of the original SPIONs. Therefore, the nature of the block copolymer that is used to form the SPIONs nanoaggregates through block copolymers self-assembly is determined by the type of interactions that are established between SPION and the block copolymer. Amphiphilic block copolymers are usually used when the SPIONs have a hydrophobic coating, being encapsulated into core-shell structures through Van der Waals interactions with the hydrophobic polymeric segment. [25-27] In addition, double hydrophilic block copolymers can be used to form SPION nanoaggregates, if one of the hydrophilic blocks can establish electrostatic interactions with the SPIONs' surface, such as cationic polymers for negatively charged stabilized SPIONs [24, 28] or anionic polymeric segments for positively charged uncoated iron oxide nanoparticles.[20, 29] Alternatively, the possibility of chemisorbing poly(glycerol (meth)acrylate) onto SPIONs surface through 1,2-diol groups[30] has been used to form aggregates of block copolymers with SPIONs, but these were limited to self-assembly at the hydrophilic surface of the block copolymers.[30, 31] These SPIONs' agglomerates have been found to be excellent contrast agents for magnetic resonance imaging (MRI) applications.[25-28, 31]

Although poly(4-vinyl pyridine) (P4VP) is known to be a strong coordinator for metallic species,[32-35] it has not yet been used for the stabilization of SPIONs in aqueous medium. We thought that the use of P4VP segments may offer the possibility of direct complexation of pyridyl groups with iron oxide moieties and further interaction through Van der Waals forces with, if existing, hydrophobic groups at the SPIONs' surface. When P4VP is combined with a hydrophilic segment in a block copolymer, well-defined core-shell nanoparticles can be formed through a self-assembly mechanism in aqueous medium.[36-37] Moreover, the strong coordinating nature of the pyridyl moieties in P4VP-based amphiphilic block copolymers has been explored for the preparation of complex structures such as the hydrophilic coating of capillary walls[38] or J- and H-aggregates with anionic porphyrins.[39] In addition, the aqueous self-assembly of P4VP-based amphiphilic block copolymers has been used to prepare water dispersions of hybrid metal-polymer nanoparticles.[40] The micellization of this amphiphilic P4VP-based block copolymers in the presence of SPIONs, through a self-assembly mechanism, can, thus, be expected to lead to uniformly sized and highly stable nanoaggregates. The possibility of tuning the type of structures that are formed based on the molecular design of the block copolymer and on the self-assembly conditions may be particularly relevant for the preparation of new magnetic-responsive materials, such as for coatings applications or for the creation of MRI contrast agents.[41]

In this chapter, we report a novel approach for preparing SPIONs hybrid core-shell nanoparticles, based on the self-assembly of amphiphilic poly(ethylene glycol)-block-poly(4-vinyl pyridine) (*m*PEG-*b*-P4VP) and on the transition metal complexation of the pyridyl groups with iron. In addition, the hydrophobic character of the P4VP block, at pH values above its pK_a, can provide an efficient way to form core-shell nanostructures even with hydrophilic SPIONs or to provide enhanced stabilization for hydrophobic-coated SPIONs, making *m*PEG-*b*-P4VP a versatile block copolymer to prepare magnetic nanoaggregates for a broad range of SPIONs. This paper compares the aggregation behavior depending on the composition and molecular weight of the block copolymers and on the original SPIONs surface functionality. In addition, the influence of the self-assembly methodology (titration and solvent exchange method) is investigated. The *in vitro* performance of the prepared SPIONs' nanoaggregates as potential MRI contrast agents was further assessed and related with their aggregates structure.

8.3 Experimental Section

8.3.1 Materials

Each poly(ethylene glycol) methyl ether (mPEG) ($mPEG_{113}$: Mw=5000 Da, and $mPEG_{45}$: M_w=2500 Da; Sigma-Aldrich) was dried by azeotropic distillation from toluene. 2-chloropropionyl chloride (CPC) (97%; Sigma-Aldrich), $CuCl_2$ (+99%+extra pure, anhydrous; Acros) were used as supplied. Cu(0) wire (99%; Acros) was activated with nitric acid, washed with acetone and dried before use. Isopropanol (IPA) (99.97%; Fisher Chemical), ethanol (96%; Panreac), diethyl ether (>99.8%; Sigma-Aldrich), methanol (>99.85%; Aldrich), chloroform (99.99%; Fisher Chemical), dimethylformamide (DMF) (+99.8%; Sigma-Aldrich), deuterated chloroform ($CDCl_3$) (+1% tetramethylsilane (TMS); Euriso-top), sodium hydroxide (pellets QP; Panreac) and hydrochloric acid solution (HCl) (37%; Aldrich) were used as received. Milli-Q water (Milli-Q®, Millipore) was obtained by reverse osmosis. 4-vinylpyridine (4VP) (96%; Fluka), triethylamine (TEA) (96%; Sigma-Aldrich) and dichloromethane (DCM) (+99.6%; Fisher Scientific) were dried and distilled under reduced pressure, prior to use. 4- Dimethylaminopyridine (DMAP) (99%; ACROS) was previously recrystallized. Tris(2-dimethylaminoethyl)amine (Me_6TREN) was synthesized according to procedures described in the literature [42]. For size exclusion chromatography (SEC), poly(methyl methacrylate) (PMMA) standards (Polymer Laboratories) (Acros, 99%, ~70 mesh) and high performance liquid chromatrography (HPLC) DMF (HPLC grade; Panreac) were used as received. Fe(III) chloride hexahydrate ($FeCl_3 \cdot 6H_2O$, >99%), Fe(II) chloride tetrahydrate ($FeCl_2 \cdot 4H_2O$, >99%), and 1-butanol were purchased from Merck Chemicals Inc.; toluene, acetone, and ethanol were purchased from Ghataran Shimi T. Co. Cetyltrimethylammonium bromide (CTAB) was purchased from Sigma-Aldrich and used as received. Oleic acid-coated hydrophobic SPIONs (OaSPIONs) with a 5±1 nm (TEM conform) average particle size and with 10.1%wt. of oleic-content, as determined by thermogravimetric analysis, were used as received (5mg/mL in toluene; Aldrich reference no. 700320). The synthesis of poly(ethylene glycol) monomethyl ether chloride (mPEG-Cl) was through an adaptation of a method reported [43] An illustrative procedure for the preparation of $mPEG_{113}$-Cl is presented section 3.2.3 Procedures. $mPEG_{113}$-*b*-P4VP block copolymers were prepared by ATRP, using the previously reported Cu(0) and [$CuCl_2$]/[Me_6TREN]=1/1 catalytic system[44], (the procedure is

presented in section 3.2.3 Procedures). Hydrophilic Fe_3O_4 SPIONs (hSPIONs) were synthesized using a micro-emulsion technique in which two water in oil microemulsions of the same composition (water/toluene/CTAB-butanol) were prepared, according to our previous work [45], (detailed procedure in section 3.2.3 Procedures).

8.3.2 Techniques

Size exclusion chromatography (SEC) was carried out using high performance size-exclusion chromatography (HPSEC), with refractive index (RI) (Knauer K-2301) detection. The column set consisted of a PL 10-μL guard column (50 x 7.5 mm^2), followed by two MIXED-B PL columns (300 x 7.5mm^2, 10 μL). The HPLC pump was set with a flow rate of 1 mL/min and the analyses were carried out at 60ºC using an Elder CH-150 heater. The eluent was DMF, containing 0.3% of LiBr. Before injection (100 μL), the samples were filtered through a polytetrafluoroethylene (PTFE) membrane with 0.2 μm pore size. The system was calibrated against PMMA standards.

400 MHz ^1H NMR spectra of the reaction mixture samples and recovered products were recorded on a Bruker Avance III 400 MHz spectrometer, with a 5-mm TXI triple resonance detection probe, in $CDCl_3$ using tetramethylsilane (TMS) as an internal standard. NMR measurements were carried out using an acquisition time of 9 s and a T_1 of 1 s (total relaxation delay of 10 s). The conversion of the monomers was determined through the integration of the monomer peak and polymer peak using MestReNova software version: 6.0.2-5475.

Transmission electron microscopy (TEM) was used to observe the size and morphology of the nanoaggregates that were prepared under different self-assembly conditions. Each aqueous dispersion was mounted on a 400 mesh copper grid and examined using a Jeol JEM 1400 transmission electron microscope. Images were digitally recorded using a Gatan SC 1000 ORIUS CCD camera.

Dynamic light scattering (DLS) measurements were performed on a Malvern Instruments Zetasizer Nano-ZS (Malvern Instruments Ltd.). The particle size distribution (in intensity), average hydrodynamic particle size average (z-average) and dispersity (*Đ*) were determined with Zetasizer 6.20 software. Measurements were made at 25 ºC and at a backward scattering angle of 173 º. All of the samples were

filtered before measurements through a membrane of poly(propylene) (PP) (0.45 μm pore size), to remove any existing dust. At least, 4 measurements were taken for each sample.

Atomic Absorption Spectroscopy (AAS) was used to evaluate the residual copper catalysts content in the block copolymers and the content of iron in the prepared hybrid samples. AAS was performed on a Perkin Elmer (Model 3300). For the copper content determination, the block copolymers were dissolved in a 0.1 M HCl solution at a known concentration between 0.5 and 1 mg/mL. The iron content in each self-assembled block copolymer and SPIONs samples was measured from dilutions of the final dispersion in a 0.1M HCl solution. At least, five measurements were taken for each sample.

For the relaxivity measurements of the different SPIONs and block copolymer formulations, the water proton longitudinal (T_1) and transverse (T_2) relaxation times were measured using a Bruker Minispec mq20, operating at a magnetic field of 0.47 T, corresponding to a Larmor frequency of 20 MHz, and at a temperature of 25 ºC. T_1 and T_2 relaxation times were obtained using the inversion-recovery (IR) and Carr-Purcell-Meiboom-Gill (CPMG) pulse sequences, respectively. The accuracy of the relaxation time determinations was better than ± 1 %. For T_1 determinations, for each measurement a relaxation delay longer than five times T_1 was used and the interpulse delay was varied between the shortest and longest values, in order to cover the full range of longitudinal magnetization recovery. For T_2 determinations, the same care was taken to choose relaxation delays longer than five times T_2 and an array of echo times was selected to allow full sampling of the transverse magnetization decay. The paramagnetic contribution to the water proton inverse relaxation times, $R_{i,p}$, varied linearly with the Fe concentration, according to the equation (1) [12].

$$R_{i,p} = R_{i,obs} + R^0_i = r_i [Fe] \quad (i = 1, 2) \tag{1}$$

In Equation 1, $R_{i,obs}$ and R^0_i are, respectively, the determined experimentally inverse relaxation time and the inverse relaxation times of aqueous solutions of the block copolymer alone at a concentration correspondent to that existing in the hybrid sample, while the relaxivities r_i (i = 1, 2) are defined as the water proton relaxation rate enhancements per mM Fe concentration. Different iron concentrations were

obtained by the sequential dilution of the original sample. This dilution was performed 3 times to obtain four concentrations.

8.3.3 Procedures

8.3.3.1 Synthesis of poly(ethylene glycol) monomethyl ether chloride ($mPEG_{113}$-Cl)

The $mPEG_{113}$-Cl was prepared through an adaptation of a reported method[43]. DMAP(0.916 g, 7.5 mmol), DCM (20 mL) and TEA (0.7 mL, 5 mmol) were placed into a round-bottom flask. A solution of CPC (1.21 mL, 12.5 mmol) in DCM (20 mL) was then added dropwise and a yellow dispersion was formed. After, $mPEG_{113}$ (10.0 g, 5.0 mmol) and DCM (30 mL) were added, under a N_2 atmosphere in an ice bath (0ºC). After the CPC solution addition, the temperature was raised to 25ºC and the reaction continued under magnetic stirring for 18 h. The obtained dispersion was then filtered, concentrated by solvent evaporation and the product recovered by precipitation in cold diethyl ether. The crude product was purified by recrystallization overnight in absolute ethanol. After being filtered and washed with cold diethyl ether, the macroinitiator was collected and dried for 48 h, under vacuum, at 40ºC. The same procedure was used for the preparation of $mPEG_{45}$-Cl.

8.3.3.2 Synthesis of $mPEG_{113}$-*b*-$P4VP_{124}$ block copolymer

$mPEG_{113}$-*b*-P4VP block copolymers were prepared by ATRP using the previously reported Cu(0) and $[CuCl_2]/[Me_6TREN]=1/1$ catalytic system [44]. In a typical procedure, a mixture of $mPEG_{113}$-Cl (0.472 g, 0.09 mmol), $CuCl_2$ (12.47 mg, 0.09 mmol), Me_6TREN (21.36 mg, 0.09 mmol) and IPA (3.11 mL) was placed in a Schlenk reactor and immediately frozen in liquid nitrogen. Activated Cu(0) wire was placed in the reactor and the system was deoxygenated with four freeze-vacuum-thaw cycles and purged with nitrogen. 4VP (3.0 mL, 28 mmol) was then added to a Schlenk reaction vessel under a nitrogen atmosphere and the reaction mixture was immediately frozen in liquid nitrogen and deoxygenated by conducting two freeze-vacuum-thaw cycles and purged with nitrogen. The Schlenk reactor was placed in a pre-heated oil bath at 50 ºC and left reacting under magnetic stirring. After 90 minutes, a sample was taken to determine the monomer conversion by ^1H NMR

spectroscopy. Then the block copolymer was precipitated in cold diethyl ether and the solid dissolved in chloroform and passed through an alumina column to remove the copper catalyst. The solution was concentrated by rotary evaporation and the product recovered by precipitation in cold diethyl ether, followed by filtration. Further catalysts removal was achieved by re-dissolving the product in methanol and dialysis for 12 h (molecular weight cut-off (MWCO) = 3500 Da). Finally, the crude product was obtained by precipitation in cold diethyl ether, filtered and then dried, under vacuum, at 40 ºC for 48 h.

8.3.3.3 Synthesis of hydrophilic Fe_3O_4 SPIONs (hSPIONs)

Hydrophilic Fe_3O_4 SPIONs were synthesized using a micro-emulsion technique in which two water in oil microemulsions, with the same water/toluene/CTAB-butanol composition, were prepared, according to our previous work [45]. One of the microemulsions contained 1.9 mL of an aqueous internal phase of ferric chloride hexahydrate (0.75 mmol, 111 mg/mL) and ferrous chloride tetrahydrate (0.37 mmol, 52.2 mg/mL). The other micro-emulsion contained the ammonium hydroxide (NH_4OH) reducing agent (30% v/v, 1.9 ml). SPIONs were formed and precipitated by blending the two microemulsions under a high purity (99.9%) argon atmosphere, at 50 ˚C for 1 h. The product was washed 3 times with 20 mL of ethanol and then washed under reflux with ethanol to remove any surfactant residues and any unreacted byproduct, before being finally collected using an external magnet.

8.3.3.4 Self-assembly of mPEG-*b*-P4VP block copolymers

The self-assembly of the mPEG-*b*-P4VP block copolymers was carried out by titration and solvent exchange methods to afford 1mg/mL of aqueous solutions. In the titration method, the block copolymer was previously dissolved in an aqueous solution of HCl (0.01 M). The solution was then titrated using a very slowly dropwise addition of a 0.1 M NaOH aqueous solution. The change in the pH with respect to the added volume of the NaOH solution was recorded. The titration was stopped when the pH stabilized at 11.5.

In the solvent exchange method[21, 27] the block copolymer was previously dissolved in DMF at a concentration of 10 mg/mL. 200 µL of the block copolymer solution were

then added dropwise to 1.8 mL of Mili-Q water, under vigorous stirring. The sample was then dialyzed against Mili-Q water for 2 days (MWCO = 1000 Da).

8.3.3.5 Self-assembly of mPEG-*b*-P4VP block copolymers in the presence of SPIONs

The self-assembly of the mPEG-*b*-P4VP block copolymers, in the presence of SPIONs, was carried out using the procedures described for the block copolymers, to afford 1 mg/mL of aqueous solutions containing a 10:1 weight ratio of the block copolymer to SPIONs. The titration method was applied only to the hydrophilic SPIONs, because of the non-dispersability of the hydrophobically coated OaSPIONs. In this method, the block copolymer and the SPIONs were dissolved at an acidic pH at a weight ratio of block copolymer to SPIONs of 10:1.

In the solvent exchange method, for the hydrophilic SPIONs, 200 μL of each block copolymer solution in DMF (10 mg/mL) were added dropwise to 1.8 mL of a previously prepared dispersion containing 0.11mg/mL of SPIONs in Mili-Q water. For the hydrophobic SPIONs, a mixture of 40 μL of SPIONs solution, in toluene (5 mg/mL), and 200 μL of the block copolymer, in DMF (10 mg/mL), was initially prepared. The required dropwise addition was carried out under vigorous stirring, in a ultra-sounds bath.

8.4 Results and discussion

8.4.1 Synthesis and characterization of mPEG-*b*-P4VP block copolymers

Block copolymers of mPEG-*b*-P4VP with different compositions and molecular weights were prepared by the SARA ATRP of 4VP using a Cu(0)/$CuCl_2$/Me_6TREN catalytic system, in isopropanol at 50 ºC[44] using mPEG-Cl macroinitiators. Table 8.1 summarizes the polymerization parameters that were used and the characteristics of the obtained block copolymers.

Table 8.1 M_n and $Đ$ values determined by ^{1}H NMR and SEC and residual copper content determined by elemental analysis for the mPEG-*b*-P4VP block copolymer product.

Block copolymer	DP	Time (h)	4VP conversion	M_n^{target} x10^{-3}	M_n^{th} x10^{-3}	M_n^{SEC} x10^{-3}	$Đ$	$Cu_{res.}$ (%wt.)
$mPEG_{45}$-*b*-$P4VP_{32}$	50	1.5	62.0 %	5.3	5.3	11.2	1.16	0.94
$mPEG_{45}$-*b*-$P4VP_{56}$	200	2.5	26.7 %	7.7	7.9	13.5	1.19	0.55
$mPEG_{45}$-*b*-$P4VP_{96}$	100	3.0	89.0 %	11.5	12.0	26.9	1.42	0.97
$mPEG_{113}$-*b*-$P4VP_{40}$	100	5.0	38.1 %	9.2	9.2	19.1	1.24	0.66
$mPEG_{113}$-*b*-$P4VP_{78}$	200	3.0	51.1 %	15.8	13.2	26.8	1.22	0.88
$mPEG_{113}$-*b*-$P4VP_{124}$	250	1.5	41.4 %	15.9	18.1	43.8	1.27	0.57

The results indicate that mPEG-Cl macroinitiators were successfully initiated to afford mPEG-*b*-P4VP block copolymers, with narrow molecular weight distributions, for the different compositions and molecular weights, (see SEC traces in Figure 8.1).

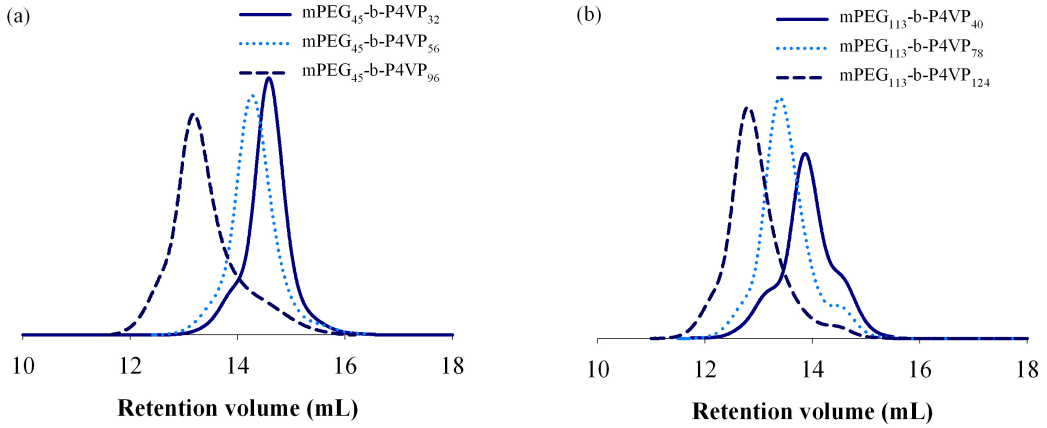

Figure 8.1 SEC traces (RI signal) of a mPEG-*b*-P4VP block copolymers obtained by SARA ATRP with : (a) $mPEG_{45}$-Cl and (b) $mPEG_{113}$-Cl macroinitiators.

The ^{1}H NMR spectrum of the $mPEG_{45}$-*b*-$P4VP_{56}$ block copolymer (Figure 8.2) shows the mPEG's terminal C-(CH_3) protons, at 0.80-1.00 ppm, the P4VP characteristic protons at 1.20-2.00 ppm (d, 3H), and its aromatic ring at 6.00-6.90 ppm (e, 2H) and 7.70-8.90 ppm (f, 2H). The average number molecular weight (M_n) of the P4VP blocks was determined through the comparison of the NMR peak integrals and from SEC measurements.

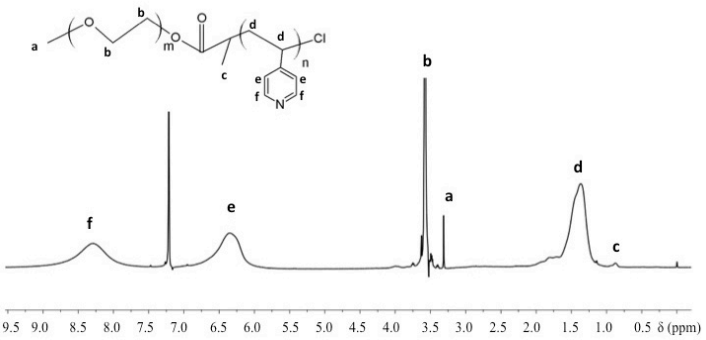

Figure 8.2 - ^{1}H NMR spectrum of mPEG$_{45}$-*b*-P4VP$_{56}$-Cl block copolymer. Their chemical structure and the proton identification scheme adopted for the NMR spectral assignments are also indicated.

The obtained narrow molecular weight distributions and the kinetic results of polymerizations [4] (Figure 8.3) suggest the success of the ATRP method that was adopted. One possible drawback that can be associated with the use of ATRP to prepare P4VP-containing structures may be the presence of copper in the final product. However, as can be observed in Table 1, the amount of copper in the block copolymers is residual, with values ranging from 0.55 and 0.94%. As an example, for the copolymer mPEG$_{45}$-*b*-P4VP$_{32,}$ this corresponds for only 2.5% of the existing pyridyl groups complexed with the copper ions (1:1 complex).

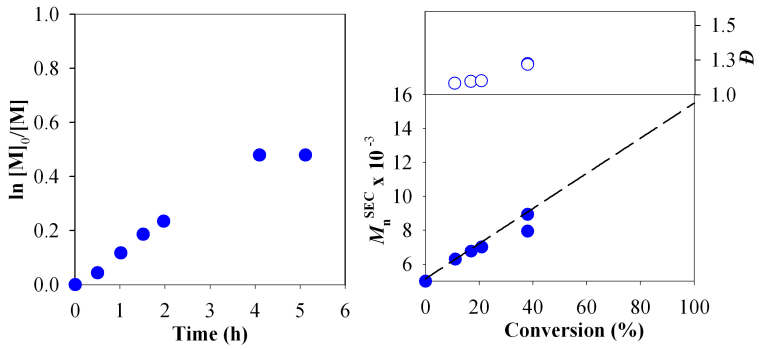

Figure 8.3 mPEG$_{113}$-*b*-P4VP$_{40}$ kinetic plots of conversion and ln[M]$_0$/[M] *vs*. time (left) and plot of number-average molecular weights (M_n^{SEC}) and *Đ* *vs*. conversion (right) for ATRP of 4VP catalyzed by CuCl$_2$/Me$_6$TREN in isopropanol at 40 °C. Conditions: [4VP]$_0$/ [IPA]= 1/1 (v/v); [4VP]$_0$/[PEG$_{113}$-Cl]$_0$/[CuCl$_2$]$_0$/[Me$_6$TREN] = 100/1/1/1 (molar).

8.4.2 Preparation and characterization of mPEG-*b*-P4VP micellar structures

Considering the pH-responsive character of P4VP, one way of preparing the block copolymer micelles involves aqueous self-assembly as a function of pH change, as previously described for amphiphilic P4VP-based block copolymers [36-37].

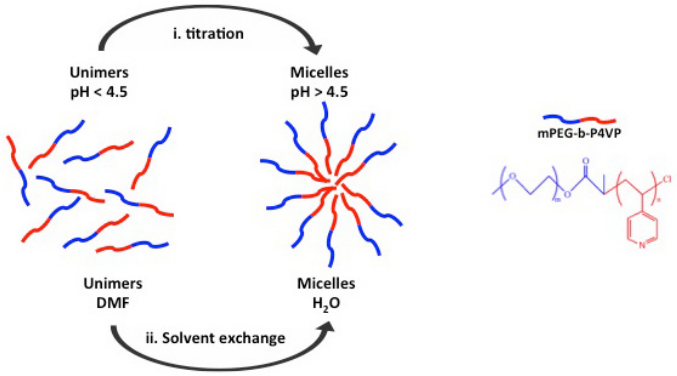

Figure 8.4 Representation of mPEG-*b*-P4VP self-assembly in aqueous media via titration and solvent exchange methods

Figure 8.4 represents a scheme of amphiphilic P4VP-based block copolymers self-assembly in aqueous media via titration and solvent exchange methods. These block copolymers are soluble under acidic conditions, but form core-shell micelles when the pH is above the pKa of P4VP (~pH 4.5 [37]), at which point the P4VP chains are deprotonated and the P4VP segments become hydrophobic. Another route to particle formation is via a solvent exchange method, as schematically represented in Figure 8.4. In this method, the block copolymer is initially dissolved in a good solvent for both blocks (such as DMF) and, due to solvability changes caused by dropwise addition into water, the particles form and are further subjected to dialysis against distilled water. The self-assembly of mPEG-*b*-P4VP could be monitored by the titration of HCl-acidic aqueous dispersions of the block copolymer, using a NaOH solution. Change from unimers to the micellized state was indicated by an increase in the solution turbidity when the pK_a of P4VP was reached, and could be confirmed by the significant increase in their hydrodynamic size, as determined by DLS (Figure 8.5). A similar process of particle formation was observed for nanoparticles produced through the use of solvent exchange process. The particle size distributions were determined by DLS and the average hydrodynamic diameters (D_h) and polydispersity index (PDI) of the obtained nanoparticles obtained are listed in Table 8.2.

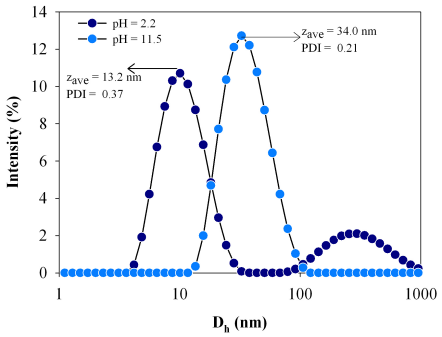

Figure 8.5 Particle size distribution in intensity determined by DLS for $mPEG_{113}$-*b*-$P4VP_{40}$ at different pH conditions.

Table 8.2 D_h and PDI of aqueous block copolymer dispersions, as determined by DLS, prepared by titration and by solvent exchange methods

Block Copolymer	Titration		Solvent Exchange	
	pH= 11.5		pH = 6.0	
	D_h (nm)	PDI	D_h (nm)	PDI
$mPEG_{45}$-*b*-$P4VP_{32}$	24.7	0.08	17.8	0.15
$mPEG_{45}$-*b*-$P4VP_{56}$	93.4	0.19	29.7	0.22
$mPEG_{45}$-*b*-$P4VP_{96}$	613.2	0.29	17.6	0.21
$mPEG_{113}$-*b*-$P4VP_{40}$	34.0	0.21	32.0	0.18
$mPEG_{113}$-*b*-$P4VP_{78}$	50.9	0.10	35.7	0.09
$mPEG_{113}$-*b*-$P4VP_{124}$	55.1	0.12	25.1	0.26

The results presented in Table 8.2 for the titration method show a tendency towards an increase in the hydrodynamic size with increase in the length of the P4VP block, while maintaining a narrow particle size distribution. The narrow size distributions can be related to the narrow molecular weight distributions of the block copolymers, which are essential to the self-assembly into uniform structures[46]. When a greater P4VP to mPEG ratio is used, larger particles with broader distributions were formed. This behavior was less pronounced when a longer mPEG segment was used, with particles of similar sizes being formed. The destabilization of micellar structures by increasing the P4VP block length was also previously observed when the titration method was used for P4VP block copolymers having poly(glycidol) as the steric stabilizer[37]. For the solvent exchange method, the self-assembly of block copolymers with greater P4VP to mPEG chain length ratios led to particles that were significantly smaller than those obtained by the titration method.

It should be noted that, in the titration method, the hydrodynamic size of the self-assembled block copolymers is only slightly affected by pH changes. In fact, specifically for the block copolymer $mPEG_{45}$-*b*-$P4VP_{56}$, the slight variation of the measured hydrodynamic size of the particles at different pH values (Figure 8.6), point out for only a negligible effect of the pH on particle size of the self-assembled SPIONs' aggregates using the titration method. Previous studies on the self-assembly of capsules that were formed from P4VP and poly(methacrylic acid)[47] have shown that, when the ionic strength was increased, the stability of the capsules decreased, leading to increasing swelling and even to the precipitation of the P4VP at higher pH values.

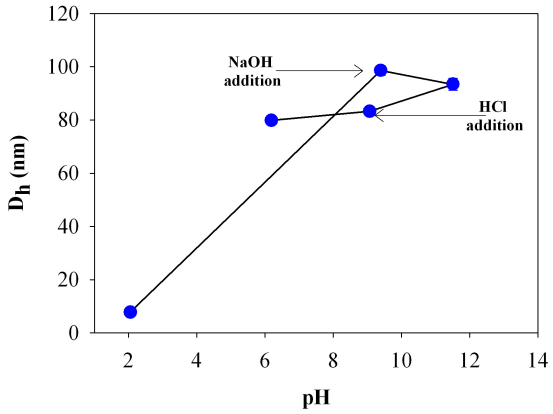

Figure 8.6 Hydrodynamic diameter (D_h) of $mPEG_{113}$-b-$P4VP_{78}$ self-assembled in the presence of Hydrophilic SPIONs (hSPIONs) measured at different pH values using the titration method.

To further inspect the effect of the ionic strength in the self-assembly of the block copolymers, $mPEG_{45}$-*b*-$P4VP_{56}$ nanoparticles were prepared by solvent exchange at different NaCl ionic strengths. The hydrodynamic size was found to increase from 29.7 nm (see Table 8.2) to 110.3 nm and 93.7 nm at, respectively, 10 mM and 200 mM of NaCl. These results support the conclusion that the observed increase in the particle size of the samples prepared by the titration method is due to the increase in the ionic strength of the medium.

Figure 8.7 presents the TEM micrographs of self-assembled block copolymers, prepared by titration and solvent exchange methods.

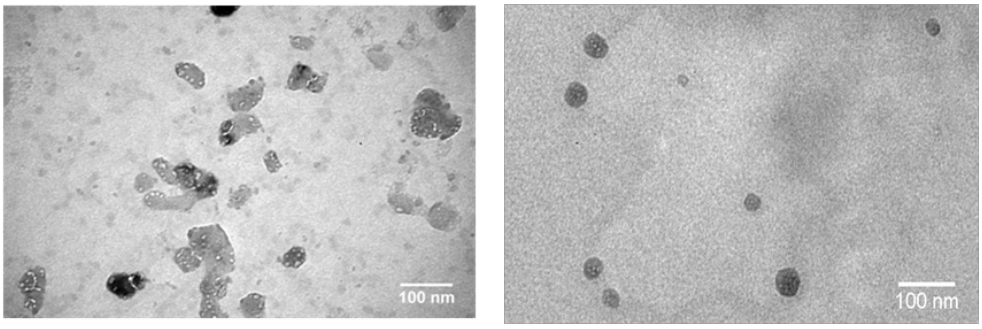

(a) **(b)**

Figure 8.7 TEM images of self-assembled block copolymers of (a) $mPEG_{113}$-*b*-$P4VP_{40}$ obtained by titration method and (b) at $mPEG_{45}$-*b*-$P4VP_{96}$ prepared by solvent exchange.

As shown in Figure 8.7 (a), after titration the block copolymer molecules are seen to be self-assembled into reasonably similar structures, with particle sizes in the 20-40 nm range. These structures seem to incorporate voids that can be attributed to a swelling effect arising from an increase in the ionic strength that occurs during titration. When the solvent exchange method was applied, only small and compacted aggregates (20-30 nm) were formed. Interestingly, these structures did not show evidence of large voids that were identified in Figure 8.7 (a). This difference in self-assembled structures suggests that the formation of ionic species during titration interferes significantly with the particle formation process and is responsible for the increased swelling of the nanoparticles.

8.1.1 Preparation and characterization of SPIONs aggregates based on mPEG-*b*-P4VP self-assembly

Hydrophilic SPIONs (hSPIONs) with an average size of 10 nm and a cubic morphology were synthesized according to our reported work.[45] The ability of mPEG-*b*-P4VP to form micellar structures in water can be used to prepare core-shell SPIONs aggregates that have the SPIONs in their core (Figure 8.8). The coordination capacity of P4VP, combined with its hydrophobicity at the self-assembled state, enables the transport of the hSPIONs into the core during micelle formation.

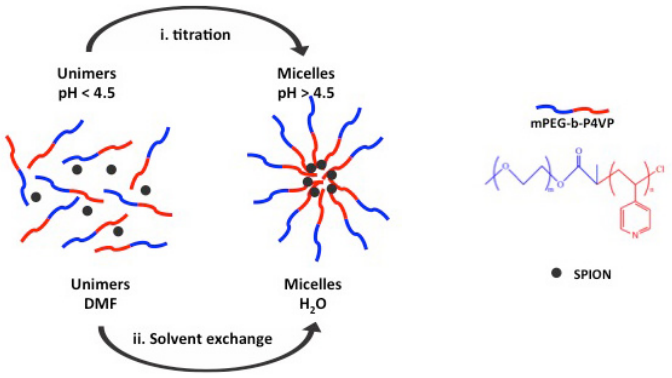

Figure 8.8 Schematic representation of the self-assembly of mPEG-*b*-P4VP in the presence of Fe_3O_4-based SPIONs, via titration and via solvent exchange methods.

In Table 8.3, it is presented the hydrodynamic diameter and polydispersity of the aggregates that were obtained by the self-assembly of mPEG-*b*-P4VP in the presence of hSPIONs. The increase in the hydrodynamic size, compared to that corresponding to the block copolymer alone, suggests that the hSPIONs are in the micelle core.

Table 8.3 - Dh and PDI values for mPEG-*b*-P4VP, self-assembled in the presence of hSPIONs

Block Copolymer	Titration		Solvent Exchange	
	z-average D_h (nm)	PDI	z-average D_h (nm)	PDI
$mPEG_{45}$-*b*-$P4VP_{32}$	66.7	0.27	66.8	0.19
$mPEG_{45}$-*b*-$P4VP_{56}$	113.1	0.20	70.2	0.25
$mPEG_{45}$-*b*-$P4VP_{96}$	*Precipitates*		55.2	0.27
$mPEG_{113}$-*b*-$P4VP_{40}$	71.8	0.25	160.0	0.36
$mPEG_{113}$-*b*-$P4VP_{78}$	78.5	0.19	69.9	0.26
$mPEG_{113}$-*b*-$P4VP_{124}$	86.5	0.22	68.8	0.28

The results that were obtained when the hSPIONs aggregates were prepared by the titration method followed the same trend as those obtained from the titration of the block copolymers alone (compare with Table 8.2), since there was tendency towards a significant increase in their particle size of the self-assembled structures as the P4VP to mPEG molar ratio was increase. This observation was particularly relevant for the block copolymer with the lowest mPEG molecular weight. In fact, $mPEG_{45}$-*b*-$P4VP_{96}$ could not even form stable aggregates of hSPIONs. This effect may be attributed to the formation of a large core that could not be stabilized by a small hydrophilic segment (recall large structures obtained by titration of $mPEG_{45}$-*b*-$P4VP_{96}$).

When the solvent exchange method was used there was also a tendency for more compacted structures to be formed when the P4VP to mPEG ratio was increased, while maintaining the low polydispersity. The only exception was obtained for the nanoaggregates prepared with $mPEG_{113}$-*b*-$P4VP_{40}$. This increase in the hybrid nanoparticles particle size suggests that, at lower P4VP to mPEG chain length ratios, the reduced amount of pyridyl groups that are available leads to an inferior capacity for coordination with the hSPIONs. Therefore, less compacted micelles including non-coordinated aggregates of hSPIONs are expected to be formed.

Figure 8.9 provides microscopic evidence for hSPIONs aggregation that can be achieved by the two self-assembly methodologies.

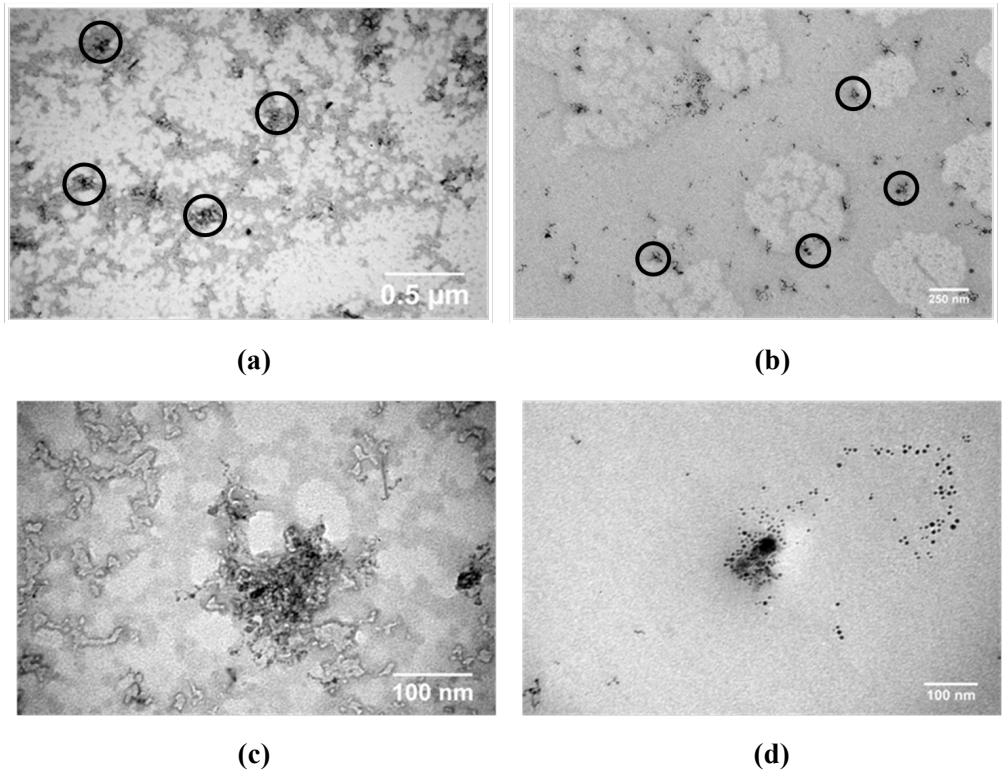

Figure 8.9 TEM micrographs of self-assembled block copolymers with hSPIONs prepared with (a, c) $mPEG_{113}$-*b*-$P4VP_{40}$ by titration and (b, d) $mPEG_{45}$-*b*-$P4VP_{32}$ by solvent exchange. (a) and (b) micrographs were taken at Mag. x60,000 and highlight the presence of the nanoaggregates (black circles), whereas (c) and (d) micrographs were taken at Mag. x200,000.

It is interesting to notice that, similarly to what occurred to the block copolymers self-assembly, is observed the disappearance of the swelled and voids-including structures when the preparation method is changed from the titration to the solvent exchange method. Another significant point is the presence of small particles outside the self-

assembled structures. This presence can be attributed to the hydrophilic nature of the hSPIONs, which may favor some particles being outside the self-assembled structures.

To understand the influence of the original coating of the SPIONs on the formation of hybrid nanoaggregates with mPEG-*b*-P4VP block copolymers, hydrophobic oleic acid-stabilized SPIONs (OaSPIONs) were evaluated. It should be noted that the hydrophobic nature of OaSPIONs makes it impossible to pre-disperse the nanoparticles in water and, therefore, only the solvent exchange method could be used. Figure 8.10 gives the particle size distributions that were obtained.

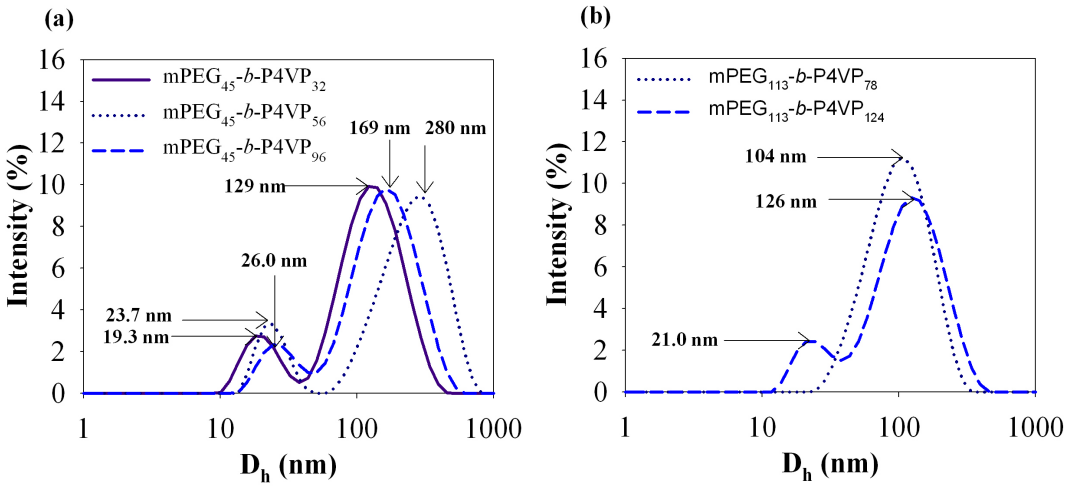

Figure 8.10 Particle size distributions, determined by DLS, for mPEG-*b*-P4VP block copolymers that were self-assembled in the presence of OaSPIONs. The block copolymers were based on (a) $mPEG_{45}$ and (b) $mPEG_{113}$ respectively as the steric stabilizer.

Similarly to what occurred for the self-assembly with hSPIONs, there is an increase in the size of the particle formed by the mPEG-*b*-P4VP self-assembly (compare with Table 8.2), suggesting an efficient encapsulation of the SPIONs in the micellar core. The size distribution of $mPEG_{113}$-*b*-$P4VP_{40}$ could not be determined because of the presence of large aggregates. In fact, this block copolymer gave larger hybrid nanoaggregates particles sizes when the solvent exchange method was used and such behavior was attributed to the reduced amount of P4VP. Thus, the precipitating behavior that was observed for this particular copolymer may be explained by a reduced ability to stabilize the core of the aggregates, when the SPIONs have a hydrophobic coating.

Additionally, when the OaSPIONs were used, bimodal size distributions were found in most of the samples. Since OaSPIONs cannot be dispersed in water, because of their hydrophobic character, the smaller sized population (20-30nm) can be attributed to the formation block copolymer micelles with no incorporation of OaSPIONs (compare values with those of Table 8.2). To support this conclusion, aggregates with 1:1 weight ratios were prepared for the block copolymers $mPEG_{45}$-*b*-$P4VP_{32}$. The DLS analysis showed only one particle size distribution in each case, with a maximum intensity peak at 163 nm, showing that increasing the block copolymer to OaSPIONs ratio can favor the formation of block copolymer micelles without OaSPIONs.

These results show that larger particles were formed when the hydrophobic SPIONs were used. The variation in the size distribution with the composition and with the molecular weight of the block copolymers seems to follow the same trend as that of the hybrid nanoaggregates prepared from hSPIONs by solvent exchange. For the block copolymer having the smaller mPEG, there is a maximum particle size in the intermediate P4VP to mPEG molar ratio ($mPEG_{45}$-*b*-$P4VP_{56}$). Block copolymers with a greater molecular weight and a greater P4VP to mPEG molar ratio, seem to lead to compacted structures, whose particle sizes are similar to those of $mPEG_{45}$-*b*-$P4VP_{32}$.

Figure 8.11 presents TEM micrographs of SPIONs aggregates that were prepared from the self-assembly of $mPEG_{45}$-*b*-$P4VP_{32}$ copolymer with OaSPIONs.

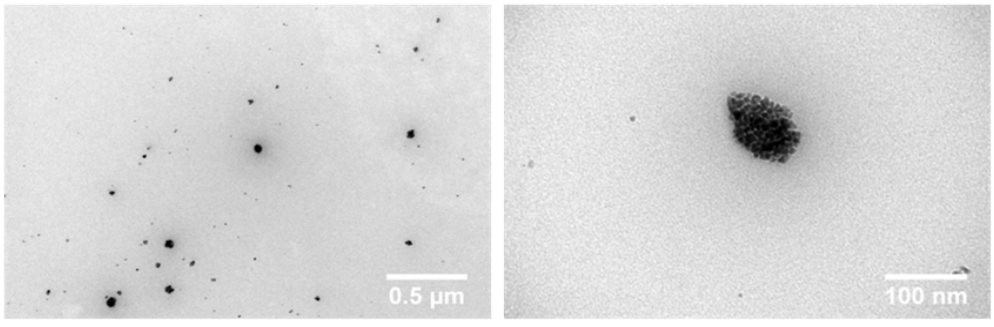

(a) **(b)**

Figure 8.11 TEM micrographs of SPIONs aggregates, prepared with oleic acid-coated SPIONs nanoaggregates based on the self-assembly of $mPEG_{45}$-*b*-$P4VP_{32}$: (a) was taken at a Mag. x60,000 and (b) at Mag. x300,000.

Compared with the aggregates that were prepared with the hSPIONs, these SPIONs tend to be more densely packed into the core of the aggregates. This effect can be attributed to greater water repulsion by the original coating of these SPIONs.

These results show that with this type of block copolymers it is possible to disperse in water nanoaggregates of SPIONs, either if they have hydrophilic or hydrophobic surfaces. Moreover, the most significant disadvantage in using non-coated iron oxide nanoparticles is their instability in an aqueous dispersion when kept for long periods of time. This instability arises because of the occurrence progressive agglomeration [14, 18-19]. In fact, the nanoaggregates prepared by self-assembly with mPEG-*b*-P4VP remained stable for months, independently on the preparation method or on the type of SPIONs that were used. However, for further application of these nanoaggregates in specific biological systems, one should evaluate the influence of other medium components in the colloidal stability.

8.1.2 Relaxometry of self-assembled mPEG-*b*-P4VP and SPIONs as aqueous dispersions

SPIONs have been clinically used as T_2-type (negative) MRI contrast agents, being commercially available under several brand names[48]. The performance of SPIONs aggregates, based on their mPEG-*b*-P4VP self-assembly behavior, as potential MRI contrast agents has been evaluated on the basis of relaxometric measurements. Figure 8.12 displays the measured r_1 and r_2 relaxivities for a representative dispersion of the hSPIONs-loaded $mPEG_{113}$-*b*-$P4VP_{78}$ and $mPEG_{45}$-*b*-$P4VP_{32}$ micelles, prepared respectively by the solvent exchange method and the titration method.

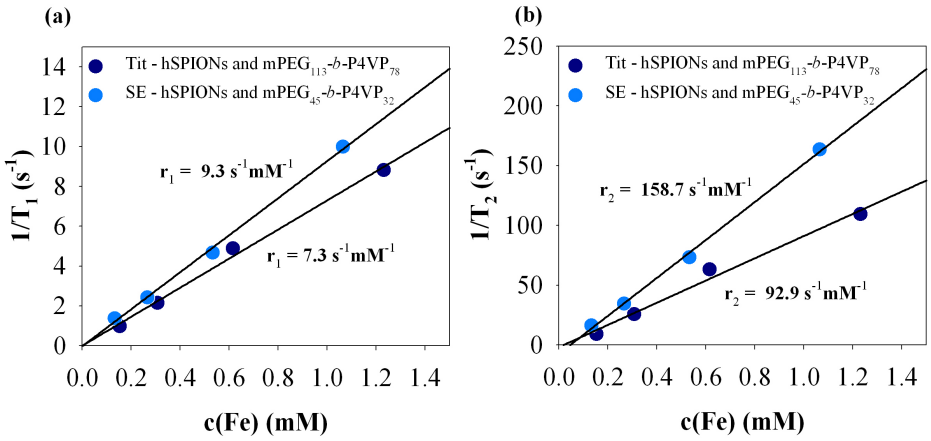

Figure 8.12 The paramagnetic contribution to the water proton relaxation rates (20 MHz, 25ºC) (a) for T_1 and (b) for T_2 relaxation rates (represented, respectively, as $r_{1,p}$ and $r_{2,p}$ in s^{-1}) as a function of iron concentration (in mM) for hSPION-loaded-$mPEG_{45}$-*b*-$P4VP_{32}$ and $mPEG_{113}$-*b*-$P4VP_{78}$ micelles, prepared, respectively, by the titration (Tit) and solvent exchange (SE) methods.

The relaxivity values that were obtained at 20 MHz for different self-assembled systems are summarized in Table 8.4.

Table 8.4 Longitudinal (r_1), transverse (r_2) relaxivities, and relaxivity ratios (r_2/r_1), obtained from relaxometry measurements, for different block copolymers and SPIONs-self-assembled samples, (at 20 MHz, 25ºC, 0.47T)

Block copolymer	SPIONs	Method	$r_1 \pm \sigma$ [s^{-1} mM^{-1}]	$r_2 \pm \sigma$ [s^{-1} mM^{-1}]	r_2/r_1
	SSPIONs [48-49]		20-40	150-160	4.0-6.0
	USPIONs [31, 48-49]		20-30	20-50	1.8-2.1
$mPEG_{45}$-*b*-$P4VP_{32}$	hSPIONs	Tit	7.7 ± 0.3	83.0 ± 1.7	10.8
$mPEG_{113}$-*b*-$P4VP_{78}$	hSPIONs	Tit	7.2 ± 0.6	92.8 ± 7.2	12.8
$mPEG_{45}$-*b*-$P4VP_{32}$	hSPIONs	SE	8.7 ± 0.4	148.3 ± 7.2	17.1
$mPEG_{113}$-*b*-$P4VP_{78}$	hSPIONs	SE	5.1 ± 0.4	96.7 ± 2.4	19.1
$mPEG_{45}$-*b*-$P4VP_{32}$	OaSPIONs	SE	2.8 ± 0.1	58.0 ± 1.4	20.4
$mPEG_{113}$-*b*-$P4VP_{78}$	OaSPIONs	SE	3.3 ± 0.0	97.5 ± 0.8	29.1

The r_1 values for mPEG-*b*-P4VP, self-assembled in the presence of SPIONs, are significantly lower than those reported for commercially available standards and for ultrasmall SPIONs (respectively, SSPIONs and USPIONs)[31, 48-49]. Values of r_1 are usually interpreted through the use of outer-sphere Curie relaxation theory, where the accessibility of water molecules to the surface of the nanoparticle is depicted to be a dominant factor, represented by the distance of closest approach[12, 50-51]. The hSPIONs-based micelle dispersions, with constant 10nm SPIONs diameter and hydrodynamic diameters in the 55.8-78.5nm range (Table 8.4), had r_1 values in the range of 5.1 – 8.7 s^{-1} mM^{-1} Fe. The reduction in r_1 that was observed for the studied nanoagregates is mainly attributed to a significant decrease in the accessibility of water to the surface of the hSPIONs because of their encapsulation in the hydrophobic mPEG-*b*-P4VP micelle core. For those aggregates that were prepared using the hydrophobic OaSPIONs (of constant 5nm size), there was a very significant reduction in r_1 values, which could be expected due to the increased water hindrance of the original SPIONs[25].

The hSPIONs mPEG-*b*-P4VP micelle formulations have r_2 values in the range of 83.0-148.3 s^{-1} mM^{-1} Fe, considerably larger than those reported for some USPIONs formulations, such as dextran-coated SPIONs (30-50 s^{-1} mM^{-1} Fe)[49] or CTAB-stabilized SPIONs (23.8 s^{-1} mM^{-1} Fe).[31] However, they have values that are comparable to those obtained by self-assembly methodologies[25, 28]. Previous studies have established that when SPIONs are present as clusters within polymeric micellar cores, r_2 can be considerably increased because of the collective effects of

nanoparticle assemblies. This effect is enhanced by having an increased SPIONs' diameter, and in some cases an increased loading density. In this work, the observed r_2 values may depend in a complex way on the extent of SPIONs encapsulation in the micelle core and on their water accessibility, which is determined by the adopted self-assembly methodology. The increased dispersability of the aggregates prepared by the solvent exchange method relative to the titration method significantly increased r_2 when the block copolymers containing shorter mPEG blocks were used, but had no significant effects for the micelles with the longer mPEG blocks.

The nanoaggregates that were prepared with OaSPIONs gave r_2 values in the range of 58.0 – 97.5 s^{-1} mM^{-1} Fe. These results suggest that, in spite of the extensive SPIONs aggregation observed for these systems, the greater hindrance of the iron oxide particles in OaSPIONs-based dispersions, resulting from their stronger hydrophobic character, may decrease r_2.

The r_2/r_1 relaxivity ratios of the micelle preparations studied are relatively high, making these systems potentially very efficient T_2 MRI contrast agents. These studies confirm that SPIONs clustering, arising from their incorporation in the hydrophobic mPEG-*b*-P4VP micelle core enhances r_2 and r_2/r_1 relaxivity ratios,[25, 28] but this effect may be limited by the hindered water accessibility to the micelle core.

Moreover, the SPIONs' nanoagregates were shown to remain stable in the aqueous dispersions after being subjected to a magnetic field. Figure 8.13 demonstrates the susceptibility of the hSPIONs-loaded $mPEG_{45}$-*b*-$P4VP_{32}$ micelles to the influence of an applied external magnetic field. When the magnetic field was removed, the particles became well dispersed in water again. Also, there was no evidence of differences in the quality of the dispersion, when compared to the dispersions that had not been subjected to the external magnetic field.

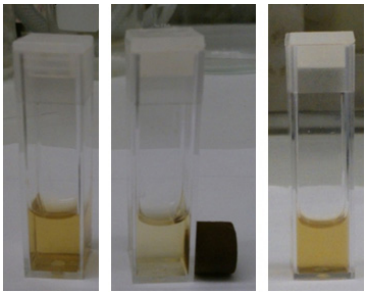

Figure 8.13 Comparison of aqueous dispersions of hSPIONs-loaded $mPEG_{45}$-*b*-$P4VP_{32}$ micelles (a) before, (b) during, and (c) after being subjected to an external magnetic field.

8.5 Conclusions

It has been shown that mPEG-*b*-P4VP block copolymers can be used to prepare hybrid nanoaggregates of SPIONs, independently of their original hydrophilic or hydrophobic coating, by self-assembly in aqueous media. Well-defined block copolymers, having different compositions and molecular weights were prepared by ATRP methodologies and were successfully used to prepare micelle structures in aqueous media. The type of structures that were formed was dependent on the preparation method, giving rise to much larger structures when prepared using a titration method (from 24.7 to 613 nm) than by a solvent exchange method (from 17.6 to 35.7 nm). Similar behavior occurred when the self-assembly was carried out in the presence of SPIONs. The block copolymer was capable of encapsulating the SPIONs with hydrophilic or hydrophobic nature in the micelle's core. The obtained hybrid SPIONs nanoaggregates perform as efficient T_2-weighted magnetic resonance imaging contrast agents, their r_1 values being significantly lower and r_2 in a similar range to those of commercially available SPIONs, giving rise to SPIONs aggregates that possessed large relaxivity ratios (r_2/r_1). The aggregates prepared in this study maintained a good stability in water for long periods of time, contrary to what occurs with native SPIONs, and after being subjected to an external magnetic field.

8.6 References

1. Nie, Z. H.; Petukhova, A.; Kumacheva, E., Properties and emerging applications of self-assembled structures made from inorganic nanoparticles, *Nat. Nanotechnol.*, *5* (1), 15-25, 2010.
2. Alexandridis, P.; Tsianou, M., Block copolymer-directed metal nanoparticle morphogenesis and organization, *Eur. Polym. J.*, *47* (4), 569-583, 2011.
3. Braunecker, W. A.; Matyjaszewski, K., Controlled/living radical polymerization: Features, developments, and perspectives, *Prog. Polym. Sci.*, *32* (1), 93-146, 2007.
4. Matyjaszewski, K., Atom Transfer Radical Polymerization: From Mechanisms to Applications, *Isr. J. Chem.*, *52* (3-4), 206-220, 2012.
5. Matyjaszewski, K.; Tsarevsky, N. V., Nanostructured functional materials prepared by atom transfer radical polymerization, *Nature Chemistry*, *1* (4), 276-288, 2009.
6. Cordeiro, R. A.; Rocha, N.; Mendes, J. P.; Matyjaszewski, K.; Guliashvili, T.; Serra, A. C.; Coelho, J. F. J., Synthesis of well-defined poly(2-(dimethylamino)ethyl methacrylate) under mild conditions and its co-polymers with cholesterol and PEG using Fe(0)/Cu(II) based SARA ATRP, *Polymer Chemistry*, *Advance Article*, 2013.

7. Rocha, N.; Mendonca, P. V.; Mendes, J. P.; Simoes, P. N.; Popov, A. V.; Guliashvili, T.; Serra, A. C.; Coelho, J. F. J., Facile Synthesis of Well-Defined Telechelic Alkyne-Terminated Polystyrene in Polar Media Using ATRP With Mixed Fe/Cu Transition Metal Catalyst, *Macromolecular Chemistry and Physics*, *214* (1), 76-84, 2013.
8. Rocha, N.; Coelho, J. F. J.; Barros, B.; Cardoso, P. M. L.; Goncalves, P. M.; Gil, M. H.; Guthrie, J. T., Deviation from the theoretical predictions in the synthesis of amphiphilic block copolymers in a wide range of compositions based on poly(vinyl chloride) by single electron transfer: Degenerative chain living radical polymerization in suspension medium, *J. Appl. Polym. Sci.*, *127* (5), 3407-3417, 2013.
9. Abreu, C. M. R.; Mendonca, P. V.; Serra, A. C.; Popov, A. V.; Matyjaszewski, K.; Guliashvili, T.; Coelho, J. F. J., Inorganic Sulfites: Efficient Reducing Agents and Supplemental Activators for Atom Transfer Radical Polymerization, *ACS Macro Lett.*, *1* (11), 1308-1311, 2012.
10. Liu, Y. B.; Wang, X. S., Recent advances in block copolymer-assisted synthesis of supramolecular inorganic/organic hybrid colloids, *Polymer Chemistry*, *2* (12), 2741-2757, 2011.
11. Lu, A.-H.; Salabas, E. L.; Schueth, F., Magnetic nanoparticles: Synthesis, protection, functionalization, and application, *Angewandte Chemie-International Edition*, *46* (8), 1222-1244, 2007.
12. Laurent, S.; Forge, D.; Port, M.; Roch, A.; Robic, C.; Elst, L. V.; Muller, R. N., Magnetic iron oxide nanoparticles: Synthesis, stabilization, vectorization, physicochemical characterizations, and biological applications, *Chemical Reviews*, *108* (6), 2064-2110, 2008.
13. Gupta, A. K.; Gupta, M., Synthesis and surface engineering of iron oxide nanoparticles for biomedical applications, *Biomaterials*, *26* (18), 3995-4021, 2005.
14. Mahmoudi, M.; Sant, S.; Wang, B.; Laurent, S.; Sen, T., Superparamagnetic iron oxide nanoparticles (SPIONs): Development, surface modification and applications in chemotherapy, *Advanced Drug Delivery Reviews*, *63* (1-2), 24-46, 2011.
15. Wang, N.; Guan, Y.; Yang, L.; Jia, L.; Wei, X.; Liu, H.; Guo, C., Magnetic nanoparticles (MNPs) covalently coated by PEO-PPO-PEO block copolymer for drug delivery, *Journal of Colloid and Interface Science*, *395*, 50-57, 2013.
16. Casula, M. F.; Corrias, A.; Arosio, P.; Lascialfari, A.; Sen, T.; Floris, P.; Bruce, I. J., Design of water-based ferrofluids as contrast agents for magnetic resonance imaging, *Journal of Colloid and Interface Science*, *357* (1), 50-55, 2011.
17. Seo, S.-B.; Yang, J.; Lee, T.-I.; Chung, C.-H.; Song, Y. J.; Suh, J.-S.; Yoon, H.-G.; Huh, Y.-M.; Haam, S., Enhancement of magnetic resonance contrast effect using ionic magnetic clusters, *Journal of Colloid and Interface Science*, *319* (2), 429-434, 2008.
18. Lee, N.; Hyeon, T., Designed synthesis of uniformly sized iron oxide nanoparticles for efficient magnetic resonance imaging contrast agents, *Chemical Society Reviews*, *41* (7), 2575-2589, 2012.
19. Oh, J. K.; Park, J. M., Iron oxide-based superparamagnetic polymeric nanomaterials: Design, preparation, and biomedical application, *Prog. Polym. Sci.*, *36* (1), 168-189, 2011.
20. Euliss, L. E.; Grancharov, S. G.; O'Brien, S.; Deming, T. J.; Stucky, G. D.; Murray, C. B.; Held, G. A., Cooperative assembly of magnetic nanoparticles and block copolypeptides in aqueous media, *Nano Letters*, *3* (11), 1489-1493, 2003.

21. Kim, B. S.; Qiu, J. M.; Wang, J. P.; Taton, T. A., Magnetomicelles: Composite nanostructures from magnetic nanoparticles and cross-linked amphiphilic block copolymers, *Nano Letters*, *5* (10), 1987-1991, 2005.
22. Berret, J. F.; Sehgal, A.; Morvan, M.; Sandre, O.; Vacher, A.; Airiau, M., Stable oxide nanoparticle clusters obtained by complexation, *Journal of Colloid and Interface Science*, *303* (1), 315-318, 2006.
23. Lecommandoux, S. B.; Sandre, O.; Checot, F.; Rodriguez-Hernandez, J.; Perzynski, R., Magnetic nanocomposite micelles and vesicles, *Advanced Materials*, *17* (6), 712-718, 2005.
24. Lattuada, M.; Hatton, T. A., Preparation and controlled self-assembly of janus magnetic nanoparticles, *J. Am. Chem. Soc.*, *129* (42), 12878-12889, 2007.
25. Ai, H.; Flask, C.; Weinberg, B.; Shuai, X.; Pagel, M. D.; Farrell, D.; Duerk, J.; Gao, J. M., Magnetite-loaded polymeric micelles as ultrasensitive magnetic-resonance probes, *Advanced Materials*, *17* (16), 1949-1956, 2005.
26. Hong, G.-b.; Zhou, J.-x.; Yuan, R.-x., Folate-targeted polymeric micelles loaded with ultrasmall superparamagnetic iron oxide: combined small size and high MRI sensitivity, *International Journal of Nanomedicine*, *7*, 2863-2872, 2012.
27. Chen, D.; Xia, X.; Gu, H.; Xu, Q.; Ge, J.; Li, Y.; Li, N.; Lu, J., pH-responsive polymeric carrier encapsulated magnetic nanoparticles for cancer targeted imaging and delivery, *Journal of Materials Chemistry*, *21* (34), 12682-12690, 2011.
28. Berret, J. F.; Schonbeck, N.; Gazeau, F.; El Kharrat, D.; Sandre, O.; Vacher, A.; Airiau, M., Controlled clustering of superparamagnetic nanoparticles using block copolymers: Design of new contrast agents for magnetic resonance imaging, *J. Am. Chem. Soc.*, *128* (5), 1755-1761, 2006.
29. Sondjaja, R.; Hatton, T. A.; Tam, M. K. C., Clustering of magnetic nanoparticles using a double hydrophilic block copolymer, poly(ethylene oxide)-b-poly(acrylic acid), *Journal of Magnetism and Magnetic Materials*, *321* (16), 2393-2397, 2009.
30. Wan, S. R.; Zheng, Y.; Liu, Y. Q.; Yan, H. S.; Liu, K. L., Fe3O4 nanoparticles coated with homopolymers of glycerol mono(meth) acrylate and their block copolymers, *Journal of Materials Chemistry*, *15* (33), 3424-3430, 2005.
31. Hu, J.; Qian, Y.; Wang, X.; Liu, T.; Liu, S., Drug-Loaded and Superparamagnetic Iron Oxide Nanoparticle Surface-Embedded Amphiphilic Block Copolymer Micelles for Integrated Chemotherapeutic Drug Delivery and MR Imaging, *Langmuir*, *28* (4), 2073-2082, 2012.
32. Aizawa, M.; Buriak, J. M., Block copolymer templated chemistry for the formation of metallic nanoparticle arrays on semiconductor surfaces, *Chem. Mat.*, *19* (21), 5090-5101, 2007.
33. Kang, N. G.; Kang, B. G.; Koh, H. D.; Changez, M.; Lee, J. S., Block copolymers containing pyridine moieties: Precise synthesis and applications, *React. Funct. Polym.*, *69* (7), 470-479, 2009.
34. Fahmi, A.; Pietsch, T.; Mendoza, C.; Cheval, N., Functional hybrid materials, *Mater. Today*, *12* (5), 44-50, 2009.
35. Koh, J. H.; Seo, J. A.; Park, J. T.; Kim, J. H., Synthesis and characterization of AgBr nanocomposites by templated amphiphilic comb polymer, *Journal of Colloid and Interface Science*, *338* (2), 486-490, 2009.
36. Zhang, W. Q.; Shi, L. Q.; Ma, R. J.; An, Y. L.; Xu, Y. L.; Wu, K., Micellization of thermo- and pH-responsive triblock copolymer of poly(ethylene glycol)-b-poly(4-vinylpyridine)-b-poly(N-isopropylacrylamide), *Macromolecules*, *38* (21), 8850-8852, 2005.

37. Mendrek, S.; Mendrek, A.; Adler, H.-J.; Dworak, A.; Kuckling, D., Synthesis and Characterization of pH Sensitive Poly(glycidol)-b-poly(4-vinylpyridine) Block Copolymers, *Journal of Polymer Science Part a-Polymer Chemistry*, *47* (7), 1782-1794, 2009.
38. Liu, H.; Shi, R.; Wan, W.; Yang, R.; Wang, Y., A well-defined diblock copolymer of poly(ethylene oxide)-block-poly(4-vinylpyridine) for separation of basic proteins by capillary zone electrophoresis, *Electrophoresis*, *29* (13), 2812-2819, 2008.
39. Zhao, L.; Ma, R.; Li, J.; Li, Y.; An, Y.; Shi, L., J- and H-Aggregates of 5,10,15,20-Tetrakis-(4-sulfonatophenyl)-porphyrin and Interconversion in PEG-b-P4VP Micelles, *Biomacromolecules*, *9* (10), 2601-2608, 2008.
40. Azzam, T.; Bronstein, L.; Eisenberg, A., Water-soluble surface-anchored gold and palladium nanoparticles stabilized by exchange of low molecular weight ligands with biamphiphilic triblock copolymers, *Langmuir*, *24* (13), 6521-6529, 2008.
41. Thevenot, J.; Oliveira, H.; Sandre, O.; Lecommandoux, S., Magnetic responsive polymer composite materials, *Chemical Society Reviews*, *42* (17), 7099-7116, 2013.
42. Ciampolini, M.; Nardi, N., Five-Coordinated High-Spin Complexes of Bivalent Cobalt, Nickel, andCopper with Tris(2-dimethylaminoethyl)amine, *Inorganic Chemistry*, *5* (1), 41-44, 1966.
43. Jankova, K.; Chen, X. Y.; Kops, J.; Batsberg, W., Synthesis of amphiphilic PS-b-PEG-b-PS by atom transfer radical polymerization, *Macromolecules*, *31* (2), 538-541, 1998.
44. Vidts, K. R. M.; Du Prez, F. E., Design of water-soluble block copolymers containing poly(4-vinylpyridine) by atom transfer radical polymerization, *Eur. Polym. J.*, *42* (1), 43-50, 2006.
45. Maleki, H.; Simchi, A.; Imani, M.; Costa, B. F. O., Size-controlled synthesis of superparamagnetic iron oxide nanoparticles and their surface coating by gold for biomedical applications, *Journal of Magnetism and Magnetic Materials*, *324* (23), 3997-4005, 2012.
46. Lynd, N. A.; Meuler, A. J.; Hillmyer, M. A., Polydispersity and block copolymer self-assembly, *Prog. Polym. Sci.*, *33* (9), 875-893, 2008.
47. Mauser, T.; Dejugnat, C.; Sukhorukov, G. B., Balance of hydrophobic and electrostatic forces in the pH response of weak polyelectrolyte capsules, *Journal of Physical Chemistry B*, *110* (41), 20246-20253, 2006.
48. Geraldes, C. F. G. C.; Laurent, S., Classification and basic properties of contrast agents for magnetic resonance imaging, *Contrast Media & Molecular Imaging*, *4* (1), 1-23, 2009.
49. Wang, Y. X. J.; Hussain, S. M.; Krestin, G. P., Superparamagnetic iron oxide contrast agents: physicochemical characteristics and applications in MR imaging, *European Radiology*, *11* (11), 2319-2331, 2001.
50. Roch, A.; Muller, R. N.; Gillis, P., Theory of proton relaxation induced by superparamagnetic particles, *Journal of Chemical Physics*, *110* (11), 5403-5411, 1999.
51. Pinho, S. L. C.; Laurent, S.; Rocha, J.; Roch, A.; Delville, M.-H.; Mornet, S.; Carlos, L. D.; Vander Elst, L.; Muller, R. N.; Geraldes, C. F. G. C., Relaxometric Studies of γ-Fe2O3@SiO2 Core Shell Nanoparticles: When the Coating Matters, *The Journal of Physical Chemistry C*, *116* (3), 2285-2291, 2011.

Part IV

Final Remarks

Chapter 9

9.1 Conclusions

Atom transfer radical polymerization is a versatile, efficient, and robust method to prepare (co)polymers with controlled molecular weight, composition, architecture, high chain end functionality, and low dispersity. The main objective of this research work was to develop strategies to obtain controlled polymerization of different monomer families using new eco-friendly SARA ATRP solvents or "greener" approaches having in mind the environmental aspect of this type of polymerizations.

Sulfolane was used for the first time as a universal solvent in SARA ATRP for methyl acrylate, methyl methacrylate, styrene and vinyl chloride polymerizations. The kinetic data show similar values as obtained using a commonly used polar solvent, dimethylsulfoxide. As proof of concept, poly(methyl acrylate)-*b*-poly(vinyl chloride)-*b*-poly(methyl acrylate) and poly(styrene)-*b*-poly(vinyl chloride)-*b*-poly(styrene) block copolymers were synthesized for the first time with controlled structure by "one pot" reaction. The addition of small amounts of water to sulfolane resulted in the significant enhance of the rate of polymerization, without compromising the properties of the final copolymers. The addition of water also allowed the use of FDA-approved sulphites as SARA agents, which could not be used before in pure sulfolane due to insolubility issues.

In the same line of research (introducing "greener" solvents) other alternative strategies were also attended: the use of ionic liquids and cyclopentyl methyl ether. The main reasons behind the choice of ionic liquids were the fact that they are considered by many authors as "green solvents" due to their intrinsic characteristic. CPME was selected because it is chemically comparable to the THF, it is "greener" than THF and, at the same time, does not act as a chain transfer agent. Using

[BMIM]-[PF_6] and CPME some very important results have been achieved: a synergistic effect between [BMIM]-[PF_6] /DMSO in the SARA ATRP of MA using $Na_2S_2O_4$/$CuBr_2$/Me_6TREN as the catalytic system was proved at room temperature; CPME was reported, for the first time in ATRP reactions as suitable solvent to replace oh THF (toxic solvent).

It is still important to mention the universal character of the ATRP system using sulfolane or [BMIM]-[PF_6] and water mixtures. However, the synergistic effect verified between DMSO/[BMIM]-[PF_6] was not observed with sulfolane/[BMIM]-[PF_6].

The SARA ATRP was successfully carried out in miniemulsion. Although the conversion rates were lower than those obtained in homogeneous systems, the polymerization was carried out successfully since it was possible to obtain polymers with controlled features.

Finally, amphiphilic block copolymer matrix, consisting of poly(ethylene glycol)-block-poly(4-vinylpyridine) with different compositions and molecular weights, were prepared by ATRP and used in the stabilization of SPIONs. This result is an important step towards the applicability of these copolymers for the stabilization of nanoparticles.

Overall, this project has contributed for the development of new ecofriendly ATRP-based systems for the polymerization of several monomer families, which have the same properties as those obtained with conventional solvents.

9.2 Future work

This work has contributed for the development of new ecofriendly ATRP solvent systems that present attractive features for further developments regarding the scale-up of the technique. Based on the results obtained in this work, the following studies will be of interest to improve the state-or-art involving the ATRP methods:

- The use of deep eutectic mixtures as an economically viable alternative to the expensive ionic liquds;
- The development of effective recycling and reusing processes involving ionic liquids that will promote their reintegration in the polymerization cycle;
- Evaluation of the application of natural based solvents in ATRP, increasing the "green" aspect of the process;
- Application of the "greener solvent" strategy to the synthesis of amphiphilic copolymers used to stabilize the SPIONs as well as the study of new ecofriendly solvents to obtain their stabilization.